

BRUNO SERENI

**Two-Stage Static Output Feedback Controller Design  
for Linear Systems Under LMI Pole Placement and  
 $\mathcal{H}_2/\mathcal{H}_\infty$  Guaranteed Cost Constraints**

Ilha Solteira  
2023



BRUNO SERENI

**Two-Stage Static Output Feedback Controller Design  
for Linear Systems Under LMI Pole Placement and  
 $\mathcal{H}_2$  /  $\mathcal{H}_\infty$  Guaranteed Cost Constraints**

Doctoral Thesis presented at the São Paulo State University (UNESP) - School of Engineering - Campus of Ilha Solteira, in fulfillment of one of the requirements for obtaining the degree of Doctor in Electrical Engineering.  
Specialty: Automation.

Prof. Dr. Edvaldo Assunção  
Advisor

Ilha Solteira  
2023

FICHA CATALOGRÁFICA

Desenvolvido pelo Serviço Técnico de Biblioteca e Documentação

S483t Sereni, Bruno.  
Two-stage static output feedback controller design for linear systems under LMI pole placement and  $H_2/H_\infty$  guaranteed cost constraints / Bruno Sereni. --Ilha Solteira: [s.n.], 2023  
155 f. : il.

Tese (doutorado) - Universidade Estadual Paulista. Faculdade de Engenharia de Ilha Solteira. Área de conhecimento: Automação, 2023

Orientador: Edvaldo Assunção  
Inclui bibliografia

1. Realimentação estática de saída. 2. Sistemas lineares. 3. Controle gain-scheduling. 4. Controle robusto. 5. Alocação de polos. 6. Desigualdades matriciais lineares.

  
Raiane da Silva Santos

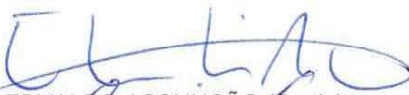
**CERTIFICADO DE APROVAÇÃO**

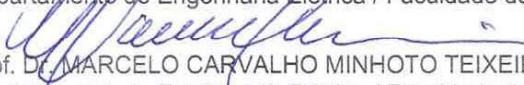
TÍTULO DA TESE: Two-Stage Static Output Feedback Controller Design for Linear Systems Under LMI Pole Placement and H<sub>2</sub>/H<sub>∞</sub> Guaranteed Cost Constraints


**AUTOR: BRUNO SERENI**

**ORIENTADOR: EDVALDO ASSUNÇÃO**

Aprovado como parte das exigências para obtenção do Título de Doutor em Engenharia Elétrica, área: Automação pela Comissão Examinadora:

  
Prof. Dr. EDVALDO ASSUNÇÃO (Participação Presencial)  
Departamento de Engenharia Elétrica / Faculdade de Engenharia de Ilha Solteira - UNESP

  
Prof. Dr. MARCELO CARVALHO MINHOTO TEIXEIRA (Participação Presencial)  
Departamento de Engenharia Elétrica / Faculdade de Engenharia de Ilha Solteira - UNESP

  
Prof. Dr. FLAVIO ANDRADÉ FARIA (Participação Presencial)  
Departamento de Matemática / Faculdade de Engenharia de Ilha Solteira - UNESP

  
Prof. Dr. JOSÉ CLAUDIO GEROMEL (Participação Virtual)  
Universidade Estadual de Campinas - UNICAMP

  
Prof. Dr. UILIAM NELSON LENZION TOMAZ ALVES (Participação Virtual)  
Departamento de Eixo de Controle e Processos Industriais / Instituto Federal de Educação, Ciência e Tecnologia do Paraná - IFPR

Ilha Solteira, 19 de janeiro de 2023

*Para a honra e glória do Senhor,*

***Ofereço.***

## **AGRADECIMENTOS**

### **Agradeço**

a Deus, por sempre iluminar o meu caminho, pelo incessante amparo, pela confiança, pela força e misericórdia nos momentos difíceis;

a Edvaldo Assunção, pela orientação, pela amizade única e pelos valiosos ensinamentos;

aos meus pais, pelo amor e apoio incondicionais;

a minha namorada, pelo carinho e suporte ao longo da caminhada;

aos amigos e colegas que fiz ao longo de tantos anos de estudo;

e a FAPESP, pelo financiamento ao longo do doutorado (Processo 2019/20839-9).

*“E qual o pai de entre vós que, se o filho lhe pedir  
pão, lhe dará uma pedra? Ou, também, se lhe pedir  
peixe, lhe dará por peixe uma serpente?”*

*Pois se vós, sendo maus, sabeis dar boas dádivas aos  
vossos filhos, quanto mais dará o Pai celestial o  
Espírito Santo àqueles que lhe pedirem?*

***Lucas, 11:11,13***

## ABSTRACT

In this work, new static output feedback (SOF) controller synthesis conditions for the stabilization of linear systems are proposed. The cases of uncertain linear time-invariant (LTI) systems and linear parameter-varying (LPV) systems are addressed in the frameworks of robust control and gain-scheduling (GS) control, respectively. The SOF controller synthesis is based on the two-stage method, in which a preliminary state feedback (SF) gain matrix is designed, and then used as input information to the second stage for obtaining the desired stabilizing SOF controller. The proposed design conditions are given in terms of sufficient linear matrix inequalities (LMI), and are obtained considering the enforcement of specific additional constraints for guaranteeing improved transient performance regarding the establishment of a lower bound on the closed-loop system decay rate and reduced oscillatory behavior. Such further control requirements are imposed through LMI pole placement constraints, designed based on the concept of the  $\mathcal{D}$ -stability of continuous-time systems. Furthermore, SOF control design conditions are also proposed for addressing noise/disturbance rejection by means of the  $\mathcal{H}_\infty$  guaranteed cost minimization, particularly for discrete-time LPV systems. Additionally, the employment of the studied SOF control strategy for dealing with uncertain LTI systems with sensors and/or actuators with non-negligible dynamics and subject to time delay is investigated. For this purpose, an augmented system model which encompasses plant, sensors, and actuator dynamics is obtained. The system augmentation procedure also takes into account the dynamic effect of the time delay. Particularly for this problem, the use of homogeneous-polynomial parameter-dependent Lyapunov functions (HPPDLF) with degree higher than 1 is considered. Disturbance rejection is also addressed through extensions to  $\mathcal{H}_2$  guaranteed cost minimization. Numerical examples are presented to illustrate the SOF controller synthesis procedure proposed in this work, as well as to highlight its features and advantages over other strategies available in the literature. Results of practical implementation of SOF controllers designed using the proposed methods are also presented, attesting for the potential of the contributions of this work to be employed in real world control problems.

**Keywords:** static output feedback; linear systems; gain-scheduling control; robust control; pole placement;  $\mathcal{H}_2/\mathcal{H}_\infty$  control; linear matrix inequalities.



## RESUMO

Neste trabalho são propostas novas condições para a síntese de controladores via realimentação estática de saída (SOF, sigla do inglês *static output feedback*) objetivando a estabilização de sistemas lineares. Os casos de sistemas incertos lineares invariantes no tempo (LTI, do inglês *linear time-invariant*) e de sistemas lineares com parâmetro variante no tempo (LPV, do inglês *linear parameter-varying*) são abordados no contexto de controle robusto e de controle *gain-scheduling* (GS), respectivamente. A síntese dos controladores SOF é baseada no método dos dois estágios, no qual uma matriz de ganhos de realimentação de estado é preliminarmente projetada, e então utilizada como parâmetro de entrada para o segundo estágio, no qual o controlador estabilizante SOF pode ser obtido. As condições de projeto propostas são dadas em termos de desigualdades matriciais lineares (LMI, do inglês *linear matrix inequalities*) suficientes, as quais são obtidas considerando a imposição de restrições adicionais para obtenção de garantias para uma performance de transitório adequada, impondo um limitante inferior para a taxa de decaimento do sistema em malha fechada e também um comportamento oscilatório mais amortecido. Tais requisitos de controle adicionais são impostos a partir da consideração de restrições LMI para a alocação de polos, projetadas baseadas no conceito da  $\mathcal{D}$ -estabilidade de sistemas contínuos no tempo. Além disso, condições de projeto SOF são também propostas para abordar a rejeição de ruído/distúrbio por meio da minimização do custo garantido  $\mathcal{H}_\infty$ , particularmente para sistemas LPV discretos no tempo. Adicionalmente, é investigado o emprego da estratégia de controle SOF em sistemas incertos LTI com atuadores e/ou sensores com dinâmica não desprezível, e sujeitos a atraso no tempo. Para tal propósito, um modelo de sistema aumentado é obtido de forma a englobar as dinâmicas da planta, dos sensores e atuadores. O procedimento de aumento de sistema também leva em consideração o efeito dinâmico do atraso. Particularmente para este problema, considera-se o uso de funções de Lyapunov polinomiais homogêneas dependentes de parâmetros (HP-PDLF, do inglês *homogeneous-polynomial parameter-dependent Lyapunov functions*). A rejeição de distúrbios também é tratada por meio de extensões para a minimização do custo garantido  $\mathcal{H}_2$ . Exemplos numéricos são apresentados para ilustrar o procedimento de síntese de controladores SOF proposto neste trabalho, assim como para destacar suas características e vantagens comparadas a outros trabalhos na literatura. Resultados de implementações práticas de controladores SOF projetados utilizando as estratégias propostas também são apresentados, atestando o potencial das contribuições deste trabalho para serem aplicadas a problemas de controle do mundo real.

**Palavras-chave:** realimentação estática de saída; sistemas lineares; controle *gain-scheduling*; controle robusto; alocação de polos; controle  $\mathcal{H}_2/\mathcal{H}_\infty$ ; desigualdades matriciais lineares.

## LIST OF FIGURES

|             |   |    |
|-------------|---|----|
| Figure 2.1  | Graphical representation the uncertainty polytope of an LTI system with two uncertain parameters in the model (four vertices). . . . .  | 32 |
| Figure 2.2  | Geometric interpretation of the minimum decay rate requirement. . . . .   | 35 |
| Figure 2.3  | Circular LMI region $\mathcal{D}(q, r)$ for pole placement. . . . .   | 36 |
| Figure 2.4  | A linear system representation in both time and frequency domains: the later enables the $\mathcal{H}_\infty$ control approach. . . . .   | 38 |
| Figure 2.5  | The $\mathcal{H}_\infty$ norm representation for SISO systems: the worst case in the system frequency response. . . . .   | 39 |
| Figure 2.6  | The $\mathcal{H}_\infty$ guaranteed cost representation for an uncertain SISO system: a upper bound for the uncertain LTI system $\mathcal{H}_\infty$ norm. . . . .                 | 40 |
| Figure 2.7  | The $\mathcal{H}_2$ norm representation for two distinct SISO LTI systems with transfer functions $H_1(j\omega)$ and $H_2(j\omega)$ , respectively. . . . .                         | 41 |
| Figure 2.8  | The $\mathcal{H}_2$ guaranteed cost representation: frequency response for three different values of $\alpha$ of a generic SISO LTI system. . . . .                                 | 42 |
| Figure 2.9  | Illustration of the gain-scheduled classic control for a parameter grid of four sections and its corresponding static controllers. . . . .  | 45 |
| Figure 2.10 | Illustration of the gain-scheduled controller generated by the convex combination of four vertex matrices, parameterized in terms of the time-varying parameters. . . . .           | 46 |
| Figure 3.1  | Feasibility region obtained in Example 3.1 using: Strategy 1 ( $\square$ ); Strategy 2 ( $\square$ and $\circ$ ); and Strategy 3 ( $\square$ , $\circ$ , and $\triangle$ ). . . . . | 63 |
| Figure 3.2  | Cloud of open (+) and closed-loop (*) eigenvalues of the uncertain row axis dynamics for arbitrary values of uncertain parameters within the specified range. . . . .               | 66 |
| Figure 3.3  | Row rate time response with controllers (3.33) (solid) and (3.34) (dash-dot) for 30 different random values of $\delta_1$ and $\delta_2$ in (3.32). . . . .                         | 67 |
| Figure 3.4  | Row control command with controllers (3.33) (solid) and (3.34) (dash-dot) for 30 different random values of $\delta_1$ and $\delta_2$ in (3.32). . . . .                            | 68 |
| Figure 3.5  | Active suspension system experimental module and model diagram. . . . .   | 69 |
| Figure 3.6  | Cloud of open (+) and closed-loop (*) of the uncertain active suspension system dynamics for arbitrary values of uncertain parameters within the specified range. . . . .           | 71 |

|             |  |     |
|-------------|--|-----|
| Figure 3.7  | Active suspension dynamic response (upper chart) and control signal (bottom chart) with $M_s(\alpha) = 1.455$ kg in: open-loop (0-8s); closed-loop (8-16s); fault: 30% power loss in the actuator (16-24s).            | 72  |
| Figure 3.8  | Active suspension dynamic response (upper chart) and control signal (bottom chart) with $M_s(\alpha) = 2.45$ kg in: open-loop (0-8s); closed-loop (8-16s); fault: 30 % power loss in the actuator (16-24s).            | 73  |
| Figure 3.9  | Open-loop (dashed lines) and closed-loop (full lines) transient response of the L-1011 lateral axis dynamics, and control input $u(t)$ (bottom chart).   | 83  |
| Figure 3.10 | Behavior of the time-varying parameters (top left charts); parametric elements of $\alpha(t)$ (top right charts); and GS-SOF gains (bottom chart) in Example 3.4 simulations.  | 83  |
| Figure 4.1  | Unitary circle and circular sub region bounded for $0 \leq \rho < 1$ .   | 86  |
| Figure 4.2  | Eigenvalue cloud for system (4.58) in open loop ( $*$ ) and closed loop ( $\times$ ) with GS-SOF controller (4.60) (dashed line: $\rho = 0.85$ ; Right chart: close-up).   | 105 |
| Figure 4.3  | Transient response of system (4.58) in open loop.  | 106 |
| Figure 4.4  | Transient response of system (4.58) in closed loop.  | 107 |
| Figure 4.5  | Control signal produced by the designed GS-SOF controller.   | 107 |
| Figure 4.6  | Variation of the values of GS-SOF controller $L(\alpha(k))$ (up) according to the instant measurement of $\alpha(k)$ (bottom).   | 107 |
| Figure 4.7  | Feasibility region obtained using: Corollary 4.1 ( $\times$ ), Corollary 1 in Rosa, Morais and Oliveira (2018) ( $\times$ and $\bigcirc$ ); and Theorem 4.2 ( $\times$ , $\bigcirc$ , and $\square$ ).                 | 109 |
| Figure 4.8  | $\mathcal{H}_\infty$ guaranteed cost with GS-SOF controller design obtained with Theorem 4.3, employed according to Algorithm 4.3, and with the techniques proposed in Rosa et al. (2017) and de Caigny et al. (2010). | 110 |
| Figure 4.9  | Controlled output and control signals obtained with the GS-SOF controller 4.64.  | 112 |
| Figure 5.1  | Closed-loop block diagram.   | 115 |
| Figure 5.2  | L-1011 lateral axis closed-loop dynamics with SOF design neglecting (SERENI <i>et al.</i> , 2020) and considering transport delay (SOF controller (5.43)).   | 128 |

|            |  |     |
|------------|--|-----|
| Figure 5.3 | L-1011 lateral axis closed-loop dynamics with SOF design with minimum decay rate $\gamma = 0.2$ and without minimum decay rate enforcement ( $\gamma = 0$ ). . . . .   | 129 |
| Figure 5.4 | Simulation results obtained for Example 5.2 system considering a conventional SMC controller (UTKIN, 1978). . . . .  | 131 |
| Figure 5.5 | Simulation results obtained for Example 2 system considering a robust SOF controller using our proposed two-stage design via Theorem 5.1. . . . .  | 132 |
| Figure 5.6 | Feasibility region obtained for the L-1011 lateral axis SOF stabilization problem without imposing a minimum decay rate when applying the polytopic PDLF SOF design strategy (SERENI <i>et al.</i> , 2018) ( $\circ$ - Corollary 5.2); and when using the HPLF extension proposed in Theorem 5.1 ( $\circ$ and $\square$ ). . . . .            | 133 |
| Figure 5.7 | Feasibility region obtained for the L-1011 lateral axis SOF stabilization problem imposing a minimum decay rate ( $\gamma_1 = \gamma_2 = 0.025$ ) when applying the polytopic PDLF SOF design strategy (SERENI <i>et al.</i> , 2020) ( $\circ$ ); and when using the HPLF extension proposed in Theorem 5.1 ( $\circ$ and $\square$ ). . . . . | 134 |
| Figure 5.8 | Feasibility regions obtained for the L-1011 lateral axis SOF stabilization problem for different choices of the polynomial degree of the decision variables associated to the first- and second-stage designs with (bottom charts) and without (top charts) minimum decay rate constraints. . . . .  | 135 |

## LIST OF ABBREVIATIONS AND ACRONYMS

|        |   |
|--------|---|
| BMI    | Bilinear matrix inequalities                                  |
| BRL    | Bounded-real lemma  |
| CQLF   | Common quadratic Lyapunov functions                           |
| DC     | Direct current  |
| DOF    | Dynamic output feedback                                       |
| GS     | Gain-scheduling/Gain-scheduled                                |
| HPPDLF | Homogeneous polynomial parameter-dependent Lyapunov functions |
| LFT    | Linear fractional transformation                              |
| LMI    | Linear matrix inequalities                                    |
| LPV    | Linear parameter-varying                                      |
| LTI    | Linear time-invariant   |
| LTV    | Linear time-varying   |
| PDLF   | Parameter dependent Lyapunov functions                        |
| SISO   | Single-input single-output                                    |
| SF     | State feedback  |
| SMC    | Sliding mode control  |
| SOF    | Static output feedback  |
| T-S    | Takagi-Sugeno   |

## LIST OF SYMBOLS

|                           |  |
|---------------------------|--|
| $M^\perp$                 | Basis for the null space of $M$ .                                      |
| $\ v\ , \ v\ _2$          | Euclidean norm of the real vector $v$ .                                |
| $\ H(s)\ $                | Magnitude of an LTI system transfer function in terms of $s = j\omega$ |
| $\ H(s)\ _\infty$         | $\mathcal{H}_\infty$ norm of a dynamic system                          |
| $\ H(s)\ _2$              | $\mathcal{H}_2$ norm of a dynamic system                               |
| $M^{-1}$                  | Inverse of the real matrix $M$ .                                       |
| $M(\alpha)$               | $M(\alpha) = \sum_{i=1}^N \alpha_i M_i, \quad \alpha \in \Lambda_N$ .  |
| $\mathbb{R}^{n \times m}$ | Set of the real matrices with $n$ rows and $m$ columns.                |
| *                         | Symmetric block of a symmetric matrix.                                 |
| $\lambda$                 | Represents the eigenvalues of a generic square matrix $M$              |
| $M + (\bullet)'$          | Represents $M + M'$ .  |
| $M \geq (>)0$             | Symmetric positive semidefinite (definite) matrix $M$ .                |
| $M \leq (<)0$             | Symmetric negative semidefinite (definite) matrix $M$ .                |
| $M'$                      | Transpose of the real matrix $M$ .                                     |
| $C'$                      | Conjugate transpose of the complex matrix $C$ .                        |

## CONTENTS

|              |  |           |
|--------------|--|-----------|
| <b>1</b>     | <b>INTRODUCTION</b>  | <b>15</b> |
| 1.1          | Motivation   | 15        |
| 1.2          | Literature Review  | 19        |
| 1.3          | Main Contributions   | 27        |
| 1.4          | Outline  | 30        |
| <b>2</b>     | <b>FUNDAMENTAL CONCEPTS AND DEFINITIONS</b>                            | <b>31</b> |
| 2.1          | Stability and Transient Performance in Linear Systems via LMI          | 31        |
| <b>2.1.1</b> | <b>LTI and LPV Systems: A Polytopic Description</b>                    | <b>31</b> |
| <b>2.1.2</b> | <b>Pole Placement Constraints</b>                                      | <b>34</b> |
| <b>2.1.3</b> | <b><math>\mathcal{H}_\infty</math> Guaranteed Cost</b>                 | <b>37</b> |
| <b>2.1.4</b> | <b><math>\mathcal{H}_2</math> Guaranteed Cost</b>                      | <b>41</b> |
| <b>2.1.5</b> | <b>Two-Stage SOF Design</b>  | <b>42</b> |
| <b>2.1.6</b> | <b>Gain-Scheduling Control</b>   | <b>44</b> |
| 2.2          | Mathematical Tools   | 47        |
| <b>3</b>     | <b>STATIC OUTPUT FEEDBACK CONTROL WITH POLE PLACEMENT CONSTRAINTS</b>  | <b>49</b> |
| 3.1          | Robust $\mathcal{D}$ -stabilization via SOF Control                    | 49        |
| <b>3.1.1</b> | <b>Problem Statement and Proposed Approach</b>                         | <b>50</b> |
| <b>3.1.2</b> | <b>Two-Stage SOF Design for <math>\mathcal{D}</math>-Stabilization</b> | <b>51</b> |
| <b>3.1.3</b> | <b>Illustrative Examples</b>   | <b>61</b> |
| <b>3.1.4</b> | <b>Practical Implementation: Active Suspension System</b>              | <b>68</b> |
| 3.2          | Gain-Scheduling Control via SOF with Pole Placement Constraints        | 73        |
| <b>3.2.1</b> | <b>Problem Statement</b>   | <b>74</b> |
| <b>3.2.2</b> | <b><math>\mathcal{D}</math>-stability: an extension to LPV systems</b> | <b>75</b> |
| <b>3.2.3</b> | <b>Gain-Scheduling Static Output Feedback</b>                          | <b>76</b> |
| <b>3.2.4</b> | <b>Illustrative Examples</b>   | <b>79</b> |
| <b>4</b>     | <b>DISCRETE-TIME GS–SOF CONTROL DESIGN</b>                             | <b>84</b> |
| 4.1          | Two-Stage Discrete-Time GS–SOF Control                                 | 84        |
| <b>4.1.1</b> | <b>Problem Statement and Proposed Approach</b>                         | <b>85</b> |
| <b>4.1.2</b> | <b>Two-Stage Discrete-Time GS–SOF Design with Decay Rate Bounding</b>  | <b>86</b> |

|              |   |            |
|--------------|---|------------|
| <b>4.1.3</b> | <b>Two-Stage Discrete-Time <math>\mathcal{H}_\infty</math> GS-SOF Design</b>  | <b>95</b>  |
| <b>4.1.4</b> | <b>Illustrative Examples</b>  | <b>103</b> |
| <b>5</b>     | <b>NON-NEGLIGIBLE SENSORS AND ACTUATORS DYNAMICS<br/>WITH TRANSPORT DELAY</b> | <b>113</b> |
| 5.1          | Problem Statement   | 113        |
| 5.2          | Proposed Strategy   | 115        |
| <b>5.2.1</b> | <b>System Augmentation</b>  | <b>115</b> |
| <b>5.2.2</b> | <b>Control Design</b>   | <b>119</b> |
| 5.3          | Illustrative Examples   | 124        |
| 5.4          | Extension to $\mathcal{H}_2$ control  | 135        |
| <b>6</b>     | <b>CONCLUSION</b>   | <b>140</b> |
|              | <b>REFERENCES</b>   | <b>144</b> |



## 1 INTRODUCTION

This first chapter begins with the presentation of ideas and concepts that motivated the exploration of the subjects of interest of this work, which are mainly related to linear control systems via static output feedback (SOF). Then, by means of a more detailed literature review, we manage to introduce the scientific development in the control theory fields that are addressed and discussed in the subsequent chapters. The idea is to give proper context regarding the current research state-of-the-art on the output-feedback stabilization problem written in the linear matrix inequality (LMI) framework, with emphasis in gain-scheduling and robust control, pole placement constraints, and  $\mathcal{H}_2/\mathcal{H}_\infty$  norm optimization. On top of that, we summarize the technical contributions that are presented, proposed, and discussed in this work. Finally, the organization of the following chapters of this text is presented.

### 1.1 MOTIVATION

A mathematical system model consists of a set of mathematical equations that describes how the state of a dynamic system changes in time according to its initial conditions and/or the influence of an external stimulus. Regardless of whether we are talking about an airplane flying in the sky, a robot in an industrial plant, or even the stock market variations, it is of great practical importance to know how these systems behave. This knowledge grants us the ability to not only have some insights on how their behavior will evolve with time but, more importantly, it gives us the possibility of acting on such systems, in order to enhance its performance, making them to operate according to our purpose.

With this, we can conduct the system state (such as its position, velocity, or temperature, for instance) to assume a specified reference value within a certain amount of time, according to some specified characteristics in terms faster and/or smoother responses. We also might want to guarantee that the system is able to maintain such features even when some unavoidable perturbation exerts influence over it, as a sudden strong gust of wind blowing over the wings of a plane during its flight, for example. All these mentioned objectives can be achieved by means of the design of an automatic controller for the considered system, based on its mathematical model, that will control its behavior

accordingly to the desired specification.

However, in practice, the parameters that compose a system model are not precisely known, *i.e.*, the mathematical model presents some amount of uncertainty on the actual values of the parameters associated to the system dynamics. For example, the vertical displacement of a vehicle while driving exhibits a different behavior depending on the total mass that is being carried. This means that the suspension has different dynamics depending whether we have just one person in the vehicle, or if it is the case of a whole family on a vacation trip, and therefore, the system model is also different for each one of these situations – or any other between these extreme cases.

These practical challenges steamed the development of the robust control theory. By means of the design of a robust controller one can guarantee acceptable performance, even when the considered system model is subject to uncertain parameters. This field of study attracted a great amount of attention over the past decades, and it is still being investigated until today through multiple perspectives. Besides robustness to model uncertainty, robust control is also applied to establish robustness over other practical conditions that some dynamic systems are subject to experience, such as power failures, loss of data in communication channels, and digital attacks – which is a matter that gained a great deal of relevance in the recent years, on the scope of cyber-security systems.

Particularly related to disturbance rejection, the robust control theory evolved around the so-called  $\mathcal{H}_\infty$  control theory. The design of  $\mathcal{H}_\infty$  robust controllers is based on a frequency domain approach, and it is concerned with rejecting the effect of disturbance input signals over the system output. In short, the idea is to identify how each particular frequency signal is amplified from the input to the output, and then try to minimize the worst-case, *i.e.*, the frequency in the spectrum for which occurs the highest gain amplification of the input to the output. In that way, if the  $\mathcal{H}_\infty$  robust controller is able to minimize the worst case, then the effect of every other possible frequency of disturbance is consequently attenuated.

By employing robust control techniques, we are also able to enhance the system performance regarding its transient response. When a system model is given in terms of a set of matrices, we might associate its corresponding eigenvalues configuration to the system transient shape. Around this concept, the theory of  $\mathcal{D}$ -stability evolved with the objective of strategically adjusting the system's eigenvalues (or poles, as sometimes referred to in the literature) configuration, in order to modify its time response, usually for making it faster and with reduced oscillations.

In addition, there are some particular occasions where the parameters associated to the system model varies over time. This is the case of a rocket during its flight: the mass is a parameter that varies along the take-off, as the fuel used for its propulsion is being

consumed. Clearly, the actual value of the mass of the rocket will dictate its aerodynamic characteristics. To address such kind of problem, we can employ robust control strategies, assuming that the time-varying parameter is an uncertainty in the system model.

However, particularly when the time-varying parameter is being measured along with the system operation, better performance results can be achieved. In such cases, we can employ the design of a controller that adapts its configuration according to the instant value of the time-varying parameter: the so-called gain-scheduled controller. The idea of “scheduled” controller gains comes from its early applications, where the range of variation of the time-varying parameter is divided into small sections, for which an individual “static” controller is designed. Then, the controller gains are selected accordingly to the actual values of the parameters and the system corresponding point of operation.

Over the past decades, gain-scheduling control techniques evolved, and its study has gained a great amount of attention in the control research community. In fact, one can find results on gain-scheduling for addressing all the above-mentioned problems and several others more. However, some controversy exists particularly associated to the application of the  $\mathcal{D}$ -stability concepts on the gain-scheduling framework. The main reason is that  $\mathcal{D}$ -stability is formally defined for time-invariant systems, as it is based on the idea of eigenvalue assignment. Since we cannot properly relate to eigenvalues when addressing time-varying matrices, a great care must be taken when transient performance improvement through  $\mathcal{D}$ -stabilization is a control objective in a gain-scheduling design. Nevertheless, we have seen a quite few works dealing with  $\mathcal{D}$ -stability in the context of time-varying systems, showing that there is some room for exploring this subject when properly approached.

On top of all that, it is imperative to observe that a control system is almost always useless if not able to be implemented in practice. One of the main cases in which this can happen is when we do not dispose of the complete set of measurements of the system state for composing a feedback loop. In such situations, in addition to the controller one might need to design a state observer in order to obtain an estimation on the missing state information. It was over this practical issue that the static output feedback arose in control theory. This technique – differently from the state feedback – considers utilizing only the available state information to form the feedback loop, representing a more direct approach to the problem.

A very popular strategy in the literature for addressing this practical issue is the dynamic output-feedback (DOF) control, which is based on the design of a controller that presents its own dynamic behavior, consisting of a separate system itself. In this kind of control system, the inputs are the measurements of the available state variables of the plant to be controlled. According to this information, the DOF controller produces a

control command as output signal.

With a simpler implementation setup, we also have the SOF control. In contrast to the dynamic controller obtained through the DOF approach, the SOF control is based on the design of a single static feedback gain that will produce the desired control signal using only a subset of the plant state variables. Although it represents an elegant and simpler approach, the SOF is for long known as one of the most challenging problems in control theory. The reasons can be summarized in two: i) the mathematical manipulation of the SOF control problem is intrinsically way more involved and difficulty to handle; ii) there is no closed solution for the problem yet until today, even for the simplest case where no uncertainties are considered in the system model, in contrast to the state-feedback case. Additionally, it is worth noting that by performing some system model augmentation, a DOF controller synthesis can be reduced to an SOF problem, which emphasizes the relevance of the SOF strategy in control theory.

At last, we must emphasize that regardless of whether we are dealing with uncertain or time-varying systems, or if we are interested in solving state or output feedback control problems, the use of the LMI framework contributed for a strong development in control theory research. One of the main features that make LMI an interesting tool for addressing control problems is that it makes possible to easily consider multiple design requirements in a single formulation. The idea behind LMI representation is that we can reduce a control problem to a convex optimization problem. In this context, after the development of efficient computational tools, the interest in describing a control problem in terms of the solution of a set of LMI grew strongly, and until today, we continue to see quite important results and contributions on control theory that are based on the LMI framework.

It is motivated by the presented scope that the main subject addressed in this work is defined: the proposition of new LMI-based synthesis conditions for SOF design. The idea is to bring new contributions in terms of new alternatives for the SOF control design, motivated by the relevance of the referred topic in the control research community, and by the fact that it still an open problem in the literature. In the next chapters, the problems of pole placement constraints and  $\mathcal{H}_2 / \mathcal{H}_\infty$  norm optimization are investigated considering the SOF background. Continuous- and discrete-time linear systems are considered for study, as well as uncertain linear time-invariant (LTI) and linear parameter-varying (LPV) cases. The goal is to embark relevant control requirements under a single design, investigating the role of  $\mathcal{D}$ -stability concepts in SOF designs for uncertain LTI systems, and also its extension to LPV systems. By means of a broader and more technical background on the subjects of interest for the development of this work, we intend to clearly point out how the proposed results are inserted among others already available in the literature.

## 1.2 LITERATURE REVIEW

As briefly introduced in the previous section, the results proposed in the present work concern the stabilization of linear systems by means of the design of SOF controllers. In that sense, is rather important to emphasize the role of the output feedback in control problems.

The state-feedback (SF) control is a very common and widely applied technique. It consists in the design of a controller that produces a control signal based on complete system state measurement. Undeniably, SF control can yield an efficient solution to a myriad of problems, under a vast universe of design requirements and constraints, with a view to stability and good transient performance. However, despite the technical guarantees, in the case of incomplete state information, the direct implementation of standard state feedback would be hindered in practice. The output-feedback control emerges from this practical issue, enabling control implementation using only the available state information.

As mentioned before, the output feedback can be addressed from the DOF or the SOF approaches. In the former, the controller consists of a whole dynamic system itself, and the problem is based on designing a set of state-space matrices that will form the dynamic feedback loop, which implies in system order augmentation. The latter is formulated in a more straightforward strategy, where the feedback loop is formed by a static feedback gain matrix, yielding a simpler control implementation (DONG; YANG, 2008; SADABADI; KARIMI, 2015).

We can find, indeed, relevant contributions on DOF control on many different scopes, as finite-time stabilization (AMATO; ARIOLA; COSENTINO, 2006), switched linear systems (GEROMEL; COLANERI; BOLZERN, 2008; DEAECTO; GEROMEL; DAAFOUZ, 2011; EGIDIO; DEAECTO, 2021), model predictive control (DING, 2010; DING; HUANG; XU, 2011), and event-triggered control (SOUZA *et al.*, 2021b; LI *et al.*, 2021), for citing a few.

On its turn, the SOF control is still considered as a major open problem in the control theory literature (TROFINO; KUCERA, 1993; SADABADI; PEAUCELLE, 2016). No closed solution is available, even in the case where the plant model is assumed to be known. In fact, the SOF stabilization is for long known as an NP-hard problem (BLONDEL; TSITSIKLIS, 1997), which characterizes its intrinsic difficult mathematical formulation (SOF control is a non-convex problem even in the stabilization of completely known systems (CRUSIUS; TROFINO, 1999)). Nevertheless, such challenging nature motivated the development of studies on this subject over the past decades, addressing several control problems.

Due to these facts, most of the available contributions on SOF control are based on severe restrictions over the problem variables or even on the system matrices. It is not rare to find sufficient design conditions in the literature that were obtained through the imposition of restrictions on the system output matrix format (GEROMEL; PERES; SOUZA, 1996; DONG; YANG, 2013), for instance. Otherwise, the SOF control must be tackled as a non-convex bilinear matrix inequality (BMI) problem by means of the use of specialized solvers and algorithms that severely depends on the initialization step, and yet may often fail to provide a solution (SADABADI; PEAUCELLE, 2016).

On the other hand, the SOF control stills to steam great interest in the research community, and several new strategies have been proposed recently, specially based on Lyapunov stability theory, modeled as convex problem stated in terms of LMI. In this context, SOF control problem have been investigated under many different design requirements and frameworks, as in works based on the cone complementarity algorithm (GHAOUI; OUSTRY; AITRAMI, 1997), iterative LMI-base (CAO; LAM; SUN, 1998), linear matrix inequality and equality constraints (CRUSIUS; TROFINO, 1999; TROFINO; KUCERA, 1993), polytopic uncertain systems (GEROMEL; KOROGUI; BERNUSSOU, 2007; DONG; YANG, 2013; AGULHARI; OLIVEIRA; PERES, 2010b), regarding norm-bounded uncertainties (QIU; FENG; GAO, 2011; GRITLI; ZEMOUCHE; BELGHITH, 2021), and  $\mathcal{H}_2$  norm optimization (AL-JIBOORY; ZHU, 2018; SPAGOLLA *et al.*, 2021), for citing a few.

There are, as briefly mentioned, several available approaches for tackling the SOF control problem. In this work, we are particularly interested in the two-stage method (PEAUCELLE; ARZELIER, 2001; MEHDI; BOUKAS; BACHELIER, 2004), which has been showing great potential in addressing SOF synthesis problems from a convex LMI-based approach. The idea lies in a preliminary design in which a state-feedback gain matrix is computed. Then, the obtained SF controller is used in the second stage, in the search for the desired SOF controller.

Several interesting contributions regarding two-stage SOF design have been published so far, as for time-delay systems (HAO; DUAN, 2015), polytopic systems (AGULHARI; OLIVEIRA; PERES, 2010b; SERENI *et al.*, 2018; SERENI; ASSUNÇÃO; TEIXEIRA, 2020), distributed SOF control systems (CHEN; XU; WANG, 2021), an heuristic two-stage approach (HAO *et al.*, 2021), and many others. This crescent interest on the subject motivates our choice for addressing the SOF control problem from the two-stage method.

When further design requirements rather than stability are on demand, new synthesis constraints need to be considered in the controller design. Here, we give a special attention to the robust  $\mathcal{D}$ -stabilization, which refers to a controller design for clustering the eigenvalues of an uncertain system in a specific region of the complex plane defined

in terms of LMI (CHILALI; GAHINET; APKARIAN, 1999). This technique enables the enforcement of a variety of performance specifications such as bounds on decay rate, damping ratio and undamped natural frequency. Using such tool, the designer can impress a more specific time response besides asymptotic stability for a dynamic system (SANTOS; PELLANDA; SIMÕES, 2018; CHILALI; GAHINET, 1996).

Indeed, the  $\mathcal{D}$ -stability has received a great deal of attention in the last decades, having been addressed from different frameworks, such as the non-smooth optimization and through LMI constraints. Interesting results on the former can be seen in Santos, Pellanda and Simões (2018), Yaesh and Shaked (2011), and Burke, Lewis and Overton (2003), for example.

In the present work, we are especially interested in LMI-based strategies. Such interest stems from the fact that LMI formulations enables an easy grouping of design criteria, *e.g.* stability, dynamic performance, and input and/or output bounds, and also that LMI-based problems can be efficiently solved with semidefinite programming tools (AGULHARI; OLIVEIRA; PERES, 2010b).

In fact, one can find results for  $\mathcal{D}$ -stability based on LMI formulation in analysis problems (EBIHARA; MAEDA; HAGIWARA, 2005; PEAUCELLE *et al.*, 2000), for SF controller synthesis (YANG; GANI; HENRION, 2007; YANG; ROTONDO; PUIG, 2019), state derivative feedback case (BETETO *et al.*, 2018), and also in the output feedback framework (ZHANG; DUAN, 2017; SAHOO *et al.*, 2019; BEHROUZ; MOHAMMADZAMAN; MOHAMMADI, 2021), for mentioning a few.

The allocation region can be specified in different manners. In special, the definition of a circular  $\mathcal{D}$ -region has demonstrated interesting results for pole placement of uncertain LTI systems, as shown in reports on state feedback (LEITE; MONTAGNER; PERES, 2002) and state derivative feedback (BETETO *et al.*, 2018). Particularly in the SOF case, in Sereni, Assunção and Teixeira (2019) the authors bring an SOF controller synthesis based on the two-stage method.

One recurrent issue in two-step SOF design strategies is that the first stage does not consider complete information about the design requirements specified in the second stage. Since the two-stage method – as any other numerically tractable SOF strategy – consists of sufficient conditions (SADABADI; PEAUCELLE, 2016), one might observe that the solution obtained in the second stage might be different depending on the SF gain used as input information. In fact, the second stage may not even be feasible for a particular choice of first-stage gain matrix. Bearing this in mind, the selection of an appropriate strategy for the SF stage is of great relevance in the two-stage method.

As seen, many interesting contributions regarding SOF control for LTI systems have

been proposed in the past decades, but they are not limited to this class of linear systems. In several practical situations, the system parameters are not constant and do change with time. This is the case of the LPV systems. LPV systems consist of an important class of linear dynamic systems in which the state-space matrices are fixed functions of a vector of time-varying parameters,  $\theta(t)$  (GAHINET; APKARIAN, 1994; RUGH; SHAMMA, 2000). The relevance of the LPV framework stems from the fact that it can be used to model linear time-varying (LTV) systems or represent linear models of nonlinear plants, then enabling the employment of powerful linear control techniques to address analysis and stabilization problems of nonlinear systems (APKARIAN; GAHINET; BECKER, 1995).

For decades, the control of LPV systems has received a great deal of attention, and different approaches have been proposed for dealing with such systems. The main strategies published so far differ depending on the available information about the time-varying parameters. If  $\theta(t)$  is treated as a parametric uncertainty, then robust control techniques can be applied for stabilizing the LPV plant (GAHINET; APKARIAN, 1994). However, if those parameters are known at all instants of time  $t > 0$  (by online measurement or estimation), then such information can be used to develop control strategies that might be able to yield higher performance (RUGH; SHAMMA, 2000), namely, LPV control or, equivalently, gain-scheduling (GS) control.

The GS is a control design strategy that is being intensively studied in the past decades (HOFFMANN; WERNER, 2014; WEI *et al.*, 2014). Further from finding a special use for dealing with nonlinear systems, the GS strategy has demonstrated to be capable of addressing a handful of control objectives when dealing with LPV systems (APKARIAN; GAHINET, 1995; CAIGNY *et al.*, 2012). In practical terms, GS control proved its efficacy in coping with systems that experience rapid changes in operating conditions. Indeed, applications on guided missiles, airplanes autopilots, robots, and others can be found in the literature (AL-JIBOORY; ZHU, 2018).

The first GS strategies were based on a problematic “divide and conquer” method, in which the space of the time-varying parameters were divided into small areas, and local LTI controllers were designed and switched according to a gain-scheduling rule on the values of  $\theta(t)$  (ÅSTRÖM; WITTENMARK, 2013; STILWELL; RUGH, 1999). The problems of this approach arise from the fact that no guarantees over the global stability or performance are provided. Also, a fine parameter gridding is necessary for achieving good performance, which implies on a high complexity control structure (RUGH; SHAMMA, 2000).

Such drawbacks were surpassed with the emergence of more modern techniques: the linear fractional transformation (LTF) and Lyapunov-based approaches for GS control. In these strategies, the controller is designed in the same parameter-dependent fashion



as the LPV plant, and then, a “smooth” scheduled controller is derived. In the LFT framework, the state-space matrices are linear fractional functions of  $\theta(t)$ . Following the pioneer work Packard *et al.* (1991), many papers have been published in the literature on LFT-based GS control (YUAN, 2017; BAN; WU, 2016; ZIN *et al.*, 2008; WU; DONG, 2006; APKARIAN; PELLANDA; TUAN, 2000). However, LFT has the drawback of considering complex variation values of  $\theta(t)$  and to be based on a restrictive block diagonal scaling, which introduces conservatism (APKARIAN; GAHINET; BECKER, 1995; WU; DONG, 2006).

In contrast, the polytopic approach considers the case of an affine dependence of the state-space matrices on  $\theta(t)$ , with  $\theta(t)$  belonging to a polytope (APKARIAN; GAHINET; BECKER, 1995). The stability and performance certificates are then obtained by employing Lyapunov’s direct method, which consists in finding an appropriate scalar function associated to the system dynamics. Works based on the polytopic approach evolved regarding the design of common quadratic Lyapunov functions (CQLF) and parameter-dependent Lyapunov functions (PDFL) (CAIGNY *et al.*, 2010). Basically, CQLF guarantees the so-called quadratic stability by means of a fixed Lyapunov matrix  $P$ , whereas PDFL incorporates the time-varying parameter in the Lyapunov function, implying on the search for a parameter-dependent matrix  $P(\theta(t))$ .

Each strategy has its own advantages. In fact, considering a fixed matrix  $P$  leads to a considerably more simple mathematical and computational problem, since no other information besides the variation range of  $\theta(t)$  needs to be known *a priori* for the controller design, in contrast to PDFL approach which also needs the information of maximum and minimum rates of  $\dot{\theta}(t)$ , particularly in the continuous-time case. However, conservatism reduction can be obtained by considering a time-varying parameter-dependent matrix  $P(\theta(t))$ , since it enables the search for multiple Lyapunov matrices that can guarantee stability and performance for the entire range of parameter variations. Undeniably, research on LPV systems is still a hot-topic in control literature, with quite innovative contributions, as for descriptor systems (CHEN; HAN; HOU, 2021; RODRIGUES *et al.*, 2014), on event-triggered control (SOUZA *et al.*, 2021a, 2021b), and also cyber-physical LPV systems (PESSIM *et al.*, 2021), for instance.

In the present work, we consider utilizing GS control via Lyapunov-based approach, which has received increasing interest over the past two decades. Particularly in the continuous-time LPV framework, one can find interesting and relevant results regarding SOF design. For instance, Al-Jiboory and Zhu Al-Jiboory and Zhu (2018) proposed conditions for the GS-SOF controller with guaranteed  $\mathcal{H}_2$  performance; and Sereni, Assunção and Teixeira (2020) developed LMI conditions for GS-SOF controller design with decay rate bounding.

We are also interested in investigating the discrete-time case of GS control, as its relevance continues to grow as digital technology becomes more present in the industry and other areas of application of control theory. For presenting some of the available results on the subject, we can mention contributions on LPV control for discrete-time state-feedback controller design considering  $\mathcal{H}_\infty$  performance in a CQLF approach (MONTAGNER *et al.*, 2005), and on  $\mathcal{H}_2/\mathcal{H}_\infty$  problem addressed via piecewise Lyapunov functions (AMATO; MATTEI; PIRONTI, 2005). Extensions to LPV systems with multiplicative noises were also investigated, where GS synthesis conditions can be found in both CQLF and PDLF frameworks (KU; CHEN, 2015). Recently, a more general proposal of LMI conditions for the synthesis of GS  $\mathcal{H}_\infty$  controller emerged (PANDEY; OLIVEIRA, 2019), along with a new approach based on the case where the time-varying parameters can be written as solutions of a linear difference equation (PALMA; MORAIS; OLIVEIRA, 2020).

A particular approach which has been intensively investigated is the use of homogeneous polynomial parameter-dependent Lyapunov functions (HPPDLF). Analysis and control synthesis conditions were presented for state-feedback control, using HPPDLF and multi-affine Lyapunov functions (OLIVEIRA; PERES, 2009). Gain-scheduling problems have also been investigated in the output-feedback case. Indeed, works on gain-scheduled static output feedback (GS-SOF) with  $\mathcal{H}_\infty$  performance problem can also be found in the literature using the HPPDLF approach (SADEGHZADEH, 2017; ROSA; MORAIS; OLIVEIRA, 2017), in addition to extensions for dealing with time-delayed LPV systems (ROSA *et al.*, 2018), and to the use of path-dependent Lyapunov functions (RODRIGUES; CAMINO; PERES, 2018). The problem of multi-objective  $\mathcal{H}_2/\mathcal{H}_\infty$  approach via PDLF was also studied for both state- and static output-feedback cases (CAIGNY *et al.*, 2010), and also on a DOF framework (CAIGNY *et al.*, 2012). The GS-DOF problem is, indeed, a topic of great interest (JUNIOR; GALVÃO; ASSUNÇÃO, 2017). Papers on the robust case considering  $l_2$ -gain performance (SADEGHZADEH, 2018) and reduced-order mixed performance objective (ROSA; MORAIS; OLIVEIRA, 2018) applying the HPPDLF approach can be found in the literature.

Further from guaranteeing closed-loop stability, performance improvement is also a desired control requirement in LPV control. As previously discussed, among other strategies, this control objective may be achieved by enforcing the closed-loop eigenvalue placement in a particular region of the complex plane, by means of the use of  $\mathcal{D}$ -stability constraints, although  $\mathcal{D}$ -stabilization is well defined for LTI systems, since it is a concept associated to closed-loop eigenvalue (or pole) placement. Nevertheless, extensions for LPV systems have been developed in the literature, based on the idea that for fixed (or “frozen”) values of the scheduling parameters, the LPV model assumes a specific LTI configuration. Particularly for polytopic models, pole placement constraints over the polytope vertices have been shown to be able to induce improved closed-loop transient performance of LPV

systems (KAJIWARA; APKARIAN; GAHINET, 1999; ROTONDO; NEJJARI; PUIG, 2014; BEHROUZ; MOHAMMADZAMAN; MOHAMMADI, 2021).

Aside from the classic control problems that have been discussed so far, the SOF control might be an interesting solution to some very important problems that arise from practical issues that several systems experience. For instance, in some situations, automatic control systems are composed of sensors and actuators with non-negligible dynamics as, for instance, in embedded controllers of modern light-weight aircraft (AL-JIBOORY *et al.*, 2017). Due to the intrinsic aeroelastic nature of such systems, we observe a strong interaction between the aircraft structure and its control and actuator systems. Such interconnection is referred in the specialized literature as aeroservoelasticity (YANG; WANG; XU, 2018). As a consequence, for properly representing the system in order to achieve desired aeroelastic characteristics, these additional dynamics must be considered in system modeling (TANG *et al.*, 2021; WANG; WYNN; PALACIOS, 2016).

In face of such practical issue, one may note that the actual plant state variables are not available for composing the feedback loop, but only the sensors outputs, hence hindering the implementation of standard state-feedback control techniques. Therefore, the employment of additional sensors, which may also present non-negligible dynamics, might be demanded. Moreover, ignoring such parasitic dynamics may incur in performance loss and, in the worst case, compromise the closed-loop stability, as been long known (LEITMANN; RYAN; STEINBERG, 1986; YOUNG; KOKOTOVIC, 1982). This fact motivated the development of studies for robust control designs that may address the problem of actuators and sensors dynamics. We may cite, for instance, contributions regarding observed-based design (KHALIL, 2005; ANFINSEN; AAMO, 2018), sliding mode control (SMC) (BANZA; TAN; MAREELS, 2020), and output feedback control (WANG; WU; LI, 2014). In this work, we particularly discuss the output-feedback control and how it emerges as a convenient approach, which can be employed by considering an augmented system representation encompassing the plant, sensors, and actuators dynamics. Then, only the sensor output signals are used in the feedback loop, as presented in (SERENI *et al.*, 2020).

However, the problem gets even more involved when the sensor and actuator dynamics involve time-delay. Due to its relevance, the effects of time delay have been investigated in several areas of engineering, such as power (WU; NI; HEYDT, 2002), communication (GUNNARSSON; GUSTAFSSON; BLOM, 2001), and control systems (SHIN; CUI, 1995). In particular, the research on network communication delay has been flagged as a relevant issue for advanced aircraft data exchange systems (WANG; PENG; YAN, 2018). Even more complicated problems arise in the case of uncertain delays. As a matter of fact, the huge amount of data flow in aircraft network buses implies in the uncertain behavior of

such systems. Furthermore, the relationship between time delay and actuator dynamics have also raised interest to the development of research on the stability margin in fighter aircraft (KIM *et al.*, 2021), for instance.

The practical relevance of the effects of time delay in dynamic systems motivated the research on modeling and control design strategies that are able to guarantee robustness over the above mentioned issues (FENG, 2016; BENAMMAR *et al.*, 2017). Many of the available methods are related to predictor-like techniques (ALBERTOS; GARCÍA, 2009; TORRICO *et al.*, 2013; RODRIGUES *et al.*, 2021), which are intended to compensate the delay effect through the transformation of the delayed system into a delay-free model through finite integrals over past control input values. Predictor-based control results can be found in the linear time-invariant scenario with (NICULESCU; LOZANO, 2001) and without considering model uncertainty (FLIESS; MARQUEZ; MOUNIER, 2001). Methods for nonlinear systems can also be found, such as input delay and additive disturbance compensation (DENG; YAO; MA, 2018), and dealing with arbitrarily large time delay (KRSTIC, 2008).

Even though predictor-like techniques are consolidated for addressing input delay (*i.e.*, delay affecting the control input), they struggle to handle systems affected by state delay, as the problem gets considerably more complicated to be modeled in this particular framework. For instance, recent works on this subject (DENG *et al.*, 2021) managed to consider dynamic actuators via backstepping control with input delay but does not include state delay nor sensor dynamics in the control design. Also, the dependence on integral terms might be sensitive to parametric uncertainty and delay mismatches (RICHARD, 2003).

The sliding mode control (KARIMI, 2012; PALRAJ; MATHIYALAGAN; SHI, 2021; SUN; ZHANG, 2018) is also an example of technique for dealing with time delay in control systems, being particularly known for its robustness characteristics. However, as a drawback, the presence of time delay has a severe destabilizing effect in conventional SMC systems. For a more complete background, we refer the reader to the survey paper (RICHARD, 2003).

A simpler yet interesting approach is based on the development of an approximation model of the delayed dynamics. In such method, the infinite-dimension delayed system is treated as a finite-dimensional one by means of the truncation of an infinite series given in terms of a rational polynomial (RICHARD, 2003). The main downside of this approach is that in some cases the rational approximation must be of high order to obtain a good representation. However, finite-dimension approximation has led to important contributions, specifically for linear systems (WU; NI; HEYDT, 2002; SUN, 2009; SONI; DUTT; DAS, 2021; SHAH; PATEL, 2019).

### 1.3 MAIN CONTRIBUTIONS

After presenting and discussing the past developments and current state-of-the-art regarding the SOF control and its extensions to areas of interest to this work, we highlight the main contributions that are brought to the theme.

Regarding the  $\mathcal{D}$ -stabilization of LTI systems through SOF control, a novel LMI-based strategy for robust pole placement in SOF control design, considering the  $\mathcal{D}$ -region for pole placement as a circle in the complex left-half plane is proposed. The SOF controller synthesis is based on the two-stage method and described in terms of LMI. The proposed LMI conditions for the robust SOF controller synthesis is based on the use of parameter-dependent Lyapunov functions. Further contributions are proposed in terms of the combined design of  $\mathcal{D}$ -stabilizing gains in both stages, which might represent a more consistent approach considering the two-stage method. Furthermore, aiming at obtaining less conservative second-stage design LMI conditions, we investigate the use of a first-stage parameter-dependent state-feedback gain as input information (AGULHARI; OLIVEIRA; PERES, 2010a), in contrast to a single robust gain. To the best of our knowledge, a two-stage SOF design method for LTI closed-loop systems pole placement based on a first-stage design considering both parameter-dependent and  $\mathcal{D}$ -stabilization constraints have not yet been proposed in the literature.

On the continuous-time LPV framework, this work proposes new LMI conditions for the design of GS-SOF controllers, under the constraints of incomplete state measurement and specific eigenvalue placement in a circular LMI-region. For that, we consider the polytopic LPV approach to propose new GS controller design methods via SOF, using the two-stage method. By exploiting the polytopic framework, we extend the LTI  $\mathcal{D}$ -stability concept to the LPV model vertices, enabling the induced enforcement of additional performance and control signal requirements, in terms of faster and less oscillatory transient, and controller norm bounding, differently from previous works on the subject (SERENI; ASSUNÇÃO; TEIXEIRA, 2020, 2019; BETETO *et al.*, 2021; ASSUNÇÃO *et al.*, 2019).

Considering the discrete-time case, new contributions regarding gain-scheduled controller synthesis for LPV systems with incomplete state information via static output feedback are also proposed in this work. In the considered strategy, the synthesis conditions are provided in terms of a finite set of LMI. Differently from most of the works on the subject at hand, our proposed control design strategy is based on a polytopic PDLF approach. With such consideration, we are able to employ a multiple matrix search on the Lyapunov matrix that does not require *a priori* information other than the range where the time-varying parameters can vary. Such feature grants our proposal less conservative

conditions when compared to CQLF, and a more simpler and straightforward control design, since it is not always possible in practice to obtain a range for the derivatives of the scheduling parameters, let alone obtain on-line information of  $\dot{\theta}$ , which is required in other available approaches in the literature (SCHERER, 1996; WU *et al.*, 1996; OLIVEIRA; PERES, 2009). The SOF controller design is based on a two-stage method. Additionally, we explore the flexibility of LMI framework for including a performance objective to improve the closed-loop transient settling time, by means of a minimum decay rate enforcement. To the best of our knowledge, such control design in a PDLF approach for discrete-time have not been extensively investigated yet, when compared to  $\mathcal{H}_\infty$  or  $\mathcal{H}_2$  problems, which motivates our studies. Nevertheless, an extension to address the  $\mathcal{H}_\infty$  optimization problem and also enforce robustness in terms of disturbance rejection is proposed in the present work.

At last, studying the problem of uncertain LTI systems whose state information and control input signals are obtained and applied by means of sensors and actuators with non-negligible dynamics, a control strategy based on robust SOF design is proposed. We assume that the communication channels between sensors, actuators and controller are susceptible to a delay in time, which is also a novelty, since the literature is usually concerned with the effects of either input or state delay, and not the joint effect of both types of delay. Furthermore, investigations on the synthesis of controllers for systems with time delays and also non-negligible dynamics in sensors and actuators are relatively scarce. In this work, such practical issues are handled by defining an augmented system, where the time-delay effect is modeled using the Padé Approximation (NIU *et al.*, 2013; ZHAO *et al.*, 2021). The resulting overall system encompasses the plant, sensors, actuators, and time-delay dynamic states. By assuming that only the sensor outputs are available for feedback, we employ a two-stage-based SOF design method defined in terms of a homogeneous-polynomial Lyapunov function (HPLF) (AGULHARI; OLIVEIRA; PERES, 2010a; PAULINO; BARA, 2021). Employing the SOF control for addressing time-delayed systems with actuators and sensors dynamics through an augmented system is a simple and direct, yet innovative approach that, to the best of the authors' knowledge, has not been considered so far. The new proposed controller synthesis strategy is formulated in the LMI framework for including the specification of a minimal performance index in terms of a lower bound on the closed-loop system decay rate, with the purpose of achieving enhanced transient performance. Robustness in terms of disturbance rejection is also taken into account by means of the closed-loop  $\mathcal{H}_2$  norm minimization.

The proposed contributions that are presented in this work culminated in the publication/submission of the following papers:

- Sereni, B., Assunção, E., and Teixeira, M. C. M. (2022). Stabilization and Disturbance Rejection with Decay Rate Bounding in Discrete-Time LPV Systems via  $\mathcal{H}_\infty$  Gain-Scheduling Static Output Feedback Control. *International Journal of Robust and Nonlinear Control*, 32(14), 7920-7945.;
- Sereni, B., Beteto, M. A. L., Assunção, E., and Teixeira, M. C. M. (2021). Pole Placement LMI Constraints for Stability and Transient Performance of LPV Systems with Incomplete State Measurement. *Journal of the Franklin Institute*, 359(2), 837-858;
- Sereni, B., Galvão, R. K. H, Assunção, E., and Teixeira, M. C. M. (2020). Synthesis of Robust Control Systems with Dynamic Actuators and Sensors Using a Static Output Feedback Method. In *Congresso Brasileiro de Automática-CBA* (Vol. 2, No. 1).
- Sereni, B., Assunção, E., and Teixeira, M. C. M. (2019). Robust D-Stabilisation of Uncertain Systems via Static Output Feedback. In *Proceedings of the XIV Brazilian Symposium on Intelligent Automation*, Ouro Preto, MG, Brazil.
- Sereni, B., Galvão, R. K. H., Assunção, E., and Teixeira, M. C. M. An Output-Feedback Design Approach for Robust Stabilization of Linear Systems with Uncertain Time-Delayed Dynamics in Sensors and Actuators. *IEEE Access* (Under review)

It is worth-noting that the new results proposed in this work are given as a continuation of the research project that has been carried out since the master's course, which established the following previous contributions:

- Sereni, B., Assunção, E., and Teixeira, M. C. M. (2019). New Gain-Scheduled Static Output Feedback Controller Design Strategy for Stability and Transient Performance of LPV Systems. *IET Control Theory & Applications*, 14(5), 717-725.
- Sereni, B., Manesco, R. M., Assunção, E., and Teixeira, M. C. M. (2018). Relaxed LMI Conditions for the Design of Robust Static Output Feedback Controllers. *IFAC-PapersOnLine, Proceedings of the 9th IFAC Symposium on Robust Control Design (ROCOND'18)*, 51(25), 428-433.

## 1.4 OUTLINE

The continuation of this text is organized as follows:

**Chapter 2 - Fundamental Concepts and Definitions:** devoted to present and define some basic yet important control theory concepts that form the foundation for the development of the contributions presented in the following chapters. Mathematical tools relevant to the proof of the proposed theorems are also formally enunciated.

**Chapter 3 - Static Output Feedback Control with Pole Placement Constraints:** presents new contribution regarding the design of robust SOF controllers for the  $\mathcal{D}$ -stabilization of continuous-time uncertain LTI systems. Results for the extension continuous-time LPV systems by means of gain-scheduled SOF controller design under pole placement constraints are also proposed.

**Chapter 4 - Discrete-Time GS-SOF Control Design:** discuss and present contributions in terms of new LMI-based strategy for discrete-time GS-SOF controller design through the two-stage method under constraints for ensuring lower bound decay rate and  $\mathcal{H}_\infty$  guaranteed cost minimization.

**Chapter 5 - Non-Negligible Sensors and Actuators Dynamics and Time Delay:** proposes an application of the two-stage robust SOF controller design for guaranteeing the robust stabilization of uncertain LTI that are subject to sensors and/or actuators that present non-negligible dynamics, as well as the presence of time delay in the information transport between plant, controller and sensors. An extension for coping with disturbance rejection by means of the minimization of the  $\mathcal{H}_2$  guaranteed cost is also proposed.

**Chapter 6 - Conclusion:** presents the final conclusions of the work and future perspectives for the conducted research.



## 2 FUNDAMENTAL CONCEPTS AND DEFINITIONS

This chapter presents some important concepts and definitions that form the technical basis of the results that are presented in the next chapters.

We begin by defining basic stability and performance LMI conditions for guaranteeing stability and performance in polytopic LTI and LPV systems. The chapter ends with some fundamental mathematical results that are going to be necessary in the proof of the proposed theorems.

### 2.1 STABILITY AND TRANSIENT PERFORMANCE IN LINEAR SYSTEMS VIA LMI

The results presented in this work are related to the stabilization and performance improvement of linear systems by means of LMI-based controller designs. In that sense, in this section we properly define the polytopic model adopted for representing LTI and LPV used in the present text. Then, the concepts of pole placement design and  $\mathcal{H}_\infty$  guaranteed cost minimization are given and fundamental LMI constraints for ensuring such design requirements are defined. In the sequence, we give some details regarding the design of SOF controllers by means of the two-stage method, and also on the design and implementation of gain-scheduled controllers, as considered in the results proposed in this work.

#### 2.1.1 LTI AND LPV SYSTEMS: A POLYTOPIC DESCRIPTION

This work studies the stabilization problem of uncertain LTI systems and also LPV systems. There are many approaches that may be employed for describing such systems dynamics in terms of a mathematical model. The strategy adopted in throughout this text is the polytopic model.

Using the polytopic model we are able to represent uncertainties or time-varying parameters in terms of a polytopic domain, that defines a convex set for representing every possible configuration that the system may assume.

In these terms, for what follows the rest of this text, we consider that generic uncertain

LTI systems are represented according to a state-space representation as

$$\begin{aligned}\dot{x}(t) &= A(\alpha)x(t) + B(\alpha)u(t) \\ y(t) &= C(\alpha)x(t) + D(\alpha)u(t),\end{aligned}\tag{2.1}$$

where  $\alpha \in \mathbb{R}^N$  is an uncertain vector whose  $N$  entries are such that belong to the simplex unitary set

$$\Delta_N = \left\{ \alpha \in \mathbb{R}^N : \sum_{i=1}^N \alpha_i = 1; \alpha_i \geq 0; i = 1, \dots, N. \right\}.$$

This allows for describing the set of matrices  $(A, B, C, D)(\alpha)$  as a convex combination of vertex matrices such as

$$(A, B, C, D)(\alpha) = \sum_{i=1}^N \alpha_i (A, B, C, D)_i,$$

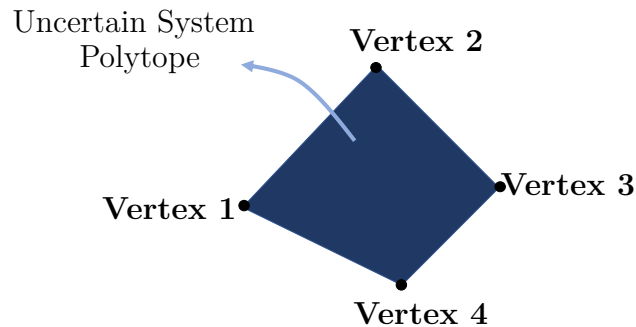
which defines a polytope whose vertices are  $(A, B, C, D)_i$ , for  $i = 1, \dots, N$ .

The system vertices are defined according to the extreme values that the uncertain parameters may assume. For example, consider a mechanical system whose mass and coefficient of friction are uncertain parameters in the system model. Therefore, the vertices of the corresponding polytope are defined by crossing the extreme cases:

- **Vertex 1:** minimum mass and minimum coefficient of friction;
- **Vertex 2:** minimum mass and maximum coefficient of friction;
- **Vertex 3:** maximum mass and minimum coefficient of friction;
- **Vertex 4:** maximum mass and maximum coefficient of friction.

As one might observe, the number of polytope vertices is defined by  $N = 2^{n_p}$ , where  $n_p$  is the number of uncertain parameters affecting the system model. For instance, an LTI system affected by  $n_p = 2$  uncertain parameters can be described as belonging to a polytope with  $N = 2^2 = 4$  vertices (Figure 2.1).

Figure 2.1 - Graphical representation the uncertainty polytope of an LTI system with two uncertain parameters in the model (four vertices).



Source: Own author.

Following an analogous concept, a generic LPV system in this work is described by a state-space representation

$$\begin{aligned}\dot{x}(t) &= A(\alpha(t))x(t) + B(\alpha(t))u(t) \\ y(t) &= C(\alpha(t))x(t) + D(\alpha(t))u(t),\end{aligned}\tag{2.2}$$

where  $\alpha(t) \in \mathbb{R}^N$  is an time-varying vector whose  $N$  entries are such that

$$\bar{\alpha}_N = \left\{ \alpha(t) \in \mathbb{R}^N : \sum_{i=1}^N \alpha_i(t) = 1; \alpha_i(t) \geq 0; i = 1, \dots, N, \forall t \geq 0 \right\}.\tag{2.3}$$

However, as in this work we address LPV system with the gain-scheduling control approach, the time-varying parameters in  $\alpha(t)$  are assumed to be known. Then, the set of matrices  $(A, B, C, D)(\alpha(t))$  are defined as a convex combination of constant vertices as

$$(A, B, C, D)(\alpha(t)) = \sum_{i=1}^N \alpha_i(t)(A, B, C, D)_i,$$

which in turn define a polytope whose vertices are  $(A, B, C, D)_i$ , for  $i = 1, \dots, N$ . At each time instant  $t$ , and corresponding values for  $\alpha(t)$ , the LPV system is exactly represented in the defined polytopic domain. Note that the polytope concept in Figure 2.1 can be equivalently extended to LPV systems.

Regarding the asymptotic stability, as our approach is based on a polytopic domain definition, we consider the employment of Lyapunov's stability criterion, which is based on the existence of a scalar function  $V(x(t))$ , such that  $V(x(t)) > 0$ , and  $\dot{V}(x(t)) < 0$ , for all trajectories  $x(t) \neq 0$  (BOYD *et al.*, 1994).

When considering uncertain LTI systems, a stability certificate can be obtained if we confirm the existence of a symmetric positive definite matrix  $P$ , such that

$$A_i'P + PA_i < 0\tag{2.4}$$

holds for  $i = 1, \dots, N$ .

This approach is referred in the literature as quadratic stabilization, since it is based on a common-quadratic Lyapunov function (CQLF), in terms of a fixed positive definite matrix  $P$ . Despite of being a simple solution, it is well-known that quadratic stability yields very conservative constraints when dealing with uncertain systems (OLIVEIRA; PERES, 2006; GEROMEL; KOROGUI, 2006). In that scope, less conservative conditions can be obtained by considering a formulation based on parameter-dependent Lyapunov functions (PDFL). This approach allows the Lyapunov function to be dependent on the

uncertain parameters. This can be achieved by considering

$$P(\alpha) = \sum_{i=1}^N \alpha_i P_i, \quad \alpha \in \Delta_N.$$

In these terms, an stability certificate for the uncertain system (2.1) can be obtained through the less conservative LMI conditions, based on PDLF, if we confirm the existence of  $N$  symmetric positive definite matrices  $P_i$ , such that

$$A_i' P_i + P_i A_i < 0 \quad (2.5)$$

holds for  $i = 1, \dots, N$ , and

$$A_i' P_j + P_j A_i + A_j' P_i + P_i A_j < 0 \quad (2.6)$$

holds for  $i = 1, \dots, N-1$  and  $j = i+1, \dots, N$ .

Even less conservative conditions can be obtained, by allowing the PDLF to have a homogeneous polynomial dependence on the uncertain parameters of degree  $g > 1$ . For instance, considering  $P(\alpha)$  to be a homogeneous polynomial matrix of degree  $g = 2$  means that

$$P(\alpha) = \alpha_1^2 P_1 + \alpha_1 \alpha_2 P_{12} + \alpha_2^2 P_2,$$

with  $P_1 = P_1'$ ,  $P_{12} = P_{12}'$ , and  $P_2 = P_2'$ , in a polytope with  $N = 2$  vertices.

Despite less conservative conditions might be obtained with progressively higher polynomial degrees, obtaining a finite set of LMI conditions as (2.5) and (2.6) may become a tedious and tricky procedure. For that, specialized computational packages, as the ROLMIP parser (AGULHARI *et al.*, 2019) can be employed for obtaining the desired set of LMI by only specifying the problem variables structure.

**Remark 2.1.** *All the aforementioned strategies are going to be investigated in the course of this work, and its advantages and drawbacks analyzed and emphasized, especially in the continuous-time LTI and discrete-time LPV case. When dealing with continuous-time LPV systems, considering PDLF approaches imply in a more involved mathematical development, and will be subject of future studies.*

### 2.1.2 POLE PLACEMENT CONSTRAINTS

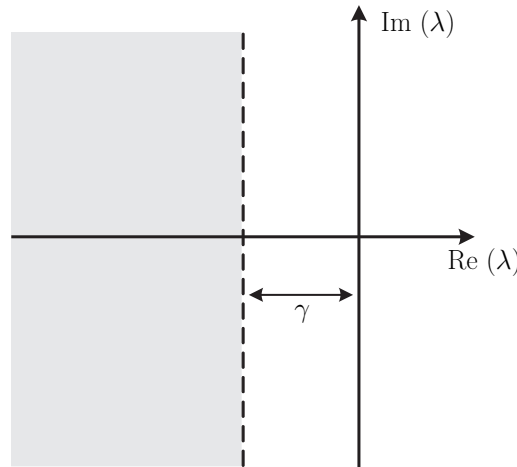
Further from guaranteeing the asymptotic stability, in several practical control problems, it is also necessary to provide improved dynamic performance to the system closed-loop response (CHILALI; GAHINET; APKARIAN, 1999). For instance, the settling time and steady-state signal overshoot are examples of indexes related to the system perfor-

mance, which can be optimized with a proper controller design (SANTOS; PELLANDA; SIMÕES, 2018).

A strategy for enhancing the system dynamic characteristics, based on the specification of desired values for such transient parameters, is to properly enforce a robust closed-loop pole placement in a particular region of the complex left-half plane, namely  $\mathcal{D}$ -stabilization (CHILALI; GAHINET, 1996). These regions, usually referred to as LMI-regions, might assume many different shapes, depending on the convex constraints used to define them.

Stability can be guaranteed by ensuring that all closed-loop system eigenvalues are allocated in the left-half complex plane. However, by imposing that the eigenvalue placement occurs at the left of a vertical line perpendicular to the real axis (Figure 2.2), we might induce a faster transient performance.

Figure 2.2 - Geometric interpretation of the minimum decay rate requirement.



Source: Adapted from Silva *et al.* (2012).

When regarding pole placement constraints, this technique is referred to  $\alpha$ -stability<sup>1</sup>. However, this control design requirement is also known as the enforcement of a minimum decay rate to the closed-loop system. The decay rate is a basic performance index associated with the system transient duration. A formal and mathematical definition is presented in Boyd *et al.* (1994), which states that the decay rate can be defined as the highest scalar,  $\gamma$ , such that

$$\lim_{t \rightarrow \infty} e^{\gamma t} \|x(t)\| = 0 \quad (2.7)$$

holds for all the trajectories of the system state,  $x(t)$ . Analyzing (2.7), we can extract the practical interpretation that the decay rate denotes the highest possible scalar  $\gamma$  such

---

<sup>1</sup>We advise the reader to not associate the pole placement nomenclature “ $\alpha$ -stability”, was established in the control literature, with the uncertainty vector notation  $\alpha$ , adopted throughout this text.

that the convergence of  $\|x(t)\|$  to the origin ( $x(t) = 0$ ) is more rapid than the growth of the exponential,  $e^{\gamma t}$ , as  $t \rightarrow \infty$ . Note that this implies that  $\gamma$  establishes the measurement based on the rapidity of the occurrence of a system transient.

As well-known, the system stability and a lower bound of the decay rate can be ensured if we consider the existence of a quadratic Lyapunov's function,  $V(x(t)) = x(t)'Px(t) > 0$ , for  $x(t) \neq 0$ , such that

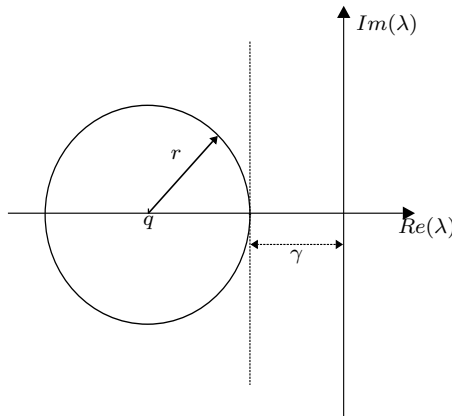
$$\dot{V}(x(t)) \leq -2\gamma V(x(t)) \quad (2.8)$$

holds for all the trajectories of the system state,  $x(t)$ , with  $\gamma > 0$  (BOYD *et al.*, 1994).

Note that even though the decay rate definition given by (2.7) does not impose constraints on the signal of the scalar  $\gamma$ , the system stability corresponds to a positive decay rate. Indeed, according to Lyapunov's stability concept, for  $x(t) \neq 0$ , the function  $V(x(t)) > 0$  must be such that  $\dot{V}(x(t)) < 0$  ensures asymptotic stability (BOYD *et al.*, 1994). Note that if  $\gamma < 0$ , then (2.8) will not hold.

For enabling a more specific transient shaping, we might consider a circle centered in the real axis, as the one in Figure 2.3. By enforcing the eigenvalue placement in a circular region, the designer is able to adjust the distance that the closed-loop eigenvalues are going to be set away from the real and imaginary axis. With such control, it is possible to provide faster transient response, and yet maintaining reasonable control signal amplitudes.

Figure 2.3 - Circular LMI region  $\mathcal{D}(q, r)$  for pole placement.



Source: Adapted from Leite, Montagner and Peres (2002).

Indeed, a system with eigenvalues of high absolute value real parts can present a short transient settling time. However, eigenvalues with high absolute value real parts tend to produce controllers with high gains, which ultimately leads to high amplitude control signals that naturally must be avoided due to practical reasons. At the same time, by enforcing an eigenvalue clustering with reduced imaginary part absolute values enables to impress less oscillatory behavior.

**Remark 2.2.** *The relation between pole placement and performance indexes such as overshoot-percent and settling time are well established for first and second order systems. For higher-order cases, the transient response can be expressed as a sum of first and second-order responses. However, the dependence between pole location and transient shaping is more involved (OGATA et al., 2010). Therefore, by considering an additional restriction to the pole placement of higher-order systems we are only indirectly inducing performance criteria over the distance of the poles from the real and imaginary axis.*

In Lemma 2.1, a classic sufficient condition for ensuring circular eigenvalue assignment is presented. This result is used as a reference for the contributions proposed in Chapter 3.

**Lemma 2.1.** *(HADDAD; BERNSTEIN, 1992) Let  $A(\alpha) \in \mathbb{R}^{n \times n}$  and  $\mathcal{D}(q, r)$  be a circular disk in the complex plane with center  $(-q, 0)$ , radius  $r > 0$  and minimum distance from the imaginary axis  $\gamma > 0$ , with  $q = \gamma + r$ . Then, the eigenvalues of  $A(\alpha)$  are contained in  $\mathcal{D}(q, r)$  if, and only if, there exists a positive definite symmetric matrix  $P \in \mathbb{R}^{n \times n}$  such that*

$$P > 0, \quad (2.9)$$

$$A(\alpha)'P + PA(\alpha) + 2\gamma P + \frac{1}{r}(A(\alpha) + \gamma I)'P(A(\alpha) + \gamma I) < 0, \quad (2.10)$$

for every  $\alpha \in \Lambda_N$ .

Based on this preliminary result, Leite, Montagner and Peres (2002), developed an LMI-based strategy for verifying the eigenvalue configuration of an uncertain LTI system  $\dot{x}(t) = A(\alpha)x(t)$ , considering a circular  $\mathcal{D}$ -region of Figure 2.3. The referred strategy consists in checking if there exists a symmetric positive definite matrix  $P$  such that

$$\begin{bmatrix} A_i'P + PA_i + 2\gamma P & (A_i + \gamma I)'P \\ P(A_i + \gamma I) & -rP \end{bmatrix} < 0 \quad (2.11)$$

holds for  $i = 1, \dots, N$ .

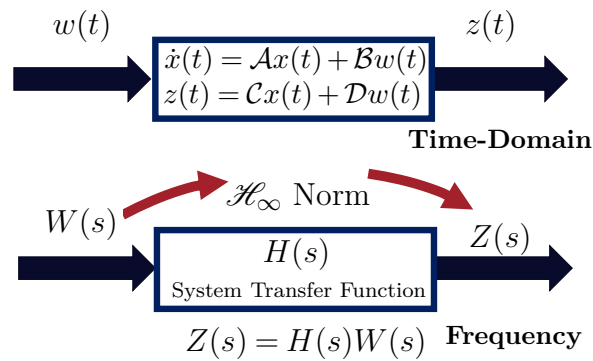
This result consist the basis for the development of the contribution presented in this work regarding the  $\mathcal{D}$ -stabilization via SOF, as detailed in Chapter 3.

### 2.1.3 $\mathcal{H}_\infty$ GUARANTEED COST

Besides transient shaping, another important design requirement in control problems is that the closed-loop system should posses some desired level of disturbance rejection. For instance, in land vehicles, it is important to minimize the impact of an irregular road profile on the dynamics for ensuring better handling and comfortable driving.

Such practical problem might be addressed by means of the so-called  $\mathcal{H}_\infty$  control (CHILALI; GAHINET, 1996). This control strategy is based on identifying the system's characteristics in the frequency domain. In particular, the goal is to minimize the system  $\mathcal{H}_\infty$ -norm, which corresponds to a measure of the impact of exogenous signals (such as bumps and holes in a road) on the system output (the vertical vehicle displacement, for instance). This idea is based on the fact that the  $\mathcal{H}_\infty$ -norm is directly associated to the system transfer function from the input to its output (Figure 2.4).

Figure 2.4 - A linear system representation in both time and frequency domains: the later enables the  $\mathcal{H}_\infty$  control approach.



Source: Own author.

For understanding this concept, consider a generic state-space representation of a linear system

$$\begin{cases} \dot{x}(t) = \mathcal{A}x(t) + \mathcal{B}w(t) \\ z(t) = \mathcal{C}x(t) + \mathcal{D}w(t) \end{cases} \quad (2.12)$$

As well-known, we can certify the asymptotic stability of (2.12) through the existence of a scalar function  $V(x(t))$  such that  $V(x(t)) > 0$  and  $\dot{V}(x(t)) < 0$ , for all  $x(t) \neq 0$  and all  $t \geq 0$ .

Now, as mentioned earlier, the dynamic behavior of (2.12) can be investigated in the frequency domain in terms of its transfer function matrix  $H(s)$ , which establishes a relation between the Laplace's Transform of the system output and input,  $Z(s)$  and  $W(s)$ , with zero initial condition, respectively, as  $Z(s) = H(s)W(s)$ . By considering (2.12), it is trivial to derive that  $H(s) = \mathcal{C}(sI - \mathcal{A})^{-1}\mathcal{B} + \mathcal{D}$ .

Clearly,  $H(s)$  dictates the effect of an exogenous signal  $w(t)$  over the system output  $z(t)$ . However, note that for different frequencies  $s = j\omega$ ,  $\forall \omega \in \mathbb{R}^+$  the system response to the exogenous signal might be different, as the transfer matrix is a function of  $s$ . In these terms, we can evaluate the magnitude the disturbance effect by analyzing the  $\mathcal{H}_\infty$ -norm of  $H(s)$  (represented by  $\|H(s)\|_\infty$ ), which according to Scherer, Gahinet and Chilali (1997), characterizes the largest gain, for all frequencies  $s = j\omega$ ,  $\forall \omega \in \mathbb{R}^+$ , for the singular



values norm. In other words,  $\|H(s)\|_\infty$  represents the maximum gain from  $w(t)$  to  $z(t)$ , for every real frequency  $\omega$ .

In the time-domain, we can associate the  $\mathcal{H}_\infty$  norm of (2.12) to the minimum scalar  $\mu$  such that  $\|z(t)\|_2 < \mu\|w(t)\|_2$ , for every possible frequency of the signal  $w(t)$ . Note that this relation indicates that the  $\mathcal{H}_\infty$  norm is associated to the worst-case, *i.e.* the minimum scalar  $\mu$  is obtained at the condition of the maximum input amplification, or equivalently, highest  $\|z(t)\|_2/\|w(t)\|_2$  ratio. Moreover, the smaller the value of  $\mu$  assumes, the less the output  $z(t)$  will be affected by the presence  $w(t)$  on the system dynamics. Upon this discussion, we can establish a joint relation between the asymptotic stability and the robust  $\mathcal{H}_\infty$  performance by means of the Bounded-Real Lemma (BRL), stated in Lemma 2.2.

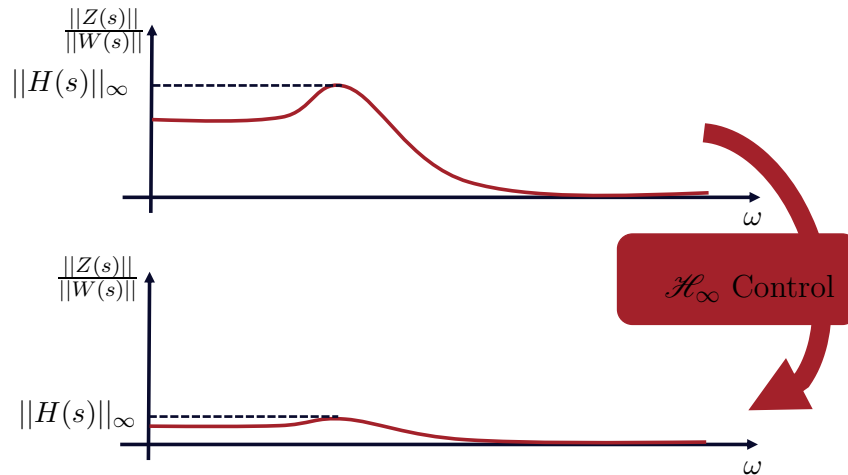
**Lemma 2.2** (Bounded-Real Lemma). *A dynamic system described as in (2.12) is asymptotic stable with  $\|H(s)\|_\infty < \mu$  if there exists symmetric matrix  $P$  such that*

$$\dot{x}(t)'Px(t) + \dot{x}(t)Px(t)' + z(t)'z(t) - \mu^2w(t)'w(t) < 0. \quad (2.13)$$

**Proof:** See Boyd *et al.* (1994). ■

The  $\mathcal{H}_\infty$ -control has the purpose of minimizing the  $\mathcal{H}_\infty$  norm, promoting the attenuation of the input to output amplification gain to every other possible frequency input signal. This idea is illustrated in Figure 2.5 for the case of a single-input single-output (SISO) system.

Figure 2.5 - The  $\mathcal{H}_\infty$  norm representation for SISO systems: the worst case in the system frequency response.



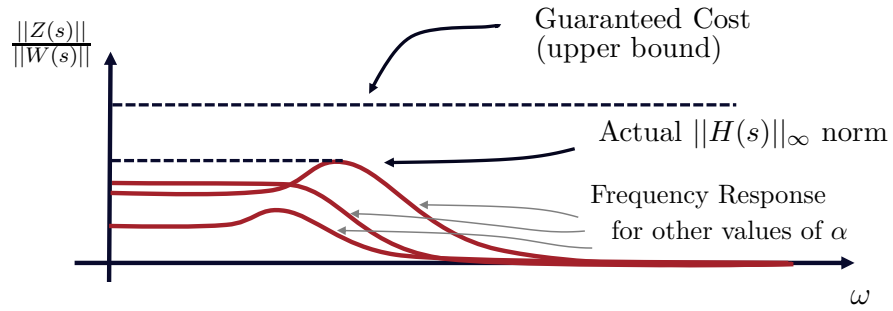
Source: Own author.

In the case of uncertain LTI systems, the  $\mathcal{H}_\infty$  norm optimization problem becomes more involved. For each possible value that the uncertain parameter  $\alpha$  affecting the plant

may assume, we have a different frequency response, and therefore, a different associated  $\mathcal{H}_\infty$  norm. Then, we have that the  $\mathcal{H}_\infty$  norm of an uncertain LTI is the “worst of all worst cases”, meaning the lower possible value for  $\mu$  among each case defined by  $\alpha$ .

However,  $\alpha$  can assume an infinite number of possible values. Thus, for finding the  $\mathcal{H}_\infty$  norm of an uncertain system we might need to test each and possible frequency domain behavior, as a function of  $\alpha$ . Naturally, this becomes impossible, especially in the case of robust controller synthesis. In this context, the  $\mathcal{H}_\infty$  guaranteed cost concept takes place for defining the system behavior in reaction to exogenous input signals. When dealing with uncertain LTI systems, instead of minimizing the actual  $\mathcal{H}_\infty$  norm, we try to minimize a guaranteed cost, that is, an upper bound on the real uncertain system  $\mathcal{H}_\infty$  norm. By minimizing such bound, the actual  $\mathcal{H}_\infty$  norm is consequently minimized. We have this concept illustrate in Figure 2.6.

Figure 2.6 - The  $\mathcal{H}_\infty$  guaranteed cost representation for an uncertain SISO system: an upper bound for the uncertain LTI system  $\mathcal{H}_\infty$  norm.



Source: Own author.

One important observation is that the BRL is well-defined for LTI systems, since it is based on the idea of transfer matrices. There are, however, extensions for dealing with the  $\mathcal{H}_\infty$  problem in the LPV framework. These extensions consider the definition of the  $l_2$ -induced norm. When we have an LPV system as

$$\begin{aligned} \dot{x}(t) &= \mathcal{A}(\alpha(t))x(t) + \mathcal{B}(\alpha(t))w(t) \\ z(t) &= \mathcal{C}(\alpha(t))x(t) + \mathcal{D}(\alpha(t))w(t) \end{aligned} \quad (2.14)$$

the  $\mathcal{H}_\infty$  guaranteed cost  $\mu$ , can be established in terms of  $\|H_{zw}\|_\infty < \mu$ , where

$$\|H_{zw}\|_\infty := \sup_{\|w(t)\|_2 \neq 0} \frac{\|z(t)\|_2}{\|w(t)\|_2},$$

holds for every possible trajectory of the time-varying parameter  $\alpha(t)$ . Following previous works on this subject (SADEGHZADEH, 2017),  $\|H_{zw}\|_\infty$  denotes the induced- $l_2$  gain

performance of the closed-loop system (2.14). However, with a slight abuse of language, we consider the use of the term  $\mathcal{H}_\infty$  guaranteed cost for referring to the bound  $\mu$ .

#### 2.1.4 $\mathcal{H}_2$ GUARANTEED COST

Another strategy for dealing with disturbance rejection is the  $\mathcal{H}_2$  norm minimization. Differently from the  $\mathcal{H}_\infty$  norm approach, which intends to reduce the peak gain of the frequency response, the  $\mathcal{H}_2$  strategy seeks to minimize the whole area under the frequency response curve, as it will be explained in the sequence.

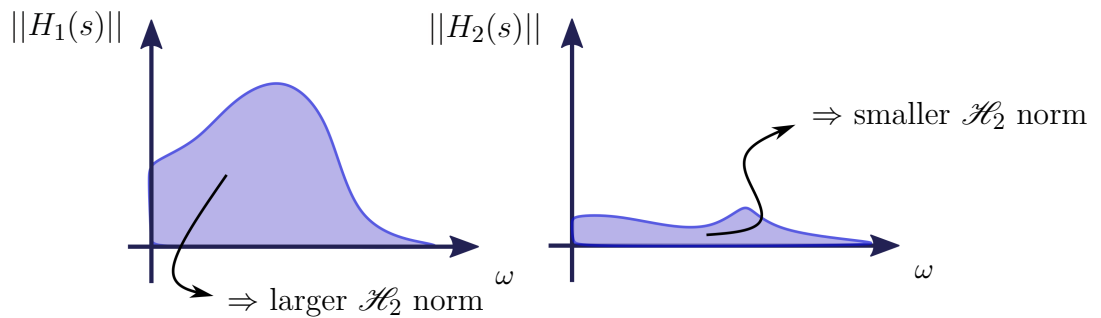
For the matter considered in this work, the  $\mathcal{H}_2$  guaranteed cost is defined as a positive scalar  $\mu$  such that  $\mu \geq \|H(\alpha, s)\|_2$  where  $\|H(\alpha, s)\|_2$  is the system (2.12)  $\mathcal{H}_2$  norm, defined as

$$\|H(\alpha, s)\|_2^2 = \sup_{\alpha \in \Lambda_N} \frac{1}{2\pi} \int_{-\infty}^{+\infty} \text{Tr}(H(\alpha, j\omega)^* H(\alpha, j\omega)) d\omega \quad (2.15)$$

and  $H(\alpha, s) = \mathcal{C}(\alpha)(sI - \mathcal{A}(\alpha)^{-1})\mathcal{B}(\alpha)$ , is the closed-loop system transfer matrix, defined over the complex variable  $s$ , here considered as the complex frequency variable  $s = j\omega$ . It is important to observe that when considering the  $\mathcal{H}_2$  problem, it is mandatory to impose the following constraint over the direct transfer matrix in (2.12):  $\mathcal{D}(\alpha) = 0$ .

In these terms, note that definition given in (2.15) relates to the area under the frequency response curve, as illustrated in Figure 2.7 for the particular single-input/single-output (SISO) LTI system case.

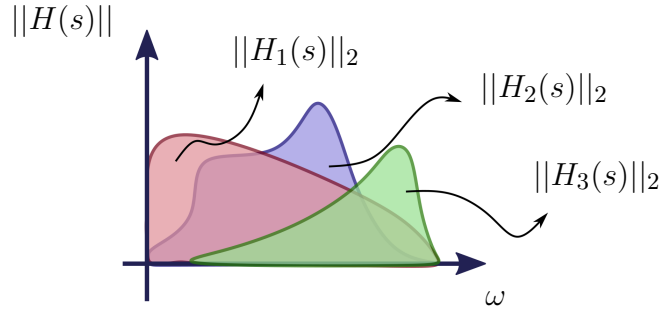
Figure 2.7 - The  $\mathcal{H}_2$  norm representation for two distinct SISO LTI systems with transfer functions  $H_1(j\omega)$  and  $H_2(j\omega)$ , respectively.



Source: Own author.

Note that the transfer defined up above incorporates the uncertainty in the system model, being a function of  $\alpha$ . Therefore, we need to discuss the concept of the  $\mathcal{H}_2$  guaranteed cost. Observe that for each  $\alpha \in \Lambda_N$  the system frequency response presents a different area under its corresponding curve (see Figure 2.8 for a simple illustration). In this perspective, the  $\mathcal{H}_2$  guaranteed cost establishes an upper bound for the largest among all possible areas associated to each  $\|H(\alpha, s)\|$ .

Figure 2.8 - The  $\mathcal{H}_2$  guaranteed cost representation: frequency response for three different values of  $\alpha$  of a generic SISO LTI system.



Source: Own author.

To give basis to our next proposed results, we consider the following lemma, which represents a condition for minimizing the closed-loop  $\mathcal{H}_2$  guaranteed cost as defined in this section.

**Lemma 2.3.** (LACERDA; OLIVEIRA; PERES, 2011) For a Hurwitz matrix  $\mathcal{A}(\alpha)$ ,  $\|\mathcal{H}(\alpha, s)\|_2^2 < \mu$  if and only if there exists parameter-dependent symmetric matrices  $P(\alpha) > 0$  and  $Y(\alpha) > 0$  such that

$$\text{trace}(Y(\alpha)) < \mu^2 \quad (2.16)$$

$$Y(\alpha) - \mathcal{B}(\alpha)'P(\alpha)\mathcal{B}(\alpha) > 0 \quad (2.17)$$

$$\mathcal{A}(\alpha)'P(\alpha) + P(\alpha)\mathcal{A}(\alpha) + \mathcal{C}(\alpha)'\mathcal{C}(\alpha) < 0. \quad (2.18)$$

### 2.1.5 TWO-STAGE SOF DESIGN

The SOF control synthesis strategy proposed in this work is fundamentally based on the two-stage method, initially proposed in Peaucelle and Arzelier (2001). For describing its core idea, assume that we want to design an SOF controller such that  $\dot{x}(t) = Ax(t) + Bu(t)$  is asymptotically stabilized considering a control law  $u(t) = Ly(t)$ , with  $y(t) = Cx(t)$ . For completing this task by means of the two-stage method, we perform a two-step design:

- **Stage 1: State-feedback design** Initially, we consider the design of a control law  $u(t) = Kx(t)$ , given in terms of a state-feedback gain matrix  $K$ , such that the system of  $\dot{x}(t) = Ax(t) + Bu(t) = (A + BK)x(t)$  is asymptotically stabilized.
- **Stage 2: Static output-feedback design** In the second stage, we use the designed SF matrix  $K$  as input information, in a second design problem, which returns, if possible, the desired SOF gain matrix  $L$ .

The two-stage method has first appeared in the work Peaucelle and Arzelier (2001).

This result comes from the observation that the SOF Lyapunov stability condition, given in terms of the existence of a symmetric matrix  $P > 0$  such that

$$(A + BLC)'P + P(A + BLC) < 0 \quad (2.19)$$

holds, can be equivalently represented by the following inequality:

$$\begin{bmatrix} I & C'L' \end{bmatrix} \begin{bmatrix} A'P + PA & PB \\ B'P & 0 \end{bmatrix} \begin{bmatrix} I \\ LC \end{bmatrix} < 0. \quad (2.20)$$

One can observe that (2.20) is in the form of one of the inequalities of the Finsler's Lemma (see the formal definition of this well-known linear algebra result at the end of this chapter), and thus can be rewritten as

$$\begin{bmatrix} A'P + PA & PB \\ B'P & 0 \end{bmatrix} + \begin{bmatrix} H_s \\ -H \end{bmatrix} \begin{bmatrix} LC & -I \end{bmatrix} + \begin{bmatrix} C'L' \\ -I \end{bmatrix} \begin{bmatrix} H'_s & -H' \end{bmatrix} < 0, \quad (2.21)$$

where  $H_s$  and  $H$  are slack variables, introduced by the application of Finsler's Lemma.

Summing the block matrices in (2.21) we have

$$\begin{bmatrix} A'P + PA + H_s LC + C'L'H'_s & PB - H_s - C'L'H' \\ B'P - H'_s - HLC & H + H' \end{bmatrix} < 0. \quad (2.22)$$

From the bottom right block of (2.22), we have that  $H + H' < 0$ , which ensures the existence of  $H^{-1}$  (BOYD *et al.*, 1994). Thus, by regarding that  $I = HH^{-1} = H^{-1}H'$ , (2.22) can be rewritten as

$$\begin{bmatrix} A'P + PA + H_s H^{-1} HLC + C'L'H'H^{-1}H'_s & PB - H_s H^{-1}H - C'L'H' \\ B'P - H'H^{-1}H'_s - HLC & H + H' \end{bmatrix} < 0. \quad (2.23)$$

Now, defining  $K' = H_s H^{-1}$  and  $J = HL$ , we have

$$\begin{bmatrix} A'P + PA + K'JC + C'J'K & PB - K'H - C'J' \\ B'P - H'K' - JC & H + H' \end{bmatrix} < 0, \quad (2.24)$$

or, as presented in Peaucelle and Arzelier (2001):

$$\begin{bmatrix} A'P + PA & PB \\ B'P & 0 \end{bmatrix} + \begin{bmatrix} K' \\ -I \end{bmatrix} \begin{bmatrix} JC & -H \end{bmatrix} + \begin{bmatrix} C'J' \\ -H' \end{bmatrix} \begin{bmatrix} K & -I \end{bmatrix} < 0. \quad (2.25)$$

Therefore, the original BMI problem (2.19) stated in terms of  $P$  and  $L$  is equivalently represented as the BMI (2.25) in terms of  $P$ , and now, with additional variables  $K$ ,  $H$ , and  $J$ . Note that both BMI are related through  $J = HL$ , with  $\det(H) \neq 0$ .

Now a very important observation: by pre multiplying (2.25) by  $\begin{bmatrix} I & K' \end{bmatrix}$  and post multiplying by its transpose we have

$$A'P + PA + PBK + K'B'P < 0. \quad (2.26)$$

This result shows that  $K$  is a stabilizing state-feedback gain matrix, considering the existence of a function  $V(x) = x'Px > 0$ . Moreover, the Lyapunov matrix  $P$  that attests the stability of  $A + BK$  is the same that guarantees the stability of  $A + BLC$ , since (2.19) is also satisfied for the same  $P$ , considering  $J = HL$  in (2.25), as already demonstrated. Concluding, we see that if a stabilizing SF gain  $K$  is found for  $A + BK$ , we can seek for a stabilizing SOF gain  $L$  to  $A + BLC$  by solving the LMI problem given in (2.25).

Any available method in the literature for the synthesis of state-feedback stabilizing controllers can be adopted. However, the feasibility of the SOF problem in the second stage depends on the matrix  $K$  provided *a priori*. Such feature implies on the fact that the LMI-based two-stage method consists of sufficient SOF control synthesis conditions. Even so, if the method fails for some particular  $K$ , the designer can employ a different SF synthesis procedure, and then the two-stage method can be applied once again.

In these terms, one may conclude that the search for a stabilizing state-feedback gain matrix  $K$  is a pivot element in the SOF problem. In fact, the existence of a stabilizing SOF controller  $L$  is conditioned to the existence of stabilizing SF controller  $K$ . This is true since that in the output-feedback case, the closed-loop system has the form

$$\dot{x}(t) = (A + BLC)x(t). \quad (2.27)$$

Therefore, an  $L$  gain matrix such that (2.27) is asymptotic stable exists if the same system is asymptotically stable via state-feedback, since  $K = LC$  in (2.27) leads to

$$\dot{x}(t) = (A + BK)x(t).$$

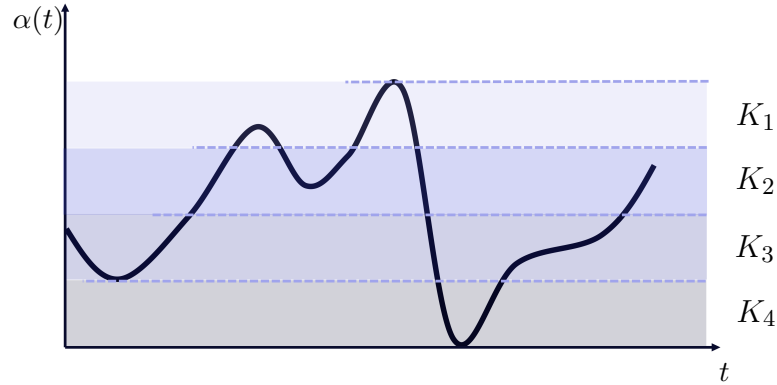
However, note that the existence of a stabilizing SF gain matrix  $K$  does not necessarily implies in the existence of a stabilizing SOF gain matrix  $L$ .

### 2.1.6 GAIN-SCHEDULING CONTROL

Gain-scheduling control is based on using available information about the time-varying behavior of the considered LPV system to instantly updated the controller gains, in order to achieve enhanced performance and robustness. As mentioned in Chapter 1, the classic gain-scheduling technique is based on the construction of a family of LTI subsystems to cover the range of operation of the nonlinear or/and time-varying plant. Then, for each

of the portioned sections of the range of variation that the time-varying parameter  $\alpha(t)$  may assume, we design a single static feedback gain, as illustrated in Figure 2.9.

Figure 2.9 - Illustration of the gain-scheduled classic control for a parameter grid of four sections and its corresponding static controllers.



Source: Own author.

Then, based on the online measurement of the time-varying parameters, the scheduled controller gains *a priori* designed are selected. As already mentioned, this strategy has some clear shortcomings: i) for better performance, a refinement on the parametric grid is required, which leads to higher complexity and computational cost for implementation; ii) serious questioning about stability guarantee in the switching zones, which might compromise global stability.

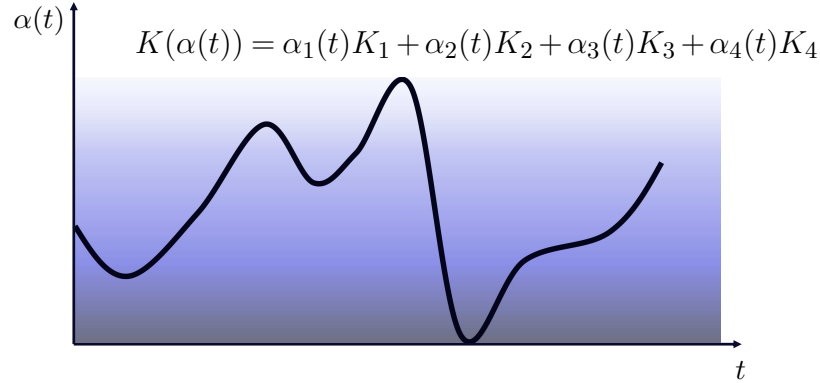
In this work, we consider the design of GS controllers via LMI formulation and a polytopic representation of LPV systems. In this approach, by having knowledge of the extreme values that the time-varying parameters might assume, we design a single static gain for each one of the polytope vertices (Figure 2.10). With that, we implement the GS controller as a convex combination of the static controller vertices, as

$$K(\alpha(t)) = \alpha_1(t)K_1 + \alpha_2(t)K_2 + \cdots + \alpha_N(t)K_N$$

providing a smooth time-varying controller, without having to worry about parameter gridding or stability issues due to gain switching.

As discussed before in this section, we consider the polytopic model for LPV systems, which is based on assuming a polytopic dependence of the model matrices with the time-varying parameters, *i.e.*  $(A, B, C)(\alpha(t))$ , where  $\alpha(t)$  belongs to the unitary simplex set (2.3).

Figure 2.10 - Illustration of the gain-scheduled controller generated by the convex combination of four vertex matrices, parameterized in terms of the time-varying parameters.



Source: Own author.

In general, the practical set of time-varying parameters that affects the model matrices,  $\theta(t)$ <sup>2</sup>, does not fall within the domain of the unitary simplex. Therefore, in such cases, the elements  $\alpha_i(t)$  must be obtained through a parametrization of each time-varying parameter  $\theta_l(t)$ , with  $l = 1, \dots, n_p$  and  $n_p$  being the number of time-varying parameters affecting the model.

The set  $\alpha(t)$  can be determined by defining a convex combination of minimum and maximum values that each  $\theta_l(t)$  may assume. For exemplifying, the model of an LPV system which is affected by a single time-varying parameter  $\theta_1(t)$  (which is measured or estimated online by assumption) can be obtained by defining

$$\alpha_1(t) = \frac{\theta_1(t) - \theta_{1min}}{\theta_{1max} - \theta_{1min}} \quad \text{and} \quad \alpha_2(t) = 1 - \alpha_1(t),$$

where  $\theta_{1min}$  and  $\theta_{1max}$  are the lower and upper limits of the range of values that  $\theta_1(t)$  can assume, also known by hypothesis.

A more complex parametrization is needed when the system is affected by two or more time-varying parameters. For exemplifying, let's assume an arbitrary LPV under the influence of two time-varying parameters,  $\theta_1(t)$  and  $\theta_2(t)$ . First, we can rewrite  $\theta_1(t)$  and  $\theta_2(t)$  as a convex combination of their extreme values,

$$\theta_1(\sigma(t)) = \sigma_1(t)\theta_{1min} + \sigma_2(t)\theta_{1max}, \quad (2.28)$$

$$\theta_2(\sigma(t)) = \xi_1(t)\theta_{2min} + \xi_2(t)\theta_{2max}, \quad (2.29)$$

with  $\sigma_1(t) + \sigma_2(t) = 1$  and  $\xi_1(t) + \xi_2(t) = 1$ ,  $\sigma_{1,2}(t) \geq 0$ , and  $\xi_{1,2}(t) \geq 0$ .

<sup>2</sup>We are considering the continuous-time case, but the same discussion and conclusion can be carried out for the discrete-time time-varying parameter case.



Considering these definitions, and we can perform the following transformation:

$$\begin{aligned}\theta_1(\sigma(t), \xi(t)) &= (\xi_1(t) + \xi_2(t))(\sigma_1(t)\theta_{1min} + \sigma_2(t)\theta_{1max}), \\ \theta_1(\sigma(t), \xi(t)) &= (\xi_1(t)\sigma_1(t) + \xi_2(t)\sigma_1(t))\theta_{1min} + (\xi_1(t)\sigma_2(t) + \xi_2(t)\sigma_2(t))\theta_{1max},\end{aligned}\quad (2.30)$$

$$\begin{aligned}\theta_2(\sigma(t), \xi(t)) &= (\sigma_1(t) + \sigma_2(t))(\xi_1(t)\theta_{2min} + \xi_2(t)\theta_{2max}), \\ \theta_2(\sigma(t), \xi(t)) &= (\sigma_1(t)\xi_1(t) + \sigma_2(t)\xi_1(t))\theta_{2min} + (\sigma_1(t)\xi_2(t) + \sigma_2(t)\xi_2(t))\theta_{2max}.\end{aligned}\quad (2.31)$$

Now, defining  $\alpha_1(t) = \xi_1(t)\sigma_1(t)$ ,  $\alpha_2(t) = \xi_1(t)\sigma_2(t)$ ,  $\alpha_3(t) = \xi_2(t)\sigma_1(t)$ , and  $\alpha_4(t) = \xi_2(t)\sigma_2(t)$ , we have

$$\theta_1(\alpha(t)) = \alpha_1(t)\theta_{1min} + \alpha_2(t)\theta_{1max} + \alpha_3(t)\theta_{1min} + \alpha_4(t)\theta_{1max}, \quad (2.32)$$

$$\theta_2(\alpha(t)) = \alpha_1(t)\theta_{2min} + \alpha_2(t)\theta_{2min} + \alpha_3(t)\theta_{2max} + \alpha_4(t)\theta_{2max}. \quad (2.33)$$

Note that every system configuration, which is defined by the instant values assumed by the two time-varying parameters,  $\theta_{1,2}(t)$ , is now expressed in as a convex combination parameterized in terms of the vector  $\alpha(t) = (\alpha_1(t) \ \alpha_2(t) \ \alpha_3(t) \ \alpha_4(t))$ , with  $\alpha(t) \in \bar{\lambda}$ .

## 2.2 MATHEMATICAL TOOLS

Before properly discussing the contributions proposed in this work, we present the following lemmas and properties, which are essential for the development of this thesis.

**Lemma 2.4** (Finsler's Lemma). *Consider  $w \in \mathbb{R}^n$ ,  $S \in \mathbb{R}^{n \times n}$ , and  $R \in \mathbb{R}^{m \times n}$  with rank  $(R) < n$ , where  $R^\perp$  is a basis for the null space of  $R$  (i.e.  $RR^\perp = 0$ ).*

*Then, the following conditions are equivalent:*

- (i)  $w'Sw < 0, \forall w \neq 0, Rw = 0$ ,
- (ii)  $R^{\perp'}SR^\perp < 0$ ,
- (iii)  $\exists \eta \in \mathbb{R} : S - \eta R'R < 0$ ,
- (iv)  $\exists X \in \mathbb{R}^{m \times n} : S + XR + R'X' < 0$ ,

*where  $\eta$  and  $X$  are additional variables (or multipliers).*

*Proof.* See Skelton, Iwasaki and Grigoriadis (1997) and Oliveira and Skelton (2007).  $\square$

**Property 2.1.** (BOYD et al., 1994) *If  $M + M' > 0$ , where  $M$  is a square matrix, then  $M$  is invertible.*

The employment of Lemma 2.4 in this work is based on deriving an equivalent stability and performance certificate for the investigated systems. Such alternative representation

allows for circumventing non-convex constraints, and then leading to tractable convex conditions. For further reference in the text, Lemma 2.5, which is obtained as a direct extension of the results proposed in Oliveira and Skelton (2007), presents stability and performance certificate regarding the minimum system decay rate.

**Lemma 2.5.** *A sufficient condition for the robust stability of  $A(\alpha)$  is that there exist a parameter-dependent positive definite matrix  $P(\alpha)$  and parameter-dependent matrices  $F(\alpha)$  and  $G(\alpha)$  such that*

$$\begin{bmatrix} A(\alpha)'F(\alpha)' + (\bullet)' + 2\gamma P(\alpha) & * \\ P(\alpha) - F(\alpha)' + G(\alpha)A(\alpha) & -G(\alpha) - G(\alpha)' \end{bmatrix} < 0, \quad (2.34)$$

holds for every  $\alpha \in \Lambda_N$ . Additionally, the system decay rate has a lower bound  $\gamma > 0$ .

**Proof:** Note that (2.34) can be rewritten as

$$\begin{bmatrix} F(\alpha) \\ G(\alpha) \end{bmatrix} \begin{bmatrix} A(\alpha) & -I \end{bmatrix} + (\bullet)' + \begin{bmatrix} 2\gamma P(\alpha) & * \\ P(\alpha) & 0 \end{bmatrix} < 0, \quad (2.35)$$

which corresponds to condition (iv) of Lemma 2.4 with

$$X = \begin{bmatrix} F(\alpha) \\ G(\alpha) \end{bmatrix}, \quad S = \begin{bmatrix} 2\gamma P(\alpha) & * \\ P(\alpha) & 0 \end{bmatrix}, \quad R' = \begin{bmatrix} A(\alpha)' \\ -I \end{bmatrix}. \quad (2.36)$$

Hence, by defining  $w = [x(t)' \quad \dot{x}(t)']'$  in condition (i) of Lemma 2.4, we have that (2.34) implies<sup>3</sup>

$$w'Sw = \begin{bmatrix} x' & \dot{x}' \end{bmatrix} \begin{bmatrix} 2\gamma P(\alpha) & * \\ P(\alpha) & 0 \end{bmatrix} \begin{bmatrix} x \\ \dot{x} \end{bmatrix} = \dot{x}'P(\alpha)x + x'P(\alpha)\dot{x} + 2\gamma x'P(\alpha)x < 0, \quad (2.37)$$

with  $Rw = 0$ , since  $\dot{x}(t) = A(\alpha)x(t)$ . By defining  $V(x) = x'P(\alpha)x$ , (2.37) becomes  $\dot{V}(x) < -2\gamma V(x)$ , *i.e.*, the Lyapunov's constraint for stability and minimum decay rate  $\gamma > 0$  (BOYD *et al.*, 1994). ■

---

<sup>3</sup>Note that in (2.37) the time dependence ( $t$ ) was omitted for shortening the notation.

### 3 STATIC OUTPUT FEEDBACK CONTROL WITH POLE PLACEMENT CONSTRAINTS

This chapter is devoted to present new contributions on the theory of static output feedback (SOF) control design with additional linear matrix inequality (LMI) constraints for pole placement.

The goal is to guarantee the asymptotic stability of linear systems while some transient performance improvement is also enforced by promoting closed-loop pole assignment to a particular region of the complex plane – namely, the  $\mathcal{D}$ -stability. The pole allocation region considered in the following developments is a disk, whose radius and center position may be set by the designer in terms of two scalar parameters.

Two main studies are presented in the sequence: first, we address the case of uncertain linear time-invariant (LTI) systems. In this scenario, the goal is to design a robust SOF controller that meets the control objective at hand; second, the extension of the concepts of  $\mathcal{D}$ -stability to the case of linear parameter-varying (LPV) systems is explored. In this second framework, the idea is to design gain-scheduled (GS) controllers under additional pole placement constraints applied over the system polytope vertex and evaluate its impact on the closed-loop system performance.

#### 3.1 ROBUST $\mathcal{D}$ -STABILIZATION VIA SOF CONTROL

In this section, the robust  $\mathcal{D}$ -stabilization of uncertain LTI systems via SOF control is addressed.

At first, the investigated problem is properly stated and defined. In the sequence, a solution in terms of a design procedure based on the two-stage method considering sufficient LMI conditions for controller synthesis is proposed. Moreover, the impacts of the design constraints considered in the first stage over the obtained robust SOF controller are also investigated. Feasibility analysis results, comparing three strategies for implementing the two-stage design procedure are presented and discussed.

## 3.1.1 PROBLEM STATEMENT AND PROPOSED APPROACH

Consider an uncertain LTI system described in a state-space representation such as

$$\begin{aligned}\dot{x}(t) &= A(\alpha)x(t) + B(\alpha)u(t) \\ y(t) &= C(\alpha)x(t),\end{aligned}\tag{3.1}$$

where  $x(t) \in \mathbb{R}^n$  is the state vector,  $u(t) \in \mathbb{R}^m$  is the control input vector, and  $y(t) \in \mathbb{R}^p$  is the measured output vector. The matrices associated to the system dynamics,  $A(\alpha) \in \mathbb{R}^{n \times n}$ ,  $B(\alpha) \in \mathbb{R}^{n \times m}$ , and the output matrix  $C(\alpha) \in \mathbb{R}^{p \times n}$ , respectively, are considered uncertain and belong to the polytopic domain  $\mathcal{P}$  defined as

$$\mathcal{P} = \left\{ (A, B, C)(\alpha) : (A, B, C)(\alpha) = \sum_{i=1}^N \alpha_i (A, B, C)_i, \quad \alpha \in \Lambda_N \right\}\tag{3.2}$$

where  $(A, B, C)_i$  denotes the  $i$ -th of the  $N$  polytope vertices. Moreover,  $\mathcal{P}$  is parameterized in terms of the vector  $\alpha = (\alpha_1, \dots, \alpha_N)$ , whose entries  $\alpha_i$  are unknown constants that belong to the unitary simplex set  $\Lambda_N$ , defined as

$$\Lambda_N = \left\{ \alpha \in \mathbb{R}^N : \sum_{i=1}^N \alpha_i = 1; \alpha_i \geq 0; i = 1, \dots, N \right\}.\tag{3.3}$$

Assume that only a subset of the system state variables is measured. Therefore, consider a control law  $u(t) = Ly(t)$  and design a robust SOF gain matrix  $L \in \mathbb{R}^{m \times p}$  such that the closed-loop system

$$\dot{x}(t) = (A(\alpha) + B(\alpha)LC(\alpha))x(t)\tag{3.4}$$

is asymptotically stable for all  $\alpha \in \Lambda_N$  (*i.e.* robustly stable).

Moreover,  $L$  must ensure that the eigenvalues of the closed-loop system (3.4) are all placed inside the circular  $\mathcal{D}$ -region represented in Figure 2.3. Observe that this region is defined in terms of its radius  $r$ , its distance  $\gamma$  from the imaginary axis, and its center  $(-q, 0)$ , with  $q = \gamma + r$ . When these requirements are met, (3.4) is said to be robustly  $\mathcal{D}$ -stable.

For addressing the considered control problem, the design of the robust SOF controller is performed by means of a two-stage procedure (PEAUCELLE; ARZELIER, 2001; MEHDI; BOUKAS; BACHELIER, 2004) (for an initial insight, see Subsection 2.1.5). In this strategy, one must first obtain a gain matrix such that the system of interest is stabilized via state feedback (SF). Then, the obtained SF controller is used as input information for the second stage, in which the desired SOF gain matrix is computed.

In these terms, we first consider a control law  $u(t) = Kx(t)$ , which when applied to (3.1) yields the closed-loop system

$$\dot{x}(t) = (A(\alpha) + B(\alpha)K)x(t). \quad (3.5)$$

Then, we design a gain matrix  $K$  such that (3.5) is robustly stable. This matrix is then fed the second stage, where the compute of  $L$  is performed.

Now, based on the results presented in Leite, Montagner and Peres (2002), by defining  $A_N(\alpha) = A(\alpha) + B(\alpha)LC(\alpha)$  one can verify that  $L$  ensures the robust eigenvalue placement in the circular  $\mathcal{D}$ -region of Figure 2.3 by checking if there exists a symmetric definite positive matrix  $P$  such that

$$\begin{bmatrix} A'_N(\alpha)P + PA_N(\alpha) + 2\gamma P & (A_N(\alpha) + \gamma I)'P \\ P(A_N(\alpha) + \gamma I) & -rP \end{bmatrix} < 0 \quad (3.6)$$

holds for all  $\alpha \in \Lambda_N$ .

On that scope, the proposed solution consists in designing the robust SOF controller  $L$  in order to satisfy (3.6). In the next section, further details on how each design stage is performed are given.

### 3.1.2 TWO-STAGE SOF DESIGN FOR $\mathcal{D}$ -STABILIZATION

In this section, a new two-stage design method for the robust pole placement of closed-loop uncertain LTI systems via SOF is proposed. Considering the sufficient nature associated to the two-stage method, the state-feedback controller synthesis performed in the first stage may be accomplished using different design strategies. Consequently, the second stage design might yield different outcomes, regarding the constraints and strategies imposed and adopted in the first step. Due to this reason, it is relevant to inquire about how the chosen SF design strategy impacts on the second-stage synthesis success.

Having said that, three different first-stage SF control design methods are considered and investigated, as listed below.

- **Strategy 1:** consists in designing a stabilizing robust SF controller  $K$  considering  $\alpha$ -stability constraints (see Section 2.1.2), which restrains the closed-loop eigenvalue allocation to a partition of the left-half complex plane defined by a vertical line parallel to the imaginary axis, in contrast to the more restrictive circular allocation region considered in second stage;
- **Strategy 2:** considers the employment of  $\mathcal{D}$ -stability control design constraints for closed-loop eigenvalue placement in a circular region in the first stage.

- **Strategy 3:** characterized by considering the design of a parameter-dependent  $\mathcal{D}$ -stabilizing SF gain  $K(\alpha)$  in the first stage that ensures closed-loop eigenvalue placement in a circular region.

As one may observe, by defining these three strategies it is possible to investigate how the region considered for pole placement in the first stage impacts on the overall two-stage procedure, regarding that in the second step the design considers a circle for enclosing the closed-loop poles. Additionally, the influence of the structure of the SF gain matrix may also be observed, comparing first-stage robust and parameter-dependent controller designs. In the sequence, the details of each one of the proposed strategies are presented and discussed.

### Strategy 1: Robust State-Feedback First-Stage Design

The implementation of Strategy 1 consists in the design of a robust SF  $\alpha$ -stabilizing gain for the first stage, based on the classic common-quadratic Lyapunov function (CQLF) formulation enunciated in Theorem 3.1.

**Theorem 3.1.** (BOYD et al., 1994) *If there exist a matrix  $Z \in \mathbb{R}^{m \times n}$  and a symmetric positive definite matrix  $W \in \mathbb{R}^{n \times n}$ , for a given scalar  $\gamma_1 > 0$ , such that*

$$A_i W + W A_i' + B_i Z + Z' B_i' + 2\gamma_1 W < 0 \quad (3.7)$$

*holds for  $i = 1, \dots, N$ , then  $K = ZW^{-1}$  robustly stabilizes  $A(\alpha) + B(\alpha)K$ , considering a minimum decay rate  $\gamma_1$  (i.e., the closed-loop system (3.5) is  $\alpha$ -stable).*

After the design of the first-stage gain matrix  $K$  solving the LMI problem presented in Theorem 3.1, the obtained gain is used for computing the desired SOF gain  $L$  in the second-stage design. The proposed solution for the problem is given in terms of new LMI synthesis conditions for the robust SOF  $\mathcal{D}$ -stabilization of system (3.4), obtained considering the existence of parameter-dependent Lyapunov functions (PDLF), as stated in Theorem 3.2.

**Theorem 3.2.** (SERENI; ASSUNÇÃO; TEIXEIRA, 2019) *Assuming that there exists a state feedback gain  $K$  such that  $A(\alpha) + B(\alpha)K$  is robustly stable, then there exists a static output feedback gain  $L$  such that  $A(\alpha) + B(\alpha)LC(\alpha)$  is robustly  $\mathcal{D}$ -stable, ensuring the closed-loop pole placement inside a circle with radius  $r_2$  and with center in  $(-q_2, 0)$ , where  $q_2 = r_2 + \gamma_2$ , if there exist symmetric matrices  $P_i > 0$  and matrices  $F_i, G_i, H$  and  $J$  such that (3.8) and (3.9) are satisfied.*

$$\begin{bmatrix} A'_i F'_i + F_i A_i + K' B'_i F'_i + F_i B_i K + \gamma_2 P_i (2r_2 + \gamma_2) & * & * \\ (r_2 + \gamma_2) P_i - F'_i + G_i A_i + G_i B_i K & P_i - G_i - G'_i & * \\ B'_i F'_i + J C_i - H K & B'_i G'_i & -H - H' \end{bmatrix} < 0 \quad (3.8)$$

for  $i = 1, 2, \dots, N$ .

$$\begin{bmatrix} \Theta_{11} & * & * \\ \Theta_{21} & P_i + P_j - G'_i - G_i - G'_j - G_j & * \\ B'_i F'_j + B'_j F'_i + J C_i + J C_j - 2H K & B'_i G'_j + B'_j G'_i & -2H - 2H' \end{bmatrix} < 0 \quad (3.9)$$

for  $i = 1, 2, \dots, N-1$  and  $j = i+1, i+2, \dots, N$ , where

$$\begin{aligned} \Theta_{11} = & A'_i F'_j + F_i A_j + K' B'_i F'_j + F_i B_j K + \gamma_2 P_i (2r_2 + \gamma_2) \\ & + A'_j F'_i + F_j A_i + K' B'_j F'_i + F_j B_i K + \gamma_2 P_j (2r_2 + \gamma_2) \end{aligned}$$

and

$$\Theta_{21} = (r_2 + \gamma_2) P_i - F'_i + G_i A_j + G_i B_j K + (r_2 + \gamma_2) P_j - F'_j + G_j A_i + G_j B_i K.$$

In the affirmative case, the robust static output feedback gain is given by  $L = H^{-1} J$ .

*Proof.* Assume that (3.8) and (3.9) hold. Then, immediately, we see that (3.8) implies in  $H + H > 0$ , which guarantees the existence of the inverse of  $H$  (BOYD *et al.*, 1994).

Now, remembering that  $\sum_{i=1}^N \alpha_i = 1$ , by multiplying (3.8) by  $\alpha_i^2$  and summing for  $i = 1, \dots, N$ , and by multiplying (3.9) by  $\alpha_i \alpha_j$  and summing for  $i = 1, \dots, N-1$  and  $j = i+1, \dots, N$ , we have that

$$\begin{bmatrix} A'(\alpha) F(\alpha)' + F(\alpha) A(\alpha) + K' B(\alpha)' F(\alpha)' + F(\alpha) B(\alpha) K + \gamma_2 P(\alpha) (2r_2 + \gamma_2) \\ (r_2 + \gamma_2) P(\alpha) - F(\alpha)' + G(\alpha) A(\alpha) + G(\alpha) B(\alpha) K \\ B(\alpha)' F(\alpha)' + J C(\alpha) - H K \\ * & * \\ P(\alpha) - G(\alpha) - G(\alpha)' & * \\ B(\alpha)' G(\alpha)' & -H - H' \end{bmatrix} < 0, \quad (3.10)$$

also holds.

Pre and post multiplying (3.10) by  $T(\alpha)$  and  $T(\alpha)'$ , where  $T(\alpha)$  is defined as

$$T(\alpha) = \begin{bmatrix} I & 0 & S(\alpha)' \\ 0 & I & 0 \end{bmatrix}, \quad (3.11)$$

with  $S(\alpha) = H^{-1}JC(\alpha) - K$ , it follows that

$$\begin{bmatrix} \Psi(\alpha) & \Phi(\alpha) \\ * & P(\alpha) - G(\alpha) - G(\alpha)' \end{bmatrix} < 0, \quad (3.12)$$

where

$$\begin{aligned} \Psi(\alpha) &= (A(\alpha) + B(\alpha)H^{-1}JC(\alpha))'F(\alpha)' \\ &\quad + F(\alpha)(A(\alpha) + B(\alpha)H^{-1}JC(\alpha)) + \gamma_2 P(\alpha)(2r_2 + \gamma_2). \end{aligned} \quad (3.13)$$

and,

$$\Phi(\alpha) = (r_2 + \gamma_2)P(\alpha) - F(\alpha) + A(\alpha)'G(\alpha)' + K'B(\alpha)'G(\alpha)' + S(\alpha)'B(\alpha)'G(\alpha)'. \quad (3.14)$$

Defining  $L = H^{-1}J$  in (3.13) and (3.14), yields

$$\begin{bmatrix} \gamma_2 P(\alpha)(2r_2 + \gamma_2) & (r_2 + \gamma_2)P(\alpha) \\ (r_2 + \gamma_2)P(\alpha) & 0 \end{bmatrix} + \left( \begin{bmatrix} (A(\alpha) + B(\alpha)LC(\alpha))' \\ -I \end{bmatrix} \begin{bmatrix} F(\alpha)' & G(\alpha)' \end{bmatrix} \right) + (\bullet)' < 0. \quad (3.15)$$

According to Finsler's Lemma (Lemma 2.4), by defining  $w = [x(t)' \quad \dot{x}(t)']'$ , we have that (3.15) leads the following equivalent inequality:

$$\begin{bmatrix} x(t)' & \dot{x}(t)' \end{bmatrix} \begin{bmatrix} \gamma_2(2r_2 + \gamma_2)P(\alpha) & (r_2 + \gamma_2)P(\alpha) \\ (r_2 + \gamma_2)P(\alpha) & P(\alpha) \end{bmatrix} \begin{bmatrix} x(t) \\ \dot{x}(t) \end{bmatrix} < 0, \quad (3.16)$$

with  $w$  under the constraint

$$\begin{bmatrix} A(\alpha) + B(\alpha)LC(\alpha) & -I \end{bmatrix} \begin{bmatrix} x(t) \\ \dot{x}(t) \end{bmatrix} = 0. \quad (3.17)$$

Initially, observe that (3.17) yields

$$\dot{x}(t) = [A(\alpha) + B(\alpha)LC(\alpha)]x(t), \quad (3.18)$$

which corresponds to the considered closed-loop system (3.4).

Additionally, omitting the time dependency of the state vectors for notation simplification, note that (3.16) yields

$$x' \gamma_2 P(\alpha)(2r_2 + \gamma_2)x + \dot{x}'(r_2 + \gamma_2)P(\alpha)x + x'(r_2 + \gamma_2)P(\alpha)\dot{x} + \dot{x}'P(\alpha)\dot{x} < 0 \quad (3.19)$$

Now, by defining  $A_N(\alpha) = A(\alpha) + B(\alpha)LC(\alpha)$ , and rearranging terms in (3.19) we



have

$$x' \left( (r_2 + \gamma_2)(A_N(\alpha)'P(\alpha) + P(\alpha)A_N(\alpha)) + (2r_2\gamma_2 + \gamma_2^2)P(\alpha) + A_N(\alpha)'P(\alpha)A_N(\alpha) \right) x < 0,$$

or, equivalently,

$$A_N(\alpha)'P(\alpha) + P(\alpha)A_N(\alpha) + 2\gamma_2P(\alpha) + (A_N(\alpha) + \gamma_2I)' \frac{P(\alpha)}{r_2} (A_N(\alpha) + \gamma_2I) < 0.$$

At this point, by means of the Schur's complement, we can obtain from (3.19) the following equivalent inequality:

$$\begin{bmatrix} A_N(\alpha)'P(\alpha) + P(\alpha)A_N(\alpha) + 2\gamma_2P(\alpha) & * \\ P(\alpha)(A_N(\alpha) + \gamma_2I) & r_2P(\alpha) \end{bmatrix} < 0, \quad (3.20)$$

which is a sufficient condition (LEITE; MONTAGNER; PERES, 2002) for the robust  $\mathcal{D}$ -stabilization of the SOF closed-loop system (3.4).  $\square$

### Strategy 2: $\mathcal{D}$ -Stabilizing State-Feedback First-Stage Design

Strategy 2 consists in designing a first-stage gain matrix  $K$  under  $\mathcal{D}$ -stabilizing constraints, considering a circular region for pole placement. Then, the obtained gain is fed to the second stage, which is performed using the LMI conditions enunciated in Theorem 3.2. The details and benefits if this new SOF  $\mathcal{D}$ -stabilizing two-stage design configuration are discussed in the sequence.

Firstly, we emphasize that designing  $K$  by means of Theorem 3.1 does not enable a precise robust closed-loop eigenvalue placement, except that they all will be settled at the left of the vertical line passing through the point  $(-\gamma_1, 0)$ , in the left complex semi-plane (BOYD *et al.*, 1994).

Since in the second stage a more specific pole placement region is imposed, it seems imperative to investigate how the method is affected, in terms of feasibility success, when the first stage is also performed considering  $\mathcal{D}$ -stabilizing constraints. With this purpose, when performing the first stage, we propose considering the employment of the results presented in Leite, Montagner and Peres (2002), which enables the synthesis of a robust  $\mathcal{D}$ -stabilizing state feedback controller considering a circular region for pole placement, by solving the LMI problem enunciated in Theorem 3.3.

**Theorem 3.3.** (LEITE; MONTAGNER; PERES, 2002) *If there exist a matrix  $Z \in \mathbb{R}^{m \times n}$  and a symmetric positive definite matrix  $W \in \mathbb{R}^{n \times n}$  such that*

$$\begin{bmatrix} A_iW + WA_i' + B_iZ + Z'B_i' + 2\gamma_1W & * \\ WA_i' + Z'B_i' + \gamma_1W & -r_1W \end{bmatrix} < 0 \quad (3.21)$$

holds for  $i = 1, \dots, N$ , then  $K = ZW^{-1}$  ensures the robust closed-loop pole placement of  $A(\alpha) + B(\alpha)K$  inside the circular region with radius  $r_1$  and center in  $(-q_1, 0)$ , where  $q_1 = r_1 + \gamma_1$ .

If Theorem 3.3 provides a feasible solution, then the designer may use the obtained robust  $\mathcal{D}$ -stabilizing gain  $K$  as input parameter to Theorem 3.2 LMIs, to seek for the desired SOF  $\mathcal{D}$ -stabilizing gain  $L$ .

Although first and second stages are not explicitly dependent, the pole placement region specified in the state feedback step might impact on the SOF design success in the second stage, as it will be demonstrated in the examples presented in Section 3.1.3.

### Strategy 3: Parameter-dependent $\mathcal{D}$ -Stabilizing State-Feedback First-Stage Design

Further from also imposing specific pole-placement constraints on both design stages, this third SOF  $\mathcal{D}$ -stabilizing controller synthesis strategy considers the design of a first-stage parameter-dependent SF controller, which is then fed to the second stage as a known parameter.

The conception of this strategy emerges from the observation that the gain designed in the first stage is not implemented in practice, being used only as input data for the second stage (AGULHARI; OLIVEIRA; PERES, 2010a). Therefore, we can employ a parameter-dependent state-feedback design for obtaining a gain matrix  $K(\alpha)$  in the first stage. As we are considering a polytopic approach, this means that a parameter-dependent first-stage design will provide a gain matrix

$$K(\alpha) = \sum_{i=1}^N \alpha_i K_i, \quad \sum_{i=1}^N \alpha_i = 1; \quad \alpha_i \geq 0; \quad i = 1, \dots, N. \quad (3.22)$$

With this, we might reduce conservatism in the second stage, since instead of feeding a single gain matrix  $K$ , we can use a set of matrices  $K_i$ , one for each polytope vertex, serving as a sort of “slack variables”.

For that intent, we extend the results of Leite, Montagner and Peres (2002), presented in Theorem 3.3, to obtain synthesis conditions for the design of a  $\mathcal{D}$ -stabilizing parameter-dependent controller, as enunciated in Theorem 3.4.

**Theorem 3.4.** *If there exist a symmetric positive definite matrix  $W \in \mathbb{R}^{n \times n}$  and matrices  $Z_i \in \mathbb{R}^{m \times n}$  such that*

$$\begin{bmatrix} A_i W + W A_i' + B_i Z_i + Z_i' B_i' + 2\gamma_1 W & * \\ W A_i' + Z_i' B_i' + \gamma_1 W & -r_1 W \end{bmatrix} < 0, \quad (3.23)$$

holds for  $i = 1, \dots, N$ , and

$$\begin{bmatrix} (A_i W + B_i Z_j + A_j W + B_j Z_i) + (\bullet)' + \gamma_1 W & * \\ W A_i' + W A_j' + Z_i' B_j' + Z_j' B_i' + 2\gamma_1 W & -2r_1 W \end{bmatrix} < 0 \quad (3.24)$$

holds for  $i = 1, \dots, N-1$  and  $j = i+1, i+2, \dots, N$ , then  $K(\alpha)$ , as defined in (3.22) with  $K_i = Z_i W^{-1}$ , ensures the robust closed-loop pole placement of  $A(\alpha) + B(\alpha)K(\alpha)$  inside the circular region with radius  $r_1$  and center in  $(-q_1, 0)$ , where  $q_1 = r_1 + \gamma_1$ .

*Proof.* Assume that (3.23) and (3.24) hold. Then, by multiplying (3.23) by  $\alpha_i^2$  and summing for  $i = 1, \dots, N$ , and by multiplying (3.24) by  $\alpha_i \alpha_j$  and summing for  $i = 1, \dots, N-1$  and for  $j = i+1, \dots, N$ , and remembering that  $\sum_{i=1}^N \alpha_i = 1$ , we have that

$$\begin{bmatrix} A(\alpha)W + W A(\alpha)' + B(\alpha)Z(\alpha) + Z(\alpha)'B(\alpha)' + 2\gamma_1 W & * \\ W A(\alpha)' + Z(\alpha)'B(\alpha)' + \gamma_1 W & -r_1 W \end{bmatrix} < 0, \quad (3.25)$$

also holds, which is equivalent to (3.21), with  $Z = Z(\alpha)$ .  $\square$

Now, it is important to note that Theorem 3.2 cannot be used for completing the second stage using a parameter-dependent state feedback gain as input information. This is due to the fact that the referred theorem considers the existence of a robust matrix  $K$ . For making use of a parameter-dependent gain matrix  $K(\alpha)$  obtained through Theorem 3.4, appropriate synthesis conditions have to be considered in the second stage. To that end, a new and less conservative second-stage SOF control design for robust  $\mathcal{D}$ -stabilization is proposed, as enunciated in Theorem 3.5.

**Theorem 3.5.** *Assuming that there exists a state feedback gain matrix  $K(\alpha)$ , defined in terms of its vertices  $K_i$  as in (3.22), such that  $A(\alpha) + B(\alpha)K(\alpha)$  is robustly stable, then there exists a static output feedback gain  $L$  such that  $A(\alpha) + B(\alpha)LC(\alpha)$  is robustly  $\mathcal{D}$ -stable, ensuring the closed-loop pole placement inside a circle with radius  $r_2$  and with center in  $(-q_2, 0)$ , where  $q_2 = r_2 + \gamma_2$ , if there exist symmetric matrices  $P_i > 0$  and matrices  $F_i, G_i, H$  and  $J$  such that (3.26), (3.27), and (3.28) are satisfied.*

$$\begin{bmatrix} A_i' F_i' + F_i A_i + K_i' B_i' F_i' + F_i B_i K_i + \gamma_2 P_i (2r_2 + \gamma_2) & * & * \\ (r_2 + \gamma_2) P_i - F_i' + G_i A_i + G_i B_i K_i & P_i - G_i - G_i' & * \\ B_i' F_i' + J C_i - H K_i & B_i' G_i' & -H - H' \end{bmatrix} < 0 \quad (3.26)$$

for  $i = 1, 2, \dots, N$ .

$$\begin{bmatrix} \Omega_{11} \\ \Omega_{21} \\ (B_i' + B_j') F_i' + B_i' F_j' + J(2C_i + C_j) - H(2K_i + K_j) \end{bmatrix}$$

$$\begin{bmatrix} * & * \\ 2P_i + P_j - 2(G_i + G'_i) - G'_j - G_j & * \\ (B'_i + B'_j)G'_i + B'_iG'_j & -3H - 3H' \end{bmatrix} < 0 \quad (3.27)$$

for  $i = 1, \dots, N$ ,  $j = 1, \dots, N$ , with  $i \neq j$ , where

$$\begin{aligned} \Omega_{11} = & \left[ (A'_i + A'_j)F'_i + A'_iF'_j + (K'_iB'_i + K'_iB'_j)F'_i \right. \\ & \left. + K'_jB_iF'_i \right] + (\bullet)' + \gamma_2(2P_i + P_j)(2r_2 + \gamma_2) \end{aligned}$$

and

$$\begin{aligned} \Omega_{21} = & (r_2 + \gamma_2)(2P_i + P_j) - 2F'_i - F'_j + G_i(A_i + A_j) \\ & + G_jA_i + G_i(B_iK_j + B_jK_i) + G_jB_iK_i. \end{aligned}$$

$$\begin{bmatrix} \Lambda_{11} & * & * \\ \Lambda_{21} & \Lambda_{22} & * \\ \Lambda_{31} & \Lambda_{32} & -6H - 6H' \end{bmatrix} < 0 \quad (3.28)$$

for  $i = 1, \dots, N-2$ ,  $j = i+1, \dots, N-1$ , and  $k = j+1, \dots, N$  where

$$\begin{aligned} \Lambda_{11} = & \left[ (A'_i + A'_j)F'_k + (A'_i + A'_k)F'_j + (A'_j + A'_k)F'_i \right. \\ & \left. + (K'_iB'_j + K'_jB'_i)F'_k + (K'_iB'_k + K'_kB'_i)F'_j + (K'_jB'_k + K'_kB'_j)F'_i \right] \\ & + (\bullet)' + \gamma_2 2(P_i + P_j + P_k)(2r_2 + \gamma_2), \end{aligned}$$

$$\begin{aligned} \Lambda_{21} = & 2(r_2 + \gamma_2)(P_i + P_j + P_k) - 2(F'_i + F'_j + F'_k) \\ & + G_i(A_j + A_k) + G_j(A_i + A_k) + G_k(A_i + A_j) \\ & + G_i(B_jK_k + B_kK_j) + G_j(B_iK_k + B_kK_i) + G_k(B_iK_j + B_jK_i), \end{aligned}$$

$$\begin{aligned} \Lambda_{31} = & (B'_i + B'_j)F'_k + (B'_i + B'_k)F'_j + (B'_j + B'_k)F'_i \\ & + 2J(C_i + C_j + C_k) - 2H(K_i + K_j + K_k), \end{aligned}$$

$$\Lambda_{22} = 2(P_i + P_j + P_k) + 2(-G_i - G_j - G_k) + (\bullet)',$$

and

$$\Lambda_{32} = (B'_i + B'_j)G'_k + (B'_i + B'_k)G'_j + (B'_j + B'_k)G'_i.$$

In the affirmative case, the robust static output-feedback gain is given by  $L = H^{-1}J$ .

*Proof.* Assume that (3.26)-(3.28) hold. Then, immediately, we see that (3.26) implies in

$H + H' > 0$ , which guarantees the existence of the inverse of  $H$  (BOYD *et al.*, 1994).

Now, remembering that  $\sum_{i=1}^N \alpha_i = 1$ , and by multiplying (3.26) by  $\alpha_i^3$  and summing for  $i = 1, \dots, N$ , by multiplying (3.27) by  $\alpha_i^2 \alpha_j$  and summing for  $i = 1, \dots, N, j = 1, \dots, N$ , with  $i \neq j$ , and by multiplying (3.28) by  $\alpha_i \alpha_j \alpha_k$ , and summing for  $i = 1, \dots, N-2, j = i+1, \dots, N-1$ , and  $k = j+1, \dots, N$ , we have that

$$\begin{bmatrix} A'(\alpha)F(\alpha)' + F(\alpha)A(\alpha) + K(\alpha)'B'(\alpha)F(\alpha)' + F(\alpha)K(\alpha) + \gamma_2 P(\alpha)(2r_2 + \gamma_2) \\ (r_2 + \gamma_2)P(\alpha) - F(\alpha)' + G(\alpha)A(\alpha) + G(\alpha)B(\alpha)K(\alpha) \\ B(\alpha)'F(\alpha)' + JC(\alpha) - HK(\alpha) \\ * & * \\ P(\alpha) - G(\alpha) - G(\alpha)' & * \\ B'(\alpha)G(\alpha)' & -H - H' \end{bmatrix} < 0, \quad (3.29)$$

also holds.

The rest of the proof follows similarly as for Theorem 3.2, and it is therefore omitted.  $\square$

In Theorem 3.5, by considering a parameter-dependent first-stage design, we allow for the use of different matrices  $K_i$  for each polytope vertex. Despite the fact that they are not direct optimization variables in the second stage, they introduce an artificial degree of freedom, as each one of them are intrinsically associated to its respective polytope vertex. In fact, whenever a solution using Theorem 3.2 exists, Theorem 3.5 will also have a solution. This result is stated in Theorem 3.6.

**Theorem 3.6.** *Suppose that there exist symmetric matrices  $P_i$  and matrices  $F_i, G_i, H, J$ , and  $K$  such that LMI conditions (3.8) and (3.9) in Theorem 3.2 hold for  $i = 1, \dots, N$ , and for  $i = 1, \dots, N-1$  and  $j = i+1, \dots, N$ , respectively. Then, the LMI conditions (3.26) - (3.28) in Theorem 3.5 also hold.*

*Proof.* Assume that  $K_i = K$ . Then, we have that (3.26) becomes (3.8), which holds for  $i = 1, \dots, N$  as our initial hypothesis.

Additionally, one can see that (3.27) becomes

$$\begin{bmatrix} \Delta_{11} \\ \Delta_{21} \\ (B'_i + B'_j)F'_i + B'_i F'_j + J(2C_i + C_j) - 3HK \\ * & * \\ 2P_i + P_j - 2(G_i + G'_i) - G'_j - G_j & * \\ (B'_i + B'_j)G'_i + B'_i G'_j & -3H - 3H' \end{bmatrix} < 0 \quad (3.30)$$

for  $i = 1, \dots, N$ ,  $j = 1, \dots, N$ , with  $i \neq j$ , where

$$\Delta_{11} = \left[ (A'_i + A'_j)F'_i + A'_i F'_j + (K' B'_i + K' B'_j)F'_i + K' B'_i F'_i \right] + (\bullet)' + \gamma_2(2P_i + P_j)(2r_2 + \gamma_2)$$

and

$$\begin{aligned} \Delta_{21} = (r_2 + \gamma_2)(2P_i + P_j) - 2F'_i - F'_j + G_i(A_i + A_j) \\ + G_j A_i + G_i(B_i K + B_j K) + G_j B_i K. \end{aligned}$$

Observe that (3.30) can be decomposed as a sum of two matrix blocks

$$\begin{aligned} & \begin{bmatrix} A'_i F'_i + F_i A_i + K' B'_i F'_j + F_i B_i K + \gamma_2 P_i (2r_2 + \gamma_2) & * & * \\ (r_2 + \gamma_2)P_i - F'_i + G_i A_i + G_i B_i K & P_i - G_i - G'_i & * \\ B'_i F'_i + J C_i - H K & B'_i G'_i & -H - H' \end{bmatrix} + \\ & \begin{bmatrix} \Sigma_{ij} \\ (r_2 + \gamma_2)(P_i + P_j) - F'_i + G_i A_j + G_i B_j K - F'_j + G_j A_i + G_j B_i K \\ B'_i F'_j + J C_i + J C_j + B'_j F'_i - 2H K \\ * & * & * \\ P_i + P_j - G'_i - G_i - G'_j - G_j & * & * \\ B'_i G'_j + B'_j G'_i & -2H - 2H' \end{bmatrix} < 0, \quad (3.31) \end{aligned}$$

for  $i = 1, \dots, N$ ,  $j = 1, \dots, N$ , with  $i \neq j$ , where

$$\begin{aligned} \Sigma_{11} = A'_i F'_j + F_i A_j + K' B'_i F'_j + F_i B_j K + \gamma_2 P_i (2r_2 + \gamma_2) \\ + A'_j F'_i + F_j A_i + K' B'_j F'_i + F_j B_i K + \gamma_2 P_j (2r_2 + \gamma_2). \end{aligned}$$

Also, note that the first term in (3.31) is negative definite, since (3.8) holds for  $i = 1, \dots, N$ . Moreover, note that the second term in (3.31) is also negative definite, since (3.9) holds for  $i = 1, 2, \dots, N - 1$  and  $j = i + 1, \dots, N$ , as our initial hypothesis. Thus, (3.30) holds.

Following the same argument, we can prove that (3.28) also holds for  $i = 1, \dots, N - 2$ ,  $j = i + 1, \dots, N - 1$ , and  $k = j + 1, \dots, N$  when (3.8) holds for  $i = 1, \dots, N$ , by splitting it into a sum of three matrix blocks.

Therefore, if Theorem 3.2 LMI are feasible, then LMI (3.26) - (3.28) in Theorem 3.5 will also be feasible for at least one set of matrices  $K_i$ .  $\square$

At this point, it is important to highlight that the choice of design parameters that define the clustering region should be made considering the performance requirements of each particular problem. Note that with smaller values for the circle radius,  $r_2$ , we have a

more specific eigenvalue assignment, with the addition of smaller imaginary components for complex conjugate eigenvalues, implying on oscillation modes with reduced amplitude<sup>1</sup>. Moreover, by adjusting the parameter  $\gamma_2$  we set a lower bound on the magnitude of real part of the system eigenvalues. For higher values of  $\gamma_2$ , the closed-loop system tends to present a fast transient response, with a trade-off in higher demands of control signal, since the controller matrix entries tends to increase proportionally with the magnitude of the real part of the system eigenvalues. This becomes clear by observing that  $\gamma_2$  is associated to the closed-loop system decay rate (BOYD *et al.*, 1994).

At last, it should be clear that only the second-stage design setting ( $\gamma_2$  and  $r_2$ ) will effectively impact on closed-loop response, as they are intrinsically related to the SOF controller, which will be indeed implemented in practice. Of course, the final transient response depends on the actual eigenvalue clustering, being  $\gamma_2$  and  $r_2$  only established bounds for the assignment region. In their turn, the first-stage parameters will only impact in the feasibility of the SF design stage. For different choices of  $\gamma_1$  and  $r_1$ , a different SF robust controller can be computed. As the second stage depends on the given matrix  $K$  designed in the first stage, a search on the parameters  $\gamma_1$  and  $r_1$  can be employed in order to achieved feasibility in the SOF design stage, if synthesis fails for a particular  $K$ .

### 3.1.3 ILLUSTRATIVE EXAMPLES

In this section, we present a series of examples to illustrate the controller synthesis procedure, as well as to demonstrate the advantages of the new proposed strategies. In Section 3.1.4, a practical control design for an active suspension system is also presented, demonstrating the practical applicability of the proposed method. In all presented examples, the LMIs were programmed with MATLAB software, and solved via YALMIP interface (LOFBERG, 2004), using the SeDuMi solver (STURM, 1999).

**Example 3.1** Consider an hypothetical uncertain system, described in terms of a polytope with two vertices as

$$A_1 = \begin{bmatrix} 2.439 & 0.683 \\ 0.933 & -2.787 \end{bmatrix} \quad B_1 = \begin{bmatrix} 0.607 \\ 0.629 \end{bmatrix}$$

and,

$$A_2 = \begin{bmatrix} 0.102 & 1.223 \\ -9.614 & 2.027 \end{bmatrix} \quad B_2 = \begin{bmatrix} 0.370 \\ 0.575 \end{bmatrix}.$$

For applying the SOF control, we assume that only the state variable  $x_1$  is available for measurement. Therefore, the output matrices for each vertex are defined as  $C_1 = C_2 = [1 \quad 0]$ .

---

<sup>1</sup>It is important to acknowledge the statement given in Remark 2.2.

With the intent of comparing the conservativeness associated with each strategy depicted in last section, we performed a feasibility analysis. This study consisted in attempting to design a robust SOF controller,  $L$ , via two-stage strategy for the considered uncertain system. The gain matrix  $L$  should guarantee a closed-loop pole placement inside a  $\mathcal{D}$ -region with specifications defined within the ranges  $0 < r \leq 40$  and  $0 \leq \gamma \leq 3$ , respectively. More clearly, the LMI conditions associated to each two-stage strategy:

- Strategy 1: Theorem 3.1 (SF  $\alpha$ -stabilization), and then Theorem 3.2
- Strategy 2: Theorem 3.3 (SF  $\mathcal{D}$ -stabilization), and then Theorem 3.2
- Strategy 3: Theorem 3.4 (PDSF<sup>2</sup>  $\mathcal{D}$ -stabilization), and then Theorem 3.5

were tested on 400 different control problems in terms of different pairs of parameters  $(r, \gamma)$ , obtained by gridding the aforementioned ranges for  $r$  and  $\gamma$  into a 20-element grid space. Note that each pair  $(r, \gamma)$  defines a different  $\mathcal{D}$ -region for pole placement, which represents a whole different control problem.

**Remark 3.1.** *Naturally, as Theorem 3.1, used in Strategy 1, does not regard the specification of the value of  $r_1$ , only the circle distance parameter  $\gamma_1$  is considered. Moreover, when testing Strategies 2 and 3, for simplicity only, the desired circular region was identically specified in both design stages, i.e.  $\gamma_1 = \gamma_2 = \gamma$  and  $r_1 = r_2 = r$ . The specification of  $\gamma_1 = \gamma$  when using Theorem 3.1 in Strategy 1 is set to provide the best possible condition for a fair comparison. Remind that in Theorems 3.3 and 3.4,  $\gamma_1$  is associated to the minimum distance that the closed-loop eigenvalues should be placed away from the imaginary axis in the left half-plane.*

The feasibility results obtained with each strategy, for each pair of design parameters  $(r, \gamma)$ , are presented in Figure 3.1. The symbols ( $\square$ ,  $\circ$ , and  $\triangle$ ) in the chart indicates that a particular strategy has succeeded in obtaining a  $\mathcal{D}$ -stabilizing gain  $L$  for the corresponding pair  $(r, \gamma)$ . Conversely, when no strategy was able to find a solution, no mark is plotted. Individually, the mark  $\square$  indicates success of Strategy 1, while Strategy 2 feasible points are represented by both  $\square$  and  $\circ$  marks, and the set of all three symbols are associated to the triumphs of Strategy 3 in yielding the desired SOF controller.

As one can observe, the feasibility success rate is considerably enhanced by also imposing  $\mathcal{D}$ -stability constraints in the first stage (Strategies 2 and 3). This can be inferred since an SOF feasible solution was able to be obtained for a significant greater number of cases when compared to Strategy 1 results, which are based on a simpler SF design in the first stage, regarding  $\alpha$ -stabilization constraints.

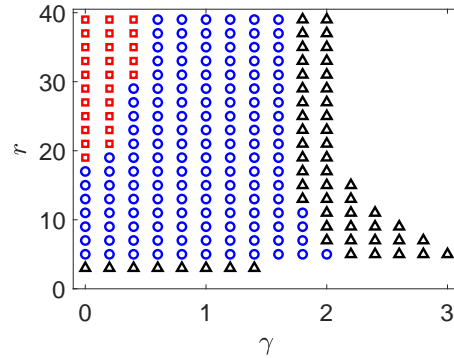
In fact, as shown in Figure 3.1, while employing Strategy 1 (Theorem 3.1 in the first stage and Theorem 3.2 in the second stage), feasibility was not able to be achieved

---

<sup>2</sup>parameter-dependent state-feedback



Figure 3.1 - Feasibility region obtained in Example 3.1 using: Strategy 1 ( $\square$ ); Strategy 2 ( $\square$  and  $\circ$ ); and Strategy 3 ( $\square$ ,  $\circ$ , and  $\triangle$ ).



Source: Author's own results.

when specifying a radius  $r$  smaller than about 20 for pole placement in the second-stage design. Furthermore, the highest value for  $\gamma$  with feasibility success in the second stage was about 0.5, which shows that when  $\mathcal{D}$ -stability is not considered in the first stage the enforcement of a lower bound on the system decay rate, associated to the value of  $\gamma$ , is also restrained. In practice, this implies that a more precise pole placement region – or, equivalently, transient performance requirements – can be specified when applying Strategy 2 or 3 (both stages executed considering  $\mathcal{D}$ -stabilization constraints).

The presented observation empirically indicates that considering  $\mathcal{D}$ -stability constraints also in the first stage might yield better feasibility performance in the SOF two-stage context. This, in fact, represents an important feature of the contributions presented in this work. Often, in previous papers on the two-stage SOF design framework, the first-stage SF design is not performed considering the same constraints as in the second-stage (AGULHARI; OLIVEIRA; PERES, 2012, 2010a). Even when similar design requirements are imposed on both stages, no further observation on the necessity of this coupled setting is presented (AGULHARI; OLIVEIRA; PERES, 2010b). However, as shown in the present study, despite that an stabilizing SF gain suffices for implementing the two-stage method for SOF control design, there might be a more suitable choice for the first-stage SF design method.

Additionally, it is possible to observe that Strategy 3, which consists in designing a parameter-dependent  $\mathcal{D}$ -stabilizing first-stage gain via Theorem 3.4 and using the obtained set of matrices  $K_i$  as input information to Theorem 3.5 second-stage LMIs led to the best performance of all three evaluated strategies, in terms of feasibility. This indicates that Theorem 3.5 LMI indeed consists of less conservative SOF design conditions. In fact, the observed results are a reflex of the relaxation certificate provided through Theorem 3.6, which states that whenever Theorem 3.2 (which makes use of a robust state-feedback

gain matrix  $K$  as input data) have a solution, Theorem 3.5 (which in turn considers a parameter-dependent  $\mathcal{D}$ -stabilizing state-feedback gain matrix  $K(\alpha)$  as input matrix) will also yield a feasible solution for some set of matrices  $K_i, i = 1, \dots, N$ .

As seen, both proposed methods (Strategies 2 and 3) are able to outperform the results achieved with Strategy 1. The common factor in our proposed methods is the enforcement of  $\mathcal{D}$ -stabilizing design constraints, as considered in the final design stage. This observation reinforces the idea that the two-stage method may indeed yield a better feasibility performance when both stages are executed accordingly.

Finally, it is important to stress the contrast between Strategies 2 and 3. Despite that both of them seem to be interesting solutions for the  $\mathcal{D}$ -stabilization problem in the SOF framework, Strategy 2 has the advantage of being presented in terms of a lesser number of LMI rows when compared to Strategy 3 (especially in the second-stage design). As well-known, the complexity associated to LMI solvers are directly linked to the numbers of variables and LMI rows (STURM, 1999), indicating that Strategy 2 leads to a lighter computational burden. However, the designer might consider employing Strategy 3 whenever the control requirements exerts more severe constraints (*e.g.* higher minimum decay rate, as illustrated in the feasibility test results in Figure 3.1), and additional flexibilization is required for obtaining a feasible solution for the problem, justifying the more complex LMI constraints of Theorem 3.5 in Strategy 3.

**Example 3.2** This second example has the purpose of illustrating the details of the controller synthesis procedure associated to the proposed strategies, as well as pointing out its the effects of the considered pole placement constraints. To this end, consider an uncertain model of the row axis dynamics of a missile, adapted from Santos, Pellanda and Simões (2018). Such dynamics are modeled as

$$\begin{aligned} \dot{x}(t) &= (A + 0.75\delta_1 A_\delta)x(t) + (B + \delta_2 B_\delta)u(t) \\ y(t) &= Cx(t), \end{aligned} \quad (3.32)$$

where

$$A = \begin{bmatrix} -180 & 0 & 0 & 0 & 0 \\ 0 & -180 & 0 & 0 & 0 \\ -21.23 & 0 & -0.6888 & -14.7 & 0 \\ 256.7 & 0 & 122.6 & -1.793 & 0 \\ -52.33 & 304.7 & 0 & 36.7 & -9.661 \end{bmatrix}, \quad A_\delta = \begin{bmatrix} 27 & 0 & 0 & 0 & 0 \\ 0 & 27 & 0 & 0 & 0 \\ 21.2 & 0 & 0.6888 & 14.96 & 0 \\ 38.6 & 0 & 122.6 & 0 & 0 \\ 52.4 & 304.8 & 0 & 36.8 & 9.66 \end{bmatrix},$$

$$B = \begin{bmatrix} 180 & 0 \\ 0 & 180 \\ 0 & 0 \\ 256.7 & 0 \\ 0 & 0 \end{bmatrix}, \quad B_\delta = \begin{bmatrix} 40.5 & 0 \\ 0 & 40.5 \\ 0 & 0 \\ 57.9 & 0 \\ 0 & 0 \end{bmatrix}, \quad C = \begin{bmatrix} 0 & 0 & 1 & 0 & 0 \\ 0 & 0 & 0 & 1 & 0 \\ 0 & 0 & 0 & 0 & 1 \end{bmatrix},$$

and  $\delta_{1,2} \in [-1, 1]$  represent the uncertain parameters. The state vector is defined as  $x = [\delta_r \ \delta_p \ r \ n_y \ p]'$ , whose entries are the yaw and roll control surface deflection, the yaw rate, the yaw acceleration and the roll rate, respectively. The control input vector is  $u = [\delta_{rc} \ \delta_{pc}]'$ , where  $\delta_{rc}$  and  $\delta_{pc}$  are the yaw and roll control commands, respectively.

Given the presented model, the missile uncertain row axis dynamics can be put into a polytopic representation in terms of four vertices, defined by the combination of the maximum and minimum values that  $\delta_{1,2}$  can assume. For the control design, we assume the requirement of a circular pole placement region with radius  $r = 100$  and  $\gamma = 10$ .

One can verify that Strategy 1 fails in providing a solution for the problem at hand. Unfortunately, Strategy 2 also does not yield a feasible solution. However, by considering Strategy 3, one can obtain in the first stage (via Theorem 3.4 with  $r_1 = 100$  and  $\gamma_1 = 10$ ), parameter-dependent gain matrix  $K(\alpha)$  with vertices

$$K_1 = \begin{bmatrix} -0.2755 & 0.0038 & 0.5345 & -0.3238 & -0.0019 \\ -0.0681 & 0.5071 & -0.1403 & -0.0462 & -0.0839 \end{bmatrix},$$

$$K_2 = \begin{bmatrix} -0.3241 & 0.0004 & 0.1458 & -0.2073 & 0.0019 \\ -0.1594 & -0.0778 & -0.1806 & -0.1128 & -0.0999 \end{bmatrix},$$

$$K_3 = \begin{bmatrix} -0.1593 & -0.0029 & 0.3609 & -0.2159 & -0.0005 \\ -0.0424 & 0.3935 & -0.0848 & -0.0234 & -0.0502 \end{bmatrix},$$

and

$$K_4 = \begin{bmatrix} -0.2154 & 0.0030 & 0.0516 & -0.1225 & 0.0018 \\ -0.1126 & -0.0864 & -0.1207 & -0.0771 & -0.0613 \end{bmatrix}.$$

Then, by feeding these gains to the second stage, and solving Theorem 3.5 LMI conditions with  $r_2 = 100$  and  $\gamma_2 = 10$ , it is possible to obtain a robust SOF gain matrix

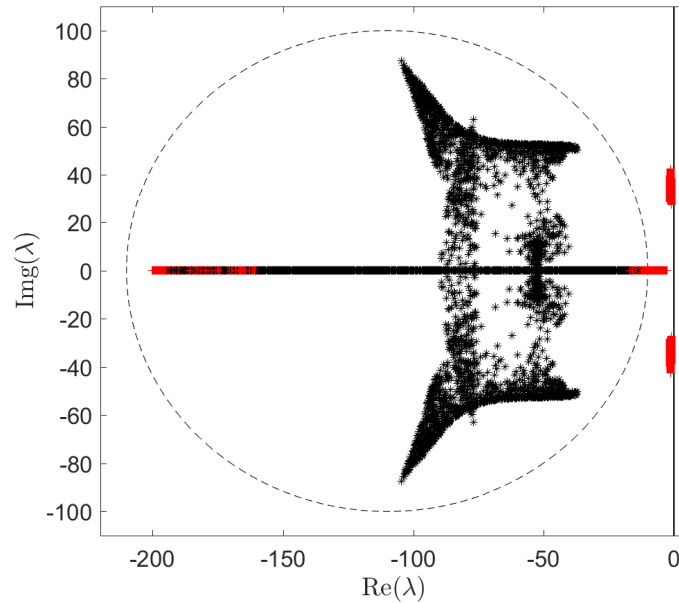
$$L = \begin{bmatrix} 0.2547 & -0.1599 & 0.0072 \\ -0.1641 & -0.0487 & -0.0874 \end{bmatrix}. \quad (3.33)$$

Firstly, we see the benefits of Strategy 3 over the other two strategies. The less conservative nature of the combined first and second stages LMIs proposed in this work (Theorems 3.4 and 3.5) is highlighted, as they made possible obtaining a feasible solution when the other two strategies have failed.

We now evaluate the practical impact of the designed robust SOF controller (3.33). The eigenvalues of the closed-loop system with the designed robust SOF gain are allocated as presented in Figure 3.2, obtained from 1000 randomly generated samples of the closed-loop system associated to different values that the uncertain parameters  $\delta_{1,2}$  may assume, according to the specified range (see the black marks \* in Figure 3.2). As one

can observe, all eigenvalues are placed inside the specified region, attesting for the efficacy of the proposed method. The open-loop ( $u(t) = 0$ ) eigenvalue configuration (see the red marks  $+$  in Figure 3.2) is also presented with illustration purposes, showing that the designed controller is indeed able to promote a drastic relocation of the system eigenvalue assignment.

Figure 3.2 - Cloud of open ( $+$ ) and closed-loop ( $*$ ) eigenvalues of the uncertain row axis dynamics for arbitrary values of uncertain parameters within the specified range.



Source: Author's own results.

**Example 3.3** This third example is dedicated to show the benefits of performing a robust SOF control design considering  $\mathcal{D}$ -stability conditions, using the same missile row axis dynamics presented in Example 3.2. With such intent, we present the time response of the row rate  $p$  and the correspondent row control command  $\delta_{pc}$  in Figures 3.3 and 3.4, respectively, starting from the initial condition  $x(0) = [0 \ 0 \ 0 \ 1 \ 0]'$ , for 30 different randomly defined values of  $\delta_1$  and  $\delta_2$  in (3.32). Note that by presenting simulation results for distinct values of  $\delta_1$  and  $\delta_2$ , we are able to observe the dynamic response of the closed-loop system for different possible models among the uncertainty polytope.

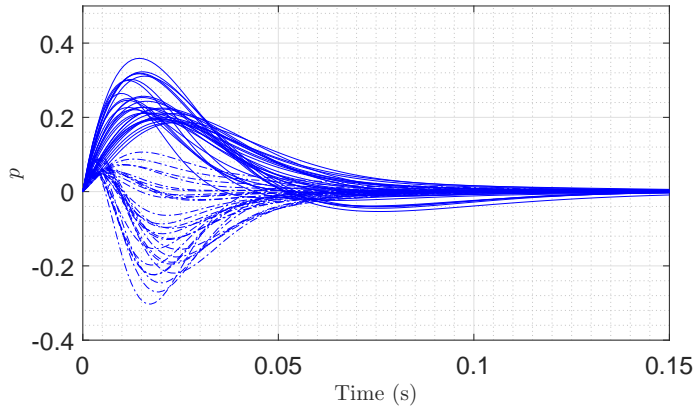
The solid lines refer to the dynamic behavior of the system and its control signal when the robust SOF controller (3.33) is used for composing the feedback loop. For comparison, we obtained a second gain matrix  $L$ , using the same strategy as in Example 3.2, but with a pole placement region with radius  $r = 250$  and distance  $\gamma = 10$ . In those terms, using

Theorem 3.4 and Theorem 3.5, the obtained gain matrix is

$$L = \begin{bmatrix} 0.9128 & -0.3476 & -0.0130 \\ 0.4497 & -0.2307 & -0.1030 \end{bmatrix}. \quad (3.34)$$

The dynamic response associated to SOF controller (3.34) is represented by the dash-dot lines.

Figure 3.3 - Row rate time response with controllers (3.33) (solid) and (3.34) (dash-dot) for 30 different random values of  $\delta_1$  and  $\delta_2$  in (3.32).

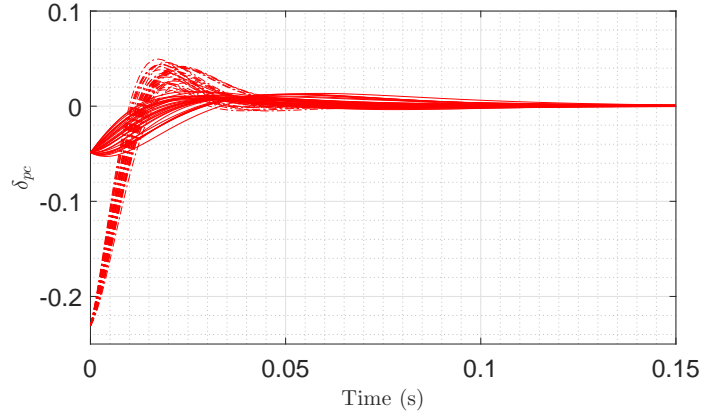


Source: Author's own results.

One may observe that with a less restrictive placement region (bigger value for the circle radius), the row rate time response with controller (3.34) (dash-dot) has a slight shorter settling time when compared to the dynamic shown with controller (3.33) (solid). This happens due to the larger value of  $r$  in the second design, which allows for the closed-loop eigenvalues to be placed farther from the imaginary axis, and then, implying in a faster response. However, as one can see in Figure 3.4, this comes at the price of a significant higher amplitude in the row control command signal for controller (3.34) (solid) when compared to controller (3.33) case (dash-dot).

Indeed, although improving performance is a desired aspect in control design, it is also important to avoid excessively high amplitudes in control signal for practical applications. In sum, it is of great interest to be able to require a specific pole placement region. In fact, with a smaller radius specification, controller (3.33) is able to provide good dynamic response (when comparable to the second studied case), but also limiting the eigenvalues distance from the imaginary axis, which in turn, impacts on smaller control signal amplitude.

Figure 3.4 - Row control command with controllers (3.33) (solid) and (3.34) (dash-dot) for 30 different random values of  $\delta_1$  and  $\delta_2$  in (3.32).



Source: Author's own results.

### 3.1.4 PRACTICAL IMPLEMENTATION: ACTIVE SUSPENSION SYSTEM

In this section, we present the design and the practical implementation results of a robust SOF controller for  $\mathcal{D}$ -stabilization of a bench scale active suspension manufactured by QUANSER<sup>®</sup>.

#### System Description

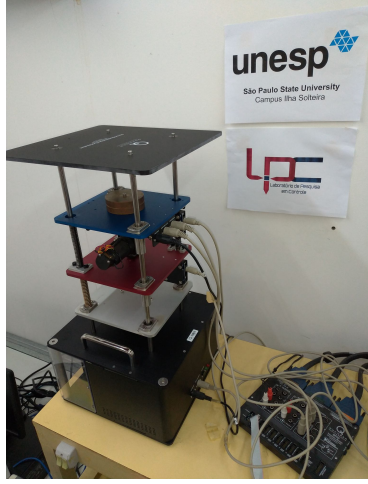
The QUANSER<sup>®</sup> Active Suspension system (Figure 3.5a) emulates a 1/4 model of a vehicle. In Figure 3.5b schematic diagram,  $M_s$  is the sprung mass, representing 1/4 of vehicle body (load) mass,  $M_{us}$  is the unsprung mass that represents the tire of the quarter-car model, and  $k_s$ ,  $b_s$ ,  $k_{us}$ , and  $b_{us}$ , are the springs and dampers in the model assembly.  $z_{us}(t)$  and  $z_s(t)$  are the unsprung and sprung mass positions related to each shown reference level.

The control objective is to mitigate the effects caused by the road surface ( $z_r(t)$ ) on the suspension travel and road handling of the car. In the considered model, these performance parameters are related to the relative movement between the vehicle body and tire ( $z_s - z_{us}$ ), and to the displacement between the tire and the road surface ( $z_{us} - z_r$ ), respectively. This goal may be achieved by properly applying a control command to drive a DC motor that acts as the active element in the suspension system (*i.e.* actuator), which in turn exerts a force  $F_c(t)$  to control the plates displacements, through a set of capstan cables attached to the plates and to the DC motor axis.

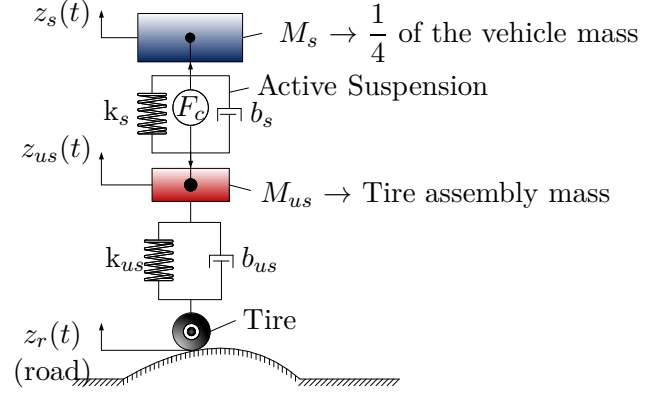
We assume that the sprung mass is an uncertain parameter lying within the interval  $1.455 \text{ kg} \leq M_s \leq 2.45 \text{ kg}$ . Moreover, we take into account that the actuator, which

Figure 3.5 - Active suspension system experimental module and model diagram.

(a) QUANSER<sup>®</sup> Active Suspension System installed at FEIS–UNESP Control Research Laboratory.



(b) Schematic diagram of the QUANSER<sup>®</sup> Active Suspension System.



Sources: (a) Own author; (b) Adapted from Silva *et al.* (2012).

applies the control signal  $u(t)$ , is susceptible to present a fault in power delivery to the DC motor, implying in the attenuation of the control signal. In this example, we assume that a maximum power fault of 30% in attenuation of the control signal is possible to occur.

This scenario was mathematically modeled by considering a second uncertain parameter  $\rho$ , such that  $0.7 \leq \rho \leq 1$ , which affects all entries of the input matrix, impressing the control signal attenuation due to the power failure on the system dynamics, similar as presented in Llins *et al.* (2017). Furthermore, it is assumed that only two of the four system state variables are available for measurement ( $x_2$  and  $x_4$ ).

In (3.35), we have a state space model for modeling the described dynamics of the active suspension system.

$$\dot{x}(t) = \begin{bmatrix} 0 & 1 & 0 & -1 \\ \frac{-k_s}{M_s} & \frac{-b_s}{M_s} & 0 & \frac{b_s}{M_s} \\ 0 & 0 & 0 & 1 \\ \frac{k_s}{M_{us}} & \frac{b_s}{M_{us}} & \frac{-k_{us}}{M_{us}} & \frac{-(b_s+b_{us})}{M_{us}} \end{bmatrix} x(t) + \begin{bmatrix} 0 \\ \frac{\rho}{M_s} \\ 0 \\ \frac{-\rho}{M_{us}} \end{bmatrix} u(t),$$

$$y(t) = \begin{bmatrix} 0 & 1 & 0 & 0 \\ 0 & 0 & 0 & 1 \end{bmatrix} x(t), \quad (3.35)$$

where state and input vectors are defined as

$$x(t) = \begin{bmatrix} z_s(t) - z_{us}(t) \\ \dot{z}_s(t) \\ z_{us}(t) - z_r(t) \\ \dot{z}_{us}(t) \end{bmatrix} \quad \text{and} \quad u(t) = F_c(t). \quad (3.36)$$

The chosen state variables allows for directly describing the dynamics that are related to the practical performance parameters of interest (*i.e* road handling and suspension travel).

Based on data presented in Table 3.1, and considering two uncertain parameters, the active suspension system may be represented as a convex combination of four vertices, defined according to the matrices

$$A_1 = A_3 = \begin{bmatrix} 0 & 1 & 0 & -1 \\ -618.56 & -5.1546 & 0 & 5.1546 \\ 0 & 0 & 0 & 1 \\ 900 & 7.5 & -2500 & -12.5 \end{bmatrix},$$

$$A_2 = A_4 = \begin{bmatrix} 0 & 1 & 0 & -1 \\ -367.35 & -3.0612 & 0 & 3.0612 \\ 0 & 0 & 0 & 1 \\ 900 & 7.5 & -2500 & -12.5 \end{bmatrix},$$

$$B_1 = \begin{bmatrix} 0 \\ 0.6873 \\ 0 \\ -1 \end{bmatrix}, \quad B_2 = \begin{bmatrix} 0 \\ 0.4082 \\ 0 \\ -1 \end{bmatrix}, \quad B_3 = \begin{bmatrix} 0 \\ 0.4811 \\ 0 \\ -0.7 \end{bmatrix}, \quad B_4 = \begin{bmatrix} 0 \\ 0.2857 \\ 0 \\ -0.7 \end{bmatrix}, \quad \text{and}$$

$$C_1 = C_2 = C_3 = C_4 = \begin{bmatrix} 0 & 1 & 0 & 0 \\ 0 & 0 & 0 & 1 \end{bmatrix}.$$

Table 3.1 - Active Suspension Parameters.

| Parameter | Value   | Parameter | Value    |
|-----------|---------|-----------|----------|
| $M_s$     | 2.45 kg | $k_{us}$  | 2500 N/m |
| $M_{us}$  | 1.0 kg  | $b_s$     | 7.5 Ns/m |
| $k_s$     | 900 N/m | $b_{us}$  | 5.0 Ns/m |

Source: Quanser (2009).



### SOF Controller Design

For the control design, we consider that the closed-loop eigenvalues should be placed inside a circle with radius  $r = 75$ , at a minimum distance  $\gamma = 1$  from the imaginary axis.

Employing the two-stage Strategy 3 proposed in this work, we start by designing an parameter-dependent SF controller using Theorem 3.4 with  $r_1 = 75$  and  $\gamma_1 = 1$ . At the synthesis condition, the obtained SF controller gains are

$$K_1 = [770.2326 \quad -19.1608 \quad -207.5085 \quad 38.3978],$$

$$K_2 = [780.8686 \quad -19.2797 \quad -378.2697 \quad 39.4382],$$

$$K_3 = [1.1271 \quad -0.0203 \quad -0.5364 \quad 0.0528] \times 10^3,$$

and

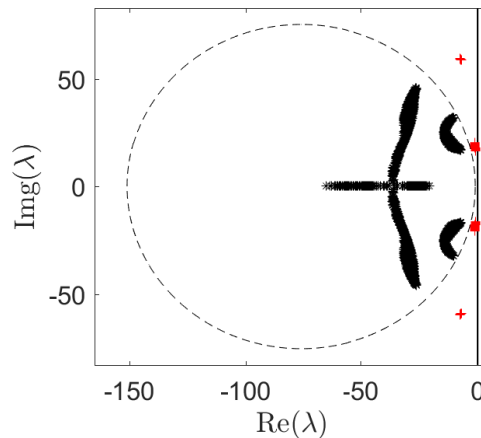
$$K_4 = [1.0220 \quad -0.0423 \quad 0.0335 \quad 0.0679] \times 10^3.$$

Then, using these SF gain matrices in Theorem (3.5), with  $r_2 = 75$  and  $\gamma_2 = 1$ , it is possible to compute the robust SOF gain matrix

$$L = [-64.5847 \quad 44.9564]. \quad (3.37)$$

As showed in Figure 3.6, which is generated in the same fashion as Figure 3.2, the designed SOF controller (3.37) is able to reallocate all system polytope eigenvalues in the required region. Additionally, note that all open-loop eigenvalues are originally positioned outside the specified region, which reaffirms the method's efficacy.

Figure 3.6 - Cloud of open (+) and closed-loop (\*) of the uncertain active suspension system dynamics for arbitrary values of uncertain parameters within the specified range.



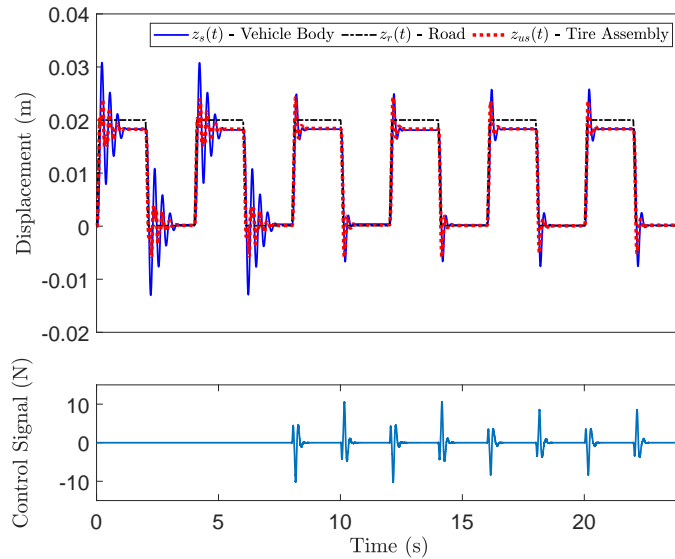
Source: Author's own results.

### Practical Dynamic Performance

The designed robust SOF controller was implemented in practice, on a physical active suspension system available at our laboratory, to evaluate the closed-loop dynamic performance. In the performed tests, the road profile ( $z_r(t)$ ) was set to a square wave with  $0.02\text{ m}$  of amplitude and frequency of  $0.25\text{ Hz}$ . Additionally, a fault of 30% power loss was programmed to occur at  $t = 16\text{ s}$ .

Two tests were performed. In the first one, the sprung mass in the system,  $M_s(\alpha)$ , was set to its minimum value, whereas in the second test  $M_s(\alpha)$  was configured to its maximum value. The observed dynamic behavior is presented in Figures 3.7 and 3.8.

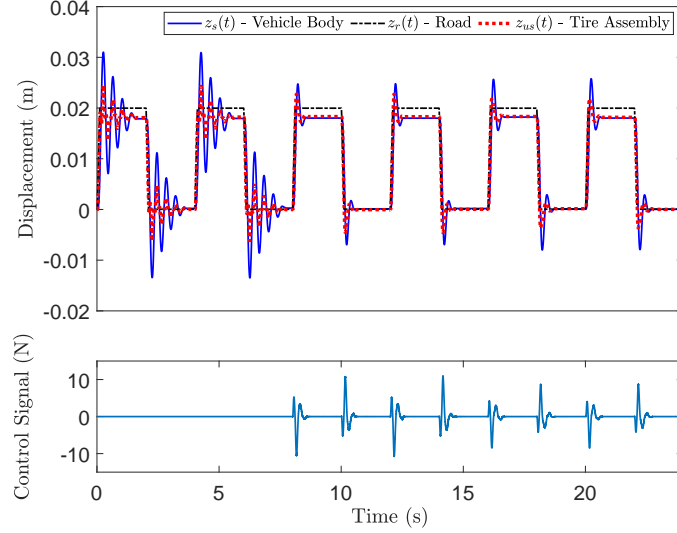
Figure 3.7 - Active suspension dynamic response (upper chart) and control signal (bottom chart) with  $M_s(\alpha) = 1.455\text{ kg}$  in: open-loop (0-8s); closed-loop (8-16s); fault: 30% power loss in the actuator (16-24s).



Source: Author's own results.

The active suspension shows its stable open-loop dynamics in the first 8 seconds of experiment. Clearly, the results show that the system response is improved in the closed-loop scenario, after the SOF control is switched on (after 8 seconds), for both studies cases (minimum and maximum load weigh), as the oscillations experienced in both sprung and unsprung levels (red and blue lines) achieved lower peaks and are extinguished almost immediately. Even in the occurrence of actuator fault (after 16 seconds – 30% in power loss), the system preserves stability and good performance. One may notice the effect of actuator fault in the lower values provided by the actuators when compared to the no-fault case (bottom chart in Figures 3.7 and 3.8).

Figure 3.8 - Active suspension dynamic response (upper chart) and control signal (bottom chart) with  $M_s(\alpha) = 2.45$  kg in: open-loop (0-8s); closed-loop (8-16s); fault: 30 % power loss in the actuator (16-24s).



Source: Author's own results.

**Remark 3.2.** *It is important to mention that the control design strategy proposed in this work is devoted to continuous-time LTI systems. However, the control system of the physical active suspension system used in the practical implementation described in this section is performed by a computer, via MATLAB<sup>®</sup> and Simulink<sup>®</sup> interface. Therefore, in practice, the control signal is generated in a discrete-time fashion. However, by setting a sufficiently high sampling rate in the Simulink<sup>®</sup> control interface, the discrete-time signals provided by the computer can properly emulate the continuous-time signals considered in our control framework.*

## 3.2 GAIN-SCHEDULING CONTROL VIA SOF WITH POLE PLACEMENT CONSTRAINTS

The main subject of this section is related to the extension of the concepts of the  $\mathcal{D}$ -stabilization to the case of linear parameter-varying (LPV) systems. First, the problem to be addressed is properly stated. A discussion is introduced in the sequence, regarding the issues of considering pole placement constraints in LPV control design. Then, new contributions are proposed for the design of gain-scheduled (GS) controllers via SOF considering additional constraints for pole placement in terms of new sufficient LMI conditions. As in the previous section, the GS-SOF controller design is based on the two-stage method. At the end, some examples are presented to illustrate the employment of the proposed strategy.

## 3.2.1 PROBLEM STATEMENT

Consider an LPV system

$$\begin{aligned}\dot{x}(t) &= A(\alpha(t))x(t) + B(\alpha(t))u(t) \\ y(t) &= C(\alpha(t))x(t),\end{aligned}\tag{3.38}$$

where  $x(t) \in \mathbb{R}^n$ ,  $u(t) \in \mathbb{R}^m$ , and  $y(t) \in \mathbb{R}^q$  are the state vector, control and measured output vectors, respectively.  $(A, B, C)(\alpha(t))$  are parameter-varying matrices which describes the time-varying nature of the system, and that can be represented in a polytopic domain  $\mathcal{Q}$  such as

$$\mathcal{Q} = \left\{ (A, B, C)(\alpha(t)) : (A, B, C)(\alpha(t)) = \sum_{i=1}^N \alpha_i(t)(A, B, C)_i, \alpha(t) \in \bar{\lambda}_N, \forall t \geq 0 \right\} \tag{3.39}$$

where  $(A, B, C)_i$  denotes the  $i$ -th of the  $N$  polytope vertices. Moreover,  $\mathcal{Q}$  is parameterized in terms of the vector  $\alpha(t) = (\alpha_1(t), \dots, \alpha_N(t))$ , whose entries  $\alpha_i(t)$  are known time-varying parameters that belong to the unitary simplex set  $\bar{\lambda}_N$ , defined as

$$\bar{\lambda}_N = \left\{ \alpha(t) \in \mathbb{R}^N : \sum_{i=1}^N \alpha_i(t) = 1; \alpha_i(t) \geq 0; i = 1, \dots, N, \forall t \geq 0 \right\}. \tag{3.40}$$

Assume that only the measured output,  $y(t)$ , is available for feedback. Then, design a control law  $u(t) = L(\alpha(t))y(t)$ , where  $L(\alpha(t)) \in \mathbb{R}^{m \times q}$  is a gain-scheduled SOF controller matrix such that the consequent closed-loop system

$$\dot{x}(t) = [A(\alpha(t)) + B(\alpha(t))L(\alpha(t))C(\alpha(t))]x(t), \tag{3.41}$$

is asymptotic stable and the eigenvalues  $\lambda(A_{SOF}(\alpha(t)))$ , for a fixed value of  $\alpha(t) \in \bar{\lambda}_N$ , are placed inside the circular region represented in Figure 2.3, for all  $(A, B, C)(\alpha(t)) \in \mathcal{Q}$ , where

$$A_{SOF}(\alpha(t)) = A(\alpha(t)) + B(\alpha(t))L(\alpha(t))C(\alpha(t)). \tag{3.42}$$

In sum, the problem addressed in this section is related to the stabilization of the LPV system (3.38) under particular constraints of incomplete state measurement and eigenvalue assignment, by means of the design of gain-scheduled controllers.

**Remark 3.3.** *In the GS control framework, the time-varying parameters  $\alpha(t) \in \bar{\lambda}_N$  are assumed to be available for measurement. Therefore, we will have a parameter-dependent control law driven by a gain-scheduled gain matrix  $L(\alpha(t))$ . With that, the entries of the feedback gain matrix will vary accordingly to the instant format of the matrices  $(A, B, C)(\alpha(t))$ , possibly yielding less conservative control synthesis conditions and enhanced transient performance, when compared to a standard robust gain matrix.*

**Remark 3.4.** *In this work, we consider that the designed GS controllers are implemented by means of the convex combination of  $N$  static matrices parameterized according to the time-varying parameters that affect the plant (which are assumed to be measured online). This means that the GS-SOF controller  $L(\alpha(t))$  is implemented in practice as*

$$L(\alpha(t)) = L_1\alpha_1(t) + \cdots + L_N\alpha_N(t),$$

where  $\alpha(t) \in \bar{\Lambda}_N$  and  $L_i$ ,  $i = 1, \dots, N$  are vertex matrices (computed offline, as products of the control design).

### 3.2.2 $\mathcal{D}$ -STABILITY: AN EXTENSION TO LPV SYSTEMS

As mentioned before, the  $\mathcal{D}$ -stability is a concept defined for LTI systems. Therefore, since that in this section we are considering LPV systems, and the addressed problems considers eigenvalue placement constraints in the control design, it is important to properly define some associated concepts.

For that, let us first consider a non-forced version of system (3.38),

$$\dot{x}(t) = A(\alpha(t))x(t). \quad (3.43)$$

It is well-known (BOYD *et al.*, 1994) that the quadratic stability of (3.43) can be analysed by means of the search for a positive definite symmetric matrix  $P \in \mathbb{R}^{n \times n}$  such that

$$A(\alpha(t))'P + PA(\alpha(t)) < 0, \quad (3.44)$$

for all  $\alpha(t) \in \bar{\Lambda}_N$ .

In the particular case of  $\alpha(t) = \alpha$ , we have that (3.43) becomes an uncertain linear time-invariant (LTI) system, and then, it is possible to investigate the system transient performance by verifying if  $A(\alpha)$  has its eigenvalues contained in a specific region of the complex plane (in particular, an LMI region), which is a concept commonly referred as  $\mathcal{D}$ -stability (CHILALI; GAHINET, 1996). Specifically, results for performing such analysis related to the concept of  $\mathcal{D}$ -stability in terms of a circular LMI region have been published in Haddad and Bernstein (1992).

By taking special care, we can directly extend this analysis to LPV systems by observing that for every possible fixed (or “frozen”) values of  $\alpha(t) \in \Lambda_N$ , the system (3.43) will have an equivalent LTI model. In that sense, for each specific value that  $\alpha(t)$  may assume in  $\Lambda_N$ , the matrix  $A(\alpha(t))$  will have a well-defined frozen eigenvalue configuration. Regarding this discussion, we enunciate in Lemma 3.1 an LPV counter part of the LTI circular eigenvalue assignment concept, based on Haddad and Bernstein (1992).

**Lemma 3.1.** *Let  $A(\alpha(t)) \in \mathbb{R}^{n \times n}$  and  $\mathcal{D}(q, r)$  be a circular disk in the complex plane with center  $(-q, 0)$ , radius  $r > 0$  and minimum distance from the imaginary axis  $\gamma > 0$ , with  $q = \gamma + r$ . Then, the frozen eigenvalues of  $A(\alpha(t))$ , obtained for each fixed value of  $\alpha(t) \in \bar{\Lambda}_N$ , are contained in  $\mathcal{D}(q, r)$  if, and only if, there exists a positive definite symmetric matrix  $P \in \mathbb{R}^{n \times n}$  such that*

$$A(\alpha(t))'P + PA(\alpha(t)) + 2\gamma P + \frac{1}{r}(A(\alpha(t)) + \gamma I)'P(A(\alpha(t)) + \gamma I) < 0, \quad (3.45)$$

for every  $\alpha(t) \in \bar{\Lambda}_N$ .

At this point, it is important to discuss the implications of Lemma 3.1. Firstly, we need stress once again that the idea of eigenvalues in LPV systems has to be taken with great care. It is well-known that we cannot infer on an LPV stability properties by only evaluating its eigenvalue configuration (WU, 1974). However, one must observe that the last two terms in (3.45) are necessarily positive definite. Therefore, when (3.45) is satisfied for a symmetric positive definite matrix, note that

$$A(\alpha(t))'P + PA(\alpha(t)) < -2\gamma P - \frac{1}{r}(A(\alpha(t)) + \gamma I)'P(A(\alpha(t)) + \gamma I) < 0$$

is also satisfied, which implies on the quadratic stability of (3.43).

Moreover, at fixed values of the time-varying parameter,  $\alpha(t) = \alpha$ , (3.45) guarantees that the eigenvalues of (3.43) are contained in  $\mathcal{D}(q, r)$  (HADDAD; BERNSTEIN, 1992).

Considering this discussion, in a control synthesis case, we may seek for inducing better transient response relying on Lemma 3.1, by enforcing a specific fixed-parameter eigenvalue assignment, without compromising stability, with the design of  $\mathcal{D}$ -stabilizing<sup>3</sup> gain-scheduled controllers.

### 3.2.3 GAIN-SCHEDULING STATIC OUTPUT FEEDBACK

To carry out the GS-SOF controller  $L(\alpha(t))$  design, the two-stage-based method is once again considered and applied. Following the same concept addressed in the previous section, for completing the first stage we must employ a state-feedback synthesis design. In that sense, by considering the control law  $u(t) = K(\alpha(t))x(t)$ , we extend to the LPV case the LTI conditions presented in Leite, Montagner and Peres (2002), enabling the compute of a GS-SF controller with eigenvalue assignment in a circular LMI region, as proposed in Theorem 3.7.

---

<sup>3</sup>Note that we consider the use of a small abuse of language, regarding the LTI nature of  $\mathcal{D}$ -stability concept.

**Theorem 3.7.** *If there exist a symmetric positive definite matrix  $W \in \mathbb{R}^{n \times n}$  and matrices  $Z_i \in \mathbb{R}^{m \times n}$  such that*

$$\begin{bmatrix} A_i W + W A_i' + B_i Z_i + Z_i' B_i' + 2\gamma_1 W & * \\ W A_i' + Z_i' B_i' + \gamma_1 W & -r_1 W \end{bmatrix} < 0, \quad (3.46)$$

holds for  $i = 1, \dots, r$ , and

$$\begin{bmatrix} (A_i W + B_i Z_j + A_j W + B_j Z_i) + (\bullet)' + 4\gamma_1 W & * \\ W A_i' + Z_i' B_j' + W A_j' + Z_j' B_i' + 2\gamma_1 W & -2r_1 W \end{bmatrix} < 0, \quad (3.47)$$

holds for  $i < j \leq r$ , then  $K_i = Z_i W^{-1}$  are the vertices of the GS-SF controller  $K(\alpha(t))$  that ensures the asymptotic stabilization of  $A(\alpha(t)) + B(\alpha(t))K(\alpha(t))$  and the closed-loop eigenvalues placement, for fixed values of  $\alpha(t)$ , inside the circular region with radius  $r_1$  and center in  $(-q, 0)$ , where  $q = r_1 + \gamma_1$ .

*Proof.* Assume that (3.46) and (3.47) hold. Then, by considering previous well-known results on the multiplication of two parameter-dependent matrices (TANAKA; IKEDA; WANG, 1998), we have that

$$\begin{bmatrix} [A(\alpha(t))W + B(\alpha(t))Z(\alpha(t))] + (\bullet)' + 2\gamma_1 W & * \\ W A(\alpha(t))' + Z(\alpha(t))' B(\alpha(t))' + \gamma_1 W & -r_1 W \end{bmatrix} < 0, \quad (3.48)$$

also holds.

In the sequence, by defining  $A_{SF}(\alpha(t)) = A(\alpha(t)) + B(\alpha(t))K(\alpha(t))$ , with  $K(\alpha(t)) = Z(\alpha(t))W^{-1}$ , and applying the Schur complement leads to

$$A_{SF}(\alpha(t))W + W A_{SF}(\alpha(t))' + 2\gamma_1 W + \frac{1}{r_1} A_{SF}(\alpha(t))W A_{SF}(\alpha(t))' < 0, \quad (3.49)$$

which consists in a dual version of (3.45).  $\square$

Now, we extend the synthesis strategy for the LTI case, given in Theorem 3.5, for completing the second stage and computing the GS-SOF controller  $L(\alpha(t))$  that asymptotically stabilizes (3.41) under closed-loop eigenvalue assignment constraints, to propose new sufficient LMI constraints as stated in Theorem 3.8, which make use of the vertex matrices  $K_i$  derived in the first stage. In the synthesis conditions, the proposed LMIs make possible to retrieve the  $N$  vertices  $L_i$  of the gain matrix  $L(\alpha(t))$ .

**Theorem 3.8.** *Assume that there exists a gain-scheduled state feedback gain matrix  $K(\alpha(t))$  such that  $A_{SF}(\alpha(t))$  is asymptotically stable. If there exist a symmetric matrix*

$P > 0$  and matrices  $F_i$ ,  $G_i$ ,  $H$ , and  $J_i$ , such that, for given vertices  $K_i$  of  $K(\alpha(t))$ ,

$$\begin{bmatrix} (A'_i F'_i + K'_i B'_i F'_i) + (\bullet)' + \gamma_2 P(2r_2 + \gamma_2) & * & * \\ (r_2 + \gamma_2)P - F'_i + G_i A_i + G_i B_i K'_i & P - G_i - G'_i & * \\ B'_i F'_i + J_i C_i - H K'_i & B'_i G'_i & -H - H' \end{bmatrix} < 0 \quad (3.50)$$

holds for  $i = 1, 2, \dots, N$ ,

$$\begin{bmatrix} \Xi_{11}^{ij} & * & * \\ \Xi_{21}^{ij} & 3P - 2(G_i + G'_i) - (G_j + G'_j) & * \\ \Xi_{31}^{ij} & B'_i(G'_i + G'_j) + B'_j G'_i & -3(H + H') \end{bmatrix} < 0, \quad (3.51)$$

with

$$\Xi_{11}^{ij} = [A'_i(F'_i + F'_j) + A'_j F'_i + K'_i(B'_i F'_j + B'_j F'_i) + K'_j B'_i F'_i] + (\bullet)' + 3\gamma_2 P(2r_2 + \gamma_2),$$

$$\Xi_{21}^{ij} = 3(r_2 + \gamma_2)P - (2F'_i + F'_j) + G_i(A_i + A_j) + G_j A_i + G_i(B_i K_j + B_j K_i) + G_j B_i K_i,$$

and

$$\Xi_{31}^{ij} = B'_i(F'_i + F'_j) + B'_j F'_i + J_i(C_i + C_j) + J_j C_i - 2H K_i - H K_j,$$

holds for  $i, j = 1, 2, \dots, N$  and  $i \neq j$ , and

$$\begin{bmatrix} \Xi_{11}^{ijk} & * & * \\ \Xi_{21}^{ijk} & 6P - 2(G_i + G'_i) - 2(G_j + G'_j) - 2(G_k + G'_k) & * \\ \Xi_{31}^{ijk} & (B'_i + B'_j)G'_k + (B'_i + B'_k)G'_j + (B'_j + B'_k)G'_i & -6(H + H') \end{bmatrix} < 0, \quad (3.52)$$

with

$$\begin{aligned} \Xi_{11}^{ijk} = & [(A'_i + A'_j)F'_k + (A'_i + A'_k)F'_j + (A'_j + A'_k)F'_i + (K'_i B'_j + K'_j B'_i)F'_k + \\ & + (K'_i B'_k + K'_k B'_i)F'_j + (K'_j B'_k + K'_k B'_j)F'_i] + (\bullet)' + 6\gamma_2 P(2r_2 + \gamma_2), \end{aligned}$$

$$\begin{aligned} \Xi_{21}^{ijk} = & 6(r_2 + \gamma_2)P - 2(F'_i + F'_j + F'_k) + (G_i + G_j)A_k + (G_i + G_k)A_j + (G_j + G_k)A_i + \\ & + G_i(B_j K_k + B_k K_j) + G_j(B_i K_k + B_k K_i) + G_k(B_i K_j + B_j K_i), \end{aligned}$$

and

$$\begin{aligned} \Xi_{31}^{ijk} = & (B'_i + B'_j)F'_k + (B'_i + B'_k)F'_j + (B'_j + B'_k)F'_i + (J_i + J_j)C_k + (J_i + J_k)C_j + \\ & + (J_j + J_k)C_i - 2H(K_i + K_j + K_k), \end{aligned}$$

hold for  $i = 1, 2, \dots, N-2$ ,  $j = i+1, \dots, N-1$ , and  $k = j+1, \dots, N$ , then  $L_i = H^{-1}J_i$  are the vertices of the controller  $L(\alpha(t))$  that ensures the asymptotic stabilization of  $A_{SOF}(\alpha(t))$  and the closed-loop eigenvalues placement, for fixed values of  $\alpha(t)$ , inside the circular region with radius  $r_2$  and center in  $(-q, 0)$ , where  $q = r_2 + \gamma_2$ .



*Proof.* Assume that (3.50)-(3.52) hold. Then, regarding Property 2.1, readily one can verify that (3.50) implies that  $H$  is invertible.

Moreover, remembering that  $\sum_{i=1}^N \alpha_i = 1$ , and by multiplying (3.50) by  $\alpha_i^3$  and summing for  $i = 1, \dots, N$ , by multiplying (3.51) by  $\alpha_i^2 \alpha_j$  and summing for  $i = 1, \dots, N$ ,  $j = 1, \dots, N$ , with  $i \neq j$ , and by multiplying (3.52) by  $\alpha_i \alpha_j \alpha_k$ , and summing for  $i = 1, \dots, N-2$ ,  $j = i+1, \dots, N-1$ , and  $k = j+1, \dots, N$ , we have that

$$\begin{bmatrix} [A(\alpha(t))'F(\alpha(t))' + K_{SF}(\alpha(t))'B(\alpha(t))'F(\alpha(t))]' + (\bullet)' + \gamma_2 P(2r_2 + \gamma_2) \\ (r_2 + \gamma_2)P - F(\alpha(t))' + G(\alpha(t))A(\alpha(t)) + G(\alpha(t))B(\alpha(t))K_{SF}(\alpha(t)) \\ B(\alpha(t))'F(\alpha(t))' + J(\alpha(t))C(\alpha(t)) - HK_{SF}(\alpha(t)) \\ \begin{matrix} * & * \\ P - G(\alpha(t)) - G(\alpha(t))' & * \\ B(\alpha(t))'G(\alpha(t))' & -H - H' \end{matrix} \end{bmatrix} < 0 \quad (3.53)$$

Now, following analogous steps as performed in Theorem 3.5, one can observe that (3.53) leads to

$$x(t)'\gamma_2 P(2r_2 + \gamma_2)x(t) + \dot{x}(t)'(r_2 + \gamma_2)Px(t) + x(t)'(r_2 + \gamma_2)P\dot{x}(t) + \dot{x}(t)'P\dot{x}(t) < 0 \quad (3.54)$$

which with  $A_{SOF}(\alpha(t)) = A(\alpha(t)) + B(\alpha(t))L(\alpha(t))C(\alpha(t))$  yields

$$A_{SOF}(\alpha(t))'P + PA_{SOF}(\alpha(t)) + 2\gamma_2 P + \frac{1}{r_2}(A_{SOF}(\alpha(t)) + \gamma_2 I)'P(A_{SOF}(\alpha(t)) + \gamma_2 I) < 0,$$

an equivalent to (3.45) with  $A(\alpha(t)) = A_{SOF}(\alpha(t))$ . The proof is concluded.  $\square$

**Remark 3.5.** *It is important to observe that the advantages of the polytopic approach comes at the price of the design complexity associated to the proposed theorems. As in any polytopic-based model, the complexity increases exponentially with number of vertices of the system polytope. Therefore, a heavier computational burden is expected when dealing with systems affected by a high number time-varying parameters.*

### 3.2.4 ILLUSTRATIVE EXAMPLES

In this section, some examples are presented to illustrate efficiency of the proposed control design strategy.

**Example 3.4** In this example, we intend to illustrate the applicability of the proposed method for GS-SOF controller design. For that extent, we consider the control problem of the lateral axis dynamics of an L-1011 aircraft, adapted from Nguyen, Chevrel and Claveau (2018). This system model is assumed to be affected by a time-varying parameter,  $\rho_1(t)$ , bounded in the interval  $-0.57 \leq \rho_1(t) \leq 2.43$ , representing the airspeed, which affects the system matrix  $A(\alpha(t))$ .

Furthermore, to increase the problem difficulty, we consider that the aileron deflection is produced by an electrical actuator whose amplifier gain may also vary in time, according to the parameter  $\rho_2(t)$ , with  $0.9 \leq \rho_2(t) \leq 1.0$  impacting on the matrix  $B(\alpha(t))$ . In this way, the actuator power vary between 90% and 100% of its nominal value. Both time-varying parameters are assumed to be measurable and available on-line.

The representing LPV state-space model matrices are given by

$$A(\alpha(t)) = \begin{bmatrix} -2.98 & \rho_1(t) & 0 & -0.034 \\ -\rho_1(t) & -0.21 & 0.035 & -0.001 \\ 0 & 0 & 0 & 1 \\ 0.39 & -1.35 - 3\rho_1(t) & 0 & -1.89 \end{bmatrix} \text{ and } B(\alpha(t)) = \begin{bmatrix} -0.032\rho_2(t) \\ 0 \\ 0 \\ -\rho_1(t)\rho_2(t) \end{bmatrix} \quad (3.55)$$

In addition, only the bank angle and the roll rate are available state information measurements (NGUYEN; CHEVREL; CLAVEAU, 2018). Thus, the output signal is defined as

$$y(t) = \begin{bmatrix} 0 & 0 & 1 & 0 \\ 0 & 0 & 0 & 1 \end{bmatrix} x(t). \quad (3.56)$$

Therefore, the system can be represented in a polytope (3.39) with four vertices, in which each vertex is defined by the combination of the minimum and maximum values of  $\rho_1(t)$  and  $\rho_2(t)$ .

A conventional state feedback technique would not be able to be directly applied. Conversely, this problem can be addressed from a robust static output feedback control framework, employing another strategy available in the literature.

In that sense, we may apply the  $\mathcal{D}$ -stability robust SOF control approach proposed in Section 3.1, treating the time-varying parameters as uncertainties. Nevertheless, a feasible control solution is not possible to be obtained, given the aforementioned time-varying parameter intervals.

Now, we apply the proposed two-stage gain-scheduling static output feedback strategy for addressing this problem. Firstly, we design a GS-SF gain matrix,  $K(\alpha(t))$ , using the proposed conditions in Theorem 3.7.

For that, we represent the system in terms of a polytope with four vertices, defined in terms of the combinations of maximum and minimum values of the time-varying parameters  $\rho_1(t)$  and  $\rho_2(t)$ , as follows.

- Vertex 1 - Minimum airspeed and minimum actuator gain

$$A_1 = \begin{bmatrix} -2.98 & -0.57 & 0 & -0.034 \\ 0.57 & -0.21 & 0.035 & -0.001 \\ 0 & 0 & 0 & 1 \\ 0.39 & 0.36 & 0 & -1.89 \end{bmatrix}, B_1 = \begin{bmatrix} -0.032 \\ 0 \\ 0 \\ 0.57 \end{bmatrix}, \text{ and } C_1 = \begin{bmatrix} 0 & 0 \\ 0 & 0 \\ 1 & 0 \\ 0 & 1 \end{bmatrix}' \quad (3.57)$$

- Vertex 2 - Minimum airspeed and maximum actuator gain

$$A_1 = A_2, B_2 = \begin{bmatrix} -0.0288 \\ 0 \\ 0 \\ 0.513 \end{bmatrix} \text{ and } C_2 = C_1 \quad (3.58)$$

- Vertex 3 - Maximum airspeed and minimum actuator gain

$$A_3 = \begin{bmatrix} -2.98 & 2.43 & 0 & -0.034 \\ -2.43 & -0.21 & 0.035 & -0.001 \\ 0 & 0 & 0 & 1 \\ 0.39 & -8.64 & 0 & -1.89 \end{bmatrix}, B_3 = \begin{bmatrix} -0.032 \\ 0 \\ 0 \\ -2.43 \end{bmatrix}, \text{ and } C_3 = C_1. \quad (3.59)$$

- Vertex 4 - Maximum airspeed and maximum actuator gain

$$A_4 = A_3, B_4 = \begin{bmatrix} -0.0288 \\ 0 \\ 0 \\ -2.187 \end{bmatrix}, \text{ and } C_4 = C_1. \quad (3.60)$$

Then, applying Theorem 3.7 conditions considering the aforementioned vertices matrices, and specifying a desired  $\mathcal{D}$ -region for pole placement with  $\gamma_1 = 0.05$  and  $r_1 = 10.5$ , yields

$$K_1 = [3.6087 \quad -2.8009 \quad 0.0145 \quad 0.0854], \quad (3.61)$$

$$K_2 = [3.1515 \quad -2.9661 \quad 0.0095 \quad -0.0273], \quad (3.62)$$

$$K_3 = [2.7114 \quad -2.9319 \quad 0.0464 \quad 0.0777], \quad (3.63)$$

and

$$K_4 = [3.3368 \quad -3.1329 \quad 0.0224 \quad 0.0701] \quad (3.64)$$

as vertices for the GS-SF controller

$$K(\alpha(t)) = \alpha_1(t)K_1 + \alpha_2(t)K_2 + \alpha_3(t)K_3 + \alpha_4(t)K_4, \quad (3.65)$$

completing the first stage. Note that  $\alpha(t)$  represents a convex parametrization of  $\rho_{(1,2)}(t)$ . Details on construction of  $\alpha_{(1,2,3,4)}(t)$  using  $\rho_{(1,2)}(t)$  are presented in Chapter 2.

Now, for the second stage, we apply the LMI conditions proposed in Theorem 3.8 for the compute of GS-SOF controllers. Considering the same polytope vertices and design requirements ( $\gamma_2 = 0.05$  and  $r_2 = 10.5$ ), (5.27)-(5.32) yields

$$L_1 = \begin{bmatrix} -0.4162 & 2.2762 \end{bmatrix}, \quad L_2 = \begin{bmatrix} -0.4092 & 2.5909 \end{bmatrix}, \quad (3.66)$$

$$L_3 = \begin{bmatrix} 1.3761 & 7.3189 \end{bmatrix}, \quad \text{and} \quad L_4 = \begin{bmatrix} 1.2469 & 7.1502 \end{bmatrix} \quad (3.67)$$

as vertices for the GS-SOF controller

$$L(\alpha(t)) = \alpha_1(t)L_1 + \alpha_2(t)L_2 + \alpha_3(t)L_3 + \alpha_4(t)L_4. \quad (3.68)$$

The results of a simulation are presented in terms of the transient response of the closed-loop system and the control input (Figure 3.9), when released from initial conditions arbitrarily set as  $x(0) = \begin{bmatrix} 0 & 1 & 0 & 0 \end{bmatrix}$ , reflecting gust perturbations. The time-varying parameters were considered to behave according to sine functions, such as

$$\rho_1(t) = 0.93 + 1.5\sin(2\pi 0.2t), \quad (3.69)$$

and,

$$\rho_2(t) = 0.95 + 0.05\sin(2\pi 0.1t). \quad (3.70)$$

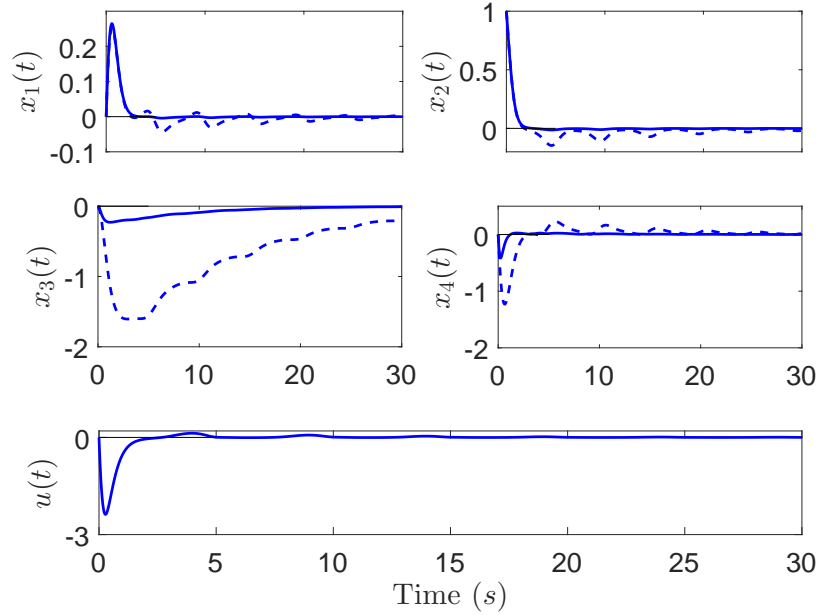
For comparison purposes, we present both open and GS-SOF closed-loop responses. In upper four charts of Figure 3.9, we can clearly see that both open and closed-loop systems exhibits an stable behavior, since all state variables converge to the origin.

However, with the designed GS-SOF controller, the state convergence occurs in a much shorter time and with reduced oscillations, due to the control input action (bottom chart of Figure 3.9).

The GS controller behavior is better understood by considering the instant values of  $\rho_1(t)$  and  $\rho_2(t)$ , in Figure 3.10. Note that as these parameters varies between its extreme values, the system dynamic matrices change.

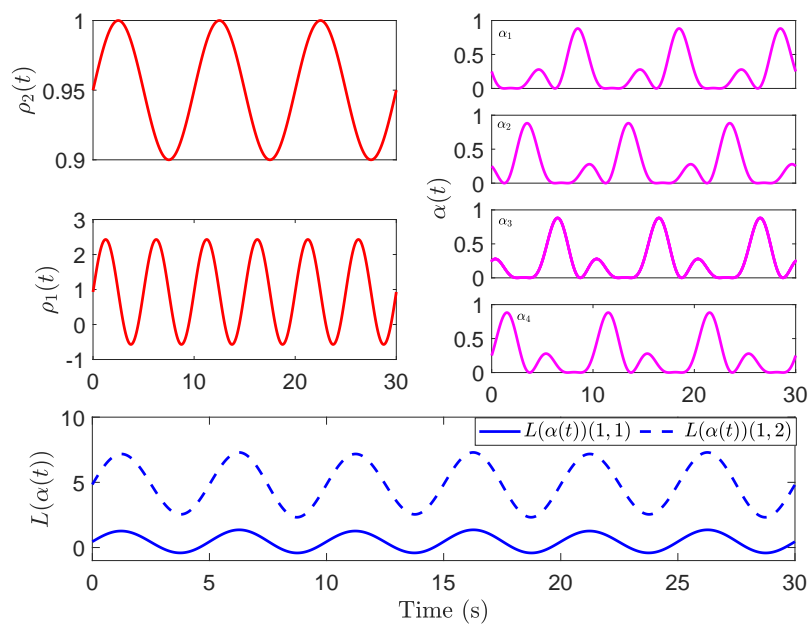
In turn, the GS-SOF controller gains are adjusted on-line, according to  $\alpha(t)$  (see the bottom and upper left charts in Figure 3.10). Remind that  $\alpha(t)$  are parameterized according to the instant values of  $\rho_1(t)$  and  $\rho_2(t)$ .

Figure 3.9 - Open-loop (dashed lines) and closed-loop (full lines) transient response of the L-1011 lateral axis dynamics, and control input  $u(t)$  (bottom chart).



Source: Author's own results.

Figure 3.10 - Behavior of the time-varying parameters (top left charts); parametric elements of  $\alpha(t)$  (top right charts); and GS-SOF gains (bottom chart) in Example 3.4 simulations.



Source: Author's own results.

## 4 DISCRETE-TIME GS–SOF CONTROL DESIGN

This fourth chapter is devoted to present new contributions on the stabilization of linear parameter-varying (LPV) systems via gain-scheduling (GS) static output feedback (SOF) control. However, the interest now is to investigate the case of discrete-time systems, and also address the problem of disturbance rejection.

The proposed results are given in terms of new sufficient linear matrix inequalities (LMI) conditions for synthesizing gain-scheduled SOF controllers that ensure asymptotic stability. The proposed LMI constraints are given in terms of the existence of an affine parameter-dependent Lyapunov function (PDLF). Differently from what happens in LPV continuous-time case, considering PDLFs yields less conservative synthesis conditions, without adding complexity to the mathematical formulation, and therefore such feature is explored for obtaining the presented contributions.

Following the results presented in Chapter 3, the discrete-time SOF controller design is also based on a two-step method: a state-feedback controller is obtained in a first-stage design, which is then used as input information in the second stage for computing the desired GS–SOF controller. In a first moment, the enforcement of a lower bound on the closed-loop decay rate, for performance improvement, is considered. In the sequence, an extension for coping with disturbance rejection is proposed in terms of the  $\mathcal{H}_\infty$  guaranteed cost optimization. Some numerical experiments are presented to illustrate the control synthesis procedure and its efficacy. Also, feasibility analysis are presented to compare and show the advantages of the proposed results over other available strategies present in literature.

### 4.1 TWO-STAGE DISCRETE-TIME GS–SOF CONTROL

In this section, a new two-stage static output feedback controller design strategy is proposed for the stabilization of discrete-time LPV systems via gain-scheduling control. The synthesis conditions are given in terms of sufficient LMI constraints that also guarantees a lower bound on the closed-loop system decay rate.

## 4.1.1 PROBLEM STATEMENT AND PROPOSED APPROACH

Consider a discrete-time LPV system described in a state-space representation as

$$\begin{aligned} x(k+1) &= A(\alpha(k))x(k) + B(\alpha(k))u(k) \\ y(k) &= C(\alpha(k))x(k), \end{aligned} \quad (4.1)$$

where  $x(k) \in \mathbb{R}^n$  is the state vector,  $u(k) \in \mathbb{R}^m$  is the input vector,  $y(k) \in \mathbb{R}^p$  is the measured output vector, and  $(A, B, C)(\alpha(k))$  are parameter-varying matrices that belong to a polytopic domain  $\mathcal{R}$  parameterized in terms of a time-varying vector  $\alpha(k) \in \mathbb{R}^N$  such as

$$\mathcal{R} = \left\{ (A, B, C)(\alpha(k)) : (A, B, C)(\alpha(k)) = \sum_{i=1}^N \alpha_i(k)(A, B, C)_i, \alpha(k) \in \bar{\bar{\Lambda}}_N, k = 0, 1, 2, \dots \right\} \quad (4.2)$$

where  $(A, B, C)_i$  denotes the  $i$ -th of the  $N$  polytope vertices. Moreover,  $\mathcal{R}$  is parameterized in terms of the vector  $\alpha(k) = (\alpha_1(k), \dots, \alpha_N(k))$ , whose entries  $\alpha_i(k)$  are known time-varying parameters that belong to the unitary simplex set  $\bar{\bar{\Lambda}}_N$ , defined as

$$\bar{\bar{\Lambda}}_N = \left\{ \alpha(k) \in \mathbb{R}^N : \sum_{i=1}^N \alpha_i(k) = 1; \alpha_i(k) \geq 0; i = 1, \dots, N, k = 0, 1, 2, \dots \right\}. \quad (4.3)$$

Assuming that  $\alpha(k)$  can be measured or estimated at each discrete time instant  $k$  during system operation, and that only the output vector  $y(k)$  is available for feedback, design a static output-feedback control law

$$u(k) = L(\alpha(k))y(k) \quad (4.4)$$

where  $L(\alpha(k)) \in \mathbb{R}^{m \times p}$  is a gain-scheduling controller matrix, such that the closed-loop system

$$x(k+1) = (A(\alpha(k)) + B(\alpha(k))L(\alpha(k))C(\alpha(k)))x(k) \quad (4.5)$$

is asymptotically stable. Furthermore,  $L(\alpha(k))$  must ensure a bound parameter  $\rho$ , associated to the convergence of the system states to the origin, described as

$$\|x(k)\|_2 < \rho^k \|x(0)\|_2, \forall k \geq 1, \quad (4.6)$$

establishing a performance criteria, namely, the decay rate bound (ROSA; MORAIS; OLIVEIRA, 2018).

For addressing the aforementioned control problem, the results given in Lemma 4.1 are considered, which are related to well-known LMI conditions that, when feasible, are sufficient for ensuring the asymptotic stability of a discrete-time LPV system  $x(k+1) =$

$A(\alpha(k))x(k)$ , with decay rate bounded by  $\rho$ .

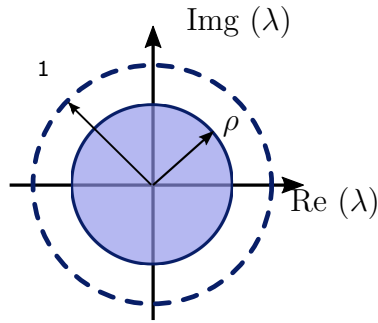
**Lemma 4.1.** *If there exists a parameter-dependent matrix  $P(\alpha(k)) = P(\alpha(k))' > 0$  such that*

$$A'(\alpha(k))P(\alpha(k+1))A(\alpha(k)) - \rho^2 P(\alpha(k)) < 0, \forall \alpha(k) \in \bar{\Lambda}_N, \quad (4.7)$$

*for  $0 \leq \rho < 1$  then system  $x(k+1) = A(\alpha(k))x(k)$  is asymptotically stable and has a decay rate bounded by  $\rho$ .*

In a linear time-invariant scenario, such conditions are necessary and sufficient for guaranteeing that all system eigenvalues ( $\lambda$ ) are contained within a particular region in the complex plane, denoted by a circle with radius  $r = \rho$ ,  $\rho < 1$  (ROSA; MORAIS; OLIVEIRA, 2018). Such interpretation is illustrated in Figure 4.1.

Figure 4.1 - Unitary circle and circular sub region bounded for  $0 \leq \rho < 1$ .



Source: Adapted from Rosa, Morais and Oliveira (2018).

Considering the presented framework, a strategy for designing discrete-time GS-SOF controllers that meet the required control objectives is proposed. The idea is to design a GS-SOF controller  $L(\alpha(k))$  associated to a symmetric positive definite matrix  $P$  that satisfies the constraints in Lemma 4.1 for  $A_{cl}(\alpha(k)) = (A(\alpha(k)) + B(\alpha(k))L(\alpha(k))C(\alpha(k)))$  as in (4.5).

#### 4.1.2 TWO-STAGE DISCRETE-TIME GS-SOF DESIGN WITH DECAY RATE BOUNDING

The first main technical contribution regarding the subject addressed in this chapter is presented in the sequence. It consists of a two-stage LMI-base strategy for the design of stabilizing GS-SOF controllers, with guaranteed lower bound  $\rho$  on the system state decay rate.

Therefore, in the same fashion as considered in Chapter 3, for the first stage, we might



consider a control law  $u(k) = Kx(k)$  where  $K \in \mathbb{R}^{m \times n}$  is a gain matrix such that

$$x(k+1) = (A(\alpha(k)) + B(\alpha(k))K)x(k) \quad (4.8)$$

is asymptotically stable.

However, as already explored in Chapter 3, the two-stage method might benefit from a search for a parameter-dependent matrix  $K(\alpha(k))$ , instead of a robust gain  $K$ . Therefore, a first theoretical contribution is proposed in terms of a state-feedback synthesis strategy based on the results presented in Montagner *et al.* (2005), which considers the LPV stabilization problem. In their paper, the authors propose that a stabilizing gain-scheduled state-feedback controller  $K(\alpha(k))$  can be obtained by solving an LMI problem.

The extension for incorporating a bound  $\rho_1^1$  in the decay rate is proposed in Theorem 4.1.

**Theorem 4.1** (First-Stage GS-SF Design). *If there exists symmetric positive definite matrices  $Q_j \in \mathbb{R}^{n \times n}$  and matrices  $X_j \in \mathbb{R}^{n \times n}$  and  $Y_j \in \mathbb{R}^{m \times n}$ ,  $j = 1, \dots, N$  such that the LMIs*

$$\begin{bmatrix} X_j + X'_j - \rho_1^2 Q_j & * \\ A_j X_j + B_j Y_j & Q_i \end{bmatrix} > 0, \quad (4.9)$$

for  $i = 1, \dots, N$ ,  $j = 1, \dots, N$ , and

$$\begin{bmatrix} X_j + X'_j + X_k + X'_k - \rho_1^2(Q_j + Q_k) & * \\ A_k X_j + A_j X_k + B_k Y_j + B_j Y_k & 2Q_i \end{bmatrix} > 0, \quad (4.10)$$

for  $i = 1, \dots, N$ ,  $j = 1, \dots, N-1$ ,  $k = j+1, \dots, N$ , have a solution, then the stability of the closed-loop system (4.8) is assured by the state-feedback control law  $u(k) = K(\alpha(k))x(k)$  with the parameter-dependent gain

$$K(\alpha(k)) = Y(\alpha(k))X(\alpha(k))^{-1}, \quad (4.11)$$

with decay rate bound  $\rho_1$ .

*Proof.* Omitted for brevity. The proof follows directly as in Montagner *et al.* (2005), with a parameter-dependent Lyapunov function  $V(x(k)) = x(k)'P(\alpha(k))x(k) > 0$  ensuring  $V(x(k+1)) - \rho_1^2 V(x(k)) < 0$ .  $\square$

**Remark 4.1.** *The LMI conditions in Theorem 4.1 are based on a parameter-dependent matrix  $X(\alpha(k))$ , which is then used for retrieving the GS-SF controller (4.11). However, despite the fact that considering a parameter-dependent matrix  $X(\alpha(k))$  yields less conservative constraints, this hinders the computation of the gain matrix  $K(\alpha(k))$ , since it*

---

<sup>1</sup>Similarly in Chapter 3, we distinguish the decay rate bound  $\rho$  considered in the first and second stages as  $\rho_1$  and  $\rho_2$ , respectively.

depends on the inverse of  $X(\alpha(k))$ , for every  $\alpha \in \bar{\bar{\Lambda}}_N$ . In this case,  $K(\alpha(k))$  would have to be computed on-line, by inverting  $X(\alpha(k))$  for every the instant value of  $\alpha$ . To avoid such implementation drawback, one might consider that  $X(\alpha(k)) = X$  (i.e.  $X_i = X$ , for  $i = 1, \dots, N$ ). Then, the GS-SF gain matrix can be computed offline, by inverting a single matrix  $X$ , for obtaining the vertices  $K_i$ ,  $i = 1, \dots, N$  of (4.11), enabling the compute of  $K(\alpha(k))$  using

$$K(\alpha(k)) = \alpha_1(k)K_1 + \dots + \alpha_N(k)K_N. \quad (4.12)$$

After obtaining a stabilizing SF gain matrix  $K(\alpha(k))$ , we move to the second stage where such controller is used as an input parameter for a second LMI problem whose solution, if feasible, yields the desired GS-SOF controller. In the next section, we propose some new sufficient LMI conditions for implementing the second stage.

As considered in the first-stage design, the basis of the proposed results consists in considering that the asymptotic stability is ensured by the existence of a polytopic parameter-dependent Lyapunov function

$$V(x(k)) = x(k)'P(x(k))x(k), \quad (4.13)$$

where

$$P(x(k)) = \sum_{i=1}^N \alpha_i(k)P_i > 0. \quad (4.14)$$

Using such definition, it is possible to obtain less conservative synthesis conditions, when compared to a classic common-quadratic Lyapunov function (CQLF) approach, which is based on the search for a single matrix  $P$  that ensures stability for the whole polytope domain.

In these terms, new LMI conditions for the asymptotic stabilization of (4.5) through the design of a GS-SOF controller are proposed in Theorem 4.2, formulated based on the strategy adopted in Montagner *et al.* (2005), which allows for arbitrarily fast variations of the time-varying parameters  $\alpha(k)$ .

**Theorem 4.2** (Second-Stage GS-SOF Design). *Assuming that there exists a gain matrix  $K(\alpha(k))$  that asymptotically stabilizes  $A(\alpha(k)) + B(\alpha(k))K(\alpha(k))$ , then there exists a static output-feedback gain-scheduled matrix  $L(\alpha(k))$  that asymptotically stabilizes  $A(\alpha(k)) + B(\alpha(k))L(\alpha(k))C(\alpha(k))$  with decay rate bounded by  $\rho_2$ , for any arbitrary time variation of the parameter  $\alpha(k)$  in (4.3), if there exist symmetric matrices  $P_i > 0$  and matrices  $F_i$ ,  $G_i$ ,  $H$ , and  $J_i$ , such that*

$$\begin{bmatrix} \rho_2^2 P_i - A_i' F_i' - F_i A_i - K_i' B_i' F_i' - F_i B_i K_i & * & * \\ F_i' - G_i A_i - G_i B_i K_i & G_i + G_i' - P_d & * \\ -B_i' F_i' + H K_i - J_i C_i & -B_i' G_i' & H + H' \end{bmatrix} > 0 \quad (4.15)$$

holds for  $d = 1, \dots, N$  and  $i = 1, \dots, N$ ,

$$\begin{bmatrix} \Theta_{1,1}^{ij} & * & * \\ \Theta_{2,1}^{ij} & 2(G_i + G'_i) + G_j + G'_j - 3P_d & * \\ \Theta_{3,1}^{ij} & -B'_i(G'_i + G'_j) - B'_j G'_i & 3H + 3H' \end{bmatrix} > 0 \quad (4.16)$$

holds for  $d = 1, \dots, N$ ,  $i = j = 1, \dots, N$ , and  $i \neq j$ , where

$$\begin{aligned} \Theta_{1,1}^{ij} &= \rho_2^2(2P_i + P_j) + (-F_i(A_i + A_j) - F_j A_i - F_i(B_i K_j + B_j K_i) - F_j B_i K_i) + (\bullet)', \\ \Theta_{1,2}^{ij} &= 2F'_i + F'_j - G_i(A_i + A_j) - G_j A_i - G_i(B_i K_j + B_j K_i) - G_j B_i K_i, \text{ and} \\ \Theta_{3,1}^{ij} &= -B'_i(F'_i + F'_j) - B'_j F'_i + 2H K_i + H K_j - J_i(C_i + C_j) - J_j C_i, \end{aligned} \quad (4.17)$$

and

$$\begin{bmatrix} \Theta_{1,1}^{ijl} & * & * \\ \Theta_{2,1}^{ijl} & \Theta_{2,2}^{ijl} & * \\ \Theta_{3,1}^{ijl} & -B'_i(G'_j + G'_l) - B'_j(G'_i + G'_l) - B'_l(G'_i + G'_j) & 6H + 6H' \end{bmatrix} > 0 \quad (4.18)$$

holds for  $d = 1, \dots, N$ ,  $i = 1, \dots, N - 2$ ,  $j = i + 1, i + 2, \dots, N - 1$ , and  $l = j + 1, j + 2, \dots, N$ , where

$$\begin{aligned} \Theta_{1,1}^{ijl} &= 2\rho_2^2(P_i + P_j + P_l) + (-F_i(A_j + A_l) - F_j(A_i + A_l) - F_l(A_i + A_j) + \\ &\quad -F_i(B_j K_l + B_l K_j) - F_j(B_i K_l + B_l K_i) - F_l(B_i K_j + B_j K_i)) + (\bullet)', \\ \Theta_{1,2}^{ijl} &= 2(F'_i + F'_j + F'_l) - G_i(A_j + A_l) - G_j(A_i + A_l) - G_l(A_i + A_j) + \\ &\quad -G_i(B_j K_l + B_l K_j) - G_j(B_i K_l + B_l K_i) - G_l(B_i K_j + B_j K_i), \text{ and} \\ \Theta_{3,1}^{ijl} &= -B'_i(F'_j + F'_l) - B'_j(F'_i + F'_l) - B'_l(F'_i + F'_j) + 2H(K_i + K_j + K_l) + \\ &\quad -J_i(C_j + C_l) - J_j(C_i + C_l) - J_l(C_i + C_j), \\ \Theta_{2,2}^{ijl} &= 2(G_i + G'_i) + 2(G_j + G'_j) + 2(G_l + G'_l) - 6P_d. \end{aligned} \quad (4.19)$$

In the affirmative case, the  $N$  vertices matrices,  $L_i$ , for composing gain-scheduled SOF controller can be retrieved with  $L_i = H^{-1} J_i$ .

*Proof.* Assume that LMIs (4.15)-(4.19) holds. Then, immediately we have that  $H + H' > 0$ . Thus, according to Boyd *et al.* (1994), the inverse of  $H$  exists.

Now, based on the procedure presented in Montagner *et al.* (2005), we may observe that by multiplying (4.15) by  $\alpha_i^3(k)$  and by  $\beta_d(k)$ , summing from  $i = 1$  to  $i = N$  and from  $d = 1$  to  $d = N$ , and that by multiplying (4.16) by  $\alpha_i^2(k)\alpha_j(k)$  and by  $\beta_d(k)$ , summing from  $i, j = 1$  to  $i, j = N$ ,  $i \neq j$  and from  $d = 1$  to  $d = N$ , and that by multiplying (4.19) by  $\alpha_i(k)\alpha_j(k)\alpha_l(k)$ , and by  $\beta_d(k)$ , summing from  $i = 1$  to  $i = N - 2$ ,  $j = i + 1$  to  $j = N - 1$ ,  $l = j + 1$  to  $l = N$ , and from  $d = 1$  to  $d = N$ , with  $\sum_{d=1}^N \beta_d(k) = 1, \beta_d(k) > 0$ , it follows that

$$\left[ \begin{array}{ccc} \rho_2^2 P(\alpha(k)) + (-F(\alpha(k))A(\alpha(k)) - F(\alpha(k))B(\alpha(k))K(\alpha(k))) + (\bullet)' \\ F(\alpha(k))' - G(\alpha(k))A(\alpha(k)) - G(\alpha(k))B(\alpha(k))K(\alpha(k)) \\ -B(\alpha(k))'F(\alpha(k))' + HK(\alpha(k)) - J(\alpha(k))C(\alpha(k)) \\ \phantom{F(\alpha(k))' - G(\alpha(k))A(\alpha(k)) - G(\alpha(k))B(\alpha(k))K(\alpha(k))} & \phantom{F(\alpha(k))' - G(\alpha(k))A(\alpha(k)) - G(\alpha(k))B(\alpha(k))K(\alpha(k))} & \phantom{F(\alpha(k))' - G(\alpha(k))A(\alpha(k)) - G(\alpha(k))B(\alpha(k))K(\alpha(k))} \\ \phantom{F(\alpha(k))' - G(\alpha(k))A(\alpha(k)) - G(\alpha(k))B(\alpha(k))K(\alpha(k))} & \begin{matrix} * \\ G(\alpha(k)) + G(\alpha(k))' - P(\beta(k)) \\ -B(\alpha(k))'G(\alpha(k))' \end{matrix} & \begin{matrix} * \\ * \\ H + H' \end{matrix} \end{array} \right] > 0 \quad (4.20)$$

also holds.

Now, performing an analogous transformation as already seen in Chapter 3, we can pre- and post-multiply (4.20) by

$$T(\alpha(k)) = \begin{bmatrix} I & 0 & S(\alpha(k))' \\ 0 & I & 0 \end{bmatrix} \quad \text{and} \quad T(\alpha(k))', \quad (4.21)$$

respectively, to obtain

$$\left[ \begin{array}{cc} \Upsilon(\alpha(k)) & * \\ \Phi(\alpha(k)) & G(\alpha(k)) + G(\alpha(k))' - P(\beta(k)) \end{array} \right] > 0 \quad (4.22)$$

where

$$\begin{aligned} \Upsilon(\alpha(k)) &= \rho_2^2 P(\alpha(k)) - A(\alpha(k))'F(\alpha(k))' - F(\alpha(k))A(\alpha(k)) - K(\alpha(k))'B(\alpha(k))'F(\alpha(k))' + \\ & - F(\alpha(k))B(\alpha(k))K(\alpha(k)) - S(\alpha(k))'B(\alpha(k))'F(\alpha(k))' + S(\alpha(k))'HK(\alpha(k)) + \\ & - S(\alpha(k))'J(\alpha(k))C(\alpha(k)) - F(\alpha(k))B(\alpha(k))S(\alpha(k)) + K(\alpha(k))'H'S(\alpha(k)) + \\ & - C(\alpha(k))'J(\alpha(k))'S + S(\alpha(k))'HS(\alpha(k)) + S(\alpha(k))'H'S(\alpha(k)). \end{aligned} \quad (4.23)$$

and

$$\Phi(\alpha(k)) = F(\alpha(k))' - G(\alpha(k))A(\alpha(k)) - G(\alpha(k))B(\alpha(k))K(\alpha(k)) - G(\alpha(k))B(\alpha(k))S(\alpha(k)). \quad (4.24)$$

Defining  $S(\alpha(k)) = H^{-1}J(\alpha(k))C(\alpha(k)) - K(\alpha(k))$  we have that (4.22) becomes

$$\left[ \begin{array}{ccc} \rho_2^2 P(\alpha(k)) + (-F(\alpha(k))A(\alpha(k)) - F(\alpha(k))B(\alpha(k))H^{-1}J(\alpha(k))C(\alpha(k))) + (\bullet)' \\ F(\alpha(k))' - G(\alpha(k))A(\alpha(k)) - G(\alpha(k))B(\alpha(k))H^{-1}J(\alpha(k))C(\alpha(k)) \\ \phantom{F(\alpha(k))' - G(\alpha(k))A(\alpha(k)) - G(\alpha(k))B(\alpha(k))H^{-1}J(\alpha(k))C(\alpha(k))} & \phantom{F(\alpha(k))' - G(\alpha(k))A(\alpha(k)) - G(\alpha(k))B(\alpha(k))H^{-1}J(\alpha(k))C(\alpha(k))} & \phantom{F(\alpha(k))' - G(\alpha(k))A(\alpha(k)) - G(\alpha(k))B(\alpha(k))H^{-1}J(\alpha(k))C(\alpha(k))} \\ \phantom{F(\alpha(k))' - G(\alpha(k))A(\alpha(k)) - G(\alpha(k))B(\alpha(k))H^{-1}J(\alpha(k))C(\alpha(k))} & \begin{matrix} * \\ G(\alpha(k)) + G(\alpha(k))' - P(\beta(k)) \end{matrix} & \begin{matrix} * \\ * \end{matrix} \end{array} \right] > 0. \quad (4.25)$$

Moreover, choosing  $L(\alpha(k)) = H^{-1}J(\alpha(k))$  and conveniently rewriting (4.25) as a sum of matrices such as

$$\begin{aligned} & \begin{bmatrix} -\rho_2^2 P(\alpha(k)) & 0 \\ 0 & P(\beta(k)) \end{bmatrix} + \begin{bmatrix} F(\alpha(k)) \\ G(\alpha(k)) \end{bmatrix} \begin{bmatrix} A(\alpha(k)) + B(\alpha(k))L(\alpha(k))C(\alpha(k)) & -I \end{bmatrix} + \\ & + \begin{bmatrix} A(\alpha(k))' + C(\alpha(k))'L(\alpha(k))'B(\alpha(k))' \\ -I \end{bmatrix} \begin{bmatrix} F(\alpha(k))' & G(\alpha(k))' \end{bmatrix} < 0, \quad (4.26) \end{aligned}$$

then, according to Lemma 2.4, we have that

$$\omega' \begin{bmatrix} -\rho_2^2 P(\alpha(k)) & 0 \\ 0 & P(\beta(k)) \end{bmatrix} \omega < 0, \quad \forall \omega \neq 0: \begin{bmatrix} A(\alpha(k)) + B(\alpha(k))L(\alpha(k))C(\alpha(k)) & -I \end{bmatrix} \omega = 0. \quad (4.27)$$

By defining  $\omega = [x'(k) \quad x'(k+1)]'$ , we note that (4.27) gives

$$\begin{aligned} x(k)' & \left[ (A(\alpha(k)) + B(\alpha(k))L(\alpha(k))C(\alpha(k)))' P(\beta(k)) (A(\alpha(k)) + B(\alpha(k))L(\alpha(k))C(\alpha(k))) \right. \\ & \left. - \rho_2^2 P(\alpha(k)) \right] x(k) < 0, \quad (4.28) \end{aligned}$$

since  $x(k+1) = (A(\alpha(k)) + B(\alpha(k))L(\alpha(k))C(\alpha(k)))x(k)$  from (4.5).

Using the strategy presented in Montagner *et al.* (2005) and defining  $P(\beta(k)) = P(\alpha(k+1))$ , (4.28) can be rewritten as

$$x(k)' \left[ A_N(\alpha(k))' P(\alpha(k+1)) A_N(\alpha(k)) - \rho_2^2 P(\alpha(k)) \right] x(k) < 0, \quad (4.29)$$

where  $A_N(\alpha(k)) = A(\alpha(k)) + B(\alpha(k))L(\alpha(k))C(\alpha(k))$ .

Finally, see that by defining  $V(x(k)) = x(k)' P(\alpha(k)) x(k)$ , (4.29) yields

$$V(x(k+1)) - \rho_2^2 V(x(k)) < 0. \quad (4.30)$$

Therefore, with  $V(x(k))$  being a parameter-dependent Lyapunov function, the feasibility of (4.15), (4.16), and (4.19) is sufficient to ensure (4.20), and consequently (4.30). Thus, the asymptotic stability of (4.5) is guaranteed with decay rate bounded by  $\rho_2$ , for any arbitrary variation of the time-varying parameters in the system polytope.  $\square$

**Remark 4.2.** Note that the first-stage SF controller enters in the second stage in terms of its vertices, similarly as already seen in Theorem 3.5. In fact, as mentioned in Remark 4.1, the gain matrix (as well as any other parameter-dependent matrix in this work) is described in a polytopic-fashion. And, similarly, Theorem 4.2 provides the desired GS-SOF controller in terms of its vertices  $L_i$ ,  $i = 1, \dots, N$ , for composing  $L(\alpha(k))$  as

$$L(\alpha(k)) = \alpha_1(k)L_1 + \dots + \alpha_N(k)L_N, \quad (4.31)$$

by means of the on-line measurement of  $\alpha(k)$ .

**Remark 4.3.** *Similar observation regarding the choice of the design parameters as seen in Chapter 3 can be derived to the results presented in this chapter. The first- and second-stage decay rate bounds  $\rho_1$  and  $\rho_2$  do not have to be set with same values (i.e.  $\rho_1 = \rho_2$ ) when applying the proposed method. In fact, if feasibility is not achieved in the second stage for a particular chose of  $\rho_1$  in the first stage, the sufficiency nature of the proposed results allows for the designer restart the procedure, by setting a different decay rate bound in the first-stage design, which will generate a different state-feedback gain matrix  $K(\alpha(k))$ . Then, another search for the second stage GS-SOF controller  $L(\alpha(k))$  can be executed, in terms of the new obtained SF gain matrix.*

**Remark 4.4.** *In the same terms of Remark 4.3, note that the application of Theorem 4.2 depends on the success in finding a stabilizing SF gain matrix. Therefore, the use of Theorem 4.1 for designing the first-stage gain is more interesting for the purposes of the two-stage method than using a robust state-feedback gain synthesis approach. In fact, finding a single robust gain  $K$  that stabilizes the considered LPV system is a rather more difficult problem than finding a set of gain matrices  $K_i$ ,  $i = 1, \dots, N$  to compose a stabilizing parameter-dependent state-feedback gain  $K(\alpha(k))$ .*

At this point, considering the remarks presented above and to bring more clarity about our method implementation, we summarize the employment of our proposed strategy to solve robust control problems in terms of an algorithm based on Theorems 4.1 and 4.2, as presented in Algorithm 4.1.

---

**Algorithm 4.1** Two-stage GS-SOF controller synthesis

---

- 1: Reset counter with  $\epsilon \leftarrow 1$  and set maximum iteration limit  $\epsilon_{max}$ .
  - 2: Step 1-1 (SF Initialization): Find the GS-SF controller  $K(\alpha(k))$  design via Theorem 4.1 with bound  $\rho_1 < 1$ .
  - 3: Step 1-2 (SF Checking): If Theorem 4.1 returns feasible  $K(\alpha(k))$ , go to Step 2-1; Otherwise, set a different first-stage decay rate bound  $\rho_1 \leftarrow \rho_1^{new}$  and restart Step 1-1; However, if Theorem 4.1 fails with  $\rho_1 \leftarrow 1$ , it might not be able to find an stabilizing GS-SF controller, then EXIT.
  - 4: Step 2-1 (SOF Design): Find the GS-SOF controller  $L(\alpha(k))$  design via Theorem 4.2 with  $K(\alpha(k))$  and decay rate bound  $\rho_2$ .
  - 5: Step 2-2 (SOF Checking): If Theorem 4.2 returns a feasible  $L(\alpha(k))$ , EXIT; Otherwise, set  $\epsilon \leftarrow \epsilon + 1$  and if  $\epsilon < \epsilon_{max}$  go to Step 1-1 with different first-stage decay rate bound  $\rho_1 \leftarrow \rho_1^{new}$  to restart the process; However, if  $\epsilon \geq \epsilon_{max}$ , the algorithm was not able to find a feasible solution for GS-SOF design, then EXIT.
- 

Source: Author's own results.

In the sequence, we show that standard quadratic stability-based approach, consisting of a single Lyapunov matrix  $P$ , is directly obtained from Theorem 4.2 by setting  $P_i = P$ ,  $i = 1, \dots, N$ , as enunciated in Corollary 4.1.

**Corollary 4.1.** *Assuming that there exists a gain matrix  $K(\alpha(k))$  that asymptotically stabilizes  $A(\alpha(k)) + B(\alpha(k))K(\alpha(k))$ , then there exists a static output-feedback gain-scheduled matrix  $L(\alpha(k))$  that asymptotically stabilizes  $A(\alpha(k)) + B(\alpha(k))L(\alpha(k))C(\alpha(k))$  with decay rate bounded by  $\rho_2$ , for any arbitrary time variation of the parameter  $\alpha(k)$  in (4.3), if there exist a symmetric matrix  $P > 0$  and matrices  $F_i$ ,  $G_i$ ,  $H$ , and  $J_i$  such that*

$$\begin{bmatrix} \rho_2^2 P - A_i' F_i' - F_i A_i - K_i' B_i' F_i' - F_i B_i K_i & * & * \\ F_i' - G_i A_i - G_i B_i K_i & G_i + G_i' - P & * \\ -B_i' F_i' + H K_i - J_i C_i & -B_i' G_i' & H + H' \end{bmatrix} > 0 \quad (4.32)$$

holds for  $i = 1, \dots, N$ ,

$$\begin{bmatrix} \Lambda_{1,1}^{ij} & * & * \\ \Lambda_{2,1}^{ij} & 2(G_i + G_i') + G_j + G_j' - 3P & * \\ \Lambda_{3,1}^{ij} & -B_i'(G_i' + G_j') - B_j' G_i' & 3H + 3H' \end{bmatrix} > 0 \quad (4.33)$$

holds for  $i = j = 1, \dots, N$  and  $i \neq j$ , where

$$\begin{aligned} \Lambda_{1,1}^{ij} &= 3\rho_2^2 P + (-F_i(A_i + A_j) - F_j A_i - F_i(B_i K_j + B_j K_i) - F_j B_i K_i) + (\bullet)', \\ \Lambda_{1,2}^{ij} &= 2F_i' + F_j' - G_i(A_i + A_j) - G_j A_i - G_i(B_i K_j + B_j K_i) - G_j B_i K_i, \text{ and} \\ \Lambda_{3,1}^{ij} &= -B_i'(F_i' + F_j') - B_j' F_i' + 2H K_i + H K_j - J_i(C_i + C_j) - J_j C_i, \end{aligned} \quad (4.34)$$

and

$$\begin{bmatrix} \Lambda_{1,1}^{ijl} & * & * \\ \Lambda_{2,1}^{ijl} & \Lambda_{2,2}^{ijl} & * \\ \Lambda_{3,1}^{ijl} & \Lambda_{3,2}^{ijl} & 6H + 6H' \end{bmatrix} > 0 \quad (4.35)$$

holds for  $i = 1, \dots, N-2$ ,  $j = i+1, i+2, \dots, N-1$ , and  $l = j+1, j+2, \dots, N$ , where

$$\begin{aligned} \Lambda_{1,1}^{ijl} &= 6\rho_2^2 P + (-F_i(A_j + A_l) - F_j(A_i + A_l) - F_l(A_i + A_j) + \\ &\quad -F_i(B_j K_l + B_l K_j) - F_j(B_i K_l + B_l K_i) - F_l(B_i K_j + B_j K_i)) + (\bullet)', \\ \Lambda_{1,2}^{ijl} &= 2(F_i' + 2F_j' + F_l') - G_i(A_j + A_l) - G_j(A_i + A_l) - G_l(A_i + A_j) + \\ &\quad -G_i(B_j K_l + B_l K_j) - G_j(B_i K_l + B_l K_i) - G_l(B_i K_j + B_j K_i), \\ \Lambda_{3,1}^{ijl} &= -B_i'(F_j' + F_l') - B_j'(F_i' + F_l') - B_l'(F_i' + F_j') + 2H K_i + 2H K_j + \\ &\quad + 2H K_l - J_i(C_j + C_l) - J_j(C_i + C_l) - J_l(C_i + C_j), \\ \Lambda_{2,2}^{ijl} &= 2(G_i + G_i') + 2(G_j + G_j') + 2(G_l + G_l') - 6P, \text{ and} \\ \Lambda_{3,2}^{ijl} &= -B_i'(G_j' + G_l') - B_j'(G_i' + G_l') - B_l'(G_i' + G_j'). \end{aligned} \quad (4.36)$$

In the affirmative case, the  $N$  vertices matrices,  $L_i$ , for composing gain-scheduled SOF controller can be retrieved with  $L_i = H^{-1} J_i$ .

*Proof.* The proof follows analogous steps as seen in Theorem 4.2 proof, considering a multiplication procedure using only  $\alpha(k)$ , and through the application of the same transformation as in Theorem 4.2, based on Mehdi, Boukas and Bachelier (2004) followed by the application of Lemma 2.4, and thus its details are omitted for conciseness.  $\square$

Additionally, we show that the proposed LMI conditions (4.15)-(4.19) can also be used to compute a gain-scheduled state-feedback controller. As previously mentioned, the feasibility in the second stage depends on the considered particular gain matrix  $K(\alpha(k))$ . If (4.15)-(4.19) fails to achieve feasibility for some  $K(\alpha(k))$ , then one can set the output matrix as  $C(\alpha(k)) = I$ .

In that case, note that  $A(\alpha(k)) + B(\alpha(k))L(\alpha(k))C(\alpha(k))$  falls into the state-feedback dynamics  $A(\alpha(k)) + B(\alpha(k))L(\alpha(k))$ , with  $L(\alpha(k))$  being a GS-SF gain matrix. Then, the obtained gain  $L(\alpha(k))$  can be used as a new input  $K(\alpha(k))$  in (4.15)-(4.19), and another search for the desired GS-SOF controller can be executed. Despite that convergence is not guaranteed, this procedure can be employed recursively, and represents another strategy for dealing with GS-SOF problems.

This feature of the proposed method is formalized in Corollary 4.2.

**Corollary 4.2.** *Assuming that there exists a gain matrix  $K(\alpha(k))$  that asymptotically stabilizes  $A(\alpha(k)) + B(\alpha(k))K(\alpha(k))$ , for any arbitrary time variation of the parameter  $\alpha(k)$  in (4.3), if there exist symmetric matrices  $P_i > 0$  and matrices  $F_i, G_i, H$ , and  $J_i$ , such that (4.15), (4.16) and (4.19) hold with  $C_i = I, i = 1, \dots, N$ , then the  $N$  vertices matrices  $L_i$ , retrieved with  $L_i = H^{-1}J_i$ , represents a state-feedback controller that asymptotically stabilizes  $A(\alpha(k)) + B(\alpha(k))L(\alpha(k))$  with decay rate bounded by  $\rho_2$ .*

*Proof.* The proof follows similarly as for Theorem 4.2, and thus is omitted for brevity.  $\square$

The application of the GS-SOF strategy using Corollary 4.2 recursively with Theorem 4.2 is depicted Algorithm 4.2.

**Remark 4.5.** *To avoid misinterpretation, remind that the decay rate bound in Theorem 4.2 is set in terms of the scalar  $\rho_2$  for distinguishing it from the first-stage decay rate bound  $\rho_1$  set in Theorem 4.1. However, it must be clear that when using Corollary 4.2 as a first-stage design,  $\rho_2$  will be the decay rate bound associated to the obtained first-stage state-feedback controller, that is  $\rho_1 = \rho_2$ .*

**Remark 4.6.** *Note that analogous results of Corollary 4.2 can be derived from the design strategies proposed in Chapter 3, for the continuous-time LTI and LPV cases, considering  $\mathcal{D}$ -stability concepts.*



**Algorithm 4.2** Two-stage GS-SOF controller synthesis recursively through Theorem 4.2

- 
- 1: Reset counter with  $\epsilon \leftarrow 1$  and set maximum iteration limit  $\epsilon_{max}$ .
  - 2: Set  $Cn_i \leftarrow C_i, i = 1, \dots, N$  to save the nominal system (4.1) output matrices.
  - 3: Step 1-1 (SF Initialization): Set  $C_i \leftarrow I, i = 1, \dots, N$  and find the GS-SF controller  $L(\alpha(k)) = K(\alpha(k))$  designed via Corollary 4.2 with bound  $\rho_1$  (see Remark 4.5).
  - 4: Step 1-2 (SF Checking): If Corollary 4.2 returns feasible  $L(\alpha(k)) = K(\alpha(k))$ , go to Step 2-1; Otherwise, set a different first-stage decay rate bound  $\rho_1 \leftarrow \rho_1^{new}$  and restart Step 1-1; However, if Corollary 4.2 fails with  $\rho_1 \leftarrow 1$ , it might not possible to find an stabilizing GS-SF controller, then EXIT.
  - 5: Step 2-1 (SOF Design): Set  $C_i \leftarrow Cn_i, i = 1, \dots, N$  and find the GS-SOF controller  $L(\alpha(k))$  design via Theorem 4.2 with  $K(\alpha(k))$  and bound  $\rho_2$ .
  - 6: Step 2-2 (SOF Checking): If Theorem 4.2 returns a feasible  $L(\alpha(k))$ , EXIT; Otherwise, set  $\epsilon \leftarrow \epsilon + 1$  and if  $\epsilon < \epsilon_{max}$  go to Step 1-1 with different first-stage decay rate bound  $\rho_1 \leftarrow \rho_1^{new}$  to restart the process; However, if  $\epsilon \geq \epsilon_{max}$ , the algorithm was not able to find a feasible solution for GS-SOF design, then EXIT.
- 

Source: Author's own results.

4.1.3 TWO-STAGE DISCRETE-TIME  $\mathcal{H}_\infty$  GS-SOF DESIGN

In this subsection, the goal is to extend the gain-scheduling control synthesis strategy proposed in Subsection 4.1.2 to address the problem of disturbance rejection for discrete-time LPV systems. With this purpose, we now consider the state-space realization

$$\begin{aligned}
 x(k+1) &= A(\alpha(k))x(k) + B_u(\alpha(k))u(k) + B_w(\alpha(k))w(k) \\
 z(k) &= C_z(\alpha(k))x(k) + D_u(\alpha(k))u(k) + D_w(\alpha(k))w(k) \\
 y(k) &= C_y(\alpha(k))x(k) + D_y(\alpha(k))w(k),
 \end{aligned} \tag{4.37}$$

where  $x(k) \in \mathbb{R}^n$  is the state vector,  $u(k) \in \mathbb{R}^m$  is the input vector,  $y(k) \in \mathbb{R}^p$  is the measured output vector,  $w(k) \in \mathbb{R}^q$  is the exogenous input vector, and  $z(k) \in \mathbb{R}^s$  is the controlled output vector. Also,  $(A, B_u, B_w, C_y, C_z, D_u, D_w, D_y)(\alpha(k))$  are parameter-dependent matrices that belong to a polytopic domain parameterized in terms of a time-varying vector  $\alpha(k) \in \mathbb{R}^N$ , following similar definitions as in (4.2) and (4.3).

The goal is to design an output-feedback control law  $u(k) = L(\alpha(k))y(k)$ , where  $L(\alpha(k))$  is a gain-scheduled SOF controller that asymptotically stabilizes the closed-loop system

$$\begin{aligned}
 x(k+1) &= (A(\alpha(k)) + B_u(\alpha(k))L(\alpha(k))C_y(\alpha(k)))x(k) + (B_w(\alpha(k)) + B_u(\alpha(k))L(\alpha(k))D_y(\alpha(k)))w(k) \\
 z(k) &= (C_z(\alpha(k)) + D_u(\alpha(k))L(\alpha(k))C_y(\alpha(k)))x(k) + (D_w(\alpha(k)) + D_u(\alpha(k))L(\alpha(k))D_y(\alpha(k)))w(k)
 \end{aligned} \tag{4.38}$$

and also guarantees a lower bound  $\rho$  in the system decay rate and an  $\mathcal{H}_\infty$  guaranteed

cost  $\mu$ , that is  $\|H_{zw}\|_\infty < \mu$ , where

$$\|H_{zw}\|_\infty := \sup_{\|w(k)\|_2 \neq 0} \frac{\|z(k)\|_2}{\|w(k)\|_2},$$

holds for every possible trajectory of the time-varying parameter  $\alpha(k)$ . Following previous works on this subject (SADEGHZADEH, 2017), we denote  $\|H_{zw}\|_\infty$  as the induced- $l_2$  gain performance of the closed-loop system (4.38). However, with a slight abuse of language, we consider the use of the term  $\mathcal{H}_\infty$  guaranteed cost for referring to the bound  $\mu$ .

To this end, we first derive a set of sufficient LMI conditions for ensuring asymptotic stability, minimum decay rate  $\rho$  and an upper bound  $\mu$  on the  $\mathcal{H}_\infty$  guaranteed cost for discrete-time systems. These base LMI constraints are defined regarding the generic non-forced (i.e.  $u(k) = 0$ ) discrete-time LPV system realization

$$\begin{aligned} x(k+1) &= \mathcal{A}(\alpha(k))x(k) + \mathcal{B}(\alpha(k))w(k), \\ z(k) &= \mathcal{C}(\alpha(k))x(k) + \mathcal{D}(\alpha(k))w(k). \end{aligned} \quad (4.39)$$

In Lemma 4.2, we have sufficient LMI conditions for ensuring the desired control objectives. This result will be used further in this subsection in order to approach the  $\mathcal{H}_\infty$  guaranteed control cost problem.

**Lemma 4.2.** *If there exist a symmetric matrix  $P(\alpha(k)) > 0$  such that*

$$\begin{bmatrix} \rho^2 P(\alpha(k)) - \mathcal{A}(\alpha(k))'F(\alpha(k))' - F(\alpha(k))\mathcal{A}(\alpha(k)) & * & * & * \\ F(\alpha(k))' - G(\alpha(k))\mathcal{A}(\alpha(k)) & G(\alpha(k)) + G(\alpha(k))' - P(\beta(k)) & * & * \\ -\mathcal{B}(\alpha(k))'F(\alpha(k))' & -\mathcal{B}(\alpha(k))'G(\alpha(k))' & \gamma I & * \\ -\mathcal{C}(\alpha(k)) & 0 & -\mathcal{D}(\alpha(k)) & I \end{bmatrix} > 0 \quad (4.40)$$

holds for every  $\alpha \in \bar{\lambda}_N$ , then system (4.39) is asymptotically stable and presents minimum decay rate  $\rho$  and  $\mathcal{H}_\infty$  guaranteed cost  $\mu = \sqrt{\gamma}$ .

*Proof.* We begin by noting that (4.40) can be equivalently rewritten in terms of a sum and product of matrices as

$$\begin{aligned} & \begin{bmatrix} -\rho^2 P(\alpha(k)) & 0 & 0 & 0 \\ 0 & P(\beta(k)) & 0 & 0 \\ 0 & 0 & -\gamma I & 0 \\ 0 & 0 & 0 & I \end{bmatrix} + \begin{bmatrix} F(\alpha(k)) & 0 \\ G(\alpha(k)) & 0 \\ 0 & 0 \\ 0 & I \end{bmatrix} \begin{bmatrix} -\mathcal{A}(\alpha(k)) & I & -\mathcal{B}(\alpha(k)) & 0 \\ -\mathcal{C}(\alpha(k)) & 0 & -\mathcal{D}(\alpha(k)) & I \end{bmatrix} + \\ & + \begin{bmatrix} -\mathcal{A}(\alpha(k))' & -\mathcal{C}(\alpha(k))' \\ I & 0 \\ -\mathcal{B}(\alpha(k))' & -\mathcal{D}(\alpha(k))' \\ 0 & I \end{bmatrix} \begin{bmatrix} F(\alpha(k))' & G(\alpha(k))' & 0 & 0 \\ 0 & 0 & 0 & I \end{bmatrix} < 0. \quad (4.41) \end{aligned}$$

Then, according to Lemma 2.4, by defining

$$\mathcal{S} = \begin{bmatrix} -\rho^2 P(\alpha(k)) & 0 & 0 & 0 \\ 0 & P(\beta(k)) & 0 & 0 \\ 0 & 0 & -\gamma I & 0 \\ 0 & 0 & 0 & I \end{bmatrix}, \quad \omega = \begin{bmatrix} x(k) \\ x(k+1) \\ w(k) \\ z(k) \end{bmatrix},$$

$$\mathcal{R} = \begin{bmatrix} -A(\alpha(k)) & I & -B(\alpha(k)) & 0 \\ -C(\alpha(k)) & 0 & -D(\alpha(k)) & I \end{bmatrix}, \quad \text{and} \quad \chi = \begin{bmatrix} F(\alpha(k)) & 0 \\ G(\alpha(k)) & 0 \\ 0 & 0 \\ 0 & I \end{bmatrix},$$

we have that (4.41) implies in

$$\omega' \mathcal{S} \omega = \begin{bmatrix} x(k)' & x(k+1)' & w(k)' & z(k)' \end{bmatrix} \begin{bmatrix} -\rho^2 P(\alpha(k)) & 0 & 0 & 0 \\ 0 & P(\beta(k)) & 0 & 0 \\ 0 & 0 & -\gamma I & 0 \\ 0 & 0 & 0 & I \end{bmatrix} \begin{bmatrix} x(k) \\ x(k+1) \\ w(k) \\ z(k) \end{bmatrix}$$

$$= x(k+1)' P(\beta(k)) x(k+1) - x(k)' \rho^2 P(\alpha(k)) x(k) + z(k)' z(k) - \gamma w(k)' w(k) < 0. \quad (4.42)$$

Once again, employing the strategy presented in Montagner *et al.* (2005) and defining  $P(\beta(k)) = P(\alpha(k+1))$ , (4.42) leads to

$$x(k+1)' P(\alpha(k+1)) x(k+1) - x(k)' \rho^2 P(\alpha(k)) x(k) + z(k)' z(k) - \gamma w(k)' w(k) < 0, \quad (4.43)$$

which corresponds to a discrete version of the bounded real lemma (BOYD *et al.*, 1994), that with  $V(k) = x(k)' P(\alpha(k)) x(k)$  guarantees the asymptotic stability of (4.39) with a lower bound  $\rho$  on the system decay rate and an  $\mathcal{H}_\infty$  guaranteed cost  $\mu = \sqrt{\gamma}$ .  $\square$

Now, in terms of the results given in Lemma 4.2, we propose new sufficient LMI conditions that enables the synthesis of  $\mathcal{H}_\infty$  gain-scheduled SOF controllers with minimum decay rate bound, as stated in Theorem 4.3.

**Theorem 4.3.** *Assuming that there exists a gain matrix  $K(\alpha(k))$  that asymptotically stabilizes  $A(\alpha(k)) + B(\alpha(k))K(\alpha(k))$ , then there exists a static output-feedback gain-scheduled matrix  $L(\alpha(k))$  that asymptotically stabilizes  $A(\alpha(k)) + B(\alpha(k))L(\alpha(k))C(\alpha(k))$  with decay rate bounded by  $\rho_2$  and  $\mathcal{H}_\infty$  guaranteed cost  $\mu_2 = \sqrt{\gamma_2}$ , for any arbitrary time variation of the parameter  $\alpha(k)$  in (4.3), if there exist symmetric matrices  $P_i > 0$  and matrices  $F_i$ ,*

$G_i$ ,  $H$ , and  $J_i$ , such that

$$\begin{bmatrix} \rho_2^2 P_i - A_i' F_i' - F_i A_i - K_i' B_{u_i}' F_i' - F_i B_{u_i} K_i & * & * & * & * \\ F_i' - G_i A_i - G_i B_{u_i} K_i & G_i + G_i' - P_d & * & * & * \\ -B_{w_i}' F_i' & -B_{w_i}' G_i' & \gamma_2 I & * & * \\ -C_{z_i} - D_{u_i} K_i & 0 & -D_{w_i} & I & * \\ -B_{u_i}' F_i' + H K_i - J_i C_{y_i} & -B_{u_i}' G_i' & -J_i D_{y_i} & -D_{u_i}' & H + H' \end{bmatrix} > 0 \quad (4.44)$$

holds for  $d = 1, \dots, N$  and  $i = 1, \dots, N$ ,

$$\begin{bmatrix} \Sigma_{1,1}^{ij} & * & * & * & * \\ \Sigma_{2,1}^{ij} & \Sigma_{2,2}^{ij} & * & * & * \\ -B_{w_i}'(F_i' + F_j') - B_{w_j}' F_i' & \Sigma_{3,2}^{ij} & 3\gamma_2 I & * & * \\ \Sigma_{4,1}^{ij} & 0 & -2D_{w_i} - D_{w_j} & 3I & * \\ \Sigma_{5,1}^{ij} & \Sigma_{5,2}^{ij} & \Sigma_{5,3}^{ij} & -2D_{u_i}' - D_{u_j}' & 3(H + H') \end{bmatrix} > 0 \quad (4.45)$$

holds for  $d = 1, \dots, N$ ,  $i = j = 1, \dots, N$ , and  $i \neq j$ , where

$$\begin{aligned} \Sigma_{1,1}^{ij} &= \rho_2^2(2P_i + P_j) + (-F_i(A_i + A_j) - F_j A_i - F_i(B_{u_i} K_j + B_{u_j} K_i) - F_j B_{u_i} K_i) + (\bullet)', \\ \Sigma_{2,1}^{ij} &= 2F_i' + F_j' - G_i(A_i + A_j) - G_j A_i - G_i(B_{u_i} K_j + B_{u_j} K_i) - G_j B_{u_i} K_i, \\ \Sigma_{2,2}^{ij} &= 2(G_i + G_i') + G_j + G_j' - 3P_d, \\ \Sigma_{3,2}^{ij} &= -B_{w_i}'(G_i' + G_j') - B_{w_j}' G_i', \\ \Sigma_{5,2}^{ij} &= -B_{u_i}'(G_i' + G_j') - B_{u_j}' G_i', \\ \Sigma_{5,3}^{ij} &= -J_i(D_{y_i} + D_{y_j}) - J_j D_{y_i}, \\ \Sigma_{4,1}^{ij} &= -2C_{z_i} - C_{z_j} - D_{u_i}(K_i + K_j) - D_{u_j} K_i, \text{ and} \\ \Sigma_{5,1}^{ij} &= -B_{u_i}'(F_i' + F_j') - B_{u_j}' F_i' + 2H K_i + H K_j - J_i(C_{y_i} + C_{y_j}) - J_j C_{y_i}, \end{aligned} \quad (4.46)$$

and

$$\begin{bmatrix} \Sigma_{1,1}^{ijl} & * & * & * & * \\ \Sigma_{2,1}^{ijl} & \Sigma_{2,2}^{ijl} & * & * & * \\ \Sigma_{3,1}^{ijl} & \Sigma_{3,2}^{ijl} & 6\gamma_2 I & * & * \\ \Sigma_{4,1}^{ijl} & 0 & -2(D_{w_i} + D_{w_j} + D_{w_l}) & 6I & * \\ \Sigma_{5,1}^{ijl} & \Sigma_{5,2}^{ijl} & \Sigma_{5,3}^{ijl} & -2(D_{u_i}' + D_{u_j}' + D_{u_l}') & 6(H + H') \end{bmatrix} > 0 \quad (4.47)$$

holds for  $d = 1, \dots, N$ ,  $i = 1, \dots, N - 2$ ,  $j = i + 1, i + 2, \dots, N - 1$ , and  $l = j + 1, j + 2, \dots, N$ , where

$$\begin{aligned}
\Sigma_{1,1}^{ijl} &= 2\rho_2^2(P_i + P_j + P_k) + (-F_i(A_j + A_l) - F_j(A_i + A_l) - F_l(A_i + A_j) + \\
&\quad -F_i(B_{u_j}K_l + B_{u_l}K_j) - F_j(B_{u_i}K_l + B_{u_l}K_i) - F_l(B_{u_i}K_j + B_{u_j}K_i)) + (\bullet)', \\
\Sigma_{2,1}^{ijl} &= 2(F'_i + F'_j + F'_l) - G_i(A_j + A_l) - G_j(A_i + A_l) - G_l(A_i + A_j) + \\
&\quad -G_i(B_{u_j}K_l + B_{u_l}K_j) - G_j(B_{u_i}K_l + B_{u_l}K_i) - G_l(B_{u_i}K_j + B_{u_j}K_i), \\
\Sigma_{3,1}^{ijl} &= -B'_{w_i}(F'_j + F'_l) - B'_{w_j}(F'_i + F'_l) - B'_{w_l}(F'_i + F'_j), \\
\Sigma_{4,1}^{ijl} &= -2(C_{z_i} + C_{z_j} + C_{z_l}) - D_{u_i}(K_j + K_l) - D_{u_j}(K_i + K_l) - D_{u_l}(K_i + K_j),
\end{aligned} \tag{4.48}$$

$$\begin{aligned}
\Sigma_{5,1}^{ijl} &= -B'_{u_i}(F'_j + F'_l) - B'_{u_j}(F'_i + F'_l) - B'_{u_l}(F'_i + F'_j) + 2H(K_i + K_j + K_l) \\
&\quad - J_i(C_j + C_l) - J_j(C_i + C_l) - J_l(C_i + C_j), \\
\Sigma_{2,2}^{ijl} &= 2(G_i + G'_i + G_j + G'_j + G_l + G'_l) - 6P_d, \\
\Sigma_{3,2}^{ijl} &= -B'_{w_i}(G'_j + G'_l) - B'_{w_j}(G'_i + G'_l) - B'_{w_l}(G'_i + G'_j), \\
\Sigma_{5,2}^{ijl} &= -B'_{u_i}(G'_j + G'_l) - B'_{u_j}(G'_i + G'_l) - B'_{u_l}(G'_i + G'_j), \text{ and} \\
\Sigma_{5,3}^{ijl} &= -J_i(D_{y_j} + D_{y_l}) - J_j(D_{y_i} + D_{y_l}) - J_l(D_{y_i} + D_{y_j}).
\end{aligned} \tag{4.49}$$

In the affirmative case, the  $N$  vertices matrices,  $L_i$ , for composing gain-scheduled SOF controller can be retrieved with  $L_i = H^{-1}J_i$ .

*Proof.* Analogously to the proof of Theorem 4.2, we readily note that when (4.44) holds, the existence of  $H^{-1}$  is ensured. Moreover, by multiplying (4.44) by  $\alpha_i^3(k)$  and by  $\beta_d(k)$ , summing from  $i = 1$  to  $i = N$  and from  $d = 1$  to  $d = N$ , and that by multiplying (4.45) by  $\alpha_i^2(k)\alpha_j(k)$  and by  $\beta_d(k)$ , summing from  $i, j = 1$  to  $i, j = N$ ,  $i \neq j$  and from  $d = 1$  to  $d = N$ , and that by multiplying (4.48) by  $\alpha_i(k)\alpha_j(k)\alpha_l(k)$ , and by  $\beta_d(k)$ , summing from  $i = 1$  to  $i = N - 2$ ,  $j = i + 1$  to  $j = N - 1$ ,  $l = j + 1$  to  $l = N$ , and from  $d = 1$  to  $d = N$ , with  $\sum_{d=1}^N \beta_d(k) = 1, \beta_d(k) > 0$ , we have

$$\left[ \begin{array}{cccc}
\rho_2^2 P(\alpha(k)) + (-F(\alpha(k))A(\alpha(k)) - F(\alpha(k))B_u(\alpha(k))K(\alpha(k))) + (\bullet)' & & & \\
F(\alpha(k))' - G(\alpha(k))A(\alpha(k)) - G(\alpha(k))B_u(\alpha(k))K(\alpha(k)) & & & \\
-B_w(\alpha(k))'F(\alpha(k))' & & & \\
-C_z(\alpha(k)) - D_u(\alpha(k))K(\alpha(k)) & & & \\
-B_u(\alpha(k))'F(\alpha(k))' + HK(\alpha(k)) - J(\alpha(k))C_y(\alpha(k)) & & & \\
* & * & * & * \\
G(\alpha(k)) + G(\alpha(k))' - P(\beta(k)) & * & * & * \\
-B_w(\alpha(k))'G(\alpha(k))' & \gamma_2 I & * & * \\
0 & -D_w(\alpha(k)) & I & * \\
-B_u(\alpha(k))'G(\alpha(k))' & -J(\alpha(k))D_y(\alpha(k)) & -D_u(\alpha(k))' & H + H'
\end{array} \right] > 0 \tag{4.50}$$

also holds.

Then, performing a transformation over (4.50) by pre- and pos-multiplying it by

$$U(\alpha(k))' = \begin{bmatrix} I & 0 & 0 & 0 & S(\alpha(k))' \\ 0 & I & 0 & 0 & 0 \\ 0 & 0 & I & 0 & V(\alpha(k))' \\ 0 & 0 & 0 & I & 0 \end{bmatrix} \quad \text{and } U(\alpha(k)),$$

with  $S(\alpha(k)) = H^{-1}J(\alpha(k))C_y(\alpha(k)) - K(\alpha(k))$  and  $V(\alpha(k)) = H^{-1}J(\alpha(k))D_y(\alpha(k))$  we obtain

$$\begin{bmatrix} \rho_2^2 P(\alpha(k)) + (-F(\alpha(k))A(\alpha(k)) - F(\alpha(k))B_u(\alpha(k))H^{-1}J(\alpha(k))C_y(\alpha(k))) + (\bullet)' \\ F(\alpha(k))' - G(\alpha(k))A(\alpha(k)) - G(\alpha(k))B_u(\alpha(k))H^{-1}J(\alpha(k))C_y(\alpha(k)) \\ -B_w(\alpha(k))'F(\alpha(k))' - D_y(\alpha(k))'J(\alpha(k))'H^{-T}B_u(\alpha(k))'F(\alpha(k))' \\ -C_z(\alpha(k)) - D_u(\alpha(k))H^{-1}J(\alpha(k))C_y(\alpha(k)) \\ * \\ G(\alpha(k)) + G(\alpha(k))' - P(\beta(k)) \\ -B_w(\alpha(k))'G(\alpha(k))' - D_y(\alpha(k))'J(\alpha(k))'H^{-T}B_u(\alpha(k))'G(\alpha(k))' \\ 0 \\ * \\ * \\ \gamma_2 I \\ * \\ -D_w(\alpha(k)) - D_u(\alpha(k))H^{-1}J(\alpha(k))D_y(\alpha(k)) \quad I \end{bmatrix} > 0. \quad (4.51)$$

Now, note that by defining  $L(\alpha(k)) = H^{-1}J(\alpha(k))$  we have that (4.51) becomes

$$\begin{bmatrix} \rho_2^2 P(\alpha(k)) + (-F(\alpha(k))A_{cl}(\alpha(k))) + (\bullet)' & * & * & * \\ F(\alpha(k))' - G(\alpha(k))A_{cl}(\alpha(k)) & G(\alpha(k)) + G(\alpha(k))' - P(\beta(k)) & * & * \\ -B_{cl}(\alpha(k))'F(\alpha(k))' & -B_{cl}(\alpha(k))'G(\alpha(k))' & \gamma_2 I & * \\ -C_{cl}(\alpha(k)) & 0 & -D_{cl}(\alpha(k)) & I \end{bmatrix} > 0. \quad (4.52)$$

where

$$\begin{aligned} A_{cl}(\alpha(k)) &= A(\alpha(k)) + B_u(\alpha(k))L(\alpha(k))C_y(\alpha(k)), \\ B_{cl}(\alpha(k)) &= B_w(\alpha(k)) + B_u(\alpha(k))L(\alpha(k))D_y(\alpha(k)), \\ C_{cl}(\alpha(k)) &= C_z(\alpha(k)) + D_u(\alpha(k))L(\alpha(k))C_y(\alpha(k)), \quad \text{and} \\ D_{cl}(\alpha(k)) &= D_w(\alpha(k)) + D_u(\alpha(k))L(\alpha(k))D_y(\alpha(k)), \end{aligned} \quad (4.53)$$

which is, according to the results given in Lemma 4.2, a sufficient condition for the closed-loop system (4.37) to be asymptotically stabilized with the gain-scheduled controller  $L(\alpha(k))$ , with closed-loop  $\mathcal{H}_\infty$  guaranteed cost  $\mu_2 = \sqrt{\gamma_2}$  and minimum decay rate  $\rho_2$ .  $\square$

As it occurs in the stabilization problem, the present proposed method requires that

a stabilizing state-feedback controller  $K(\alpha(k))$  is feed as input parameter in the second-stage LMIs. Considering this fact, we propose an extension of results presented in Montagner *et al.* (2005) to address the state-feedback stabilization of discrete-time LPV systems considering a minimum decay rate specification and an upper bound on the system  $\mathcal{H}_\infty$  guaranteed cost. This proposition is enunciated in Theorem 4.4.

**Theorem 4.4** (First-Stage  $\mathcal{H}_\infty$  GS-SF Design). *If there exists symmetric positive matrices  $Q_j \in \mathbb{R}^{n \times n}$ , matrices  $X_j \in \mathbb{R}^{n \times n}$  and  $Y_j \in \mathbb{R}^{m \times n}$ ,  $j = 1, \dots, N$ , and given scalars  $\rho_1$  and  $\gamma_1$  such that the LMIs*

$$\begin{bmatrix} X_j + X'_j - \rho_1^2 Q_j & * & * & * \\ 0 & I & * & * \\ A_j X_j + B_{u_j} Y_j & B_{w_j} & Q_i & * \\ C_{z_j} X_j + D_{u_j} Y_j & D_{w_j} & 0 & \gamma_1 I \end{bmatrix} > 0, \quad (4.54)$$

for  $i = 1, \dots, N$ ,  $j = 1, \dots, N$ , and

$$\begin{bmatrix} X_j + X'_j + X_k + X'_k - \rho_1^2(Q_j + Q_k) & * & * & * \\ 0 & 2I & * & * \\ A_j X_k + B_{u_j} Y_k + A_k X_j + B_{u_k} Y_j & B_{w_j} + B_{w_k} & 2Q_i & * \\ C_{z_j} X_k + D_{u_j} Y_k + C_{z_k} X_j + D_{u_k} Y_j & D_{w_j} + D_{w_k} & 0 & 2\mu_1 I \end{bmatrix} > 0, \quad (4.55)$$

for  $i = 1, \dots, N$ ,  $j = 1, \dots, N-1$ ,  $k = j+1, \dots, N$  have a solution, then the stability of the closed-loop system (4.8) is assured with decay rate bound  $\rho_1$  and  $\mathcal{H}_\infty$  guaranteed cost  $\mu_1 = \sqrt{\gamma_1}$  by the state-feedback control law  $u(k) = K(\alpha(k))x(k)$  with the parameter-dependent gain

$$K(\alpha(k)) = Y(\alpha(k))X(\alpha(k))^{-1}, \quad (4.56)$$

for any arbitrary time variation of the parameter  $\alpha(k)$  in (4.3).

*Proof.* Omitted for brevity. The proof follows directly as in Montagner *et al.* (2005), with a parameter-dependent Lyapunov function  $V(x(k)) = x(k)'P(\alpha(k))x(k) > 0$  ensuring  $V(x(k+1)) - \rho^2 V(x(k)) < 0$ .  $\square$

**Remark 4.7.** *The employment of the proposed method aiming at the  $\mathcal{H}_\infty$  guaranteed cost minimization via GS-SOF control design in a two-stage procedure involves the specification of three design parameters: the first-stage decay rate bound  $\rho_1$  and  $\mathcal{H}_\infty$  guaranteed cost bound  $\mu_1 = \sqrt{\gamma_1}$ ; and the second-stage minimum decay rate bound  $\rho_2$ . The second-stage parameter  $\gamma_2$  can be considered as a scalar variable to be minimized in order to obtain an optimal  $\mathcal{H}_\infty$  guaranteed cost  $\mu_2$ , for the considered problem variables ( $K(\alpha(k))$  and the other three design parameters).*

**Remark 4.8.** *With respect to the decay rate bounds, the user might consider setting the minimum decay rate parameters to assume equal values (i.e.  $\rho_1 = \rho_2$ ), to simplify the*

design procedure. However, since the choice of  $\rho_1$  directly impacts on the second-stage feasibility, it is possible to consider a linear search over these two parameters, with the goal of obtaining the best possible solution for the LMI problem, in terms of the smallest second-stage decay rate bound  $\rho_2$  such that the LMIs are feasible, aiming at guaranteeing a faster closed-loop transient performance. Regarding the specification of the parameter  $\gamma_1$ , associated to the first-stage  $\mathcal{H}_\infty$  bound, a linear search over a pre-specified range can be performed. Once again, it is important to emphasize that for different  $K(\alpha(k))$  designed in the first-stage and used as input data to the second stage, a different SOF problem is set in terms of the LMIs (4.44)-(4.48). Therefore, the  $\mathcal{H}_\infty$  guaranteed cost problem in Theorem 4.3, when configured to minimize the variable  $\gamma_2 = \mu_2^2$ , might yield a different solution depending on the choices of the first-stage design parameters  $\rho_1$  and  $\gamma_1$ .

In Algorithm 4.3 we summarize the  $\mathcal{H}_\infty$  GS-SOF design procedure proposed in the present subsection. The method is based on designing a first-stage  $\mathcal{H}_\infty$  state-feedback gain controller  $K(\alpha(k))$  through Theorem 4.4 and then using the obtained vertex matrices as input information for designing the desired  $\mathcal{H}_\infty$  gain-scheduling static output-feedback controller by solving the problem stated in Theorem 4.3 minimizing the variable  $\gamma_2$ .

---

**Algorithm 4.3** Two-stage  $\mathcal{H}_\infty$ GS-SOF controller synthesis

---

- 1: Reset counter with  $\epsilon \leftarrow 1$  and set maximum iteration limit  $\epsilon_{max}$ .
  - 2: Step 1-1 (SF Initialization): Find a GS-SF controller  $K(\alpha(k))$  design via Theorem 4.4 with bounds  $\rho_1 < 1$  and  $\gamma_1 = \mu_1^2$ .
  - 3: Step 1-2 (SF Checking): If Theorem 4.4 returns feasible  $K(\alpha(k))$ , go to Step 2-1; Otherwise, set a different pair of first-stage decay rate bound  $\rho_1 \leftarrow \rho_1^{new}$  and  $\gamma_1 \leftarrow \gamma_1^{new}$ , and restart Step 1-1; However, if Theorem 4.4 fails with  $\rho_1 \leftarrow 1$ , it might not exist an stabilizing GS-SF controller, then EXIT.
  - 4: Step 2-1 (SOF Design): Find the GS-SOF controller  $L(\alpha(k))$  design via Theorem 4.3 with  $K(\alpha(k))$ , decay rate bound  $\rho_2$  and minimum  $\gamma_2 = \mu_2^2$ .
  - 5: Step 2-2 (SOF Checking): If Theorem 4.3 returns a feasible  $L(\alpha(k))$ , EXIT; Otherwise, set  $\epsilon \leftarrow \epsilon + 1$  and if  $\epsilon < \epsilon_{max}$  go to Step 1-1 with a different pair of first-stage decay rate bound  $\rho_1 \leftarrow \rho_1^{new}$  and  $\mathcal{H}_\infty$  guaranteed cost bound  $\gamma_1 \leftarrow \gamma_1^{new}$  to restart the process; However, if  $\epsilon \geq \epsilon_{max}$ , the algorithm was not able to find a feasible solution for GS-SOF design, then EXIT.
- 

Source: Author's own results.

**Remark 4.9.** *It is important to observe that the proposed Algorithms 4.1–4.3 represent an immediate strategy for employing our proposed two-stage method. However, as mentioned in Remarks 4.3 and 4.7, the designer might consider different strategies for setting the decay rate and  $\mathcal{H}_\infty$  norm bound parameters in order to obtain best optimization results. In fact, by performing some tests using the proposed strategy, it was possible to observe that the  $\mathcal{H}_\infty$  norm bound imposed in the first stage severely impacts on the results obtained in the second stage. For instance, employing an optimization  $\mathcal{H}_\infty$ -SF design might hinder*



feasibility in the SOF design stage. Other preliminary tests showed that by considering a line search over the imposed first-stage  $\mathcal{H}_\infty$  norm bound, an optimal  $\mathcal{H}_\infty$  guaranteed cost in the second-stage design can be obtained. However, at the present state of development of this work, the focus is to derive new LMI conditions for GS-SOF controller synthesis. The development of an optimized two-stage algorithm for this problem is a subject that is going to be addressed in futures works.

#### 4.1.4 ILLUSTRATIVE EXAMPLES

In this section, we present some numerical experiments aiming to illustrate the synthesis procedure proposed in this chapter and its features, as well as comparing it with other strategies available in the literature. All experiments were performed using the SeDuMi (STURM, 1999) solver, via YALMIP (LOFBERG, 2004) interface.

**Example 4.1** For this first example, consider a discrete-time LPV system (SADEGHZADEH, 2017), whose state-space matrices are dependent on a time-varying parameter  $\theta$ , such as

$$\begin{aligned}
 A(\theta) &= \begin{bmatrix} 0.0429 & -0.0931 & 0.6249 & 0.3441 \\ -0.4705 & 0.4222 & 0.3410 & -0.2100 \\ -0.3855 & -0.5937 & 0.1346 & -0.4270 \\ 0.3841 & 0.1436 & 0.4203 & -0.3100 \end{bmatrix} + \theta \begin{bmatrix} 0.0725 & 0.0415 & 0.1360 & 0.0798 \\ 0.0802 & 0.1609 & 0.1265 & -0.0853 \\ -0.0430 & -0.1672 & 0.1674 & -0.0854 \\ 0.1354 & -0.0016 & -0.0511 & 0.0032 \end{bmatrix}, \\
 B(\theta) &= \begin{bmatrix} -1.0302 & 1.4171 \\ 0 & -0.2532 \\ 1.6270 & 0.4504 \\ 0.6604 & 0 \end{bmatrix} + \theta \begin{bmatrix} -0.5881 & -0.1067 \\ 0.6866 & -0.2186 \\ 0 & 0 \\ -0.4438 & -0.2880 \end{bmatrix}, \\
 C(\theta) &= [-0.7000 \quad 0.2876 \quad 0.6224 \quad 0] + \theta [-0.0652 \quad -0.2943 \quad 0 \quad -0.2982].
 \end{aligned} \tag{4.57}$$

The time-varying parameter  $\theta$  is bounded in the interval  $[0, 1]$ , but its measurement is assumed to be available on-line during control operation.

First, we notice that all space-state matrices in (4.57) are affected by  $\theta$ , including the output matrix  $C$ . Different from the first SOF control approaches (GEROMEL; PERES; SOUZA, 1996), our proposed method is able to cope with parameter-dependent output matrix case. Furthermore, no particular structure is imposed to any of the system matrices, which is an inherent limitation in other strategies that have attempted to address the SOF problem in this more general formulation (CRUSIUS; TROFINO, 1999; DONG; YANG, 2008).

Now, we proceed to the GS-SOF controller design using the method proposed in this

work. Immediately, see that (4.57) can be easily put in a polytopic format, by means of a convex combination of two vertices via  $\alpha(k) \in \bar{\bar{\Lambda}}_N$ . Note that, for this particular example, the relationship between  $\alpha$  and  $\theta$  is direct. In fact, one can see that  $\alpha$  have the same bounds  $([0,1])$  as  $\theta$ . In those terms, (4.57) can be represented in a polytopic form as

$$\begin{aligned}
A(\alpha(k)) = & \alpha_1(k) \begin{bmatrix} 0.0429 & -0.0931 & 0.6249 & 0.3441 \\ -0.4705 & 0.4222 & 0.3410 & -0.2100 \\ -0.3855 & -0.5937 & 0.1346 & -0.4270 \\ 0.3841 & 0.1436 & 0.4203 & -0.3100 \end{bmatrix} + \\
& + \alpha_2(k) \begin{bmatrix} 0.1154 & -0.0516 & 0.7609 & 0.4239 \\ -0.3903 & 0.5831 & 0.4675 & -0.2953 \\ -0.4285 & -0.7609 & 0.3020 & -0.5124 \\ 0.5195 & 0.1420 & 0.3692 & -0.3069 \end{bmatrix}, \tag{4.58} \\
B(\alpha(k)) = & \alpha_1(k) \begin{bmatrix} -1.0302 & 1.4171 \\ 0 & -0.2532 \\ 1.6270 & 0.4504 \\ 0.6604 & 0 \end{bmatrix} + \alpha_2(k) \begin{bmatrix} -1.6183 & 1.3104 \\ 0.6866 & -0.4718 \\ 1.6270 & 0.4504 \\ 0.2166 & -0.2880 \end{bmatrix}, \\
C(\alpha(k)) = & \alpha_1(k) [-0.7000 \quad 0.2876 \quad 0.6224 \quad 0] + \\
& + \alpha_2(k) [-0.7652 \quad -0.0067 \quad 0.6224 \quad -0.2982].
\end{aligned}$$

Then, by setting a decay rate bound  $\rho_1 = 0.85$  and using Theorem 4.1 conditions, considering  $X(\alpha(k)) = X$ , we obtain

$$\begin{aligned}
K_1 = & \begin{bmatrix} 0.1718 & 0.2371 & -0.0403 & 0.2986 \\ 0.0545 & 0.3104 & -0.3695 & -0.0637 \end{bmatrix} \quad \text{and} \\
K_2 = & \begin{bmatrix} 0.2407 & 0.2787 & -0.0916 & 0.3124 \\ 0.1826 & 0.5205 & -0.4687 & 0.0099 \end{bmatrix}
\end{aligned} \tag{4.59}$$

as the first-stage parameter-dependent gain matrix  $K(\alpha(k))$  vertices.

In the sequence, we advance to the second stage, by applying Theorem 4.2 conditions, using the obtained SF gain matrices (4.59) and setting  $\rho_2 = 0.85$ . Then, the solution under the LMIs constraints (4.15),(4.16) and (4.19) yields

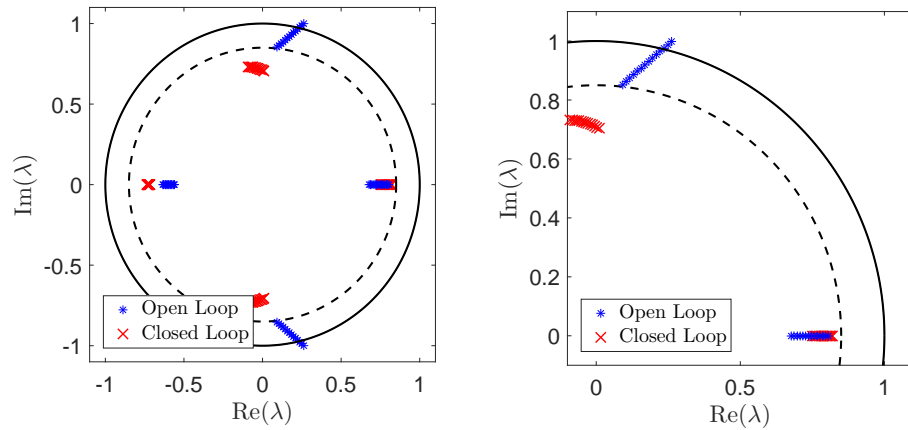
$$L_1 = \begin{bmatrix} -0.3502 \\ -0.1945 \end{bmatrix} \quad \text{and} \quad L_2 = \begin{bmatrix} -0.3667 \\ -0.3540 \end{bmatrix} \tag{4.60}$$

as the vertices matrices for the desired GS-SOF controller  $L(\alpha(k))$ .

By inspection, we see that (4.60) have a very simple format when compared to its correspondent SF gains (4.59). Such feature is typical in SOF problems, as only the

available state information is used for composing the feedback loop. This is one of the advantages of SOF over dynamic output feedback (DOF) approaches, which require a system order augmentation, as the DOF controller states must be incorporated to the problem (CRUSIUS; TROFINO, 1999).

Figure 4.2 - Eigenvalue cloud for system (4.58) in open loop (\*) and closed loop (x) with GS-SOF controller (4.60) (dashed line:  $\rho = 0.85$ ; Right chart: close-up).



Source: Author's own results.

For illustration purposes, in Figure 4.2 we present the eigenvalue placement of system (4.58) in open loop (\*), and also in closed loop via GS-SOF controller (x) formed by the designed vertices matrices (4.60). This result is obtained by calculating the eigenvalues  $\lambda(A(\alpha(k)))$  and  $\lambda(A(\alpha(k)) + B(\alpha(k))L(\alpha(k))C(\alpha(k)))$  for 50 different values of  $\alpha(k) \in \bar{\bar{\Lambda}}_N$ . The solid line circle denotes the unitary circle and the dashed one represents the region inherent to the decay rate bound  $\rho = 0.85$ . At first, we can see that system (4.58) presents unstable eigenvalue configuration for some  $\alpha(k) \in \bar{\bar{\Lambda}}_N$ . However, by applying the proposed method, the closed-loop eigenvalues, for all  $\alpha(k) \in \bar{\bar{\Lambda}}_N$ , are all contained in the dashed circle for  $\rho = 0.85$ . Of course, it is important to remember that when dealing with LPV systems, the concept of eigenvalue configuration for a fixed value of  $\alpha(k)$  must be taken with care. This analysis alone is not sufficient for inferring about the system asymptotic stability, and it is used here only for illustrating the effects of the decay rate constraint over the polytope system vertices, as already discussed in Section 3.2.

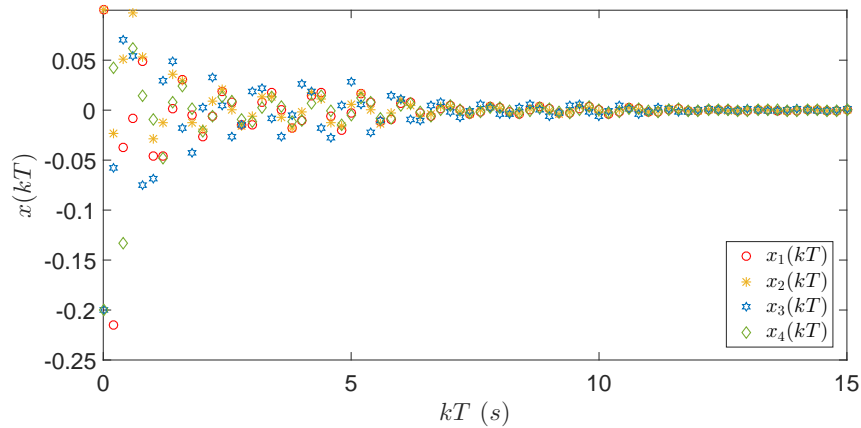
Completing the analysis, the results of a simulation of system (4.58) response is presented in the sequence. Both open and closed loop with the designed GS-SOF controller are considered. The simulation occurred in terms of the state evolution and the produced control signal behavior, after being released from initial conditions arbitrarily defined as  $x(0) = [0.1 \ 0.1 \ -0.2 \ -0.2]'$ . For this study, we set a sampling period  $T$  of 0.2 s.

Moreover, the time-varying parameter is considered as a sinusoidal wave with frequency  $f = 0.2$  Hz defined as<sup>2</sup>

$$\begin{aligned}\alpha_1(k) &= 0.5 + 0.5\sin(2\pi 0.2kT), \\ \alpha_2(k) &= 1 - \alpha_1(k).\end{aligned}\tag{4.61}$$

In Figure 4.3 the transient behavior of (4.58) in open loop is presented. Note that for this particular set of initial conditions, (4.58) states converge to the origin<sup>3</sup>. In Figure 4.4, we present the transient response obtained in closed loop with the designed GS-SOF controller. We can see that the system state also converges to the origin in closed loop. However, differently from the open-loop configuration, (4.58) now has guaranteed asymptotic stability, and also has ensured bound  $\rho = 0.85$  over the state decay rate. In fact, we can see that the states converge to the origin in 3 seconds (almost 3 times faster when compared with the open-loop transient).

Figure 4.3 - Transient response of system (4.58) in open loop.



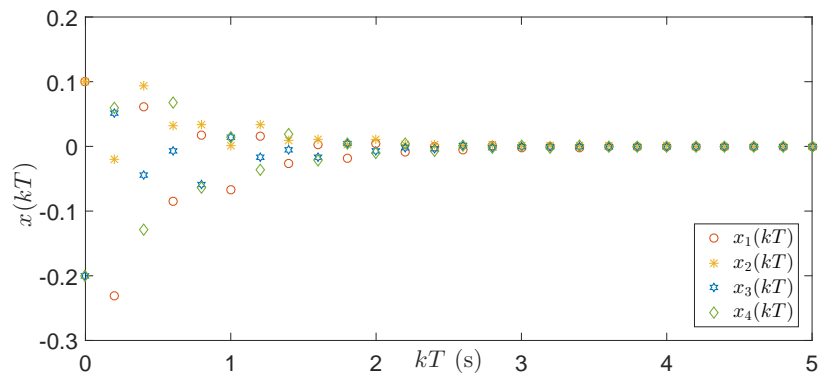
Source: Author's own results.

At last, in Figure 4.5 we can see the control signal produced by the designed GS-SOF controller gains during the closed-loop simulation. Note that the controller gains have a time-varying behavior (Figure 4.6 upper charts), changing accordingly to the instant system configuration – which is determined by the actual values of  $\alpha(k)$  (bottom chart in Figure 4.6).

<sup>2</sup>The time-varying behavior of  $\alpha(k)$  is defined *a priori* just for illustration purposes. In a real practical application, only the bounds on  $\alpha(k)$  are needed in the design stage. However,  $\alpha(k)$  has to be available on-line in the implementation stage of gain-scheduled control systems.

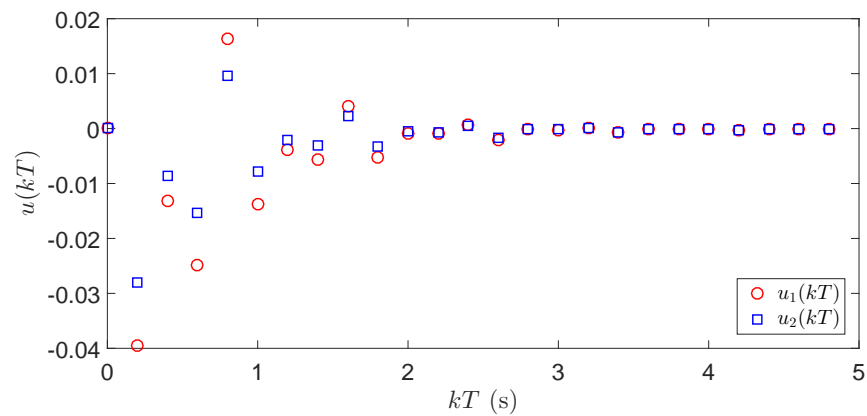
<sup>3</sup>It is important to clarify that despite that Figure 4.2 shows that (4.58) presents unstable set of eigenvalues for some  $\alpha(k)$  in open loop, the state convergence to the origin is possible for some particular initial condition. However, asymptotic stability is not guaranteed, which means that the state convergence to the origin cannot be ensured for every possible initial condition.

Figure 4.4 - Transient response of system (4.58) in closed loop.

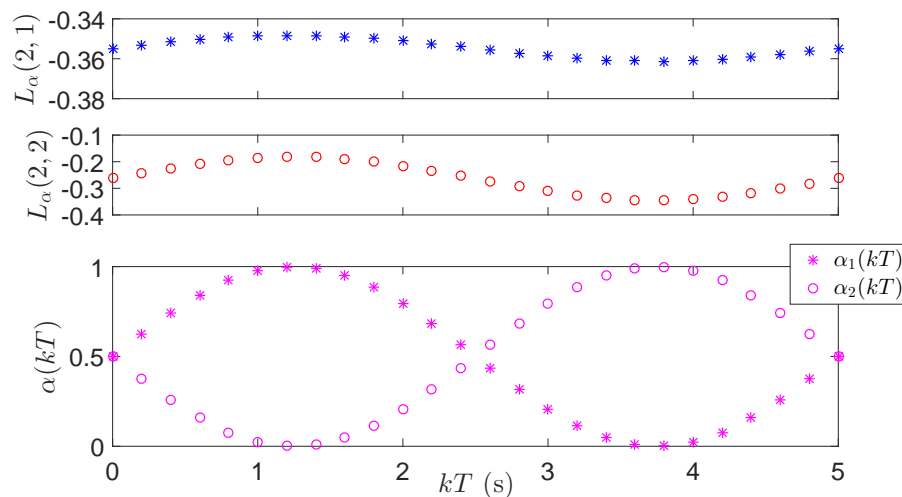


Source: Author's own results.

Figure 4.5 - Control signal produced by the designed GS-SOF controller.



Source: Author's own results.

Figure 4.6 - Variation of the values of GS-SOF controller  $L(\alpha(k))$  (up) according to the instant measurement of  $\alpha(k)$  (bottom).

Source: Author's own results.

**Example 4.2** In this second example, the proposed results are compared with the GS-SOF discrete-time control design strategy presented in Rosa, Morais and Oliveira (2018), which is a particular result for dealing with polytopic LPV systems, regarding the inclusion of a decay rate bound  $\rho$ .

For such comparison, we consider a polytopic discrete-time system (CAIGNY *et al.*, 2009), whose vertices are described by the following matrices:

$$A_1 = \eta \begin{bmatrix} 1 & 0 & -2 \\ 2 & -1 & 1 \\ -1 & 1 & 0 \end{bmatrix}, \quad A_2 = \eta \begin{bmatrix} 0 & 0 & -1 \\ 1 & -1 & 0 \\ 0 & -2 & -1 \end{bmatrix}, \quad B_1 = B_2 = \begin{bmatrix} 1 \\ 0 \\ 0 \end{bmatrix}, \quad \text{and} \quad C_1 = C_2 = \begin{bmatrix} 1 & 0 \\ 0 & 1 \\ 0 & 0 \end{bmatrix}' \quad (4.62)$$

The GS-SOF stabilization strategy proposed in this work (in terms of Theorem 4.2 and Corollary 4.1) and the method presented in Rosa, Morais and Oliveira (2018) were tested for a grid of values of  $\rho$  and  $\eta$ , bounded by the intervals

$$0.4 \leq \eta \leq 0.5 \quad \text{and} \quad 0.8 \leq \rho \leq 1.0.$$

For simplicity, when testing the performance of the two-stage strategy proposed in the present work, for each tested value of  $\rho$ , the decay rate bound was set to be the same in both first (Theorem 4.1) and second (Theorem 4.2 and Corollary 4.1) stages (*i.e.*  $\rho_1 = \rho_2$ ). Moreover, it is important to mention that the same designed gain  $K(\alpha(k))$  – for a given  $\rho_1$  – was used as input information in the second-stage design in both Theorem 4.2 and Corollary 4.1 tests.

Despite the fact that the strategy proposed in Rosa, Morais and Oliveira (2018) is not a two-stage based, it depends on the *a priori* information of scalars  $\gamma^4$  and  $\xi$ , as well as a matrices  $Q_i(\alpha(k)) \in \mathbb{R}^{p \times n}$ ,  $i = 1, 2$ . Otherwise, their strategy falls into the form of a bilinear matrix inequality (BMI) problem, which has a considerably higher computational cost. For employing their method, we set  $\gamma = 10^{-5}$  and  $Q_i(\alpha(k)) = C(\alpha(k))$ , and defined  $\xi$  belonging to the set  $\{-0.9, -0.8, \dots, 0.8, 0.9\}$ , following the setting that the authors adopted in Rosa, Morais and Oliveira (2018). Moreover, as in their paper a stability criterion in terms homogeneous-polynomial Lyapunov function is considered, while employing their strategy, the polytopic structure (degree  $g = 1$ ) was considered for the variable matrices<sup>5</sup>, since Theorem 4.2 is based on a polytopic parameter-dependent matrix  $P(\alpha(k))$ .

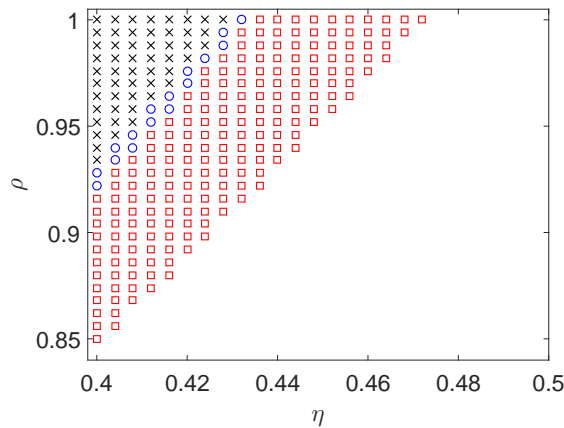
The result of the tests are compiled in Figure 4.7. As one can observe, the CQLF

<sup>4</sup>Note that in Rosa, Morais and Oliveira (2018) the parameter  $\gamma$  is not associated to the  $\mathcal{H}_\infty$  guaranteed cost bound, as  $\gamma_1$  and  $\gamma_2$  in the present work.

<sup>5</sup>Except for matrix  $S(\alpha(k))$ , which is set to have degree 0, for the same reason that we adopted  $X(\alpha(k)) = X$  in Theorem 4.1.

approach (Corollary 4.1) indeed shows to impose more restrictive conditions for the GS-SOF design than the strategy proposed in Rosa, Morais and Oliveira (2018), as expected. However, the polytopic PDLF approach based on Theorems 4.1 and 4.2 of the present work shows to be less conservative than the strategy presented in Rosa, Morais and Oliveira (2018) (for the considered comparison, setting degree  $g = 1$  for the decision variables). This can be inferred since our method was able to provide a feasible solution for a wider number of systems (represented by the different values of  $\eta$ ), and also for a tighter decay rate bound  $\rho$ . Additionally, note that, as expected, the results achieved with Theorem 4.2 outperforms its CQLF version (Corollary 4.1).

Figure 4.7 - Feasibility region obtained using: Corollary 4.1 ( $\times$ ), Corollary 1 in Rosa, Morais and Oliveira (2018) ( $\times$  and  $\circ$ ); and Theorem 4.2 ( $\times$ ,  $\circ$ , and  $\square$ ).



Source: Author's own results.

It is also worth-noting that the method in Rosa, Morais and Oliveira (2018) is tested for each value of  $\xi$  in the previously defined set, in the search for a solution. Of course, a finer grid on  $\xi$  or a parallel line search on  $\gamma$  could yield better results. However, this implies on a higher computational burden. Such complexity is not present in the strategy proposed in this work, as the only information needed is a state-feedback gain matrix.

Furthermore, it is also interesting to mention that despite that in the time-invariant scenario the existence of higher-order polynomial Lyapunov functions (HOPLFs) is a necessary and sufficient condition for robust stability, this does not apply to the LPV case. In fact, using HOPLFs is not effective in time-varying scenario, especially when bounds on the variation rates of the time-varying parameters are considered in the control design (PANDEY; OLIVEIRA, 2019).

**Example 4.3** In this third example we illustrate the efficiency of the extension of the proposed method for addressing the  $\mathcal{H}_\infty$  norm optimization problem. With this goal in mind, we once again consider the uncertain discrete time-varying system borrowed from

Caigny *et al.* (2009), now encompassing the exogenous input impact, which is affected by a time-varying parameter  $\theta_1(k)$ , and therefore can be represented in terms of a set of two vertex matrices as

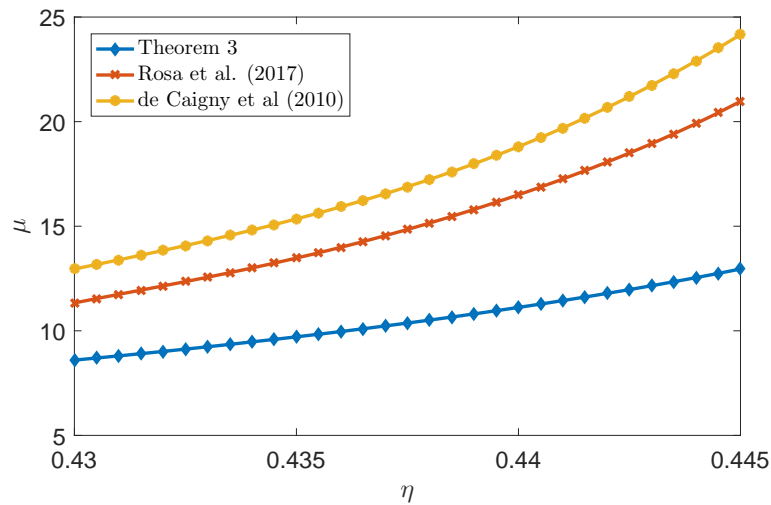
$$A_1 = \eta \begin{bmatrix} 1 & 0 & -2 \\ 2 & -1 & 1 \\ -1 & 1 & 0 \end{bmatrix}, \quad A_2 = \eta \begin{bmatrix} 0 & 0 & -1 \\ 1 & -1 & 0 \\ 0 & -2 & -1 \end{bmatrix}, \quad B_{u_1} = B_{u_2} = \begin{bmatrix} 1 \\ 0 \\ 0 \end{bmatrix}, \quad B_{w_1} = \begin{bmatrix} 0 \\ 1 \\ 0 \end{bmatrix}, \quad B_{w_2} = \begin{bmatrix} 0 \\ 0 \\ 1 \end{bmatrix},$$

$$C_{y_1} = C_{y_2} = \begin{bmatrix} 1 & 0 & 0 \\ 0 & 1 & 0 \end{bmatrix}, \quad C_{z_1} = C_{z_2} = [1 \quad 1 \quad 1],$$

$$D_{u_1} = D_{u_2} = 0, \quad D_{w_1} = D_{w_2} = 0, \quad \text{and} \quad D_{y_1} = D_{y_2} = \begin{bmatrix} 0 \\ 0 \end{bmatrix}.$$

The goal is to evaluate the method proposed in this work in the minimizing the  $\mathcal{H}_\infty$  guaranteed cost through the employment of Theorem 4.3 according to Algorithm 4.3, and compare the obtained results with other strategies available in the literature, namely Corollary 1 from Rosa, Morais and Oliveira (2017) and Theorem 8 from Caigny *et al.* (2010). Since none of the compared strategies can address minimum decay rate imposition, for the performed study we set  $\rho_1 = \rho_2 = 1$  in Theorems 4.3 and 4.4. Moreover, the first-stage  $\mathcal{H}_\infty$  guaranteed cost bound was set<sup>6</sup> in terms of  $\gamma_1 = \mu_1^2 = 20$  in Theorem 4.4.

Figure 4.8 -  $\mathcal{H}_\infty$  guaranteed cost with GS-SOF controller design obtained with Theorem 4.3, employed according to Algorithm 4.3, and with the techniques proposed in Rosa *et al.* (2017) and de Caigny *et al.* (2010).



Source: Author's own results.

<sup>6</sup>This choice of  $\gamma_1$  was defined after performing a few tests with other values for this parameter. However, as already stated in Remark 4.8, a linear search on  $\gamma_1$  can be employed to obtain better results.



In Figure 4.8 we show the obtained  $\mathcal{H}_\infty$  guaranteed cost achieved with the mentioned methods when varying the parameter  $\eta$  in the interval  $0.43 \leq \eta \leq 0.445$ . One can observe that the technique proposed in the present work outperforms both strategies by yielding a gain-scheduled SOF control design that grants a smaller  $\mathcal{H}_\infty$  guaranteed cost for all evaluated values of  $\eta$ , which implies in a better disturbance rejection performance.

For a further comparison, we consider the work of Sadeghzadeh (2017), in which the author considers that the scheduling parameter have limited variation rate, bounded by  $\Delta_1$ , such that  $|\theta_1(k+1) - \theta_1(k)| \leq \Delta_1$ . For different specified bound  $\Delta_1$  on the parameter deviation, a different  $\mathcal{H}_\infty$  bound can be obtained using his method. For the same system considered in the present example, the strategy presented in Sadeghzadeh (2017), for the particular value of  $\eta = 0.4525$ , was able to achieve an  $\mathcal{H}_\infty$  guaranteed cost in the range  $12.1861 \leq \mu_2 \leq 24.6150$ , associated to a deviation bound on the scheduling parameters  $0 \leq \Delta_1 \leq 0.5$ . The approach proposed in the present work does not need that a bound on the parameter variation rate has to be informed in the control design, and therefore is able to deal with arbitrarily variation rates. For the same value  $\eta = 0.4525$  our method was able to obtain an  $\mathcal{H}_\infty$  guaranteed cost  $\mu_2 = 17.329$  (with  $\rho_1 = \rho_2 = 1$ , and  $\gamma_1 = \mu_1^2 = 20$ ), which is comparable to the results presented in Sadeghzadeh (2017).

**Example 4.4** In this final example, we demonstrate our method application in a real control problem for the stabilization of an inverted pendulum on a cart, adapted from Sadeghzadeh (2017). Here we seek to illustrate the proposed GS-SOF controller efficacy over the disturbance rejection during control implementation. The considered system model is obtained through an Euler's first-order approximation over a quasi-LPV representation of the original nonlinear inverted pendulum model (SADEGHZADEH, 2017), for a sampling period  $T_s = 0.05$  seconds, yielding a polytopic model that can be described in terms of the following vertex matrices:

$$A_1 = A_2 \begin{bmatrix} 1 & 0.05 \\ 0.9705 & 1 \end{bmatrix}, \quad A_3 = A_4 = \begin{bmatrix} 1 & 0.0500 \\ 1.3531 & 1 \end{bmatrix}, \quad (4.63)$$

$$B_{u_1} = B_{u_3} = \begin{bmatrix} 0 \\ -0.0892 \end{bmatrix}, \quad B_{u_2} = B_{u_4} = \begin{bmatrix} 0 \\ -0.0409 \end{bmatrix}, \quad B_{w_1} = B_{w_2} = B_{w_3} = B_{w_4} = \begin{bmatrix} 0 \\ 0 \end{bmatrix},$$

$$D_{u_1} = D_{u_2} = D_{u_3} = D_{u_4} = 0, \quad D_{y_1} = D_{y_2} = D_{y_3} = D_{y_4} = 0,$$

$$C_{z_1} = C_{z_2} = C_{z_3} = C_{z_4} = [1 \ 0], \quad C_{y_1} = C_{y_2} = C_{y_3} = C_{y_4} = [1 \ 1],$$

which define a polytope with four vertices (two time-varying parameters). We refer the reader to Sadeghzadeh (2017) and references within for more details on the inverted pendulum system modeling.

By employing the proposed strategy with Theorems 4.4 and 4.3 for completing the

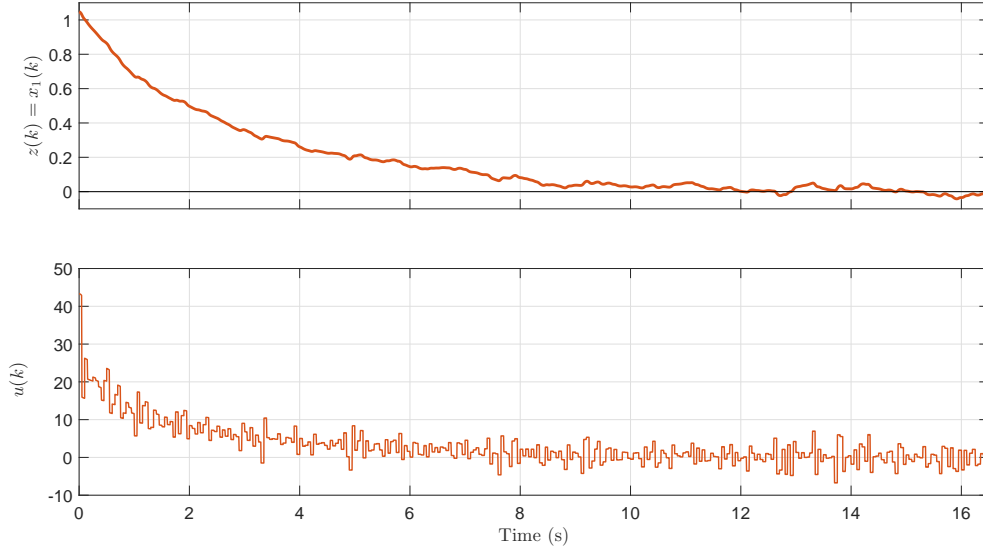
two-stage design, considering the design parameters  $\rho_1 = \rho_2 = 1$ , and  $\gamma_1 = \mu_1^2 = 50$ , one might obtain the GS-SOF controller

$$L_\alpha = \alpha_1(k)15.7811 + \alpha_2(k)31.1018 + \alpha_3(k)19.4399 + \alpha_4(k)37.0305, \quad (4.64)$$

which ensures a  $\mathcal{H}_\infty$  guaranteed cost  $\mu_2=11.674$ .

In this example, we consider that both time-varying parameters are available for measurement. In these terms, the scheduling parameters  $\alpha_i(k)$  for  $i = 1, 2, 3, 4$ , can be obtained following the procedure described in Chapter 2. Running a computational simulation of controller (4.64) applied to the original nonlinear model of the inverted pendulum, considering a disturbance input  $w(k)$  as a zero-mean Gaussian white noise, with standard deviation 0.1 (SADEGHZADEH, 2017), we obtain the transient response shown in Figure 4.9. As seen, after being released from the initial condition  $x_0 = [\pi/3 \ 0]^T$ , the controlled output  $z(k)$  asymptotically converges to the origin, even in with the presence of a disturbance input signal  $w(k) \neq 0$ .

Figure 4.9 - Controlled output and control signals obtained with the GS-SOF controller 4.64.



Source: Author's own results.

It is important to observe that the specification of the first-stage design parameters  $\rho_1$  and  $\mu_1$  drastically impacts the results obtained in the second stage. For instance, by setting  $\mu_1^2 = 25$ , while maintaining  $\rho_1 = 1$ , the second-stage design leads to a  $\mathcal{H}_\infty$  guaranteed cost of  $\mu_2 = 12.791$ . This highlights the importance of an adequate first-stage design.

## 5 NON-NEGLIGIBLE SENSORS AND ACTUATORS DYNAMICS WITH TRANSPORT DELAY

This chapter presents results obtained with the application of the two-stage SOF design method studied in this work on the particular problem of uncertain LTI systems subject to sensors and/or actuators with non-negligible dynamics. In such practical cases, the actual system states are not available for feedback, but only the measurement signals at the sensors output. Therefore, full state-feedback employment is hindered. By modeling the plant, sensors, and actuators dynamics into a single augmented system, static output feedback control might be applied for solving the problem.

Using the same idea, the dynamic effects of time delay can also be incorporated in the controller design. Considering the Padé approximation, the delay dynamics are encompassed in the augmented system and the SOF control technique can be applied to design a robust controller for asymptotic stabilization under the presence of non-negligible additional dynamics and time delay.

Differently from the previous results proposed in this thesis, in this chapter, we explore the benefits of establishing stability certificates in terms of homogeneous-polynomial Lyapunov functions when compared to conventional parameter-dependent Lyapunov functions and common quadratic Lyapunov functions.

Moreover, in a problem extension, we consider the presence of a disturbance signal that affect the uncertain LTI system dynamics. For coping with this additional issue, we extend the two-stage SOF controller synthesis LMI conditions for minimizing the closed-loop  $\mathcal{H}_2$  guaranteed cost.

In the sequence, the augmented system modeling as well as the design procedure for addressing the aforementioned problem are proposed and discussed. At the end of the chapter, illustrative examples are also presented to evaluate the efficiency of the proposed strategy.

### 5.1 PROBLEM STATEMENT

Consider the uncertain linear system described as

$$\dot{x}(t) = A(\alpha)x(t) + B(\alpha)z(t) \quad (5.1)$$

where  $x(t) \in \mathbb{R}^n$  is a vector with system states and  $z(t) \in \mathbb{R}^m$  is a vector with control input signals. The parameter-dependent matrices  $A(\alpha) \in \mathbb{R}^{n \times n}$  and  $B(\alpha) \in \mathbb{R}^{n \times m}$  belong to a polytopic domain  $\mathcal{D}$  parametrized in terms of a vector of uncertain time-invariant parameters  $\alpha = (\alpha_1, \dots, \alpha_N)$  such as

$$\mathcal{D} = \left\{ (A, B)(\alpha) : (A, B)(\alpha) = \sum_{r=1}^N \alpha_r (A_r, B_r), \alpha \in \Lambda_N \right\}, \quad (5.2)$$

where  $(A_r, B_r)$  denotes the  $r$ -th polytope vertex, and

$$\Lambda_N = \left\{ \alpha \in \mathbb{R}^N : \sum_{r=1}^N \alpha_r = 1; \alpha_r \geq 0; r = 1, \dots, N \right\}. \quad (5.3)$$

The state information is measured through  $q$  sensors, with dynamics described by

$$\dot{v}_i(t) = a_{v,i} v_i(t) - a_{v,i} \left( \sum_{j=1}^n c_{i,j} x_j(t) \right), \quad (5.4)$$

where  $v_i(t)$  are the sensor outputs, composing the vector  $v(t) = [v_1(t) \cdots v_q(t)]'$ ,  $a_{v,i} < 0$  are time-invariant (but possibly uncertain) parameters for  $i = 1, 2, \dots, q$ , and  $c_{i,j}$  are known constants for  $j = 1, 2, \dots, n$ .

Also, consider the existence of  $m$  actuators whose dynamics are described by

$$\dot{z}_k(t) = a_{z,k} z_k(t) - a_{z,k} \left( \sum_{l=1}^p d_{k,l} u_{D_l}(t) \right), \quad (5.5)$$

composing the vector of control signals  $z(t) = [z_1(t) \cdots z_m(t)]'$ . Moreover, in (5.5),  $u_{D_l}(t)$  are the actuator input commands, forming the vector  $u_D(t) = [u_{D_1}(t) \cdots u_{D_p}(t)]'$ ,  $a_{z,k} < 0$  are time-invariant (but possibly uncertain) parameters for  $k = 1, 2, \dots, m$ , and  $d_{k,l}$  are known constants for  $l = 1, 2, \dots, p$ .

The overall control system block diagram, represented in Figure 5.1, helps to illustrate the considered system and control structure.

Note that we assume that each sensor output  $v_i(t)$ , used in feedback, is available for the controller with time delay,  $\tau_{s_i}$ , in terms of a delayed sensor output signal  $v_{D_i}(t)$ . Likewise, each command signal produced by the controller,  $u_i(t)$ , is received by the actuator with time delay  $\tau_{a_i}$ , in terms of a delayed actuator command signal  $u_{D_i}(t)$ .

Under these definitions, the problem addressed herein consists in designing a control law  $u(t) = Lv_D(t)$  where  $v_D(t) \in \mathbb{R}^q$  is the vector of time-delayed sensor outputs and  $L \in \mathbb{R}^{p \times q}$  is a gain matrix to be determined in order to ensure the closed-loop asymptotic stability of the overall system. Moreover, the controller  $L$  must be designed in order to

ensure that the decay rate is greater than a given lower bound  $\gamma$ , following the definitions given in Subsection 2.1.2.

## 5.2 PROPOSED STRATEGY

In this section, a system representation that allows for encompassing plant and additional dynamics in a single model is presented, as well as a control synthesis strategy based on LMIs for designing an SOF controller that guarantees closed-loop stability and minimum decay rate.

### 5.2.1 SYSTEM AUGMENTATION

For dealing with this control problem, we propose the definition of an augmented system that encompass the plant, actuators, and sensors dynamics, and also the time delay effect. To this end, we first consider that the time delay is modeled using the Padé approximation (NIU *et al.*, 2013).

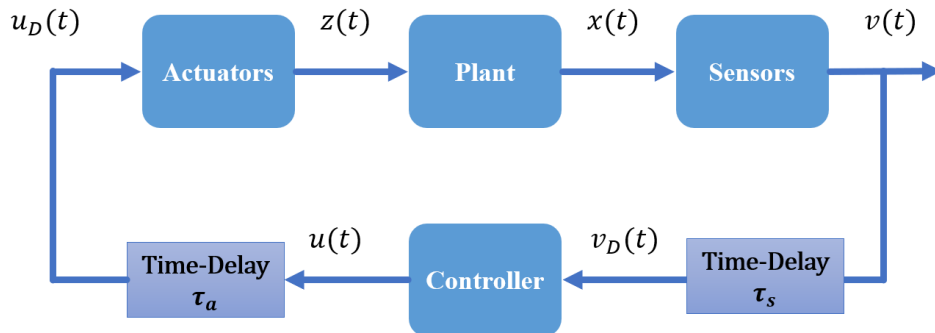
When analyzed in the frequency domain, a time delay  $\tau$  can be represented by the transfer function  $e^{-\tau s}$ . Using the Padé method,  $e^{-\tau s}$  can be approximated by a rational polynomial function  $R(s)$  as

$$e^{-\tau s} \approx R(s) = \frac{b_0 + b_1 \tau s + \dots + b_c (\tau s)^c}{a_0 + a_1 \tau s + \dots + a_k (\tau s)^k}, \quad (5.6)$$

where usually  $c = k$ , and  $k$  denotes the order of the approximated model.

Considering that every sensor output signal  $v_i(t)$ ,  $i = 1, \dots, q$ , is received by the con-

Figure 5.1 - Closed-loop block diagram.



Source: Own author.

troller with time delay  $\tau = \tau_s$  (possibly uncertain), the function  $R(s)$  in (5.6) can be transformed into an equivalent state-space model of order  $k = k_s$  that represents the delay effect on the sensor output signal by using the following realization (NIU *et al.*, 2013):

$$\begin{cases} \dot{\delta}_{sd_i}(t) = A_{sd}(\alpha)\delta_{sd_i}(t) + B_{sd}v_i(t) \\ v_{D_i}(t) = C_{sd}(\alpha)\delta_{sd_i}(t) + D_{sd}v_i(t) \end{cases}, \quad (5.7)$$

where  $\delta_{sd_i}(t) \in \mathbb{R}^{k_s}$  is the vector of phase variables,  $v_{D_i}(t)$  is the  $i$ -th time-delayed sensor output, and

$$A_{sd_i}(\alpha) = \begin{bmatrix} 0 & 1 & 0 & \cdots & 0 \\ 0 & 0 & 1 & \cdots & 0 \\ \vdots & \vdots & \vdots & \ddots & \vdots \\ 0 & 0 & 0 & \cdots & 1 \\ \frac{-a_0\tau_s^{-k_s}}{a_{k_s}} & \frac{-a_1\tau_s^{-k_s+1}}{a_{k_s}} & \frac{-a_2\tau_s^{-k_s+2}}{a_{k_s}} & \cdots & \frac{-a_{k_s-1}\tau_s^{-1}}{a_{k_s}} \end{bmatrix}, \quad (5.8)$$

$$B_{sd_i} = [0 \ 0 \ 0 \ \cdots \ 1]', \quad (5.9)$$

$$C_{sd_i}(\alpha) = \frac{1}{a_{k_s}^2} \left[ (a_{k_s}b_0 - a_0b_{k_s})\tau_s^{-k_s} \quad (a_{k_s}b_1 - a_1b_{k_s})\tau_s^{-k_s+1} \right. \\ \left. \cdots \quad (a_{k_s}b_{k_s-1} - a_{k_s-1}b_{k_s})\tau_s^{-1} \right], \quad (5.10)$$

$$D_{sd_i} = \frac{b_{k_s}}{a_{k_s}}, \quad (5.11)$$

with

$$a_j = \frac{(c_s + k_s - j)!k_s!}{j!(k_s - j)!}, \quad b_f = (-1)^f \frac{(c_s + k_s - f)!c_s!}{f!(c_s - f)!}, \quad (5.12)$$

for  $j = 1, \dots, k_s$ , and  $f = 1, \dots, c_s$ , where  $c_s$  is the numerator degree for the sensor delay model approximation in (5.6).

In that sense, we can model the sensor dynamics affected by a time delay  $\tau = \tau_s$  by defining an augmented vector  $s(t) \in \mathbb{R}^{q(1+k_s)}$  defined as

$$s(t) = [v(t)' \quad \delta_{sd}(t)']',$$

with  $\delta_{sd}(t) = [\delta_{sd_1}(t) \cdots \delta_{sd_{k_s}}(t)]'$ , which combines the sensor dynamics (5.4) subject to a time-delay effect (5.7), yielding the following augmented state-space model

$$\begin{cases} \dot{s}(t) = A_s(\alpha)s(t) + B_s(\alpha)x(t) \\ v_D(t) = C_s(\alpha)s(t) \end{cases}, \quad (5.13)$$

where

$$A_s(\alpha) = \begin{bmatrix} A_v(\alpha) & 0_{q \times qk_s} \\ B_{sd} & A_{sd}(\alpha) \end{bmatrix}, \quad B_s(\alpha) = \begin{bmatrix} -A_v(\alpha)C \\ 0_{qk_s \times n} \end{bmatrix}, \quad \text{and } C_s(\alpha) = \begin{bmatrix} D_{sd} & C_{sd}(\alpha) \end{bmatrix}$$

with

$$A_v(\alpha) = \text{diag}\{a_{v,1}, a_{v,2}, \dots, a_{v,q}\}, \quad C = \begin{bmatrix} c_{1,1} & c_{1,2} & \dots & c_{1,n} \\ c_{2,1} & c_{2,2} & \dots & c_{2,n} \\ \vdots & \vdots & \ddots & \vdots \\ c_{q,1} & c_{q,2} & \dots & c_{q,n} \end{bmatrix},$$

and

$$(A, B, C, D)_{sd}(\alpha) = \text{diag}\{(A, B, C, D)_{sd_1}, (A, B, C, D)_{sd_2}, \dots, (A, B, C, D)_{sd_q}\}, \quad (5.14)$$

with  $(A, B, C, D)_{sd_i}$  as in (5.8) - (5.11) (with the subindex “s” referring to the sensor time-delay), implying in  $A_{sd} \in \mathbb{R}^{qk_s \times qk_s}$ ,  $B_{sd} \in \mathbb{R}^{qk_s \times q}$ ,  $C_{sd} \in \mathbb{R}^{q \times qk_s}$ , and  $D_{sd} \in \mathbb{R}^{q \times q}$ .

Similarly, we can model the actuator dynamics affected by time-delayed command signals by considering a  $k_a$ -th order Padé approximation, incorporated in an augmented vector  $a(t) \in \mathbb{R}^{m(1+k_a)}$

$$a(t) = \begin{bmatrix} z(t)' & \delta_{ad}(t)' \end{bmatrix}',$$

with  $\delta_{ad}(t) = [\delta_{ad_1}(t) \cdots \delta_{ad_{k_a}}(t)]'$ , combining the actuator dynamics (5.5) subject to a time-delay effect modeled as in (5.7) (now with  $k = k_a$  and  $\tau = \tau_a$ ), yielding the following augmented state-space model

$$\begin{cases} \dot{a}(t) = A_a(\alpha)a(t) + B_a(\alpha)u_D(t) \\ z(t) = C_a(\alpha)a(t) \end{cases}, \quad (5.15)$$

where

$$A_a(\alpha) = \begin{bmatrix} A_z(\alpha) & -A_z(\alpha)DC_{ad} \\ 0_{mk_a \times m} & A_{ad}(\alpha) \end{bmatrix}, \quad B_a(\alpha) = \begin{bmatrix} -A_z(\alpha)DD_{ad} \\ B_{ad} \end{bmatrix}, \quad C_a(\alpha) = \begin{bmatrix} I_{m \times m} & 0_{m \times mk_a} \end{bmatrix}$$

$$A_z(\alpha) = \text{diag}\{a_{z,1}, a_{z,2}, \dots, a_{z,m}\}, \quad D = \begin{bmatrix} d_{1,1} & d_{1,2} & \dots & d_{1,p} \\ d_{2,1} & d_{2,2} & \dots & d_{2,p} \\ \vdots & \vdots & \ddots & \vdots \\ d_{m,1} & d_{m,2} & \dots & d_{m,p} \end{bmatrix}, \quad \text{and} \quad (5.16)$$

$$(A, B, C, D)_{ad} = \text{diag}\{(A, B, C, D)_{ad_1}, (A, B, C, D)_{ad_2}, \dots, (A, B, C, D)_{ad_m}\}, \quad (5.17)$$

with  $(A, B, C, D)_{ad_i}$  as in (5.8) - (5.11) (with the subindex “a” referring to the actuator time-delay), implying in  $A_{ad} \in \mathbb{R}^{mk_a \times mk_a}$ ,  $B_{ad} \in \mathbb{R}^{mk_a \times m}$ ,  $C_{ad} \in \mathbb{R}^{m \times mk_a}$ , and  $D_{ad} \in \mathbb{R}^{m \times m}$ .

**Remark 5.1.** *In this work, for simplifying the notation and without loss of generality, we considered that every sensor output signal is subject to the same amount of time delay  $\tau_s$ , likewise assumed for the actuator commands, with a time delay  $\tau_a$ . Therefore, the matrices in (5.7) will be the same for each of the  $q$  sensor output signals and each of the  $m$  actuator commands, respectively. However, note that a more general approach can be directly employed by assuming that the time delay  $\tau$ , and also its approximation model order  $k$ , are different for every considered signal, defining parameters such as  $\tau_{s_i}$  and  $k_{s_i}$ ,  $i = 1, \dots, q$ , and  $\tau_{a_l}$  and  $k_{s_l}$ , for  $l = 1, \dots, p$ .*

Next, to incorporate the time-delayed sensor and actuator dynamics in the LTI system (5.1), we promote a system augmentation, by defining the augmented state vector  $w(t) \in \mathbb{R}^{n+q(k_s+1)+m(k_a+1)}$  as

$$w(t) = \begin{bmatrix} x(t)' & s(t)' & a(t)' \end{bmatrix}'. \quad (5.18)$$

Then, we have the following augmented state-space representation

$$\begin{cases} \dot{w}(t) = \bar{A}(\alpha)w(t) + \bar{B}(\alpha)u(t) \\ y(t) = \bar{C}(\alpha)w(t) \end{cases}, \quad (5.19)$$

where

$$\bar{A}(\alpha) = \begin{bmatrix} A(\alpha) & 0_{n \times q(k_s+1)} & B(\alpha)C_a(\alpha) \\ B_s(\alpha) & A_s(\alpha) & 0_{q(1+k_s) \times m(1+k_a)} \\ 0_{m(1+k_a) \times n} & 0_{m(1+k_a) \times q(1+k_s)} & A_a(\alpha) \end{bmatrix}, \quad \bar{B}(\alpha) = \begin{bmatrix} 0_{n \times p} \\ 0_{q(k+1) \times p} \\ B_a(\alpha) \end{bmatrix},$$

and

$$\bar{C}(\alpha) = \begin{bmatrix} 0_{q \times n} & C_s(\alpha) & 0_{q \times m(1+k_a)} \end{bmatrix}.$$

The output vector  $y(t)$  corresponds to the delayed-sensor output  $v_D(t)$  in (5.13), which is available for feedback, in contrast to the actual system state vector  $x(t)$ . Therefore, the aforementioned problem may be addressed as a static output-feedback control design with  $u(t) = Lv_D(t) = Ly(t)$ .

At this point, we give emphasis to the first main contribution of this chapter. This new modeling strategy is able to represent, in a single set of matrices, not only the dynamics associated to sensors and actuators but also the effect of delay in the communication channels that deliver the information generated in the sensors output and received in the actuators input, respectively, enabling to address more complex and general control problems.

**Remark 5.2.** *It is important to note that the polytopic approach enables our strategy to easily cope with uncertainties on sensors and/or actuators parameters, simply by considering them as additional uncertain parameters along with the plant uncertainties. The*



same procedure can be employed to consider uncertain time delays  $\tau_s$  and/or  $\tau_a$ . This is possible since these parameters will be part of the overall system matrices, generating an augmented polytope encompassing plant, sensor, actuator, and delay uncertainties.

**Remark 5.3.** *Our method considers the Padé approximation for modeling the time delay effect over the system dynamics. The approximation error can be reduced by choosing a higher-order rational polynomial function (5.6). With higher values of  $k_s$  we obtain a better approximation on the exact dynamic effect of the delay  $e^{-\tau s}$ . Note that the order of the delay approximation  $k_s$  is directly incorporated in our proposed system augmented model. Of course, the direct trade-off is that a higher-order state-space model is needed, as the parameter  $k_s$  will define the dimension of the sensor delay model matrices (5.8)-(5.11), and similarly in the actuator delay model given in (5.17).*

### 5.2.2 CONTROL DESIGN

For the SOF controller design, we consider the use of a two-stage SOF controller synthesis strategy, based on the pioneer works of Peaucelle *et al.* (2000) and Mehdi, Boukas and Bachelier (2004).

The two-stage method employment in our work consists in first computing a state-feedback gain  $K(\alpha)$  such that

$$\dot{w}(t) = (\bar{A}(\alpha) + \bar{B}(\alpha)K(\alpha))w(t),$$

*i.e.*, the augmented system (5.19), is robustly stable in closed-loop with  $u(t) = K(\alpha)w(t)$ . In the sequence, this gain matrix  $K(\alpha)$  is fed to a second-stage controller syntheses, in which the desired SOF stabilizing robust gain  $L$  is effectively computed.

As already mentioned in the previous chapters, the first-stage state-feedback design can be performed using any available strategy in the literature. Here, we consider well-known conditions (BOYD *et al.*, 1994), based on the existence of matrices  $W = W' > 0$  and  $Z(\alpha)$  such that

$$\bar{A}(\alpha)W + W\bar{A}(\alpha)' + \bar{B}(\alpha)Z(\alpha) + Z(\alpha)'\bar{B}(\alpha)' + 2\gamma_1 W < 0 \quad (5.20)$$

holds for every  $\alpha \in \Lambda_N$ . In the synthesis conditions,  $K(\alpha) = Z(\alpha)W^{-1}$  guarantees the robust state-feedback stabilization of  $\dot{w}(t) = (\bar{A}(\alpha) + \bar{B}(\alpha)K(\alpha))w(t)$  with lower bound  $\gamma_1$  on the closed-loop system decay rate.

**Remark 5.4.** *Clearly, the conditions presented in (5.20) are of infinite-dimension, as they are dependent on the uncertain parameter  $\alpha$ . Therefore, some manipulation over these constraints has to be performed to obtain an equivalent finite-dimension problem.*

This issue is left to be properly discussed more ahead in the text, since the second-stage synthesis conditions are also presented in terms of parameter-dependent LMIs.

In this work, we bring a generalization of the SOF synthesis conditions proposed in Sereni *et al.* (2018) for computing SOF gains for the stabilization of the augmented system encompassing sensor and actuator dynamics. The results in Sereni *et al.* (2018) are achieved by considering that the LMI decision matrices have polytopic dependence on the uncertain parameter  $\alpha$ . Here, we assume that the decision variables have a homogeneous-polynomial dependence on  $\alpha$  of arbitrary degree  $g$  (AGULHARI; OLIVEIRA; PERES, 2010a), and also extend the synthesis conditions for enabling the enforcement of a minimum decay rate criterion.

For applying such strategy, we first formally enunciate in Theorem 5.1 a parameter-dependent LMI condition set that encompasses the results presented in Sereni *et al.* (2018).

**Theorem 5.1.** *Assuming that there exists a state-feedback gain  $K(\alpha)$  such that  $\bar{A}(\alpha) + \bar{B}(\alpha)K(\alpha)$  is asymptotically stable, then there exists a stabilizing static output-feedback gain  $L$  such that  $\bar{A}(\alpha) + \bar{B}(\alpha)L\bar{C}(\alpha)$  is asymptotically stable, considering a decay rate greater than or equal to  $\gamma_2 > 0$ , if there exist a symmetric parameter-dependent matrix  $P(\alpha) > 0$ , parameter-dependent matrices  $F(\alpha)$ ,  $G(\alpha)$ , and matrices  $H$  and  $J$  such that*

$$\begin{bmatrix} (F(\alpha)\bar{A}(\alpha) + F(\alpha)\bar{B}(\alpha)K(\alpha)) + (\bullet)' + 2\gamma_2 P(\alpha) & * & * \\ P(\alpha) - F(\alpha)' + G(\alpha)\bar{A}(\alpha) + G(\alpha)\bar{B}(\alpha)K(\alpha) & -G(\alpha) - G(\alpha)' & * \\ \bar{B}(\alpha)'F(\alpha)' + J\bar{C}(\alpha) - HK(\alpha) & \bar{B}'(\alpha)G(\alpha)' & -H - H' \end{bmatrix} < 0. \quad (5.21)$$

*In the synthesis condition, the robust static output-feedback gain is given by  $L = H^{-1}J$ .*

**Proof:** Readily note that (5.21) implies in  $H$  being invertible (BOYD *et al.*, 1994). In the sequence, applying a transformation on (5.21) with  $T(\alpha)$  and  $T(\alpha)'$  (MEHDI; BOUKAS; BACHELIER, 2004), where

$$T(\alpha) = \begin{bmatrix} I & 0 & S(\alpha)' \\ 0 & I & 0 \end{bmatrix}, \quad (5.22)$$

one can achieve

$$\begin{bmatrix} \Psi(\alpha) & \Phi(\alpha) \\ * & -G(\alpha) - G(\alpha)' \end{bmatrix} < 0, \quad (5.23)$$

where

$$\begin{aligned} \Psi(\alpha) = & \left[ (\bar{A}(\alpha) + \bar{B}(\alpha)(K(\alpha) + S(\alpha)))'F(\alpha)' \right. \\ & \left. + S(\alpha)'(J\bar{C}(\alpha) - H(K(\alpha) + S(\alpha))) \right] + (\bullet)' + 2\gamma_2 P(\alpha), \end{aligned} \quad (5.24)$$

and

$$\Phi(\alpha) = P(\alpha) - F(\alpha) + (\bar{A}(\alpha) + \bar{B}(\alpha)(K(\alpha) + S(\alpha)))'G'(\alpha) \quad (5.25)$$

By defining  $S(\alpha) = H^{-1}J\bar{C}'(\alpha) - K(\alpha)$ , and  $L = H^{-1}J$  in (5.24) and (5.25), we have that (5.23) becomes

$$\left[ \begin{array}{c} [(\bar{A}(\alpha) + \bar{B}(\alpha)L\bar{C}'(\alpha))'F(\alpha)'] + (\bullet)' + 2\gamma_2 P(\alpha) \\ * \\ P(\alpha) - F(\alpha) + (\bar{A}(\alpha) + \bar{B}(\alpha)L\bar{C}'(\alpha))'G'(\alpha) \\ -G(\alpha) - G(\alpha)' \end{array} \right] < 0, \quad (5.26)$$

which is a sufficient condition for the robust stabilization with a lower bound  $\gamma_2$  on the system decay rate according to Lemma 2.5, with  $\dot{w}(t) = (\bar{A}(\alpha) + \bar{B}(\alpha)L\bar{C}'(\alpha))w(t)$ . ■

The LMI conditions given in (5.21) are of infinite dimension. In order to make them computationally tractable, we need to convert them into a finite set of LMI conditions, by imposing some particular structure to the decision variables. Following previous works on the subject, by assuming that the parameter-dependent matrices are modeled as homogeneous polynomials of sufficiently large degree  $g$  on the uncertain parameter  $\alpha$ , we may obtain a finite set of LMIs with no loss of generality (AGULHARI; OLIVEIRA; PERES, 2010b). This means that the higher the degree  $g$  considered for the polynomial matrices, the lesser is the conservatism introduced in the constraint formulation. For a sufficient large  $g$ , the obtained finite set of LMI will exactly represent the constraints in (5.21).

For an arbitrary degree  $g$  considered for the homogeneous-polynomial matrices in (5.21), we can obtain a finite set of LMIs in order to solve the control design problem using semidefinite programming tools. For the particular case of  $g = 1$ , we have a polytopic parameter-dependent Lyapunov function (PDLF) such as

$$P(\alpha) = \alpha_1 P_1 + \alpha_2 P_2 + \dots + \alpha_N P_N.$$

In this case, sufficient conditions for the LMIs in Theorem 5.1 can be obtained by checking a finite set of LMI constraints over the vertices of the polytopic parameter-dependent matrices. This result is formally stated in the following corollary.

**Corollary 5.1.** *By assuming that  $P(\alpha)$ ,  $F(\alpha)$ , and  $G(\alpha)$  in Theorem 5.1 are homogeneous-polynomial matrices of degree  $g = 1$ , as well as the state-feedback first-stage gain matrix  $K(\alpha)$ , then a sufficient condition for (5.21) to hold is that there exist symmetric matrices*

$P_i > 0$ , and matrices  $F_i$ ,  $G_i$ ,  $H$ , and  $J$  such that

$$\begin{bmatrix} (F_i \bar{A}_i + F_i \bar{B}_i K_i) + (\bullet)' + 2\gamma_2 P_i & * & * \\ P_i - F'_i + G_i \bar{A}_i + G_i \bar{B}_i K_i & -G_i - G'_i & * \\ \bar{B}'_i F'_i + J_i \bar{C}_i - H K_i & \bar{B}'_i G'_i & -H - H' \end{bmatrix} < 0 \quad (5.27)$$

holds for  $i = 1, 2, \dots, N$ ,

$$\begin{bmatrix} \Xi_{11}^{ij} & * & * \\ \Xi_{21}^{ij} & -2(G_i + G'_i) - (G_j + G'_j) & * \\ \Xi_{31}^{ij} & \bar{B}'_i(G'_i + G'_j) + \bar{B}'_j G'_i & -3(H + H') \end{bmatrix} < 0, \quad (5.28)$$

with

$$\Xi_{11}^{ij} = [\bar{A}'_i(F'_i + F'_j) + \bar{A}'_j F'_i + K'_i(\bar{B}'_i F'_j + \bar{B}'_j F'_i) + K'_j \bar{B}'_i F'_i] + (\bullet)' + 2\gamma_2(2P_i + P_j), \quad (5.29)$$

$$\Xi_{21}^{ij} = 2P_i + P_j - (2F'_i + F'_j) + G_i(\bar{A}_i + \bar{A}_j) + G_j \bar{A}_i + G_i(\bar{B}_i K_j + \bar{B}_j K_i) + G_j \bar{B}_i K_i, \quad (5.30)$$

and

$$\Xi_{31}^{ij} = \bar{B}'_i(F'_i + F'_j) + \bar{B}'_j F'_i + J(2\bar{C}_i + \bar{C}_j) - H(2K_i + K_j), \quad (5.31)$$

holds for  $i, j = 1, 2, \dots, N$  and  $i \neq j$ , and

$$\begin{bmatrix} \Xi_{11}^{ijk} & * & * \\ \Xi_{21}^{ijk} & \Xi_{22}^{ijk} & * \\ \Xi_{31}^{ijk} & \Xi_{23}^{ijk} & -6(H + H') \end{bmatrix} < 0, \quad (5.32)$$

with

$$\begin{aligned} \Xi_{11}^{ijk} = & [(\bar{A}'_i + \bar{A}'_j)F'_k + (\bar{A}'_i + \bar{A}'_k)F'_j + (\bar{A}'_j + \bar{A}'_k)F'_i + \\ & + (K'_i \bar{B}'_j + K'_j \bar{B}'_i)F'_k + (K'_i \bar{B}'_k + K'_k \bar{B}'_i)F'_j + \\ & + (K'_j \bar{B}'_k + K'_k \bar{B}'_j)F'_i] + (\bullet)' + 4\gamma_2(P_i + P_j + P_k), \end{aligned}$$

$$\begin{aligned} \Xi_{21}^{ijk} = & 2(P_i + P_j + P_k) - 2(F_i + F_j + F_k)' \\ & + (G_i + G_j)\bar{A}_k + (G_i + G_k)\bar{A}_j + (G_j + G_k)\bar{A}_i + \\ & + G_i(\bar{B}_j K_k + \bar{B}_k K_j) + G_j(\bar{B}_i K_k + \bar{B}_k K_i) + G_k(\bar{B}_i K_j + \bar{B}_j K_i), \end{aligned}$$

$$\begin{aligned} \Xi_{31}^{ijk} = & (\bar{B}'_i + \bar{B}'_j)F'_k + (\bar{B}'_i + \bar{B}'_k)F'_j + (\bar{B}'_j + \bar{B}'_k)F'_i + \\ & + 2J(\bar{C}_i + \bar{C}_j + \bar{C}_k) - 2H(K_i + K_j + K_k), \end{aligned}$$

$$\Xi_{22}^{ijk} = -2(G_i + G'_i + G_j + G'_j + G_k + G'_k),$$

$$\Xi_{23}^{ijk} = (\bar{B}'_i + \bar{B}'_j)G'_k + (\bar{B}'_i + \bar{B}'_k)G'_j + (\bar{B}'_j + \bar{B}'_k)G'_i,$$

holds for  $i = 1, 2, \dots, N-2$ ,  $j = i+1, \dots, N-2$ , and  $k = j+1, \dots, N$ .

**Proof:** Note that by multiplying (5.27) by  $\alpha_i^3$  and summing for  $i = 1, \dots, N$ , by multiplying (5.28) by  $\alpha_i^2 \alpha_j$ , and summing for  $i, j = 1, 2, \dots, N$ ,  $i \neq j$ , and by multiplying (5.32) by  $\alpha_i \alpha_j \alpha_k$ , and summing for  $i = 1, 2, \dots, N-1$ ,  $j = i+1, \dots, N-2$ , and  $k = j+1, \dots, N$ , bearing in mind that  $\alpha \in \wedge_N$ , we directly obtain the parameter-dependent form (5.21). ■

It is important to observe that both Theorem 5.1 and, consequently, Corollary 5.1 encompass the conditions proposed in Sereni *et al.* (2018), showing that this previous work is a particular case of the LMI formulation proposed in the present work. Observe that by considering a robust first-stage gain matrix (i.e.,  $K(\alpha) = K$ ), the LMI conditions in Corollary 5.1 are reduced to Theorem 2 in Sereni *et al.* (2018), as they will no longer have a cross-product between three parameter-dependent matrices, and thus only sums in  $i$  and  $j$  will be needed. This result is stated in Corollary 5.2.

**Corollary 5.2.** *By assuming that, in Theorem 5.1,  $P(\alpha)$ ,  $F(\alpha)$ , and  $G(\alpha)$  are homogeneous polynomials of degree  $g = 1$ , and that the state-feedback first-stage gain matrix is such that  $K(\alpha) = K$ , then a sufficient condition for (5.21) hold is that there exist symmetric matrices  $P_i > 0$ , and matrices  $F_i$ ,  $G_i$ ,  $H$ , and  $J$  such that*

$$\begin{bmatrix} (F_i \bar{A}_i + F_i \bar{B}_i K) + (\bullet)' + 2\gamma_2 P_i & * & * \\ P_i - F_i' + G_i \bar{A}_i + G_i \bar{B}_i K & -G_i - G_i' & * \\ \bar{B}_i' F_i' + J_i \bar{C}_i - H K & \bar{B}_i' G_i' & -H - H' \end{bmatrix} < 0 \quad (5.33)$$

holds for  $i = 1, 2, \dots, N$ ,

$$\begin{bmatrix} \Xi_{11}^{ij} & * & * \\ \Xi_{21}^{ij} & -(G_i + G_i') - (G_j + G_j') & * \\ \Xi_{31}^{ij} & \bar{B}_i' G_j' + \bar{B}_j' G_i' & -2(H + H') \end{bmatrix} < 0, \quad (5.34)$$

with

$$\Xi_{11}^{ij} = [\bar{A}_i' F_j' + \bar{A}_j' F_i' + K'(\bar{B}_i' F_j' + \bar{B}_j' F_i')] + (\bullet)' + 2\gamma_2(P_i + P_j), \quad (5.35)$$

$$\Xi_{21}^{ij} = P_i + P_j - (F_i' + F_j') + G_i \bar{A}_j + G_j \bar{A}_i + G_i \bar{B}_j K + G_j \bar{B}_i K, \quad (5.36)$$

and

$$\Xi_{31}^{ij} = \bar{B}_i' F_j' + \bar{B}_j' F_i' + J(\bar{C}_i + \bar{C}_j) - H(K_i + K_j), \quad (5.37)$$

holds for  $i = 1, 2, \dots, N-1$  and  $j = i+1, i+2, \dots, N$ .

**Proof:** Note that by multiplying (5.33) by  $\alpha_i^2$  and summing for  $i = 1, \dots, N$ , and by multiplying (5.34) by  $\alpha_i \alpha_j$ , and summing for  $i = 1, 2, \dots, N-1$  and  $j = i+1, i+2, \dots, N$ , bearing in mind that  $\alpha \in \wedge_N$ , we directly obtain the parameter-dependent form (5.21), with  $K(\alpha) = K$ . ■

As mentioned before, one can find a finite set of LMI conditions that ensure (5.21) by assuming that the decision variables are homogeneous-polynomial parameter-dependent matrices. Corollary 5.1 presents the sufficient conditions for (5.21) to hold for the case of  $g = 1$ . Progressively less conservative conditions might be obtained with higher order polynomials in  $\alpha$ . However, deriving such finite set of LMI could be a laborious task, as can be seen from the complexity associated to the case of  $g = 1$ . Fortunately, one can employ computational packages available in the literature to computationally generate the finite set of LMI, as for instance the specialized parser ROLMIP (AGULHARI *et al.*, 2019), which is adopted in the present work.

A final remark needs to be made on how to define the degree of the polynomial variables in the first-stage design conditions (5.20). Note that the two-stage method consists of sufficient conditions, since the first-stage design is performed independently from the second stage, as long as the obtained feedback matrix  $K(\alpha)$  is a stabilizing one. Therefore, the designer can impose different restrictions in the first stage, either on the decay rate or on the degree of the polynomial variables. This means it is not mandatory to impose  $\gamma_1 = \gamma_2$  in the design procedure (as already discussed in the previous chapters), nor to specify the same degree on the decision variables  $Z(\alpha)$ ,  $P(\alpha)$ ,  $F(\alpha)$ , or  $G(\alpha)$ . Nevertheless, feasibility in the second stage is directly affected by these choices, as illustrated by the examples in the next section.

### 5.3 ILLUSTRATIVE EXAMPLES

In this section, two examples are presented in order to illustrate the application and benefits of the proposed approach for addressing the problem of robust stabilization of uncertain LTI systems subject to non-negligible sensor and actuator dynamics, and time delay, by means of the definition of an augmented system and the employment of a two-stage-based SOF control design. Also, we intend to show that the generalization of previous results proposed in this work is indeed relevant for addressing complex SOF designs as the one exploited herein. The LMIs associated to the investigated problems are coded in the MATLAB software, with YALMIP interface (LOFBERG, 2004), and the SDPT3 solver (TOH; TODD; TÖTÜNCÜ, 1999).

**Example 5.1** In this first example, we demonstrate the benefits of our proposed method. For that, we consider the control design of the lateral axis dynamics for an L-1011 aircraft.

The system state-space model is adapted from Nguyen, Chevrel and Claveau (2018) as

$$\dot{x}(t) = \begin{bmatrix} -2.980 & \theta & 0 & -0.034 \\ -\theta & -0.210 & 0.035 & -0.001 \\ 0 & 0 & 0 & 1 \\ 0.390 & -1.350 - 3\theta & 0 & -1.890 \end{bmatrix} x(t) + \begin{bmatrix} -0.032 \\ 0 \\ 0 \\ -\theta \end{bmatrix} u(t), \quad (5.38)$$

where the four state variables  $x(t) = (x_1(t), x_2(t), x_3(t), x_4(t))$  are the yaw rate, the sideslip angle, the bank angle and the roll rate, respectively. The control input  $u(t)$  is the aileron deflection. Note that both system and input matrices are affected by an uncertain parameter  $\theta$ , such that

$$-1.0 \leq \theta \leq -0.5$$

which represents the airspeed.

We assume that only the state variables  $x_3(t)$  and  $x_4(t)$  are measured on-line by means of two sensors with dynamics described as in (5.4), with

$$A_v = \text{diag}(-1, -1) \quad \text{and} \quad C = \begin{bmatrix} 0 & 0 & 1 & 0 \\ 0 & 0 & 0 & 1 \end{bmatrix}.$$

The control input  $u(t)$  is applied through an actuator with dynamics as in (5.5), with

$$A_z = -1 \quad \text{and} \quad D = 1.$$

The sensors and actuator information channels are subject to time delay in such way that the measured state information,  $v(t)$ , and actuator command,  $u(t)$ , experience a time delay  $\tau = \tau_s = \tau_a = 350$  ms (a realistic value considering Avionics Full Duplex Switched Ethernet (AFDX) aviation data buses (FENG, 2016)) before being delivered to the controller and to the system actuator, respectively.

To apply the proposed method, we start by modeling the time delay effect using a Padé approximation of order 2. Therefore, regarding (5.12) with  $k_s = k_a = 2$  and  $\tau = \tau_s = \tau_a = 350$ , we have that the state-space matrices of (5.7) for the delayed sensors and actuator are

- *Sensor Channel 1*

$$A_{sd_1} = \begin{bmatrix} 0 & 1 \\ -59.2593 & -13.3333 \end{bmatrix}, \quad B_{sd_1} = \begin{bmatrix} 0 \\ 1 \end{bmatrix}, \quad C_{sd_1} = [0 \quad -26.6667], \quad D_{sd_1} = 1. \quad (5.39)$$

- *Sensor Channel 2*

$$A_{sd_2} = A_{sd_1}, \quad B_{sd_2} = B_{sd_1}, \quad C_{sd_2} = C_{sd_1} \quad \text{and} \quad D_{sd_2} = D_{sd_1}. \quad (5.40)$$

- Actuator Channel 1

$$A_{ad_1} = \begin{bmatrix} 0 & 1 \\ -59.2593 & -13.3333 \end{bmatrix}, \quad B_{ad_1} = \begin{bmatrix} 0 \\ 1 \end{bmatrix}, \quad C_{ad_1} = [0 \quad -26.6667], \quad D_{ad_1} = 1. \quad (5.41)$$

Firstly, by considering that  $\theta$  may only assume values within the given interval, we can represent the uncertain system (5.38) in terms of the convex combination of two vertices

- **Vertex 1**

$$A_1 = \begin{bmatrix} -2.980 & -1 & 0 & -0.034 \\ 1 & -0.210 & 0.035 & -0.001 \\ 0 & 0 & 0 & 1 \\ 0.390 & 1.650 & 0 & -1.890 \end{bmatrix}, \quad B_1 = \begin{bmatrix} -0.032 \\ 0 \\ 0 \\ 1.000 \end{bmatrix}$$

- **Vertex 2**

$$A_2 = \begin{bmatrix} -2.980 & -0.500 & 0 & -0.034 \\ 0.500 & -0.210 & 0.035 & -0.001 \\ 0 & 0 & 0 & 1 \\ 0.390 & 0.150 & 0 & -1.890 \end{bmatrix}, \quad B_1 = \begin{bmatrix} -0.032 \\ 0 \\ 0 \\ 0.500 \end{bmatrix}$$

defined according to the minimum and maximum values of  $\theta$ , following the polytopic definition (5.2).

Given the two vertices  $(A_1, B_1)$ ,  $(A_2, B_2)$ , as well as the sensor and actuator matrices, and the Padé delay model, a thirteenth-order augmented system is obtained as in (5.19).

We now proceed to the design phase where we aim at computing an SOF gain  $L$  such that the augmented system  $\bar{A} + \bar{B}L\bar{C}$  is asymptotic stable, relying only on the available sensors output signal. For that, we apply the extended two-stage HPLF-based LMI strategy to search for the desired stabilizing gain  $L$  with minimum decay rate specification.

To this end, we first design a stabilizing state-feedback controller by solving the LMI problem under the conditions given in (5.20). For this design, we consider a polynomial parameter-dependent variable  $Z(\alpha)$  with degree<sup>1</sup>  $g = 2$ , and also impose a minimum first-stage decay rate specification  $\gamma_1 = 0.02$ . The obtained state-feedback controller is

$$K(\alpha) = \alpha_1^2 K_1 + \alpha_1 \alpha_2 K_2 + \alpha_2^2 K_3 \quad (5.42)$$

---

<sup>1</sup>For a more detailed review on the use of ROLMIP for computationally defining polynomial variables and parameter-dependent LMIs, we refer the reader to the work of Agulhari *et al.* (2019).



with

$$K_1 = \begin{bmatrix} -0.9624 & -0.8310 & -3.6782 & -4.4970 & 0.5890 & 0.6020 & & \\ & 0.1047 & -0.0117 & -0.0141 & 0.0199 & -0.4611 & -144.5650 & 14.4716 \end{bmatrix},$$

$$K_2 = \begin{bmatrix} -0.8498 & -1.3383 & -6.8547 & -7.4811 & 1.2836 & 0.8902 & & \\ & 0.2097 & -0.0216 & -0.0279 & 0.0378 & -0.6510 & -279.7175 & 29.5492 \end{bmatrix},$$

$$K_3 = \begin{bmatrix} 0.0614 & -0.76541 & -3.4788 & -2.8447 & 0.7254 & 0.2582 & & \\ & 0.1071 & -0.0111 & -0.0135 & 0.0189 & -0.5118 & -142.6304 & 14.3959 \end{bmatrix}.$$

In the sequence, we use  $K(\alpha)$  (in terms of the vertex matrices  $K_1$ ,  $K_2$ , and  $K_3$ ) in the second-stage LMIs of Theorem 5.1, which are based on homogeneous-polynomial functions. We set the polynomial Lyapunov function  $P(\alpha)$  and auxiliary polynomial variables  $F(\alpha)$  and  $G(\alpha)$  to be of degree  $g = 2$ . In addition, by enforcing a minimum second-stage decay rate  $\gamma_2 = 0.2$ , we find

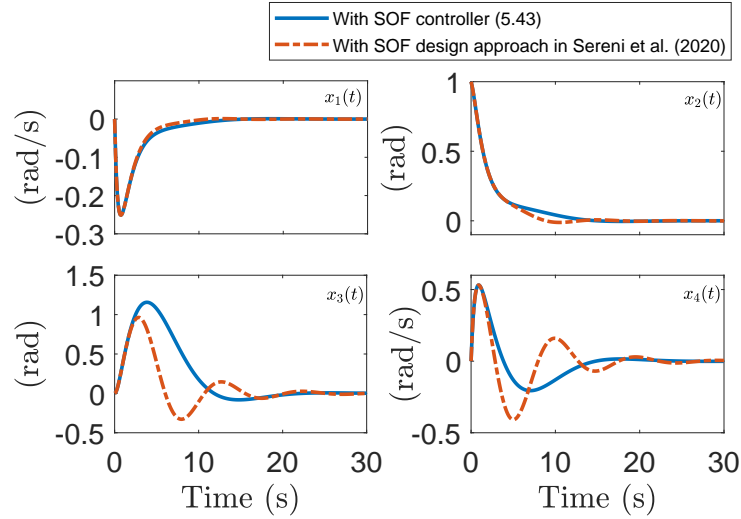
$$L = \begin{bmatrix} -0.5219 & -0.3148 \end{bmatrix}. \quad (5.43)$$

We begin analyzing this result by emphasizing the simplicity of the obtained SOF gain. Since our method considers only the available measured system information (which, in this case, consists of the two sensors outputs), the designed feedback gain (5.43) is a vector with two gains. In a hypothetical full-state feedback implementation, the gain matrix would be a vector with thirteen gains, as obtained in the first-stage design (5.42), in order to encompass plant, sensors and actuators states, if they were possible to be measured.

In Figure 5.2, we present the closed-loop time-response of each of the four states of system (5.38), with its dynamic sensors and actuators as given in (5.39)-(5.41), considering an initial condition  $x(0) = \begin{bmatrix} 0 & 1 & 0 & 0 \end{bmatrix}$ , which represents the aircraft state after a gust perturbation (ANDRY; CHUNG; SHAPIRO, 1984). We can see that the SOF controller (5.43) (solid lines) enforced a stable behavior, even with sensor and actuator delayed communication channels in  $\tau = 350$  ms.

Additionally, to illustrate the impact of neglecting the delay in the control design, we also plotted (dashed lines) the transient response of the closed-loop system with an SOF gain designed for an augmented system that only considers the sensors and actuator additional dynamics, as considered in the preliminary work of the results proposed in the

Figure 5.2 - L-1011 lateral axis closed-loop dynamics with SOF design neglecting (SERENI *et al.*, 2020) and considering transport delay (SOF controller (5.43)).



Source: Author's own results.

present thesis (SERENI *et al.*, 2020). Comparing both responses in this example, we can clearly see a degradation in the system performance, observed in terms of smaller damping during system transient, especially with  $x_3(t)$  and  $x_4(t)$  state variables (the ones used in the feedback loop).

For completing the analysis of our proposed method, we illustrate the impact of the minimum decay rate  $\gamma$  in the control design. For that, we present a comparison of the control design (5.43) – which considered a minimum decay rate constraint  $\gamma_2 = 0.2$  – with another design, carried out without imposing restrictions on the decay rate of the closed-loop system (i.e.  $\gamma_2 = 0$ ).

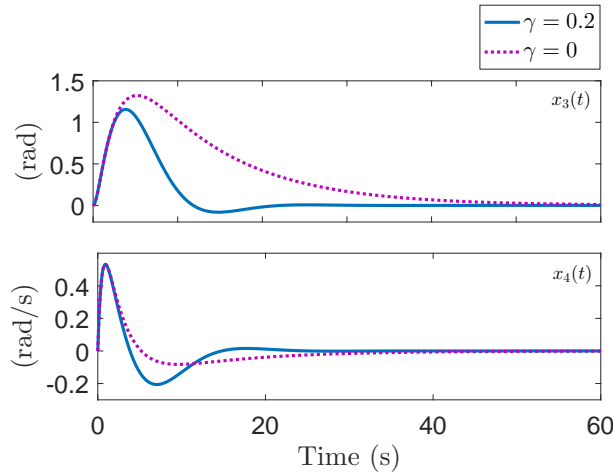
By employing the same procedure adopted in the synthesis of the SOF gain matrix (5.43), but now considering  $\gamma_1 = \gamma_2 = 0$  we obtain

$$L = \begin{bmatrix} -0.2332 & -0.0502 \end{bmatrix}. \quad (5.44)$$

A comparison of the closed-loop responses obtained with the SOF gains (5.43) and (5.44) is presented in Figure 5.3 in terms of the state variables  $x_3(t)$  and  $x_4(t)$ . One can clearly see that without imposing a minimum decay rate constraint, the closed-loop system exhibits a worse performance in terms of a longer settling-time.

**Remark 5.5.** *The decay rate bound  $\gamma_1$  considered in the first part of this example, imposed in the first-stage design (and the resulting gain  $K(\alpha)$ ) directly impacts the feasibility in*

Figure 5.3 - L-1011 lateral axis closed-loop dynamics with SOF design with minimum decay rate  $\gamma = 0.2$  and without minimum decay rate enforcement ( $\gamma = 0$ ).



Source: Author's own results.

the second-stage phase. For this particular example, by setting  $\gamma_1 = 0.02$  we obtained feasibility in the second-stage with  $\gamma_2 = 0.2$ . If desired, a search on  $\gamma_1$  can be employed for obtaining an “optimal” maximum value for the second-stage decay rate bound  $\gamma_2$ , since with higher bounds we enforce faster transient responses (BOYD et al., 1994).

**Remark 5.6.** A final yet important remark regarding Example 5.1 is that by considering a design approach via Corollary 5.1 or 5.2 we obtain some interesting results. If we consider a parameter-dependent first-stage design, by setting  $Z(\alpha)$  with degree  $g = 1$  and use the obtained matrix gains in Corollary 5.1 we do not find a feasible solution for the same decay rate design parameters. Corollary 5.2 also fails in obtaining feasibility in the second-stage design. These results illustrate the benefits of considering a higher-degree Polya's relaxation associated to the HPLF approach, when compared to the polytopic method in Sereni et al. (2018), which will be more properly discussed in Example 5.3.

**Example 5.2** In this second example, we give more emphasis to the importance of considering the delay effect in the control design. To that end, we show that methods known for its robustness characteristics, such as conventional sliding mode control (SMC) techniques, suffers destabilization in the presence of time delay.

Consider an uncertain linear system such as (5.1), described in terms of the following vertex matrices:

- **Vertex 1**

$$A_1 = \begin{bmatrix} -0.277 & -32.980 & -5.432 \\ 0.365 & -0.319 & -9.490 \\ 0 & 0 & -5 \end{bmatrix}, B_1 = \begin{bmatrix} 0 \\ 0 \\ -5 \end{bmatrix}$$

- **Vertex 2**

$$A_2 = \begin{bmatrix} -4.277 & -50 & -5.432 \\ 0.365 & -1.318 & -9.490 \\ 0 & 0 & -5 \end{bmatrix}, B_2 = B_1$$

We consider the design of an sliding-mode controller in terms of the control law

$$u(t) = Rx(t) + \rho \frac{Nx(t)}{\|Mx(t)\| + \delta},$$

where  $R, M$ , and  $N$  are constant matrices, and  $\rho$  a constant scalar. Such parameters are obtained through the employment of the classic SMC as described in Utkin (1978). For the considered example, one might obtain:

$$\rho = 0.1, \quad R = \begin{bmatrix} -0.58 & -7.96 & 17.09 \end{bmatrix},$$

$$N = \begin{bmatrix} 0.1 & -1 & 0.1 \end{bmatrix}, \quad \text{and}$$

$$M = \begin{bmatrix} -0.1 & 1 & -0.1 \end{bmatrix}.$$

The constant parameter  $\delta$  is a small scalar included for avoiding the chattering phenomenon, often present in sliding mode control structures (BAG; SPURGEON; EDWARDS, 2002). For this example, we set  $\delta = 10^{-2}$ .

In a simulation considering an arbitrary initial condition  $x_0 = [0.15 \ 0.15 \ 0.15]^T$ , the SMC controller is able to stabilize the considered system in closed-loop, yielding the transient response presented in Figure 5.4 (top).

However, when a time delay  $\tau_a = 0.02$  is inserted in the control signal channel, such that  $\dot{x} = A(\alpha)x(t) + Bu(t - \tau_a)$ , the same SMC controller is not able to maintain stability, as the simulation results for the same initial conditions show in Figure 5.4 (bottom).

By employing our robust SOF method that encompasses the input signal delay in the controller design, we obtain a stabilizing controller

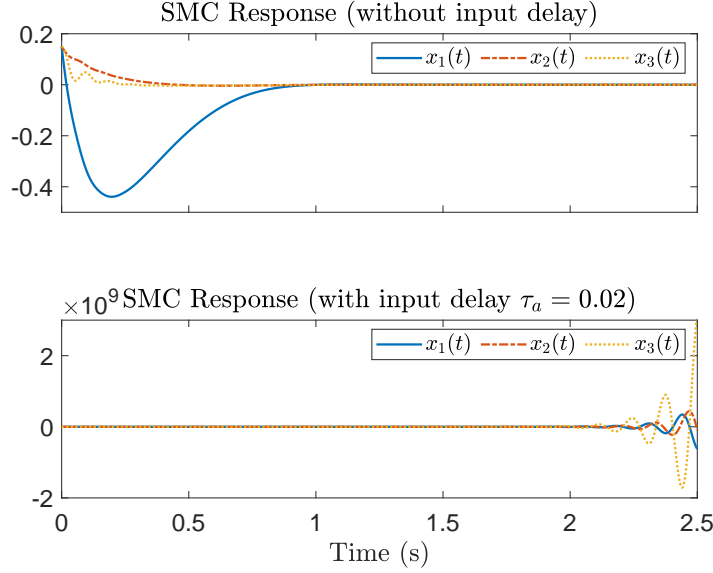
$$L = \begin{bmatrix} -0.0484 & -1.4265 & 2.2506 \end{bmatrix},$$

with sensor and actuator models matrices<sup>2</sup>  $A_v = \text{diag}(-100, -100, -100)$ ,  $A_z = -100$ , and

---

<sup>2</sup>Note that we considered actuators and sensors with fast dynamics. With that, only the delay effect will have a significant impact in the controllers simulation responses, which is the objective in this comparison example.

Figure 5.4 - Simulation results obtained for Example 5.2 system considering a conventional SMC controller (UTKIN, 1978).



Source: Author's own results.

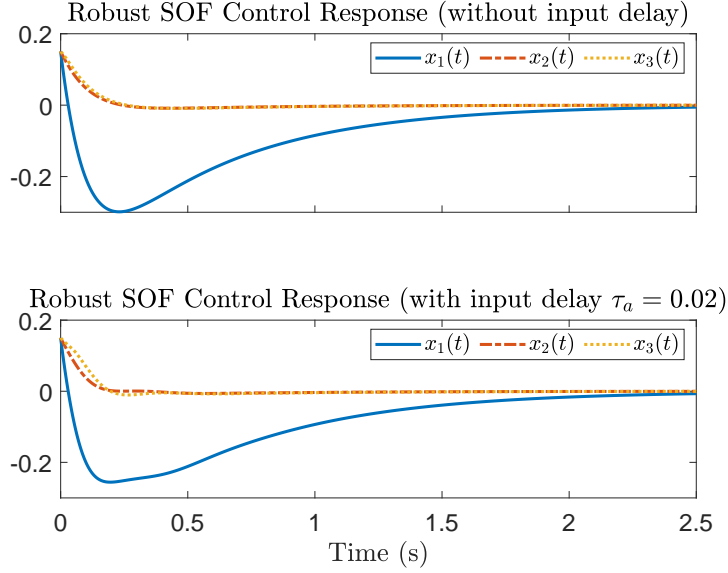
a  $2^{nd}$  order delay Padé approximation model. The first- and second-stage LMI variables degrees are set as  $degP = degF = degG = 2$ ,  $degZ = 0$ , and  $\gamma_1 = \gamma_2 = 0$ . As we can see in Figure 5.5, in contrast to the SMC strategy, our method presents stability robustness with respect to the presence of time delay in the control input channel, since closed-loop transient when input delay is considered exhibits only small variations when compared to delay-free transient.

**Remark 5.7.** *It is very important to stress that the SMC technique addressed in Utkin (1978), which is considered in this example, was designed and analyzed for ensuring robustness to uncertainties and unmatched non linearities. Therefore, such method is not suited for coping delay effects. The purpose of this example is to show that even techniques well-known for presenting robustness to several practical control issues are susceptible to present undesired dynamic characteristics in the presence of time-delay effects.*

**Example 5.3** This third example is aimed at illustrating the benefits of considering an HPLF-based two-stage robust SOF design strategy with minimum decay rate constraints for uncertain LTI systems with sensor and actuator time-delayed dynamics.

For that purpose, a set of feasibility tests is performed, which consisted in attempting to find a feasible solution for the control design of the L-1011 lateral axis dynamics (presented in Example 5.1) using a polytopic parameter-dependent strategy (SERENI

Figure 5.5 - Simulation results obtained for Example 2 system considering a robust SOF controller using our proposed two-stage design via Theorem 5.1.



Source: Author's own results.

*et al.*, 2018, 2020) (Corollary 5.2) and the HPLF generalization proposed in this work (Theorem 5.1).

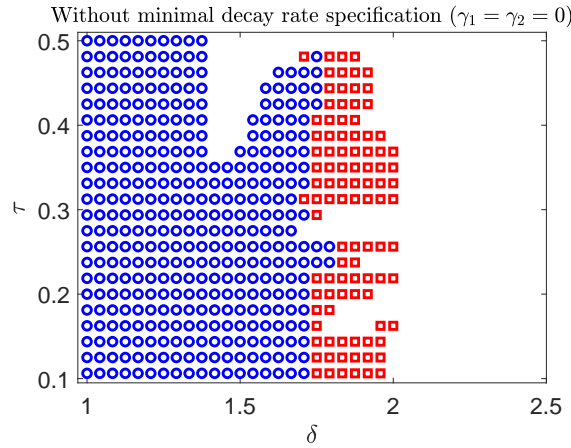
Note that for different ranges for the uncertain parameter  $\theta$  and different values for the time delay  $\tau$  we have a different control design problem. We consider that the uncertain parameter  $\theta$  lies in the range specified by  $-1.0 - \delta \leq \theta \leq -0.5 + \delta$ , with  $1.0 \leq \delta \leq 2.5$ . At the same time, we consider a range of test values for the time-delay defined by  $0.05 \leq \tau \leq 0.5$ . Therefore, for each pair  $(\delta, \tau)$  in the specified ranges, we have a different problem in terms of uncertain parameter and time delay. Moreover, observe that for higher values of  $\delta$ , we are assuming that the uncertain parameter belongs to a wider uncertainty range.

In a first study, we assume that no minimum decay rate is enforced in the control designs of both stages (i.e.  $\gamma_1 = \gamma_2 = 0$ ). Then, for each pair  $(\delta, \tau)$  we seek to find a first-stage state-feedback gain<sup>3</sup> using (5.20), and then we feed the obtained controller information to the LMI problems stated in Corollary 5.2 and Theorem 5.1.

In Figure 5.6 we present for which pairs  $(\delta, \tau)$  each strategy succeeded in finding a stabilizing robust SOF gain  $L$ . As we can clearly see, the HPLF strategy considered in

<sup>3</sup>Since the second-stage design is sensitive to the state-feedback gain designed in the first stage, we perform both tests assuming that the first stage is executed considering the degree of  $Z(\alpha)$  to be equal to 0 ( $\text{deg}Z = 0$ ), enabling the use of the same gain  $K(\alpha) = K$  in both second-stage synthesis conditions of Theorem 5.1 and Corollary 5.2 (SERENI *et al.*, 2018).

Figure 5.6 - Feasibility region obtained for the L-1011 lateral axis SOF stabilization problem without imposing a minimum decay rate when applying the polytopic PDLF SOF design strategy (SERENI *et al.*, 2018) ( $\circ$  - Corollary 5.2); and when using the HPLF extension proposed in Theorem 5.1 ( $\circ$  and  $\square$ ).



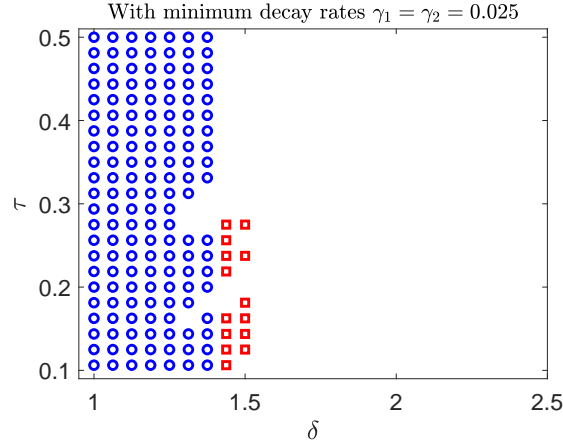
Source: Author's own results.

this work (Theorem 5.1) outperforms the polytopic PDLF approach used in Sereni *et al.* (2020), and proposed in Sereni *et al.* (2018) (Corollary 2), as Theorem 5.1 is able to provide a feasible solution for a larger number of problems. For this test, the variables  $(P, F, G)(\alpha)$  in Theorem 5.1 were assumed to be polynomials with degree  $g = 2$ . In practical terms, the result presented in Figure 5.6 shows that Theorem 5.1 guarantees the robust SOF stabilization of the L-1011 lateral axis dynamics for a wider range of uncertainty on the airspeed parameter  $\theta$ , by allowing the decision variables to be defined as homogeneous polynomials with degree higher than  $g = 1$ , in contrast as considered in Sereni *et al.* (2018).

In a second feasibility test, we now consider that a minimum decay rate is imposed in both stages of design. Repeating the same procedure as in the first test, the feasibility region in Figure 5.7 is obtained. Once again, we see that the HPLF strategy outperformed the polytopic PDLF approach used in Sereni *et al.* (2020). However, a comparison with the results in Figure 5.6 reveals that the additional constraint of a minimum decay rates increases the difficulty of providing a stabilizing SOF gain. Indeed, the feasibility region in Figure 5.7 covers a smaller range of model uncertainty, which is defined by the value of  $\delta$ .

For completing the analysis of the results proposed in our work, we present a study of the influence that the degree of the polynomial matrix  $K(\alpha)$ , chosen in the first-stage design, exerts over the feasibility in the second stage.

Figure 5.7 - Feasibility region obtained for the L-1011 lateral axis SOF stabilization problem imposing a minimum decay rate ( $\gamma_1 = \gamma_2 = 0.025$ ) when applying the polytopic PDLF SOF design strategy (SERENI *et al.*, 2020) ( $\circ$ ); and when using the HPLF extension proposed in Theorem 5.1 ( $\circ$  and  $\square$ ).



Source: Author's own results.

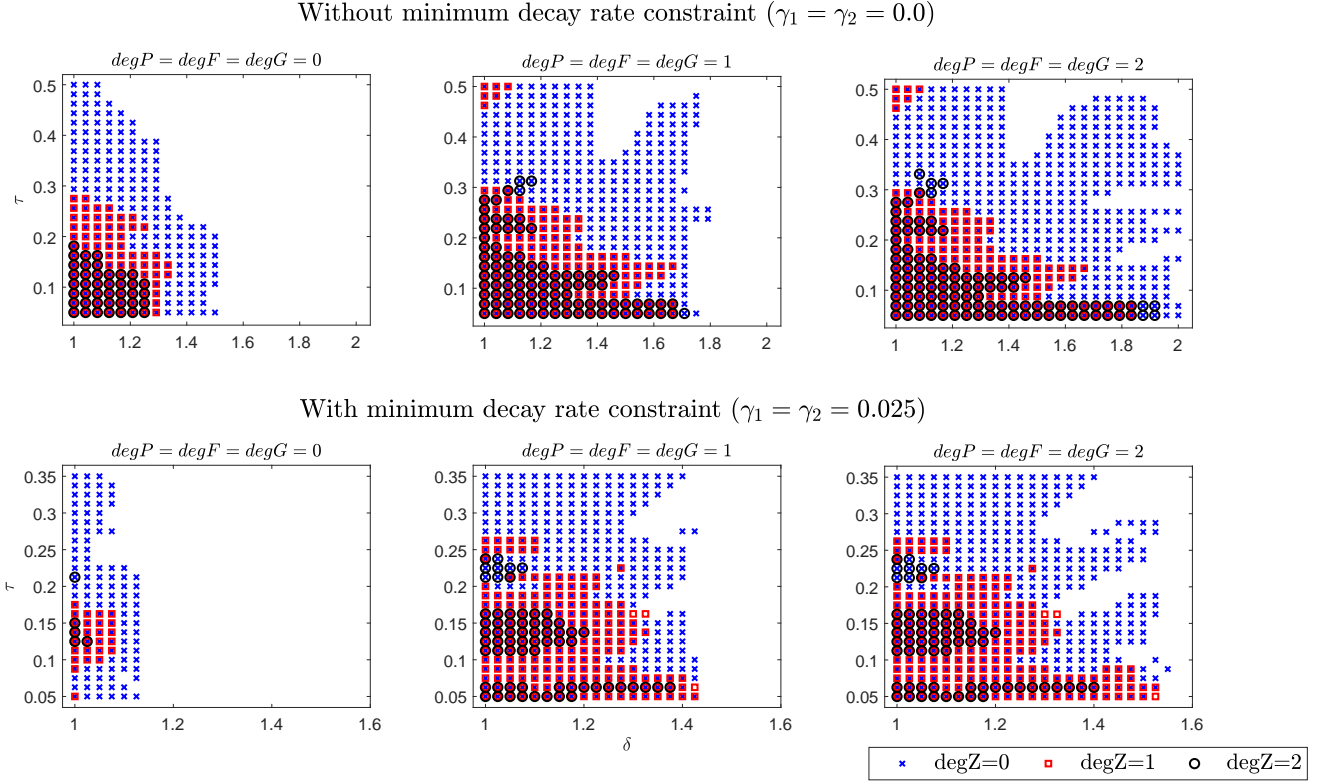
New feasibility tests – on the same basis of the two previous ones – were conducted, by combining different choices for the polynomial degrees of the decision variables in both first and second stages. In the first stage, three values were tested for the degree  $\deg Z$  of the polynomial variable  $Z(\alpha)$ , namely  $\deg Z = 0$ ,  $\deg Z = 1$ , and  $\deg Z = 2$ . It is worth recalling that  $\deg Z$  also corresponds to the degree of  $K(\alpha)$ , as  $K(\alpha) = W^{-1}Z(\alpha)$ . In the second stage, the polynomial variables  $P(\alpha)$ ,  $F(\alpha)$ , and  $G(\alpha)$  were also chosen to be of the same degree  $\deg PFG$  (*i.e.*  $\deg P = \deg F = \deg G = \deg PFG$ ), which was set to either 0, 1, or 2. For each pair  $(\deg Z, \deg PFG) \in \{0, 1, 2\} \times \{0, 1, 2\}$ , the feasibility of the LMI (5.1) in Theorem (5.21) was assessed. The results are presented in Figure 5.8.

As expected in light of the previous results, by allowing the decision variables to be homogeneous-polynomially dependent on the uncertain parameter we obtain a wider feasibility region, which increases with higher polynomial degrees.

However, the inverse result is observed regarding the polynomial degree established for the first-stage gain  $K(\alpha)$ . As seen from both scenarios (with and without minimal decay rate specification), the best feasibility results in the second-stage design are obtained when the first-stage gain is set to be independent from the uncertain parameter. Moreover, the higher degree set for the polynomial gain matrix  $K(\alpha)$ , the smaller is the resulting feasibility region in the second stage.



Figure 5.8 - Feasibility regions obtained for the L-1011 lateral axis SOF stabilization problem for different choices of the polynomial degree of the decision variables associated to the first- and second-stage designs with (bottom charts) and without (top charts) minimum decay rate constraints.



Source: Author's own results.

## 5.4 EXTENSION TO $\mathcal{H}_2$ CONTROL

Now consider the state-space realization

$$\begin{aligned} \dot{x}(t) &= A(\alpha)x(t) + B(\alpha)z(t) + B_d(\alpha)d(t) \\ \zeta(t) &= C_z(\alpha)x(t) + D_z(\alpha)z(t) \end{aligned} \quad (5.45)$$

where  $\zeta(t) \in \mathbb{R}^{q_z}$  and  $d(t) \in \mathbb{R}^{m_d}$  are the controlled output and disturbance input vectors, respectively. Additionally,  $B_d(\alpha) \in \mathbb{R}^{n \times m_d}$  is the disturbance input matrix to the system dynamics,  $C_z(\alpha) \in \mathbb{R}^{q_z \times n}$  is the controlled output matrix, and  $D_z(\alpha) \in \mathbb{R}^{q_z \times m}$  is the control input direct transmission matrix.

Assuming that sensor and actuator dynamics are modeled as described in Section II,

an augmented system can be derived such as

$$\begin{aligned} \dot{w}(t) &= \bar{A}(\alpha)w(t) + \bar{B}(\alpha)z(t) + \bar{B}_d(\alpha)d(t) \\ \zeta(t) &= \bar{C}_z(\alpha)w(t) + \bar{D}_z(\alpha)z(t) \\ y(t) &= \bar{C}(\alpha)w(t), \end{aligned} \quad (5.46)$$

where  $w(t)$  is defined as in (5.18) and  $\bar{A}(\alpha)$ ,  $\bar{B}(\alpha)$ , and  $\bar{C}(\alpha)$  are given as in (5.19), while

$$\bar{B}_d(\alpha) = \begin{bmatrix} B_d(\alpha) \\ 0_{q(1+k_s) \times m_d} \\ 0_{m(1+k_a) \times m_d} \end{bmatrix}, \quad \bar{D}_z(\alpha) = D_z(\alpha)$$

and

$$\bar{C}_z(\alpha) = \begin{bmatrix} C_z(\alpha) & 0_{q_z \times q(1+k_s)} & 0_{q_z \times m(1+k_a)} \end{bmatrix}.$$

In such fashion, the augmented system (5.46) models the effect of an exogenous input signal  $d(t)$  over the system dynamics. Moreover, it indicates the vector  $\zeta(t)$ , which consists of a linear combination of the original system state vector  $x(t)$ , defined according to the shape of the matrix  $C_z(\alpha)$ .

The  $\mathcal{H}_2$  problem here considered consists in finding a robust controller  $L$  such that the augmented system (5.46) is asymptotically stable and also that the closed-loop  $\mathcal{H}_2$  guaranteed cost is bounded by  $\mu$ . The system decay rate is also imposed to have a lower bound  $\gamma$ . Such performance criteria are desired to be met assuming a control law  $u(t) = Ly(t)$ .

For achieving such control objective, we consider the  $\mathcal{H}_2$  conditions presented in Subsection 2.1.4 and that the closed-loop system (2.12) is such that, with

$$\mathcal{A}(\alpha) = \bar{A}(\alpha) + \bar{B}(\alpha)L\bar{C}(\alpha), \quad \mathcal{B}(\alpha) = \bar{B}_d(\alpha), \quad (5.47)$$

$$\mathcal{C}(\alpha) = \bar{C}_z(\alpha) + \bar{D}_z(\alpha)L\bar{C}(\alpha) \quad \text{and} \quad \mathcal{D}(\alpha) = 0. \quad (5.48)$$

Now, based on the considered two-stage procedure, we propose new sufficient LMI conditions for computing the robust  $\mathcal{H}_2$  controller  $L$  based on the state-feedback controller  $K(\alpha)$  obtained in the previous stage, as enunciated in Theorem 5.2.

**Theorem 5.2.** *Assuming that there exists a state-feedback gain  $K(\alpha)$  such that  $\bar{A}(\alpha) + \bar{B}(\alpha)K(\alpha)$  is asymptotically stable, then there exists a stabilizing static output-feedback gain  $L$  such that  $\bar{A}(\alpha) + \bar{B}(\alpha)L\bar{C}(\alpha)$  is asymptotically stable, considering a decay rate greater than or equal to  $\gamma > 0$ , if there exist parameter-dependent symmetric matrices  $P(\alpha) > 0$  and  $Y(\alpha) > 0$ , parameter-dependent matrices  $F(\alpha)$ ,  $G(\alpha)$ , and matrices  $H$  and*

$J$  such that are a solution to the following optimization problem:

$$\min \nu$$

subject to

$$\text{trace}(Y(\alpha)) \leq \nu, \quad (5.49)$$

$$\begin{bmatrix} Y(\alpha) & \bar{B}_d(\alpha)'P(\alpha) \\ P(\alpha)\bar{B}_d(\alpha) & P(\alpha) \end{bmatrix} > 0, \quad (5.50)$$

and

$$\begin{bmatrix} (F(\alpha)\bar{A}(\alpha) + F(\alpha)\bar{B}(\alpha)K(\alpha)) + (\bullet)' + 2\gamma P(\alpha) & & & & \\ P(\alpha) - F(\alpha)' + G(\alpha)\bar{A}(\alpha) + G(\alpha)\bar{B}(\alpha)K(\alpha) & & & & \\ \bar{C}_z(\alpha) + \bar{D}_z(\alpha)K(\alpha) & & & & \\ \bar{B}(\alpha)'F(\alpha)' + J\bar{C}(\alpha) - HK(\alpha) & & & & \\ & * & * & * & \\ & -G(\alpha) - G(\alpha)' & * & * & \\ & 0 & -I & * & \\ & \bar{B}(\alpha)'G(\alpha)' & \bar{D}_z(\alpha) & -H - H' & \end{bmatrix} < 0 \quad (5.51)$$

Then, at the optimal solution, system (5.46) in closed-loop with  $u(t) = Ly(t)$ , where  $L = H^{-1}J$ , has a lower bound  $\gamma > 0$  on the system decay rate and the closed-loop system  $\mathcal{H}_2$  norm is bounded by  $\mu$  such that  $\mu = \sqrt{\nu} \geq \|\mathcal{H}(s)\|_2$ .

**Proof:** Assuming that (5.51) holds, we have that  $H$  is invertible. Now, by pre- and post-multiplying (5.51) by  $U(\alpha)$  and  $U(\alpha)'$ , where

$$U(\alpha) = \begin{bmatrix} I & 0 & 0 & S(\alpha)' \\ 0 & I & 0 & 0 \\ 0 & 0 & I & 0 \end{bmatrix}, \quad (5.52)$$

where  $S(\alpha) = H^{-1}J\bar{C}(\alpha) - K(\alpha)$ , we have after some algebraic manipulation:

$$\begin{bmatrix} (F(\alpha)(\bar{A}(\alpha) + \bar{B}(\alpha)H^{-1}J\bar{C}(\alpha))) + (\bullet)' + 2\gamma P(\alpha) & * & * \\ P(\alpha) - F(\alpha)' + G(\alpha)(\bar{A}(\alpha) + \bar{B}(\alpha)H^{-1}J\bar{C}(\alpha)) & -G(\alpha) - G(\alpha)' & * \\ \bar{C}_z(\alpha) + \bar{D}_z(\alpha)H^{-1}J\bar{C}(\alpha) & 0 & -I \end{bmatrix} < 0. \quad (5.53)$$

Defining  $L = H^{-1}J$  comes

$$\begin{bmatrix} (F(\alpha)(\bar{A}(\alpha) + \bar{B}(\alpha)L\bar{C}(\alpha))) + (\bullet)' + 2\gamma P(\alpha) & * & * \\ P(\alpha) - F(\alpha)' + G(\alpha)(\bar{A}(\alpha) + \bar{B}(\alpha)L\bar{C}(\alpha)) & -G(\alpha) - G(\alpha)' & * \\ \bar{C}_z(\alpha) + \bar{D}_z(\alpha)L\bar{C}(\alpha) & 0 & -I \end{bmatrix} < 0. \quad (5.54)$$

Following the definition given in (5.47) and (5.48), we have

$$\begin{bmatrix} F(\alpha)\mathcal{A}(\alpha) + (\bullet)' + 2\gamma P(\alpha) & * & * \\ P(\alpha) - F(\alpha)' + G(\alpha)\mathcal{A}(\alpha) & -G(\alpha) - G(\alpha)' & * \\ \mathcal{C}(\alpha) & 0 & -I \end{bmatrix} < 0. \quad (5.55)$$

At this point, one should observe that the upper-left  $2 \times 2$  block matrix in (5.55) represents the robust stability condition for  $\dot{w}(t) = \mathcal{A}w(t)$ , as seen in Lemma 2.5. Therefore, (5.55) is equivalently represented by

$$\begin{bmatrix} \mathcal{A}(\alpha)'P(\alpha) + P(\alpha)\mathcal{A}(\alpha) + 2\gamma P(\alpha) & \mathcal{C}(\alpha)' \\ \mathcal{C}(\alpha) & -I \end{bmatrix} < 0. \quad (5.56)$$

Note that by applying the Schur complement on (5.56), we have

$$\begin{aligned} & \mathcal{A}(\alpha)'P(\alpha) + P(\alpha)\mathcal{A}(\alpha) + 2\gamma P(\alpha) + \mathcal{C}(\alpha)'\mathcal{C}(\alpha) < 0 \\ \Rightarrow & \mathcal{A}(\alpha)'P(\alpha) + P(\alpha)\mathcal{A}(\alpha) + \mathcal{C}(\alpha)'\mathcal{C}(\alpha) < -2\gamma P(\alpha) < 0, \end{aligned}$$

as  $P(\alpha) > 0$  and  $\gamma > 0$ .

Finally, also by means of the Schur complement, we have that (5.50) is equivalent to  $Y(\alpha) - \mathcal{B}(\alpha)'P(\alpha)\mathcal{B}(\alpha) > 0$ . Therefore, according to Lemma 2.3, with  $\nu = \mu^2$  we have  $\mu = \sqrt{\nu} > \|\mathcal{H}(\alpha, s)\|_2$ , and by minimizing  $\nu$  and consequently the trace of  $Y(\alpha)$ , we minimize the system's  $\mathcal{H}_2$  guaranteed cost. The proof is then finished. ■

It is important to stress that in the two-stage approach the first-stage gain matrix  $K(\alpha)$  can be designed using any stabilizing state-feedback control synthesis. In this work, we consider the use of the conditions presented in (5.20). Investigating the efficiency of the proposed robust SOF  $\mathcal{H}_2$  controller synthesis with different first-stage control design techniques are beyond the scope of this work.

Finally, as in Theorem 5.1, the LMI conditions in Theorem 5.2 are of infinite dimension. Therefore, the same procedure of defining a finite set of LMI by considering a homogeneous-polynomial structure for the decision variables using the specialized parser ROLMIP (AGULHARI *et al.*, 2019) is adopted for employing Theorem 5.2.

**Remark 5.8.** *Despite of the fact that our mathematical development unravels based on the augmented system (5.46), which serves for modeling the sensor/actuator dynamics and delay effect, the proposed conditions in Theorem 5.2 are generic and can be applied to any uncertain LTI system that could be modeled as in (5.46).*

**Example 5.4** Now we aim at illustrating the efficacy of the  $\mathcal{H}_2$  control strategy proposed in Theorem 5.2. To this, consider the uncertain continuous-time system borrowed

from Dong and Yang (2007), defined in terms of polytope with vertex matrices:

- **Vertex 1**

$$A_1 = \begin{bmatrix} 1 & 2 \\ 0 & -4 \end{bmatrix}, B_1 = \begin{bmatrix} 1 \\ 0 \end{bmatrix}, B_{d1} = \begin{bmatrix} 2 \\ 1 \end{bmatrix}, C_1 = [1 \ 0], C_{z1} = [1 \ 2], D_{d1} = 1.$$

- **Vertex 2**

$$A_2 = \begin{bmatrix} 2 & -1 \\ 0 & -5 \end{bmatrix}, B_2 = \begin{bmatrix} 1 \\ 1 \end{bmatrix}, B_{d2} = \begin{bmatrix} 1 \\ 1 \end{bmatrix}, C_2 = [2 \ 1], C_{z2} = [1 \ 1], D_{d2} = 2.$$

Adapting the example for employing our proposed method, we also consider sensor and actuator with non-negligible dynamics, which are modeled as described in Subsection 5.2.1, with  $A_v = -100$ ,  $A_z = -100$ . We also assume that the information in both state and input channels are delayed in 30 ms, whose dynamic effects are modeled using a  $2^{nd}$  order delay Padé approximation model.

Now, applying our two-stage procedure over the consequent augmented system, we first design a stabilizing state-feedback gain  $K(\alpha)$  using (5.20), with  $\gamma_1 = 0$  and  $\text{deg}Z = 0$  for obtaining:

$$K(\alpha) = \begin{bmatrix} -1.9710 & -0.1149 & 0.9088 & -0.0047 \\ -4.7203 \times 10^{-5} & 0.8105 & -898.7575 & -7.8539 \end{bmatrix}.$$

Then, by solving the minimization problem stated in Theorem 5.2, with variables degrees set as  $\text{deg}P = \text{deg}F = \text{deg}G = \text{deg}Y = 1$  and  $\gamma = 0$ , we obtain a stabilizing robust SOF controller

$$L = -4.3039,$$

which ensures a  $\mathcal{H}_2$  guaranteed cost  $\mu = 6.9858$ . For comparison purposes, observe that in Dong and Yang (2007), the proposed  $\mathcal{H}_2$  control strategy achieved a more conservative guaranteed cost  $\mu = 8.0343$ , even without the additional complexity associated to our approach, which considers delay and sensor/actuator non-negligible dynamics.

## 6 CONCLUSION

This thesis compiles new contributions to control theory field related to the design of SOF controllers. In the presented chapters, different control problems related to SOF design were addressed, and new alternatives for controller synthesis were proposed and its features were demonstrated and illustrated in numerical and practical examples.

Among the proposed results, a new robust  $\mathcal{D}$ -stabilising SOF control design LMI-based method was proposed. Differently from other results available in the literature, that also addressed the robust pole placement in a circular  $\mathcal{D}$ -region for uncertain LTI systems, the LMI conditions proposed in Theorem 3.2 offers a solution for incomplete state measurement by means of a static output feedback controller design. Moreover, we demonstrated that when considering  $\mathcal{D}$ -stability constraints, the two-stage method might yield better feasibility performance when closed-loop pole placement is enforced in both stages of design. In that scope, the robust SOF  $\mathcal{D}$ -stabilization Strategy 3 regarding new LMI synthesis conditions for first (Theorem 3.4) and second (Theorem 3.5) stages showed to be capable of outperform simpler strategies.

Such enhanced performance stems from the less conservative nature of the second-stage LMI proposed in Theorem 3.5, which makes use of a parameter-dependent state-feedback gain matrix design in the first stage, using Theorem 3.4. One of the advantages of the results proposed in this work is that with less conservative conditions the designer might specify a smaller allocation region, enabling a more precise shaping of the dynamic behavior in closed-loop.

The presented examples in Chapter 3 support this conclusion, and also illustrates that by means of the proposed strategy it is possible to establish good compromise between performance and control signal magnitude. The practical applicability of our method was also attested by the results of a practical control implementation on a real active suspension system.

Also in Chapter 3, a new gain-scheduled controller synthesis strategy was proposed for LPV systems under incomplete state measurement and closed-loop pole placement constraints. As seen from the design examples and simulation results, the proposed strategy is capable of improving the transient performance an LPV system without compromising its stability, even in the absence of some state information, by means of the enforcement

of the eigenvalue placement of the closed-loop LPV system in a specific circular region of the complex plane, for a fixed value of the time-varying parameters.

In addition, we showed that our gain-scheduling approach is indeed suitable for dealing with LPV systems, while other strategies, such as robust control for uncertain systems, failed to yield a feasible controller for the time-varying parameters intervals considered in the presented example. Different from other gain-scheduling techniques, our strategy does not rely on online, nor offline information about the derivatives of the time-varying parameters that affects the system dynamics. This feature yields a simpler yet efficient mathematical approach, as it does not involve the inversion of literal matrices. In these terms, the proposed method shows to have a promising development perspective in analyzing the benefits of imposing pole placement constraints in LPV controller designs.

On the discrete-time case, we proposed a new LMI-based control design strategy for LPV systems via gain-scheduled static output-feedback. Using a two-stage procedure, our method demonstrated to be capable of improving the system performance in terms of a shorter transient time, by means of the inclusion of a minimum decay rate bound in the controller synthesis, as illustrated in Example 4.1.

Also, the proposed strategy presented to yield less conservative results in the GS-SOF stabilization problem with additional bound on the closed-loop decay rate when compared to another method available in the literature, as seen from the results in Example 4.2. Moreover, the presented examples attest the versatility and potentiality of our contribution, since it was able to address a general case, where all state-space matrices are affected by time-varying parameters, without imposing any particular structure, as seen in other SOF control strategies in literature.

We also showed that the extension of the proposed method for addressing more complex problems, as the  $\mathcal{H}_\infty$  control problem in LPV scenario by means of affine PDLFs, could outperform other available techniques, according to the results presented in Example 4.3. Additionally, we observed that allowing for the arbitrary variation of the scheduling parameters in the controller design might not represent a major issue. In fact, for some particular cases, while other available strategies managed to yield a lower bound on the  $\mathcal{H}_\infty$  guaranteed cost when slow variation deviation bounds are assumed, the opposite is observed for higher deviation bounds, as also discussed in Example 4.3. Therefore, the employment of a more straight-forward approach that only requires the range on which the scheduling parameters can vary might be interesting for problems where the information about the deviation bounds is not previously available, inclusive in real control problems, as addressed in the inverted pendulum stabilization, showed in Example 4.4.

At last, while exploring additional practical issues in real control problems, we were able to propose the employment of an strategy that is able to address additional sensors

and actuator non-negligible dynamics subject to time delay by means of an SOF control design applied to an augmented system representation. The simulation results show the importance of considering such practical issues in the control design, attesting to the relevance of the synthesis method presented in this work. In practical terms, the results attest for the potential of the proposed approach to be applied in the control design for others attitude angles in aircraft.

By confronting the results observed in Examples 5.1 and 5.3, we see that a minimum decay rate specification is of value to improve the closed-loop dynamics. However, enforcing this specification may be a challenging issue, as the feasibility of the LMIs involved in the synthesis of the robust controller may be compromised. This fact indicates the importance of being able to employ less conservative synthesis condition, in order to obtain a better transient response in closed-loop, justifying the employment of the HPLF approach proposed in Theorem 5.1.

Furthermore, our proposed augmented system designed in terms of the Padé approximation shows to be able to outperform other classic robust control strategies, such as the sliding-mode control (SMC), as presented in Example 5.2. Disturbance rejection is also possible to be coped with by employing our extended LMI synthesis conditions for  $\mathcal{H}_2$  guaranteed cost minimization. The proposed controller design showed to yield a less conservative bound on the  $\mathcal{H}_2$  norm, when compared to other available strategies, even considering more complex control requirements (additional sensor/actuator dynamics and time delay effect).

At last, it is important to highlight that the polytopic system modeling strategy considered in our work not only enables the designer to consider uncertain sensor and actuator parameters, and uncertain time delays, but also that these parameters can be time-varying. Therefore, the proposed method can be directly applied to address linear parameter-varying (LPV) systems through a gain-scheduling control design.

### Future Perspectives

The SOF stabilization is an open problem in the literature. The two-stage design strategy shows to be a very interesting way for dealing with such a challenging control problem. Based on the obtained results, presented in this thesis, we can infer that much work can still be done, and there is plenty room for exploring the potential of the proposed theorems. In the sequence, some future research topics on the subject addressed in this thesis are enlisted.

#### Two-Stage SOF Control Design:

- investigate the improvement of the two-stage method, by incorporating information about the second-stage design on the first-stage LMIs;



- extend the proposed LMI conditions to fuzzy Takagi-Sugeno models of nonlinear systems;
- develop new experiments for comparing the proposed results with other similar available in the literature.

**Robust and GS–SOF  $\mathcal{D}$ -stabilization:**

- development of extensions for coping with disturbance rejection via  $\mathcal{H}_2$  and/or  $\mathcal{H}_\infty$  norm minimization;
- investigation of more complex pole placement regions, as in Chilali and Gahinet (1996), and less conservative pole placement LMI conditions;
- evaluate the use of parameter-dependent Lyapunov functions in the LPV case;
- develop a more profound investigation regarding the performance improvement achieved through LMI pole placement constraints in LPV controller design;

**Discrete-time GS–SOF stabilization:**

- derive extensions to cope with mixed  $\mathcal{H}_2/\mathcal{H}_\infty$  problem;

## REFERENCES

- AGULHARI, C. M.; FELIPE, A.; OLIVEIRA, R. C. L. F.; PERES, P. L. D. Algorithm 998: The robust LMI parser - A toolbox to construct LMI conditions for uncertain systems. *ACM Transactions on Mathematical Software*, New York, v. 45, n. 3, p. 1–25, 2019.
- AGULHARI, C. M.; OLIVEIRA, R. C. L. F.; PERES, P. L. D. Robust  $\mathcal{H}_\infty$  static output-feedback design for time-invariant discrete-time polytopic systems from parameter-dependent state-feedback gains. In: AMERICAN CONTROL CONFERENCE - ACA, 15., 2010, Baltimore. *Proceedings [...]*. Piscataway: IEEE, 2010. p. 4677–4682.
- AGULHARI, C. M.; OLIVEIRA, R. C. L. F.; PERES, P. L. D. Static output feedback control of polytopic systems using polynomial Lyapunov functions. In: CONFERENCE ON DECISION AND CONTROL - CDC, 49., 2010, Atlanta. *Proceedings [...]*. Piscataway: IEEE, 2010. p. 6894–6901.
- AGULHARI, C. M.; OLIVEIRA, R. C. L. F.; PERES, P. L. D. LMI relaxations for reduced-order robust  $\mathcal{H}_2/\mathcal{H}_\infty$  control of continuous-time uncertain linear systems. *IEEE Transactions on Automatic Control*, Piscataway, v. 57, n. 6, p. 1532–1537, 2012.
- AL-JIBOORY, A. K.; ZHU, G. Static output-feedback robust gain-scheduling control with guaranteed  $\mathcal{H}_2$  performance. *Journal of the Franklin Institute*, Amsterdam, v. 355, n. 5, p. 2221–2242, 2018.
- AL-JIBOORY, A. K.; ZHU, G.; SWEI, S. S.-M.; SU, W.; NGUYEN, N. T. LPV modeling of a flexible wing aircraft using modal alignment and adaptive gridding methods. *Aerospace Science and Technology*, Amsterdam, v. 66, p. 92–102, 2017.
- ALBERTOS, P.; GARCÍA, P. Robust control design for long time-delay systems. *Journal of Process Control*, Amsterdam, v. 19, n. 10, p. 1640–1648, 2009.
- AMATO, F.; ARIOLA, M.; COSENTINO, C. Finite-time stabilization via dynamic output feedback. *Automatica*, Amsterdam, v. 42, n. 2, p. 337–342, 2006.
- AMATO, F.; MATTEI, M.; PIRONTI, A. Gain scheduled control for discrete-time systems depending on bounded rate parameters. *International Journal of Robust and Nonlinear Control*, New Jersey, v. 15, n. 11, p. 473–494, 2005.
- ANDRY, A.; CHUNG, J.; SHAPIRO, E. Modalized observers. *IEEE Transactions on Automatic Control*, Piscataway, v. 29, n. 7, p. 669–672, 1984.
- ANFINSSEN, H.; AAMO, O. M. Stabilization of a linear hyperbolic PDE with actuator and sensor dynamics. *Automatica*, Amsterdam, v. 95, p. 104–111, 2018.
- APKARIAN, P.; GAHINET, P. A convex characterization of gain-scheduled  $\mathcal{H}_\infty$

- controllers. *IEEE Transactions on Automatic Control*, Pistacaway, v. 40, n. 5, p. 853–864, 1995.
- APKARIAN, P.; GAHINET, P.; BECKER, G. Self-scheduled  $\mathcal{H}_\infty$  control of linear parameter-varying systems: a design example. *Automatica*, Amsterdam, v. 31, n. 9, p. 1251–1261, 1995.
- APKARIAN, P.; PELLANDA, P. C.; TUAN, H. D. Mixed  $\mathcal{H}_2/\mathcal{H}_\infty$  multi-channel linear parameter-varying control in discrete time. *Systems & Control Letters*, Amsterdam, v. 41, n. 5, p. 333–346, 2000.
- ASSUNÇÃO, E.; BETETO, M. A. L.; TEIXEIRA, M. C. M.; SILVA, E. R. P. D. Robust LQR-LMI state-derivative controller: A novel approach. In: EUROPEAN WORKSHOP ON ADVANCED CONTROL AND DIAGNOSIS - ACD, 15., 2019, Bologna. *Proceedings [...]*. Berlin: Springer, 2019.
- ÅSTRÖM, K. J.; WITTENMARK, B. **Adaptive control**. Massachusetts: Courier Corporation, 2013.
- BAG, S. K.; SPURGEON, S. K.; EDWARDS, C. Dynamic output feedback sliding mode design for linear uncertain systems. In: IEEE CONFERENCE ON DECISION AND CONTROL, 35., 1996, Kobe. *Proceedings [...]*. Pistacaway: IEEE, 2002. p. 4613–4618.
- BAN, X.; WU, F. Output feedback control of linear fractional transformation systems subject to actuator saturation. *International Journal of Systems Science*, Abingdon, v. 47, n. 15, p. 3646–3655, 2016.
- BANZA, A. T.; TAN, Y.; MAREELS, I. Integral sliding mode control design for systems with fast sensor dynamics. *Automatica*, Amsterdam, v. 119, p. 109093, 2020.
- BEHROUZ, H.; MOHAMMADZAMAN, I.; MOHAMMADI, A. Robust static output feedback  $\mathcal{H}_2/\mathcal{H}_\infty$  control synthesis with pole placement constraints: An LMI approach. *International Journal of Control, Automation and Systems*, Berlin, v. 19, n. 1, p. 241–254, 2021.
- BENAMMAR, N.; RIDOUARD, F.; BAUER, H.; RICHARD, P. Forward end-to-end delay for AFDX networks. *IEEE Transactions on Industrial Informatics*, Pistacaway, v. 14, n. 3, p. 858–865, 2017.
- BETETO, M. A. L.; ASSUNÇÃO, E.; TEIXEIRA, M. C. M.; SILVA, E. R. P. da; BUZACHERO, L. F. S.; CAUN, R. P. Design of robust LQR-derivative controller for the  $\mathcal{D}$ -stabilization of linear systems. In: CONGRESSO BRASILEIRO DE AUTOMÁTICA - CBA, 22., 2010, João Pessoa. *Anais [...]*. Campinas: SBA, 2018.
- BETETO, M. A. L.; ASSUNÇÃO, E.; TEIXEIRA, M. C. M.; SILVA, E. R. P. d.; BUZACHERO, L. F. S.; CAUN, R. da P. Less conservative conditions for robust LQR-state-derivative controller design: an LMI approach. *International Journal of Systems Science*, Abingdon, p. 1–20, 2021.
- BLONDEL, V.; TSITSIKLIS, J. N. NP-hardness of some linear control design problems. *SIAM Journal on Control and Optimization*, Philadelphia, v. 35, n. 6, p. 2118–2127,

1997.

BOYD, S.; GHAOUI, L. E.; FERON, E.; BALAKRISHNAN, V. **Linear matrix inequalities in system and control theory**. Philadelphia: SIAM, 1994.

BURKE, J. V.; LEWIS, A. S.; OVERTON, M. L. A nonsmooth, nonconvex optimization approach to robust stabilization by static output feedback and low-order controllers. In: IFAC SYMPOSIUM ON ROBUST CONTROL DESIGN, 4., 2003, Milan. *Proceedings [...]*. Amsterdam: Elsevier, 2003.

CAIGNY, J. D.; CAMINO, J. F.; OLIVEIRA, R. C. L. F.; PERES, P. L. D.; SWEVERS, J. Gain-scheduled  $\mathcal{H}_\infty$ -control for discrete-time polytopic LPV systems using homogeneous polynomially parameter-dependent Lyapunov functions. In: IFAC SYMPOSIUM ON ROBUST CONTROL DESIGN, 6., 2009, Haifa. *IFAC Proceedings Volumes*. Amsterdam: Elsevier, 2009. v. 42, p. 19–24.

CAIGNY, J. D.; CAMINO, J. F.; OLIVEIRA, R. C. L. F.; PERES, P. L. D.; SWEVERS, J. Gain-scheduled  $\mathcal{H}_2$  and  $\mathcal{H}_\infty$  control of discrete-time polytopic time-varying systems. *IET Control Theory & Applications*, Stavenage, v. 4, n. 3, p. 362–380, 2010.

CAIGNY, J. D.; CAMINO, J. F.; OLIVEIRA, R. C. L. F.; PERES, P. L. D.; SWEVERS, J. Gain-scheduled dynamic output feedback control for discrete-time LPV systems. *International Journal of Robust and Nonlinear Control*, Oxford, v. 22, n. 5, p. 535–558, 2012.

CAO, Y. Y.; LAM, J.; SUN, Y. X. Static output feedback stabilization: an ILMI approach. *Automatica*, Amsterdam, v. 34, n. 12, p. 1641–1645, 1998.

CHEN, X.; XU, H.; WANG, H. Distributed static output feedback control for interconnected systems in finite-frequency domain. *IET Control Theory & Applications*, New Jersey, v. 15, n. 8, p. 1068–1081, 2021.

CHEN, Z.; HAN, L.; HOU, Y. Robust fault estimation and isolation for a descriptor LPV system with disturbance. *Journal of the Franklin Institute*, Amsterdam, v. 358, n. 2, p. 1635–1655, 2021.

CHILALI, M.; GAHINET, P.  $\mathcal{H}_\infty$  design with pole placement constraints: an LMI approach. *IEEE Transactions on Automatic Control*, Piscataway, v. 41, n. 3, p. 358–367, 1996.

CHILALI, M.; GAHINET, P.; APKARIAN, P. Robust pole placement in LMI regions. *IEEE Transactions on Automatic Control*, Piscataway, v. 44, n. 12, p. 2257–2270, 1999.

CRUSIUS, C. A. R.; TROFINO, A. Sufficient LMI conditions for output feedback control problems. *IEEE Transactions on Automatic Control*, Piscataway, v. 44, n. 5, p. 1053–1057, 1999.

DEAECTO, G. S.; GEROMEL, J. C.; DAAFOUZ, J. Dynamic output feedback  $\mathcal{H}_\infty$  control of switched linear systems. *Automatica*, Amsterdam, v. 47, n. 8, p. 1713–1720, 2011.

- DENG, W.; YAO, J.; MA, D. Time-varying input delay compensation for nonlinear systems with additive disturbance: An output feedback approach. *International Journal of Robust and Nonlinear Control*, New Jersey, v. 28, n. 1, p. 31–52, 2018.
- DENG, W.; YAO, J.; WANG, Y.; YANG, X.; CHEN, J. Output feedback backstepping control of hydraulic actuators with valve dynamics compensation. *Mechanical Systems and Signal Processing*, Amsterdam, v. 158, p. 107769, 2021.
- DING, B. Constrained robust model predictive control via parameter-dependent dynamic output feedback. *Automatica*, Amsterdam, v. 46, n. 9, p. 1517–1523, 2010.
- DING, B.; HUANG, B.; XU, F. Dynamic output feedback robust model predictive control. *International Journal of Systems Science*, Abingdon, v. 42, n. 10, p. 1669–1682, 2011.
- DONG, J.; YANG, G.-H. Static output feedback control synthesis for linear systems with time-invariant parametric uncertainties. *IEEE Transactions on Automatic Control*, Piscataway, v. 52, n. 10, p. 1930–1936, 2007.
- DONG, J.; YANG, G.-H. Robust static output feedback control for linear discrete-time systems with time-varying uncertainties. *Systems & Control Letters*, Amsterdam, v. 57, n. 2, p. 123–131, 2008.
- DONG, J.; YANG, G.-H. Robust static output feedback control synthesis for linear continuous systems with polytopic uncertainties. *Automatica*, Amsterdam, v. 49, n. 6, p. 1821–1829, 2013.
- EBIHARA, Y.; MAEDA, K.; HAGIWARA, T. Robust  $\mathcal{D}$ -stability analysis of uncertain polynomial matrices via polynomial-type multipliers. In: IFAC WORLD CONGRESS, 16., 2005, Prague. *IFAC Proceedings Volumes*. Amsterdam: Elsevier, 2005. v. 38, p. 191–196.
- EGIDIO, L. N.; DEAECTO, G. S. Dynamic output feedback control of discrete-time switched affine systems. *IEEE Transactions on Automatic Control*, Piscataway, 2021.
- FENG, T. *Ethernet-based AFDX simulation and time delay analysis*. 2016. 133 f. Dissertation (Master's in Aerospace Computational Engineering) – Cranfield University, Cranfield, 2016.
- FLIESS, M.; MARQUEZ, R.; MOUNIER, H. PID-like regulators for a class of linear delay systems. In: PISTACAWAY. *2001 European Control Conference (ECC)*. 2001. p. 178–183.
- GAHINET, P.; APKARIAN, P. A linear matrix inequality approach to  $\mathcal{H}_\infty$  control. *International Journal of Robust and Nonlinear Control*, New Jersey, v. 4, n. 4, p. 421–448, 1994.
- GEROMEL, J. C.; COLANERI, P.; BOLZERN, P. Dynamic output feedback control of switched linear systems. *IEEE Transactions on Automatic Control*, Piscataway, v. 53, n. 3, p. 720–733, 2008.

- GEROMEL, J. C.; KOROGUI, R. H. Analysis and synthesis of robust control systems using linear parameter dependent Lyapunov functions. *IEEE Transactions on Automatic Control*, Pistacaway, v. 51, n. 12, p. 1984–1989, 2006.
- GEROMEL, J. C.; KOROGUI, R. H.; BERNUSSOU, J.  $\mathcal{H}_2$  and  $\mathcal{H}_\infty$  robust output feedback control for continuous time polytopic systems. *IET Control Theory & Applications*, Stavenage, v. 1, n. 5, p. 1541–1549, 2007.
- GEROMEL, J. C.; PERES, P. L. D.; SOUZA, S. R. Convex analysis of output feedback control problems: Robust stability and performance. *IEEE Transactions on Automatic Control*, Pistacaway, v. 41, n. 7, p. 997–1003, 1996.
- GHAOUI, L. E.; OUSTRY, F.; AITRAMI, M. A cone complementarity linearization algorithm for static output-feedback and related problems. *IEEE Transactions on Automatic Control*, Pistacaway, v. 42, n. 8, p. 1171–1176, 1997.
- GRITLI, H.; ZEMOUCHE, A.; BELGHITH, S. On LMI conditions to design robust static output feedback controller for continuous-time linear systems subject to norm-bounded uncertainties. *International Journal of Systems Science*, Abingdon, v. 52, n. 1, p. 12–46, 2021.
- GUNNARSSON, F.; GUSTAFSSON, F.; BLOM, J. Dynamical effects of time delays and time delay compensation in power controlled DS-CDMA. *IEEE Journal on Selected Areas in Communications*, Pistacaway, v. 19, n. 1, p. 141–151, 2001.
- HADDAD, W. M.; BERNSTEIN, D. S. Controller design with regional pole constraints. *IEEE Transactions on Automatic Control*, Pistacaway, v. 37, n. 1, p. 54–69, 1992.
- HAO, S.; LIU, T.; PASZKE, W.; GAŁKOWSKI, K.; WANG, Q.-G. Robust static output feedback based iterative learning control design with a finite-frequency-range two-dimensional specification for batch processes subject to nonrepetitive disturbances. *International Journal of Robust and Nonlinear Control*, New Jersey, v. 31, n. 12, p. 5745–5761, 2021.
- HAO, Y.; DUAN, Z. Static output-feedback controller synthesis with restricted frequency domain specifications for time-delay systems. *IET Control Theory & Applications*, Stavenage, v. 9, n. 10, p. 1608–1614, 2015.
- HOFFMANN, C.; WERNER, H. A survey of linear parameter-varying control applications validated by experiments or high-fidelity simulations. *IEEE Transactions on Control Systems Technology*, Pistacaway, v. 23, n. 2, p. 416–433, 2014.
- JUNIOR, J. R. C.; GALVÃO, R. K. H.; ASSUNÇÃO, E. A new OFRMPC formulation with on-line synthesis of the dynamic output feedback controller. *International Journal of Robust and Nonlinear Control*, New Jersey, v. 27, n. 17, p. 3921–3936, 2017.
- KAJIWARA, H.; APKARIAN, P.; GAHINET, P. LPV techniques for control of an inverted pendulum. *IEEE Control Systems Magazine*, Pistacaway, v. 19, n. 1, p. 44–54, 1999.
- KARIMI, H. R. A sliding mode approach to  $\mathcal{H}_\infty$  synchronization of master–slave

- time-delay systems with Markovian jumping parameters and nonlinear uncertainties. *Journal of the Franklin Institute*, Amsterdam, v. 349, n. 4, p. 1480–1496, 2012.
- KHALIL, H. K. A note on the robustness of high-gain-observer-based controllers to unmodeled actuator and sensor dynamics. *Automatica*, Amsterdam, v. 41, n. 10, p. 1821–1824, 2005.
- KIM, C.-S.; JI, C.-H.; KOH, G.-O.; KIM, B. S. Stability margin and structural coupling analysis of a hybrid INDI control for the fighter aircraft. *International Journal of Aeronautical and Space Sciences*, Berlin, p. 1–16, 2021.
- KRSTIC, M. Lyapunov tools for predictor feedbacks for delay systems: Inverse optimality and robustness to delay mismatch. *Automatica*, Amsterdam, v. 44, n. 11, p. 2930–2935, 2008.
- KU, C.-C.; CHEN, G.-W. Gain-scheduled controller design for discrete-time linear parameter varying systems with multiplicative noises. *International Journal of Control, Automation and Systems*, Berlin, v. 13, n. 6, p. 1382–1390, 2015.
- LACERDA, M. J.; OLIVEIRA, R. C. L. F.; PERES, P. L. D. Robust  $\mathcal{H}_2$  and  $\mathcal{H}_\infty$  filter design for uncertain linear systems via LMIs and polynomial matrices. *Signal Processing*, Amsterdam, v. 91, n. 5, p. 1115–1122, 2011.
- LEITE, V. J. S.; MONTAGNER, V. F.; PERES, P. L. D. Robust pole location by parameter dependent state feedback control. In: IEEE CONFERENCE ON DECISION AND CONTROL - CDC, 41., 2002. *Proceedings* [...]. Piscataway: IEEE, 2002. v. 2, p. 1864–1869.
- LEITMANN, G.; RYAN, E.; STEINBERG, A. Feedback control of uncertain systems: robustness with respect to neglected actuator and sensor dynamics. *International Journal of Control*, Abingdon, v. 43, n. 4, p. 1243–1256, 1986.
- LI, W.; DU, H.; FENG, Z.; NING, D.; LI, W. Dynamic output-feedback event-triggered  $\mathcal{H}_\infty$  control for singular active seat suspension systems with a human body model. *IET Control Theory & Applications*, New Jersey, 2021.
- LLINS, L. I. H.; ASSUNÇÃO, E.; TEIXEIRA, M. C. M.; CARDIM, R.; CADALSO, M. R.; OLIVEIRA, D. R. d.; SILVA, E. R. da. Design of gain scheduling control using state derivative feedback. *Mathematical Problems in Engineering*, Cairo, v. 2017, 2017.
- LOFBERG, J. YALMIP: A toolbox for modeling and optimization in MATLAB. In: IEEE INTERNATIONAL SYMPOSIUM ON COMPUTER AIDED CONTROL SYSTEMS DESIGN, 2004, Taipei. *Proceedings* [...]. Piscataway: IEEE, 2004. p. 284–289.
- MEHDI, D.; BOUKAS, E.; BACHELIER, O. Static output feedback design for uncertain linear discrete time systems. *IMA Journal of Mathematical Control and Information*, Oxford, v. 21, n. 1, p. 1–13, 2004.
- MONTAGNER, V. F.; OLIVEIRA, R. C. L. F.; LEITE, V. J. S.; PERES, P. L. D. Gain scheduled state feedback control of discrete-time systems with time-varying uncertainties:

- an LMI approach. In: IEEE CONFERENCE ON DECISION AND CONTROL, 44., 2005, Seville. **Proceedings** [...]. Piscataway: IEEE, 2005. p. 4305–4310.
- NGUYEN, A.; CHEVREL, P.; CLAVEAU, F. Gain-scheduled static output feedback control for saturated LPV systems with bounded parameter variations. *Automatica*, Kidlington, v. 89, p. 420–424, 2018.
- NICULESCU, S.-I.; LOZANO, R. On the passivity of linear delay systems. *IEEE Transactions on Automatic Control*, Piscataway, v. 46, n. 3, p. 460–464, 2001.
- NIU, X.; YE, H.; LIU, Y.; LIU, X. Padé approximation based method for computation of eigenvalues for time delay power system. In: INTERNATIONAL UNIVERSITIES' POWER ENGINEERING CONFERENCE - UPEC, 48., 2013, Dublin. **Proceedings** [...]. 2013. p. 1–4.
- OGATA, K. *et al.* **Modern control engineering**. New Jersey: Prentice Hall, v. 5, 2010.
- OLIVEIRA, M. C. de; SKELTON, R. E. Stability tests for constrained linear systems. In: MOHEIMANI, S. O. R. (Ed.). **Perspectives in Robust Control**. : London: Springer, 2007. p. 241–257.
- OLIVEIRA, R. C. L. F.; PERES, P. L. D. LMI conditions for robust stability analysis based on polynomially parameter-dependent Lyapunov functions. *Systems & Control Letters*, Kidlington, v. 55, n. 1, p. 52–61, 2006.
- OLIVEIRA, R. C. L. F.; PERES, P. L. D. Time-varying discrete-time linear systems with bounded rates of variation: Stability analysis and control design. *Automatica*, Amsterdam, v. 45, n. 11, p. 2620–2626, 2009.
- PACKARD, A.; ZHOU, K.; PANDEY, P.; BECKER, G. A collection of robust control problems leading to LMIs. In: IEEE CONFERENCE ON DECISION AND CONTROL, 30., 1991, Birghton. **Proceedings** [...]. Piscataway: IEEE, 1991. p. 1245–1250.
- PALMA, J. M.; MORAIS, C. F.; OLIVEIRA, R. C. L. F. A less conservative approach to handle time-varying parameters in discrete-time linear parameter-varying systems with applications in networked control systems. *International Journal of Robust and Nonlinear Control*, New Jersey, v. 30, n. 9, p. 3521–3546, 2020.
- PALRAJ, J.; MATHIYALAGAN, K.; SHI, P. New results on robust sliding mode control for linear time-delay systems. *IMA Journal of Mathematical Control and Information*, Oxford, v. 38, n. 1, p. 320–336, 2021.
- PANDEY, A. P.; OLIVEIRA, M. C. Discrete-time  $\mathcal{H}_\infty$  control of linear parameter-varying systems. *International Journal of Control*, Abingdon, v. 92, n. 12, p. 2750–2760, 2019.
- PAULINO, A. C. S.; BARA, G. I. Homogeneous polynomial Lyapunov functions for the analysis of polytopic parameter-dependent descriptor systems. *International Journal of Control*, Abingdon, p. 1–14, 2021.



- PEAUCELLE, D.; ARZELIER, D. An efficient numerical solution for  $\mathcal{H}_2$  static output feedback synthesis. In: EUROPEAN CONTROL CONFERENCE - ECC, 2001, Porto. *Proceedings* [...]. Piscataway: IEEE, 2001. p. 3800–3805.
- PEAUCELLE, D.; ARZELIER, D.; BACHELIER, O.; BERNUSSOU, J. A new robust  $\mathcal{D}$ -stability condition for real convex polytopic uncertainty. *Systems & Control Letters*, Amsterdam, v. 40, n. 1, p. 21–30, 2000.
- PESSIM, P. S.; PEIXOTO, M. L. C.; PALHARES, R. M.; LACERDA, M. J. Static output-feedback control for cyber-physical LPV systems under DoS attacks. *Information Sciences*, Amsterdam, v. 563, p. 241–255, 2021.
- QIU, J.; FENG, G.; GAO, H. Approaches to robust  $\mathcal{H}_\infty$  static output feedback control of discrete-time piecewise-affine systems with norm-bounded uncertainties. *International Journal of Robust and Nonlinear Control*, New Jersey, v. 21, n. 7, p. 790–814, 2011.
- QUANSER. *Active Suspension System: User Manual*. 2009.
- RICHARD, J.-P. Time-delay systems: an overview of some recent advances and open problems. *Automatica*, Amsterdam, v. 39, n. 10, p. 1667–1694, 2003.
- RODRIGUES, L. A.; CAMINO, J. F.; PERES, P. L. D. Gain-scheduled  $\mathcal{H}_\infty$  control for discrete-time polynomial LPV systems using homogeneous polynomial path-dependent Lyapunov functions. *IFAC-PapersOnLine*, Amsterdam, v. 51, n. 26, p. 179–184, 2018.
- RODRIGUES, M.; HAMDI, H.; BRAIEK, N. B.; THEILLIOL, D. Observer-based fault tolerant control design for a class of LPV descriptor systems. *Journal of the Franklin Institute*, Amsterdam, v. 351, n. 6, p. 3104–3125, 2014.
- RODRIGUES, R. C. S.; SOMBRA, A. K. R.; TORRICO, B. C.; PEREIRA, R. D.; FORTE, M. D. d. N.; FILHO, M. P. de A.; NOGUEIRA, F. G. Tuning rules for unstable dead-time processes. *European Journal of Control*, Amsterdam, v. 59, p. 250–263, 2021.
- ROSA, T. E.; FREZZATTO, L.; MORAIS, C. F.; OLIVEIRA, R. C.  $\mathcal{H}_\infty$  static output-feedback gain-scheduled control for discrete LPV time-delay systems. *IFAC-PapersOnLine*, Amsterdam, v. 51, n. 26, p. 137–142, 2018.
- ROSA, T. E.; MORAIS, C. F.; OLIVEIRA, R. C. L. F.  $\mathcal{H}_\infty$  output-feedback gain-scheduled control for discrete-time linear systems affected by time-varying parameters. *IFAC-PapersOnLine*, Amsterdam, v. 50, n. 1, p. 8618–8623, 2017.
- ROSA, T. E.; MORAIS, C. F.; OLIVEIRA, R. C. L. F. New robust LMI synthesis conditions for mixed  $\mathcal{H}_2/\mathcal{H}_\infty$  gain-scheduled reduced-order DOF control of discrete-time LPV systems. *International Journal of Robust and Nonlinear Control*, New Jersey, v. 28, n. 18, p. 6122–6145, 2018. ISSN 1049-8923.
- ROTONDO, D.; NEJJARI, F.; PUIG, V. Robust state-feedback control of uncertain LPV systems: An LMI-based approach. *Journal of the Franklin Institute*, Amsterdam, v. 351, n. 5, p. 2781–2803, 2014.
- RUGH, W. J.; SHAMMA, J. S. Research on gain scheduling. *Automatica*, Amsterdam,

v. 36, n. 10, p. 1401–1425, 2000.

SADABADI, M. S.; KARIMI, A. Fixed-order control of LTI systems subject to polytopic uncertainty via the concept of strictly positive realness. In: AMERICAN CONTROL CONFERENCE - ACC, 2015, Chicago. *Proceedings [...]*. Piscataway: IEEE, 2015. p. 2882–2887.

SADABADI, M. S.; PEAUCELLE, D. From static output feedback to structured robust static output feedback: A survey. *Annual Reviews in Control*, Amsterdam, v. 42, p. 11–26, 2016.

SADEGHZADEH, A. Gain-scheduled static output feedback controller synthesis for discrete-time LPV systems. *International Journal of Systems Science*, Abingdon, v. 48, n. 14, p. 2936–2947, 2017.

SADEGHZADEH, A. LMI relaxations for robust gain-scheduled control of uncertain linear parameter varying systems. *IET Control Theory & Applications*, Stavenage, v. 13, n. 4, p. 486–495, 2018.

SAHOO, P. R.; GOYAL, J. K.; GHOSH, S.; NASKAR, A. K. New results on restricted static output feedback  $\mathcal{H}_\infty$  controller design with regional pole placement. *IET Control Theory & Applications*, Stavenage, v. 13, n. 8, p. 1095–1104, 2019.

SANTOS, J. F. S. dos; PELLANDA, P. C.; SIMÕES, A. M. Robust pole placement under structural constraints. *Systems & Control Letters*, Amsterdam, v. 116, p. 8–14, 2018.

SCHERER, C.; GAHINET, P.; CHILALI, M. Multiobjective output-feedback control via LMI optimization. *IEEE Transactions on Automatic Control*, Piscataway, v. 42, n. 7, p. 896–911, 1997.

SCHERER, C. W. Mixed  $\mathcal{H}_2/\mathcal{H}_\infty$  control for time-varying and linear parametrically-varying systems. *International Journal of Robust and Nonlinear Control*, New Jersey, v. 6, n. 9-10, p. 929–952, 1996.

SERENI, B.; ASSUNÇÃO, E.; TEIXEIRA, M. C. M. Robust  $\mathcal{D}$ -stabilization of linear systems. In: SIMPÓSIO BRASILEIRO DE AUTOMAÇÃO INTELIGENTE - SBAI, 14., 2019, Ouro Preto. *Proceedings [...]*. Campinas: SBA, 2019. v. 1.

SERENI, B.; ASSUNÇÃO, E.; TEIXEIRA, M. C. M. New gain-scheduled static output feedback controller design strategy for stability and transient performance of LPV systems. *IET Control Theory & Applications*, Stavenage, v. 14, n. 5, p. 717–725, 2020.

SERENI, B.; GALVÃO, R. K. H.; ASSUNÇÃO, E.; TEIXEIRA, M. C. M. Synthesis of robust control systems with dynamic actuators and sensors using a static output feedback method. In: CONGRESSO BRASILEIRO DE AUTOMÁTICA - CBA, 23., 2020, Rio Grande. *Proceedings [...]*. Campinas: SBA, 2020. v. 2, n. 1.

SERENI, B.; MANESCO, R.; ASSUNÇÃO, E.; TEIXEIRA, M. Relaxed LMI conditions for the design of robust static output feedback controllers. *IFAC-PapersOnLine*, Amsterdam, v. 51, n. 25, p. 428–433, 2018.

- SHAH, D. H.; PATEL, D. M. Design of sliding mode control for quadruple-tank MIMO process with time delay compensation. *Journal of Process Control*, Amsterdam, v. 76, p. 46–61, 2019.
- SHIN, K. G.; CUI, X. Computing time delay and its effects on real-time control systems. *IEEE Transactions on control systems technology*, Piscataway, v. 3, n. 2, p. 218–224, 1995.
- SILVA, E. R. P. D.; ASSUNÇÃO, E.; TEIXEIRA, M.; BUZACHERO, L. F. S. Less conservative control design for linear systems with polytopic uncertainties via state-derivative feedback. *Mathematical Problems in Engineering*, London, v. 2012, 2012.
- SKELTON, R. E.; IWASAKI, T.; GRIGORIADIS, D. E. ***A unified algebraic approach to control design.*** : Florida: CRC Press, 1997.
- SONI, T.; DUTT, J. K.; DAS, A. Dynamic behavior and stability of energy efficient electro-magnetic suspension of rotors involving time delay. *Energy*, Amsterdam, v. 231, p. 120906, 2021.
- SOUZA, C.; LEITE, V. J. S.; TARBOURIECH, S.; CASTELAN, E. B. Event-triggered policy for dynamic output stabilization of discrete-time LPV systems under input constraints. *Systems & Control Letters*, Amsterdam, v. 153, p. 104950, 2021.
- SOUZA, C.; TARBOURIECH, S.; LEITE, V. J. S.; CASTELAN, E. B. Co-design of an event-triggered dynamic output feedback controller for discrete-time LPV systems with constraints. *Journal of the Franklin Institute*, Amsterdam, 2021.
- SPAGOLLA, A.; MORAIS, C. F.; OLIVEIRA, R. C. L. F.; PERES, P. L. D. Stabilization and  $\mathcal{H}_2$  static output-feedback control of discrete-time positive linear systems. *IEEE Transactions on Automatic Control*, Piscataway, 2021.
- STILWELL, D. J.; RUGH, W. J. Interpolation of observer state feedback controllers for gain scheduling. *IEEE Transactions on Automatic Control*, Piscataway, v. 44, n. 6, p. 1225–1229, 1999.
- STURM, J. F. Using SeDuMi 1.02, a MATLAB toolbox for optimization over symmetric cones. *Optimization Methods and Software*, Abingdon, v. 11, n. 1-4, p. 625–653, 1999.
- SUN, J.-Q. A method of continuous time approximation of delayed dynamical systems. *Communications in Nonlinear Science and Numerical Simulation*, Amsterdam, v. 14, n. 4, p. 998–1007, 2009.
- SUN, X.; ZHANG, Q. Observer-based adaptive sliding mode control for T–S fuzzy singular systems. *IEEE Transactions on Systems, Man, and Cybernetics: Systems*, Piscataway, v. 50, n. 11, p. 4438–4446, 2018.
- TANAKA, K.; IKEDA, T.; WANG, H. O. Fuzzy regulators and fuzzy observers: relaxed stability conditions and LMI-based designs. *IEEE Transactions on Fuzzy Systems*, Piscataway, v. 6, n. 2, p. 250–265, 1998.
- TANG, M.; BÖSWALD, M.; GOVERS, Y.; PUSCH, M. Identification and assessment of

- a nonlinear dynamic actuator model for controlling an experimental flexible wing. *CEAS Aeronautical Journal*, Berlin, p. 1–14, 2021.
- TIAN, W.; GU, Y.; LIU, H.; WANG, X.; YANG, Z.; LI, Y.; LI, P. Nonlinear aeroservoelastic analysis of a supersonic aircraft with control fin free-play by component mode synthesis technique. *Journal of Sound and Vibration*, Amsterdam, v. 493, p. 115835, 2021.
- TOH, K.-C.; TODD, M. J.; TÛTÛNCÛ, R. H. SDPT3 - a MATLAB software package for semidefinite programming, version 1.3. *Optimization methods and software*, Abingdon, v. 11, n. 1-4, p. 545–581, 1999.
- TORRICO, B. C.; CAVALCANTE, M. U.; BRAGA, A. P.; NORMEY-RICO, J. E.; ALBUQUERQUE, A. A. M. Simple tuning rules for dead-time compensation of stable, integrative, and unstable first-order dead-time processes. *Industrial & Engineering Chemistry Research*, Washington, v. 52, n. 33, p. 11646–11654, 2013.
- TROFINO, A.; KUCERA, V. Stabilization via static output feedback. *IEEE Transactions on Automatic Control*, Pistacaway, v. 38, n. 5, p. 764–765, 1993.
- UTKIN, V. I. **Sliding modes and their applications in variable structure systems**. Mir: Moscow, 1978.
- WANG, J.; PENG, G.; YAN, Y. A testing method of measuring time delay of the flight test AFDX avionic system caused by data acquiring network. In: INTERNATIONAL TELEMETERING CONFERENCE PROCEEDINGS, 54., 2018, Glendale. *Proceedings [...]*. San Diego: International Foundation for Telemetry, 2018.
- WANG, J.-W.; WU, H.-N.; LI, H.-X. Static output feedback control design for linear MIMO systems with actuator dynamics governed by diffusion PDEs. *International Journal of Control*, Abingdon, v. 87, n. 1, p. 90–100, 2014.
- WANG, Y.; WYNN, A.; PALACIOS, R. Nonlinear modal aeroservoelastic analysis framework for flexible aircraft. *AIAA Journal*, Reston, v. 54, n. 10, p. 3075–3090, 2016.
- WEI, G.; WANG, Z.; LI, W.; MA, L. A survey on gain-scheduled control and filtering for parameter-varying systems. *Discrete Dynamics in Nature and Society*, Cairo, v. 2014, 2014.
- WU, F.; DONG, K. Gain-scheduling control of LFT systems using parameter-dependent Lyapunov functions. *Automatica*, Amsterdam, v. 42, n. 1, p. 39–50, 2006.
- WU, F.; YANG, X. H.; PACKARD, A.; BECKER, G. Induced L2-norm control for LPV systems with bounded parameter variation rates. *International Journal of Robust and Nonlinear Control*, New Jersey, v. 6, n. 9-10, p. 983–998, 1996.
- WU, H.; NI, H.; HEYDT, G. T. The impact of time delay on robust control design in power systems. In: IEEE POWER ENGINEERING SOCIETY WINTER MEETING, 2002, New York. *Proceedings [...]*. : Pistacaway: IEEE, 2002. v. 2, p. 1511–1516.
- WU, M. A note on stability of linear time-varying systems. *IEEE Transactions on*

*Automatic Control*, Pistacaway, v. 19, n. 2, p. 162–162, 1974.

YAESH, I.; SHAKED, U.  $\mathcal{H}_\infty$  optimization with pole constraints of static output-feedback controllers - A non-smooth optimization approach. *IEEE Transactions on Control Systems technology*, Pistacaway, v. 20, n. 4, p. 1066–1072, 2011.

YANG, F.; GANI, M.; HENRION, D. Fixed-order robust  $\mathcal{H}_\infty$  controller design with regional pole assignment. *IEEE Transactions on Automatic Control*, Pistacaway, v. 52, n. 10, p. 1959–1963, 2007.

YANG, R.; ROTONDO, D.; PUIG, V.  $\mathcal{D}$ -stable controller design for Lipschitz NLPV system. *IFAC-PapersOnLine*, Amsterdam, v. 52, n. 28, p. 88–93, 2019.

YANG, S.-B.; WANG, L.-B.; XU, D. Computational analysis on actuator failures of flexible aircraft. *International Journal of Computational Materials Science and Engineering*, Singapore, v. 7, n. 01&02, p. 1850014:1–19, 2018.

YOUNG, K.-K. D.; KOKOTOVIC, P. V. Analysis of feedback-loop interactions with actuator and sensor parasitics. *Automatica*, Amsterdam, v. 18, n. 5, p. 577–582, 1982.

YUAN, C. Leader-following consensus of parameter-dependent networks via distributed gain-scheduling control. *International Journal of Systems Science*, Abingdon, v. 48, n. 10, p. 2013–2022, 2017.

ZHANG, K.; DUAN, G.-R. Robust  $\mathcal{H}_\infty$  dynamic output feedback control for spacecraft rendezvous with poles and input constraint. *International Journal of Systems Science*, Abingdon, v. 48, n. 5, p. 1022–1034, 2017.

ZHAO, D.; WANG, Y.; XU, L.; WU, H. Adaptive robust control for a class of uncertain neutral systems with time delays and nonlinear uncertainties. *International Journal of Control, Automation and Systems*, Berlin, v. 19, n. 3, p. 1215–1227, 2021.

ZIN, A.; SENAME, O.; GASPAR, P.; DUGARD, L.; BOKOR, J. Robust LPV- $\mathcal{H}_\infty$  control for active suspensions with performance adaptation in view of global chassis control. *Vehicle System Dynamics*, Abingdon, v. 46, n. 10, p. 889–912, 2008.